

von Karman Institute for Fluid Dynamics
Chaussée de Waterloo, 72
B - 1640 Rhode Saint Genèse - Belgium

RTO-AVT-VKI Lecture Series 2007

**ADVANCES ON PROPULSION TECHNOLOGY
FOR HIGH-SPEED AIRCRAFT**

Volume I

March 12-15, 2007

Edited by: G. Paniagua & J. Steelant
von Karman Institute for Fluid Dynamics, Belgium & ESTEC, France

**Distribution A:
Approved for public release;
distribution is unlimited.**

AQ F08-02-00543

20071113018

RTO-AVT-VKI LS 2007

©2007 by the von Karman Institute

*The contents of this book are the property of the von Karman Institute for Fluid Dynamics.
No part of this book may be reproduced or distributed in any form of by any means, or stored in a
database or retrieval system, without the prior written permission of the von Karman Institute.*

REPORT DOCUMENTATION PAGE			Form Approved OMB No. 0704-0188		
Public reporting burden for this collection of information is estimated to average 1 hour per response, including the time for reviewing instructions, searching existing data sources, gathering and maintaining the data needed, and completing and reviewing the collection of information. Send comments regarding this burden estimate or any other aspect of this collection of information, including suggestions for reducing the burden, to Department of Defense, Washington Headquarters Services, Directorate for Information Operations and Reports (0704-0188), 1215 Jefferson Davis Highway, Suite 1204, Arlington, VA 22202-4302. Respondents should be aware that notwithstanding any other provision of law, no person shall be subject to any penalty for failing to comply with a collection of information if it does not display a currently valid OMB control number. PLEASE DO NOT RETURN YOUR FORM TO THE ABOVE ADDRESS.					
1. REPORT DATE (DD-MM-YYYY) 09-05-2007		2. REPORT TYPE Conference Proceedings		3. DATES COVERED (From - To) 12 March 2007 - 15 March 2007	
4. TITLE AND SUBTITLE Advances on Propulsion Technology for High-Speed Aircraft Volume I			5a. CONTRACT NUMBER FA8655-07-1-5052		
			5b. GRANT NUMBER		
6. AUTHOR(S) Conference Committee			5c. PROGRAM ELEMENT NUMBER		
			5d. PROJECT NUMBER		
			5d. TASK NUMBER		
7. PERFORMING ORGANIZATION NAME(S) AND ADDRESS(ES) von Karman Institute Chaussee de Waterloo 72 Sint Genesius Rode B-1640 Belgium			8. PERFORMING ORGANIZATION REPORT NUMBER N/A		
			9. SPONSORING/MONITORING AGENCY NAME(S) AND ADDRESS(ES) EOARD PSC 821 BOX 14 FPO AE 09421-0014		
			11. SPONSOR/MONITOR'S REPORT NUMBER(S) CSP 07-5052		
12. DISTRIBUTION/AVAILABILITY STATEMENT Approved for public release; distribution is unlimited. (approval given by local Public Affairs Office)					
13. SUPPLEMENTARY NOTES Volume I					
14. ABSTRACT The Final Proceedings for Advances on Propulsion Technology for High-Speed Aircraft, 12 March 2007 - 15 March 2007 The demand for supersonic vehicles is believed to boost in the coming years. This VKI/RTO lecture series will review the current state of the art of high speed propulsion for both airplanes and space launchers. Hypersonic air-breathing vehicles technology benefits and challenges will be discussed, with particular attention to the recent hypersonic activities in the USA. Then recommendations for future technology development will be presented. A series of specific talks will address advanced engine technology cycles, pulsed detonation engines and turbine based cycles. A couple of lectures dedicated to rocket engines will discuss turbomachinery issues and recent developments on materials and the combustion chamber. Afterwards, ramjets, scram jets and dual mode operation will be examined. Dedicated sessions will present the experience acquired in recent years in developing advanced demonstrators in the USA, Russia, Australia and the European Union. In the light of existing environmental concerns, the program will be completed with specific sessions on noise generation from high-speed jets and chemical pollution. The requirements to implement a complete hydrogen technology will be analyzed based on the experience gained in the Cryoplane project. The Directors of this VKI/RTO Lecture Series are Prof. G. Paniagua of the von Karman Institute and Prof. J. Steelant of the European Space Agency ESTEC.					
15. SUBJECT TERMS EOARD, Propulsion, Combustion, Hypersonics					
16. SECURITY CLASSIFICATION OF:			17. LIMITATION OF ABSTRACT UL	18. NUMBER OF PAGES	19a. NAME OF RESPONSIBLE PERSON SURYA SURAMPUDI
a. REPORT UNCLAS	b. ABSTRACT UNCLAS	c. THIS PAGE UNCLAS			19b. TELEPHONE NUMBER (Include area code) +44 (0)20 7514 4299

TABLE OF CONTENTS

- McCLINTON, C.R. - *Retired NASA LaRC, USA*
High speed/hypersonic aircraft propulsion technology development
- BALEPIN, V. - *ATK GASL, USA*
High speed propulsion cycles
- SCHAUER, F. - *Wright-Patterson AFB, USA*
Pulsed detonation propulsion
- BOND, A. - *Reaction Engines Ltd, United Kingdom*
Turbine based combined cycles
- MÅRTENSSON, H.; ANDERSSON, S.; TROLLHEDEN, S.; BRODIN, S. - *Volvo Aero Corporation, Sweden*
Rocket engines: turbomachinery
- HAIND, O.J. - *DLR, Germany*
Advanced rocket engines
- FALEMPIN, F. - *MBDA, France*
Ramjet and dual mode operation
Continuous detonation wave engine
- SMART, M. - *The University of Queensland, Australia*
Scramjets
- BAKOS, R. - *ATK GASL, USA*
Current hypersonic research in USA
- SMART, M.¹; STALKER, R.¹; MORGAN, R.¹; PAULL, A.² - ¹*The University of Queensland &*
²*Defense Science and Technology Organisation, Australia*
Hypersonics Research in Australia
- KOPCHENOV, V.I. - *CIAM, Russia*
Some fundamental gasdynamic and physical-chemical aspects of combustion in high velocity flow
- STEELANT, J. - *ESA-ESTEC, The Netherlands*
LAPCAT: High-speed propulsion technology
- KOPIEV, V.F. - *TsAGI, Russia*
High speed jet noise
- WESTENBERGER, A. - *Airbus, Germany*
LH₂ as alternative fuel for aeronautics – Study on aircraft concepts
- STARIK, A.M. - *Central Institute of Aviation Motors, Russia*
Gaseous and particulate emissions with jet engine exhaust and atmospheric pollution

von Karman Institute for Fluid Dynamics

RTO-AVT-VKI Lecture Series 2007

**ADVANCES ON PROPULSION TECHNOLOGY
FOR HIGH-SPEED AIRCRAFT**

March 12-15, 2007

HIGH SPEED/HYPERSONIC AIRCRAFT
PROPULSION TECHNOLOGY DEVELOPMENT

Charles R. McClinton
Retired NASA LaRC, USA

High Speed/Hypersonic Aircraft Propulsion Technology Development

Charles R. McClinton
Retired NASA LaRC
3724 Dewberry Lane
Saint James City, FL 33956

Chuck.mcclinton@comcast.net

Abstract

H. Julian Allen made an important observation in the 1958 21st Wright Brothers Lecture [1]: "Progress in aeronautics has been brought about more by revolutionary than evolutionary changes in methods of propulsion." Numerous studies performed over the past 50 years show potential benefits of higher speed flight systems – for aircraft, missiles and spacecraft. These vehicles will venture past classical supersonic speed, into hypersonic speed, where perfect gas laws no longer apply. The revolutionary method of propulsion which makes this possible is the Supersonic Combustion RAMJET, or SCRAMJET engine. Will revolutionary applications of air-breathing propulsion in the 21st century make space travel routine and intercontinental travel as easy as intercity travel is today? This presentation will reveal how this high speed propulsion system works, what type of aerospace systems will benefit, highlight challenges to development, discuss historic development (in the US as an example), highlight accomplishments of the X-43 scramjet-powered aircraft, and present what needs to be done next to complete this technology development.

1.0 HIGH SPEED AIRBREATHING ENGINES

1.1 Scramjet Engines

The scramjet uses a slightly modified Brayton Cycle [2] to produce power, similar to that used for both the classical ramjet and turbine engines. Air is compressed; fuel injected, mixed and burned to increase the air – or more accurately, the combustion products - temperature and pressure; then these combustion products are expanded. For the turbojet engine, air is mechanically compressed by work extracted from the combustor exhaust using a turbine. In principle, the ramjet and scramjet works the same. The forward motion of the vehicle compresses the air. Fuel is then injected into the compressed air and burned. Finally, the high-pressure combustion products expand through the nozzle and over the vehicle after body, elevating the surface pressure and effectively pushing the vehicle. Thrust is the result of increased kinetic energy between the initial and final states of the working fluid, or the summation of forces on the engine and vehicle surfaces. This is a modified Brayton cycle because the final state in the scramjet nozzle is generally not ambient.

Engine specific impulse, or the efficiency of airbreathing ramjet, scramjet and turbine engines, compared to the rocket is illustrated Figure 1. Specific impulse is the thrust (Nts) produced per unit mass flow (Kg/s) of propellant utilized, i.e. propellant which is carried on board. For the rocket, propellant includes fuel and oxidizer; for the air breather, fuel is the only propellant carried. Note the significant improvement in efficiency of the air breather vis-à-vis a rocket. For example, the scramjet is about 7 times more efficient than the rocket at Mach 7. The revolutionary aspect of the scramjet is extending the airbreathing engine way beyond traditional aircraft limits. Subsonic combustion in the ramjet produces high static pressure and temperature and high heat transfer

(heat load) to the engine combustor structure – especially at higher flight Mach number. These static temperature and heat loads place a practical upper limit on ramjet operation somewhere between Mach 6 and 8. The scramjet overcomes this limit using supersonic combustion. The scramjet has no nozzle throat at the end of the combustor. Supersonic combustion occurs at significantly reduced static pressure and temperature and hence combustor wall heat load. Reduced static temperature allows the practical upper limit of the scramjet to be somewhere between Mach 13 and 15. At the lower limit, the scramjet can be operated below Mach 6 using mixed-mode

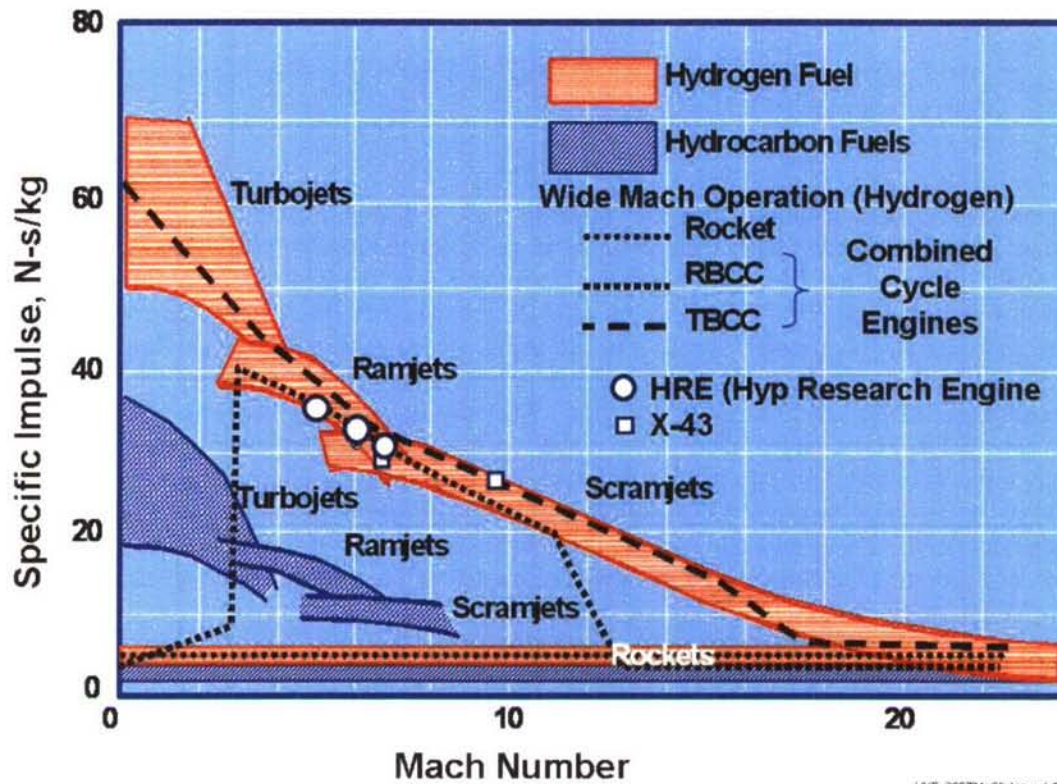


Figure 1. Hypersonic Engine Efficiency

combustion. At these speeds fuel is injected near the exit of the expanding combustor. Combustion pressure rise disturbs and separates the inflowing boundary layer. This disturbance propagates upstream through the boundary layer, creating a large recirculation region. The supersonic inlet flow is further compressed by this separated/recirculating flow to Mach 1, which then persists through the initial combustion region, before again accelerating supersonically through the remaining combustor and nozzle. Combustion in this process occurs both in the recirculating flow and in the sonic/supersonic core – hence the term mixed mode combustion. The fact that a scramjet can be designed to operate in both pure supersonic or mixed combustion modes, covering both the ramjet and scramjet operating speeds, led to the label dual-mode scramjet.

1.2 Combination/Combined Cycle Engines

The dual-mode scramjet can operate over the ramjet and scramjet speed range, from about Mach 3 to at least Mach 15. Any application of the scramjet will require an alternate means of accelerating to scramjet takeover speeds. For an aircraft application alternate power will be required to allow

efficient operation below Mach 3-4 for take off, acceleration, and deceleration to powered landing. A study [3] performed by Marquardt, Rocketdyne and Lockheed, in the early 1960's, provided a low-level (of fidelity) assessment of numerous propulsion options for space access. In all, 36 potential rocket/airbreathing systems were compared. These combined cycle engines included rocket, air-augmented rocket, ramjet, and scramjet cycles. In addition, various "air compression" concepts for low-speed operation were considered, including ejector, fan, and the liquid air cycle (LACE). These studies evaluated as a figure of merit vehicle capability (payload to space for a 1-million pound vehicle). Two conclusions from this study are: Scramjet operation to high Mach provides a significant increase in payload capability; Lox usage below scramjet takeover Mach number greatly lowers the payload capability. Three engines were recommended for additional study: Turbine-scramjet combination engine; ScramLACE; and Supercharged Ejector Ramjet (SERJ). The ScramLACE is an ejector-scramjet with real-time liquid-air collection and compression feeding a hydrogen-air rocket ejector. The SERJ is an ejector ramjet with fan for operation during acceleration to Mach 2 and cruise. The three systems were studied in the USA, and only the turbine-scramjet approach was carried forward. For airbreathing launch vehicles, an additional propulsion system is required for higher-speed operation to achieve orbital velocity, and rockets are the only option. Because the rocket is required for high speed and orbital insertion for single-stage-to-orbit (SSTO) concepts, several studies have also reconsidered it for low-speed operation (albeit inconsistent with the previous [3] conclusions). The resulting engine is called a rocket-based combined cycle engine. Dashed lines in figure 1 illustrate the potential efficiency of the turbine-scramjet-rocket combination (TBCC) engine and the RBCC engines studied extensively in the late 1990's by NASA.

The RBCC design challenges include rocket placement, rocket fuel-oxidized mixture ratio, and the impact of rocket integration on scramjet performance. One RBCC concept is illustrated in figure 2. This concept [4] operates in air-augmented rocket (AAR) mode from Mach 0 to about 3. This mode includes some ejector benefit by entraining air into the dual-mode scramjet duct. Above Mach 3 the rocket is turned off, and the engine operates as a dual-mode scramjet. The final mode of operation, rocket, begins at Mach 10. In rocket mode the engine inlet is eventually closed before the vehicle leaves the atmosphere.

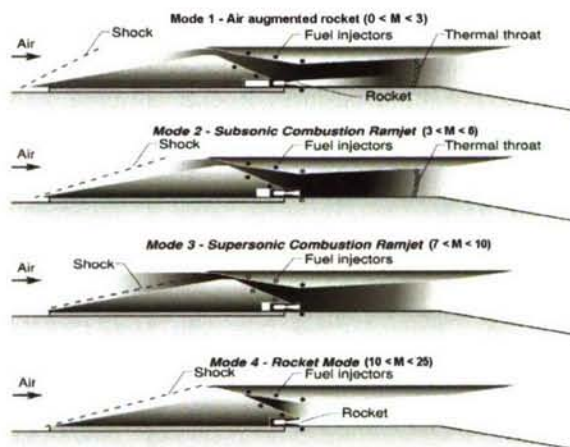


Figure 2. - RBCC Operating Modes

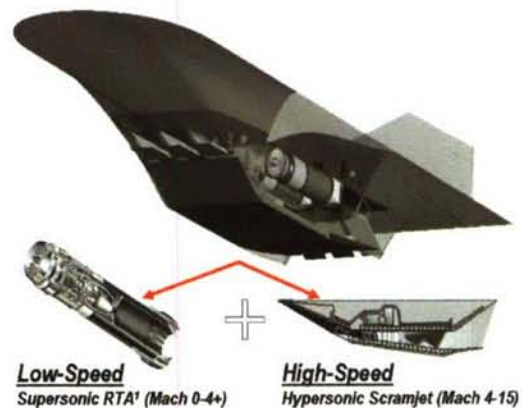


Figure 3. - Typical TBCC

NASA and the USAF have studied turbine-based "over-under" combination engine (TBCC) approaches at a low level for over 40 years. Most of the studies use "simple" over-under designs

[5], as illustrated in figure 3. These designs all utilized variable geometry inlet and nozzles which can fully close to seal off either engine.

2.0 AIRCRAFT APPLICATIONS

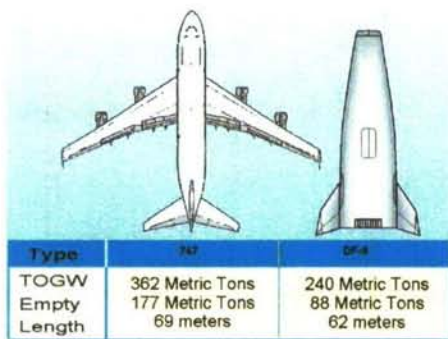
Numerous studies performed over past 50 years show potential benefits of higher speed flight systems – aircraft, missiles and space craft. Potential airbreathing high speed/hypersonic vehicle applications include endoatmospheric and space access. These vehicles may be military or civilian, manned or unmanned, reusable or expendable, hydrocarbon or hydrogen fueled. Potential applications include tactical supersonic cruise—hypersonic dash, hypersonic cruise strategic aircraft, hypersonic tactical or strategic missile, hypersonic transports, and fully or partially reusable single or two-stage-to-orbit (TSTO) launch systems.

2.1 Military Applications

Military benefits of hypersonic vehicles are versatility, response time, survivability, and unfueled range [6]. Civilian benefits are long range rapid commercial transportation and safe, affordable reliable and flexible transportation to low-earth orbit [7]. One example of a potential hypersonic cruise military aircraft is the Dual-Fuel Global-Reach concept shown in Figure 4. It would employ hydrocarbon-fueled turbo-ramjet engines for low-speed flight (Mach 0 to 4.5) and liquid hydrogen-fueled scramjet engines for high-speed flight (Mach 4.5 to 10). This vehicle concept was developed to perform two candidate operational scenarios. The baseline mission involves takeoff, climb to cruising altitude and Mach number, complete a cruise to a mission range of 15,000 Km, followed by a 2.5 g turn at the target at minimum power, and unpowered, maximum L/D descent for rendezvous with a tanker, and a subsonic return to base. The vehicle contains sufficient hydrogen to reach and engage the target, turn, and begin the unpowered descent. Sufficient hydrocarbon fuel is retained on board to allow a 10 minute loiter waiting for the tanker. An alternate mission scenario is a first stage platform for satellite launch. The resulting vehicle is comparable in size and weight to today’s air liners, as illustrated in figure 4.

2.2 Space Launch Applications

Benefits [7] of air-breathing launch systems are improved safety, mission flexibility, vehicle design robustness and reduced operating costs. Air-breathing vehicles, capable of hypersonic speeds, can transform access to space, just like turbojets transformed the airline business. Rocket-powered



Attributes	Baseline ELV	Baseline Space Shuttle	Mach 7 Stage	Mach 10 Stage	Mach 15 Stage	SSTO
	Expendable	Partially Reusable	Expendable 2 nd Stage	Reusable	Reusable	Reusable
Payload Fraction	3%	1%	1-2%	3%	4%	5%
Loss of Vehicle/Payload	1:50	1:100	1:4,000	1:60,000	1:110,000	1:160,000
Cost per Lb to LEO	\$2,500	\$10,000	\$1,700	\$2,000	\$1,400	\$1,000

Figure 4. –Strategic Hypersonic Aircraft

Table 1. Attribute of Space Launch Systems

vehicles are approaching their limits in terms of these parameters [7]; switching to a new approach is the only way to achieve significant improvements [5].

Safety benefits result from characteristics such as enhanced abort capability and moderate power density. Horizontal takeoff and powered landing allows the ability to abort over most of the flight, both ascent and decent. High lift/drag (L/D) allows longer-range glide for large landing footprint. Power density, or the quantity of propellant pumped for a given thrust level, is 1/10 that of a vertical take off rocket due to lower thrust loading (T/W), lower vehicle weight and higher specific impulse. Power density is a large factor in catastrophic failures. Recent analysis [8] indicates that safety increases by several orders of magnitude are possible using air-breathing systems. Mission flexibility results from horizontal takeoff and landing, the large landing (unpowered) footprint and high L/D. Utilization of aerodynamic forces rather than thrust allows efficient orbital plane changes during ascent, and expanded launch window. Robustness and reliability can be built into airbreathing systems because of large margins and reduced weight growth sensitivity, and the low thrust required for smaller, horizontal takeoff systems. Cost models [7] indicate about one-order magnitude reduction in operating cost is possible, vis-à-vis the space shuttle. Attributes for selected air-breathing assisted launch systems categorized by staging Mach number and reusable or expendable second stage are listed in Table 1.

NASA's Next Generation Launch Technology Program identified and quantified these attributes [7, 8]. For example, staging at Mach 7, and using an expendable second stage allows nearly an order of magnitude gain in safety (loss of vehicle/payload), with a small improvement in payload fraction and operating cost, compared with current systems (Space Shuttle or ELV's). Increasing staging Mach number (the fraction of airbreathing contribution to orbital velocity) plus adding a reusable second stage and more advanced engine and airframe technology, increases the payload fraction and reliability, and reduces both loss of vehicle (LOV) and operating cost. The most significant benefit is in safety, quantified by the attribute "Loss of Vehicle."

Airbreathing hypersonic flight is truly the next frontier for air vehicle design, and continues to excite and challenge the next generation of engineers and scientists. What will be the first application?? That depends on political forces more than on technology development challenges. In terms of difficulty, easiest first: hypersonic cruise missile; supersonic cruise - hypersonic dash tactical aircraft; Mach 7 first stage launch vehicle; Mach 7 hypersonic cruise strategic aircraft; Mach 10-15 first stage launch vehicle; Mach 10 cruise; and finally single-stage to orbit launch vehicle.

3.0 CHALLENGES

Challenges facing development and applications of scramjet engines to hypersonic airbreathing propulsion systems are technical and political. Political challenges are beyond the scope of this discussion – but must be seriously addressed in any effort to apply this technology. Technical challenges can be divided into the following categories: Flow physics; Experimental facilities and test methods; Design methods; Scramjet propulsion-airframe integration; High/low-speed engine integration; Flight testing; and Technology development tracking.

3.1 Airframe Integrated Scramjet Design Challenges

The most significant challenges facing design and development of a hypersonic vehicle are propulsion related: scramjet engine design; scramjet-airframe integration; integration of the scramjet with a Mach 4 capable low-speed engine. Effective utilization of scramjets requires careful integration of the airframe and engine. This is required because of the large airflow requirements at high speed. As flight speed increases, the air flow enthalpy approaches, then at about Mach 8 exceeds, the incremental enthalpy increase from combustion, so thrust per unit air flow decreases. This effect is captured by Aaron Auslender's "rule of 69": $T \sim m_{air} * \text{SQRT}(69 / M^2)$ for Mach numbers greater than 7.

With a high degree of propulsion-airframe integration, vehicle flight operations affect the engine operation, mostly through changes in air mass capture. Conversely, engine operation affects vehicle performance, such as lift and trim. Challenges in design/development of airframe integrated scramjets are illustrated using the 2-D cross section of the X-43 scramjet-powered research vehicle in figure 5. The X-43 was a sharp-leading edge lifting body configuration. That is, vehicle lift is

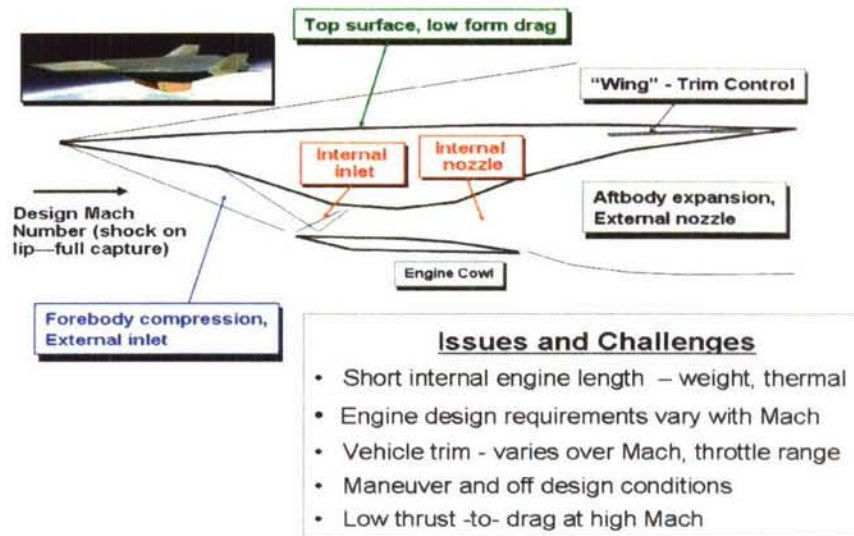


Figure 5. Airframe Integrated Scramjet Design Challenges

generated by the vehicle fuselage and engine, not wings. The vehicle wings were really all moving elevon surfaces for maintaining and controlling vehicle pitch and roll attitude. The entire lower surface of the X-43 was designed to perform scramjet functions, within the limit of acceptable hypersonic aerodynamics, stability and control. The top surface was designed to minimize form drag, enclosing the vehicle between the inlet leading edge (vehicle nose), and the nozzle trailing edge (vehicle tail). Generally good scramjet cycle performance requires that the nozzle is about 30% larger than the inlet capture cross-sectional area. Much of the scramjet inlet compression and nozzle expansion is performed on the vehicle forebody and after body respectively, so that the engine module can remain as short as possible. Short internal engine length is desirable because it is the densest structure on the vehicle, and large surface areas will drive up weight and cooling requirements, potentially exceeding fuel flow requirements. The engine cowl, or lower surface is positioned to capture all of the flow compressed (behind the bow shock wave) on the lower surface at the most critical flight condition, or design point. For hypersonic cruise the design point is the fully loaded cruise condition; for an accelerator it is somewhere close to the peak airbreathing Mach number.

Airframe integration and scramjet engine design is challenged because the vehicle must operate over a large Mach number range, and be capable of maneuvering. Airframe integration includes the effect of the vehicle on the engine performance, as well as engine on the vehicle. At lower than design Mach number the shock waves and hence the compressed flow moves away from the vehicle, so some compressed air is not captured. As the vehicle maneuvers, the shocks move closer on the lifting side, again changing the air capture. Conversely, the engine performance affects the vehicle design and operation. One significant integration issue is the vehicle pitching moment change with flight Mach number. Generally the higher mass capture at high Mach number allows

the engine to produced higher pressure on the external nozzle than that on the forebody produced by aerodynamic compression, so the vehicle tends to pitch down. At lower Mach number, much of the air compressed by the forebody is not captured by the engine. Fortunately, the combustor pressure rise is greater at lower Mach number, but generally not sufficient to make up for spilled air mass flow. So, at low Mach the vehicle tends to have a nose-up pitching moment, which is balanced by the control surfaces. Clearly, as the thrust requirement from the engine changes, the nozzle pressure will change the vehicle pitching moment and trim requirement, because the inlet forces are essentially constant.

In addition to these challenges, even the engine flowpath design requirements vary with Mach number. For example, the inlet compression, expressed by contraction ratio, must be smaller at low Mach number, and increase nearly 1:1 with flight Mach at constant flight dynamic pressure. This is required to allow the inlet to start and function at lower speeds, and provide adequate static pressure in the combustor for good combustion at higher speeds. The shape of the combustor and/or fuel injection location must vary with Mach number to assure good combustor operation. Combustion must start close to the combustor entrance for very high Mach operation, and the combustor must be short. For low speed, the fuel must be injected at a point in the combustor where sufficient expansion has already occurred to minimize the potential for un-starting the inlet. At low speed, an inlet isolator is critical for good performance, at high speed it is a serious detriment to performance. These challenges are addressed by variable geometry, multiple fuel injection stations, or both.

Many different shapes of scramjets were studied in the USA and around the world. Many have focused on the quasi two-dimensional shape selected for the X-43 engine. Others utilized swept sidewall compression [10], conical axisymmetric [11], inward turning axisymmetric [12] (with and without a centerbody), and fully three-dimensional [13]. These concepts all share the same challenges in regards to high speed/hypersonic physics – and they all have about the same performance at the design point. The discriminator between competing configurations has generally been off design performance, operability and weight. Performance issues are often associated with combustor flow distortion. For operation over a significant flight envelope (more than a range of a few Mach numbers), variable geometry is inevitable. Generally this is limited to inlet contraction and throttling the air flow to the inlet, for inlet starting, thrust control and inlet close-off. This variable geometry is accomplished by linear movement of body panels, engine cowl, center body plugs, or fuel injectors.

Hypersonic propulsion physics challenges include: Natural and forced boundary layer transition; Boundary layer turbulence; Separation caused by shock-boundary layer interaction; Shock-shock interaction heating; Inlet isolator shock trains; Cold-wall heat transfer; Fuel injection, penetration and mixing; Finite rate chemical kinetics; Turbulence-chemistry interaction; Boundary layer relaminarization; Recombination chemistry; and Catalytic wall effects. Each of these phenomena must be understood and either modeled or avoided, to successfully develop a scramjet engine. Models for these phenomena are usually developed from test data gathered in “unit” experiments which isolated and focus on the phenomena.

Integration of the high speed scramjet with the low speed engine – such as a turbo-ramjet – requires blending/sharing structure, systems and flowpaths where ever possible. Interestingly, many studies have shown the major design consideration is thrust per unit volume, not per unit engine weight for TBCC engines. Another challenge is flight acceptance testing of these propulsion systems.

3.2 Design methods

Systems studies are required to identify potential vehicle configurations, and focused technology development. For an airbreathing vehicle, systems studies are complicated by the highly integrated and coupled nature of the airframe and engine [14]. Integration aspects previously discussed confirm the need to develop the engine in concert with a specific class of vision or reference vehicle. “Coupled” means that performance of each successive component is dependent on performance of the previous components. For example, the nozzle component efficiency can not be independently determined; it is dependent on flight Mach number and vehicle attitude, as well as inlet, isolator, and combustor design, operability and performance. Therefore, the vehicle and engine are designed together, using sophisticated analysis methods. A typical design process is illustrated in Figure 6. This process requires a vehicle characterized to the point that meaningful analysis can be performed. Engine and aerodynamic performance, structure, weight, systems and packaging, and thermal management are iterated as the vehicle is “flow” to determine the volume

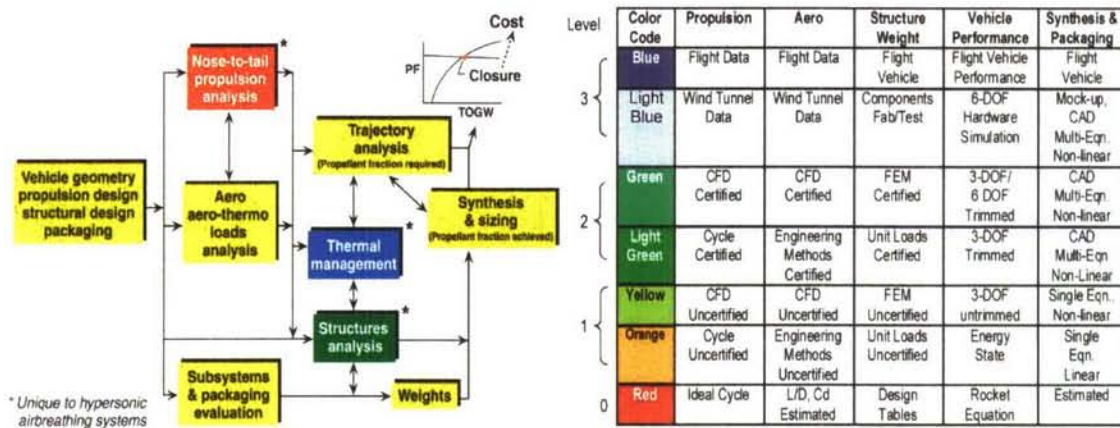


Figure 6. – Hypersonic Vehicle Design System Table 2. – Design Methods and Vehicle Level of Fidelity Assessment.

of propellant “required”. Finally, the vehicle is resized to package the propellant required to meet the mission, thus defining a “closed” configuration.

Systems analysis methods for airbreathing vehicles have evolved dramatically, yet a wide range in usage remains. These methods can be executed at several levels [14], as noted in Table 2. This discussion will focus only on propulsion tools. The lowest level scramjet design tool is ideal or approximate cycle analysis. The next level is cycle analysis using plug in efficiencies which are externally estimated or determined for a particular configuration as a function of flight Mach number only. The next level is CFD – which has its own sublevels. If the CFD analysis is validated by comparison with representative unit and engine component test data, it represents a step up in fidelity. The highest fidelity is obtained by engine tests in a wind tunnel, or preferably in flight. The wind tunnel tests are a lower fidelity than flight because the results must be scaled by analysis to flight conditions. Uncertainty in predicted performance and operability decreases with higher level analysis methods. At the lowest 0th level performance could easily be off by 50-100% or more, and the engine not operable. At the highest level, performance within 1-2% is anticipated. This table is presented as a guide to help assess the large disparity in analytical results and projected vehicle capabilities. A good design process requires synergistic utilization of experimental, analytical and computational analysis. Configurations discussed in section 2 were developed using level 2 methods, and uncertainty on the order of 10% is expected. In fact, the

payload fraction for the Mach 15 first stage vehicle in Table 1 is approximately 50% of the payload fraction estimated in the original 0th level 1965 study [3] discussed in section 1.2.

3.3 Design Optimization.

Due to the relatively small excess thrust generated by a scramjet, some method is needed to refine designs to improved performance and to define operability limits. Scramjets are particularly benefited by a formal optimization process because of significant propulsion-airframe interdependence, large number of independent variables, large potential range of variables, significant interactions, non-linearity and the current low level of design optimization. In addition, it has been clearly demonstrated that component optimization does not provide the best engine or vehicle. Figure of merit (FOM) in this optimization can be engine thrust, but vehicle level FOMs are better, such as minimum vehicle size/weight for mission, cost, safety, or other system level factors.

Several optimization approaches were considered for hypersonic systems. Design-of-experiments (DOE) [15, 16] was selected by the USA hypersonic community because it can be used with existing analysis and experimental methods. By using DOE, a large number of independent variables can be investigated efficiently. DOE uses statistical methods to build polynomial approximate models for the response (component or system performance) to multiple independent design variables. Because of the analytical nature of these models, multiple regression analysis can be used to evaluate these models. The performance model can either be optimized or quantified to determine most significant design variables.

Design-of-experiments (DOE) studies within the Hyper-X community utilized the central composite design (CCD) approach [16] to define an experimental test or analysis matrix. The CCD technique is a part of response surface methodology [17] by which the relationship between the response (dependent variable) and a set of independent variables can be established. Responses are generated for all points in the test or analysis matrix. For Hyper-X, this was accomplished either by CFD, analytical, experimental, or complete system analysis. Response surfaces are then generated for the individual responses.

For a complicated system such as a scramjet or hypersonic vehicle, non-linearity and strong two-parameter interactions are expected. Thus, at least three levels for each of the design parameters are required in order to capture nonlinear effects. Therefore, a second-order model as shown in eqn. (1) is essential: x_i terms are the independent design parameters that affect the response variable y , and the b terms are regression coefficients.

$$y = b_0 + \underbrace{\sum_{i=1}^k b_i x_i}_{\text{linear}} + \sum_{i=1}^n b_{ii} x_i^2 + \underbrace{\sum_{i=1}^k \sum_{\substack{j=1 \\ j \neq i}}^n b_{ij} x_i x_j^2}_{\text{two-parameter interaction}} \quad (1)$$

The number of analyses or experiments for the CCD method compared to those for a full factorial design is illustrated in Table 2 of reference [18]. Many studies focus on 8 variables, which represent 6587 points in a full factorial design, but only require 81 points in a CCD.

An example application for design of flush wall fuel injectors [18], included the following independent variables: θ , Injection angle (90 degrees is normal to the wall); $P_{t,j}$, Injector total

pressure; ϕ , Fuel equivalence ratio; FS, Fuel splits (film fraction of total injectant); HS, Injector spacing to gap ratio (h/Gap – where Gap is the smallest dimension of the combustor cross section at injector plane); M, Flight Mach number; and Xc, Combustor length (Normalized by Gap). The CCD matrix was solved using 3-D CFD in the combustor and nozzle, and 2-D for the forebody and inlet. Responses extracted from the solutions and modelled included mixing and combustion efficiency, total pressure recovery and entropy, combustor wall heat transfer (peak and total), combustor shear drag, one-dimensional variation of pressure, temperature, Mach number and flow distortion [9] through the combustor, nozzle thrust coefficient, and combustor thrust potential [2]. An example of the response models - the fuel mixing efficiency is:

$$\begin{aligned} \eta_{\text{mix}} = & 0.0364 + 0.5668*(FS) + 0.249*(HS) + 0.2223*(\Phi) + 0.0002026*(\theta) - 0.2973*M + 0.000011925*P_{T,J} \\ & + 0.0002031*(\theta)*M - 0.3492*(FS)*(\Phi - 0.2133*(FS)*(HS) - 0.003980*(FS)*(\theta) - 0.0857*(HS)*(\Phi) + 1.696*Xc \\ & - 0.1103*(Xc^3) - 0.00588*(FS)*Xc^2 - 0.3104*(FS)*Xc - 0.4134*(HS)*EXP(-24*EXP(-2*Xc)) \\ & + 0.0376*(\Phi)*EXP(-20*EXP(-2*Xc)) + 0.063*M*((Xc-2)^2) - 0.00035*(\theta)*Xc^2 + 0.00004*P_{T,J}*(Xc-0.5)^{0.6} \quad (2) \end{aligned}$$

This study was performed without a complete vehicle design team, so it used combustor thrust potential to define the optimum flush wall injector design. Thrust potential is the best estimate of engine thrust resulting from changes in fuel injector design. Figure 7 illustrates the best engine

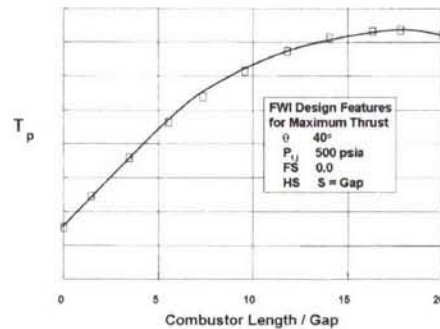


Figure 7. Typical Result from DOE Study: Combustor Thrust Potential

thrust potential from this study at Mach 10 with $\phi = 1.0$. Characteristics of the “best” fuel injector are presented in figure 7. Note that thrust potential peaks at a combustor length of 18 gaps, then decreases if the combustor is extended. This is a result of slow fuel mixing/combustion adding less energy than that removed by friction, heat transfer and nozzle energy lost to combustor dissociation. The corresponding fuel mixing efficiency for this “optimum thrust” design is about 80% at a combustor length of 18 gaps. A combustor length of about 35 Gaps is required to achieve 95% mixing with this injector, and the thrust loss incurred by extending the combustor is large. This example illustrates the necessity of designing each component to benefit the system, not just the component efficiency itself. Comparison with high quality non-reacting data has shown that the CFD prediction of fuel mixing for this study is accurate to within 5% [19]. (This is an example of design tools, not a recommended design solution).

3.4 Experimental facilities, measurements and test methodology

Scramjet engine and hypersonic vehicle development requires an integral design and systems engineering approach. Experimental testing is utilized for developing an understanding of physics, developing models, and validating design concepts and design tools. The enthalpy and pressure requirements for hypersonic combustion simulation are summarized in [9]. The sensible total enthalpy of flight increases from 6 to 12 MJ/kg as flight Mach increases from Mach 10 to 15. The forebody flow field and inlet compression process reduce the local Mach number and raise the flow

static pressure along a nearly constant total enthalpy path. The combustor entrance Mach number, stagnation temperature, and stagnation pressure for Mach 10 flight simulation are 3, 3800 K, and 100 atm, and for Mach 15 are 5, 7000 K and 2000 atm, respectively. As pointed out above, combustion heat release produces about the same energy increment as the air kinetic energy at Mach 8. Thus, simulation of supersonic combustion flow conditions for propulsion studies in ground test facilities often utilizes so-called direct-combustion heating with oxygen replenishment as a means of generating the test environment. Other sources of energy such as storage heaters, electric arc heaters, or shock compression can also provide the required energy and pressure levels for some tests. Combustion heated facilities and combustion heated storage facilities are capable of generating enthalpy and pressure requirements for simulation to about Mach 8. Arc heated facilities are capable of extremely high enthalpy, but are limited to 50 atmospheres pressure, about Mach 8 requirements. Shock heated wind tunnels are required for higher flight Mach simulation. Reflected shock tunnels, with stagnated test gas expanded in converging-diverging nozzle, are capable of a few millisecond test time, at up to about Mach 10 flight simulation; expansion tunnels are capable of flight simulation to over Mach 15 with less than one millisecond test duration.

Four types of scramjet testing are generally performed: Unit problems – to understand the hypersonic flow field physics; Component tests – to verify inlet, isolator, combustor or nozzle component performance and operability before testing the complete engine; Integrated flowpath (inlet, combustor nozzle including or not including vehicle effects); And engine tests – to verify the thermal management heat exchanger durability, engine structure, and systems.

Some unit experiment simulations require full enthalpy. Boundary layer transition, shock impingement heating, and fuel mixing simulation requirements do not necessitate full enthalpy. However, combustion and recombination finite rate chemistry unit studies require full enthalpy. Component testing of inlets, isolators and nozzles to some extent, allow partial simulation of enthalpy at full Mach and Reynolds number. Simulation of the combustor, or the nozzle recombination chemistry, or component integration requires full flight enthalpy. Four methods of scramjet engine and/or flowpath testing are typically utilized: direct-connect, semi direct connect, semi free jet, and free jet tests.

Direct-connect tests are utilized for combustor or combustor nozzle integration studies and combustor nozzle thermal/structural validation. The scramjet combustor (or inlet isolator) is connected directly to the test gas heater by a supersonic facility nozzle, to provide the correct Mach, total pressure and enthalpy of the air flow. This approach allows the highest flight Mach number simulation for any pressure-limited heater, by bypassing inlet losses. Semi-direct-connect experiments are similar – although the combustor does not capture all of the heated airflow. This approach is useful to bypass hardware development. These two approaches are useful for combustor development, but do not provide the inflow required to refine the combustor design, or assess inlet interaction (issue only at lower Mach, $M < 8$). Integrated flow path or engine testing is generally performed using the semi-free-jet approach. The engine module (internal flowpath) is fully replicated, but the external inlet and nozzle parts of the vehicle are only partially or not at all included, allowing a larger scale test. This approach has been used extensively in the USA, and is discussed in numerous papers [20-22]. Free-jet testing includes the entire length of the engine flowpath, generally from the vehicle nose to tail. This type of test can only be performed at small scale or for small engines. The NASA Hypersonic Research Engine, the Central Institute of Aviation Motors (CIAM) scramjet [23] and the X-43 full vehicle were all tested in this fashion.

Measurements in high enthalpy and pressure supersonic or hypersonic flow are difficult. Therefore measurements are generally limited to pre combustion flow surveys, forces and moment, wall pressure and temperature, and non-intrusive optical approaches. Much of the information of interest

must be deduced from measurements which are sensitive to competing unknowns. Wall pressure, the easiest measurement, is dependent on combustion, shear, heat transfer, fuel injection, mixing and shock entropy losses. Some of these effects can be measured, others modeled, but the net effect is increased uncertainty on combustion efficiency deduced from wall pressure measurements. Never the less, this deduced combustion efficiency has proven adequate at lower Mach numbers, in continuous flow facilities. At higher speeds this deduced combustion efficiency becomes large, as the impact of combustion on pressure rise becomes smaller. An in-depth study of measurement requirements was performed by Bittner [24, 9]. This study showed that for flight Mach 10-15 scramjet designs, fuel mixing and combustion efficiency are the most important combustor performance parameters (i.e., engine thrust is about proportional to combustion efficiency). Considering the measurement uncertainty and sensitivity of indirect measurements for deducing mixing and combustion efficiency, Bittner concluded that these performance parameters must be directly measured. The best experimental measurement for determining combustion efficiency is combustor exit water mass fraction (determined by line-of-sight laser absorption), and for mixing efficiency, is fuel mass fraction distribution. Bittner demonstrated, by evaluation of typical CFD solutions, that 3 or 4 - 0.50 mm diameter laser absorption paths for a combustor with 3 cm gap are adequate to resolve the combustion efficiency at any cross section to +/- 5 percent uncertainty. To isolate finite rate chemistry from fuel mixing completeness, a measure of fuel mixing is also important. Bittner's recommendation was to use the process Rogers [25] defined as fuel plume imaging, by tracing the injected fluid with very small (0.2 microns in diameter) particles. Illumination of a cross plane in the flow with laser light can then produce a Mie scattering image of the particles which can be recorded with a fast electronic camera and thus visualize the fuel distribution in the experiment. The local amount of reflected light in each image, normalized by the average reflected light in each plane, becomes a measure of the local fuel concentration relative to the average concentration in the overall bulk flow. Thus, this technique allows a quantitative measure of the fuel distribution to be determined with successive pictures at successive planes downstream from the injection location in the duct. This method has been shown consistent with CFD to less than $\pm 10\%$ uncertainty.

3.5 Flight Testing

Flight testing remains an important element in hypersonic propulsion and vehicle development. Flight not only provides the real environment, it also requires a different look at priorities. In wind tunnels, fuel equivalence ratio is important and thrust produced is secondary – in flight thrust is the priority, and how you get it is secondary. In the wind tunnel testing, engine pitching moment and lift are interesting concepts, and occasionally measured. In flight pitching moment is critical to vehicle survival. In the wind tunnel, inlet starting is an exercise about the ideal design condition – in flight it is a multidimensional challenge involving not only the current flight condition, but the flight history. Flight is expensive, and the benefits are not fully known. Flight testing immature concepts is expensive, high risk, and gives flight testing a bad reputation. But flight testing previously developed and wind-tunnel tested concepts is essential to completing the technology development.

3.6 Technology Development Tracking.

Significant advancements in hypersonic technology were made over the past 50 years. These technologies address hypersonic airframe, engine and systems development. The state of technology, expressed by Technology Readiness Level (TRL), was documented by the National Aerospace Plane Program [26] (NASP), NASA Langley Research Center [27] (LaRC), NASA Space Launch Initiative's Next Generation Launch Vehicle Technology program [28], the 2004 National Research Council (NRC) review [29] of The National Aerospace Initiative (NAI) Hypersonics Pillar, and Boeing [30]. A typical vehicle-based work breakdown structure (WBS) used to guide TRL tracking [28] of hypersonic launch vehicle technology development progress is

presented in Appendix A of reference [31]. A work breakdown structure (WBS) is required to define the system elements or needed products to assure that the reported TRL is relevant. Tracking technology development is important to help focus development. It is also important for the end user to assure technology is truly ready for application to his needs. NASA research was established to elevate the TRL to "6", i.e. test of integrated system in a relevant environment – at which point it may be considered for system development [32].

Technology status for the Mach 7 first stage of a two stage-to-orbit launch system and estimates to complete the technology will be discussed in the final section of this paper.

4.0 HISTORICAL PERSPECTIVE

Early history of scramjet development is documented by Curran [33] and Anderson [9]. A well known Air Force view of what followed the early feasibility studies is of cyclic "fits and starts" [34]. This resulted from over zealous efforts to simultaneously develop and apply hypersonic technology to programs which were on a classical 5-year development cycle. NASA perspective is of an incremental development process, which benefited from the "fits and starts" to fund major advancements.

NASA has, for nearly 50 years, funded hypersonic airbreathing vehicle technology development, aiming at futuristic space launch capabilities. NASA's activities can be divided into five generations of technology development. The first was associated with the DOD Dyna Soar/Aerospace Plane and NASA's focus on developing hypersonic vehicle technology. This phase included hypersonic airframe and engine, aerothermodynamics, structures and propulsion performance. The propulsion focus was proof of scramjet cycle efficiency, flight weight engine structure, and engine system integration. Starting in the mid 60's, NASA built and tested a hydrogen fueled and cooled scramjet engine [11] which verified scramjet cycle efficiency, structural integrity, first generation design tools and engine system integration. The axisymmetric engine selected allowed a low risk approach to validate the scramjet cycle and elementary design tools of the day.

NASA's second generation hypersonic technology starting in the early 1970's focused on scramjet-airframe integration [10]. NASA designed and demonstrated, in wind tunnels, a fixed-geometry airframe-integrated scramjet "flowpath" and companion vehicle capable of accelerating to Mach 7. In the process, wind tunnels, test techniques, leading-edge cooling, and analytical methods were all advanced, and 3-D CFD was first applied to the scramjet reacting flow.

Starting in the early 80's, NASA teamed with the DOD in the National AeroSpace Plane (NASP) Program to advance and demonstrate hypersonic technologies required for a scramjet based combined cycle powered, single-stage to orbit (SSTO) launch vehicle. Under the NASP program NASA focused on technology development and risk reduction, including: system analysis, aerodynamics, flight controls, high temperature structures, aerothermodynamics, hypersonic physics, scramjet engine detailed analysis and testing, hydrogen cooled engine structure, and hypersonic flight testing.

Following NASP, NASA's fourth generation hypersonic technology development focused on flight validation of hypersonic technology and evaluation of alternate concepts (rather than SSTO) for the next generation of space access. Flight tests included a scramjet [23] designed and flown by the Central Institute of Aviation Motors (CIAM), a low-speed takeoff and landing version of the X-43 [35], and finally the X-43 at Mach 7 and 10. Highlights of the X-43 flight program are presented in the next section. All of these tests demonstrated the need for flight testing to re-focus technology development. They also prove that flight testing does not have to be expensive. Evaluation of

alternate, near term space access configurations was instrumental in developing advanced system analysis methods, particularly assessment of system level benefits, and system engineering tracking of technology development status and requirements.

Fifth generation hypersonic technology development within NASA started in 2005. President Bush's unfunded redirection of NASA to manned space exploration resulted in significant programmatic changes within NASA aeronautics and sciences. NASA management was required to maintain NASA's unique hypersonic capability (manpower and some facilities), and did this by refocusing on low-cost in-house low-TRL research studies [32, 36], avoiding even low-cost high payoff higher TRL efforts such as developing a durable metallic scramjet combustor as mentioned in section 6.0. Fortunately, DOD is continuing hypersonic technology advancements within some of the National Aerospace Initiative (NAI) [6] programs, and some NASA's expertise is being applied to support these DOD programs, particularly the USAF X-51 missile research demonstrator [37].

5.0 X-43 FLIGHT HIGHLIGHTS

5.1 Hyper-X Program Development

NASA developed the concept for the Hyper-X Program and X-43 vehicle in 1995/96 in response to several "blue-ribbon" panel recommendations that flight demonstration of airframe-integrated scramjet propulsion be the next step in hypersonic research. The experts agreed that at a minimum and as a first step a vehicle must fly with scramjet power to validate airframe-integrated scramjet performance and design methods. A two-phase flight and ground based research program was approved by the NASA administrator in 1996: focus of the first phase was the X-43; focus of the second phase was to be development and flight test of the "low speed" turbojet engine integrated with the scramjet forming a complete hypersonic propulsion system. This section discusses accomplishments of the Phase 1 program. The next section presents results from the planning for the Phase 2 program.

The NASA Hyper-X Program employed a low cost approach to design, build, and flight test three small, airframe integrated scramjet-powered research vehicles at Mach 7 and 10. The Hyper-X team developed the X-43 phase 1 vehicle [38] as a small-scale, hydrogen-fueled research vehicle to provide flight data for an airframe-integrated scramjet engine flowpath. (The engines were heat sink cooled to meet program budget and schedule. Regenerative cooling was not needed due to the short test times afforded with a small vehicle.) In addition, data were obtained for aerodynamic, thermal, structure, guidance, flush-air-data-system and integrated system analysis design method validation. Test plans called for boosting each of three X-43 research vehicles to the required test condition by a drop-away booster. The research vehicles were dropped from the NASA B-52, rocket-boosted to test point by a modified Pegasus first stage, separated from the booster, and then operated in autonomous flight. Tests were conducted at approximately 30 kilometre altitude at a nominal dynamic pressure of 0.47 atm (1000 psf). The resulting vehicle was 3.7 km long and weighed about 1270 kg. Development of the X-43 and its systems are well documented [23, 38-49]. The first Mach 7 flight was attempted June 2, 2001. This flight failed when the Pegasus booster went out of control early in the flight. The second and third flights were successfully conducted March 27 and November 16, 2004. This section provides an overview of results (with engine focus) from the second and third flight of the X-43. Details of the launch vehicle development, verification, validation and integration, flight operations [50-54] and other results are well documented.

5.2 Flight Test Trajectory

For the second (Mach 7) flight (F2) the launch vehicle was dropped from the B-52 flying at Mach 0.8 and 12.2 km altitude. The booster ignited after a 5-second free fall. The launch vehicle executed

a 1.9g pull-up, followed by a 0.7g pushover to achieve nearly level flight at 30 km. altitude. Following burnout, stage separation, and X-43 vehicle stabilization, the engine cowl was opened for about 30 seconds: 5 seconds of fuel-off tare, 10 seconds of powered flight (at about Mach 6.83 and dynamic pressure of 463 atm), another 5-seconds of un-powered steady tare, followed by 10 seconds of Parameter IDentification (PID) maneuvers [55]. The PID maneuver was designed to quantify the aerodynamic stability and control parameters for the vehicle, including drag, to allow more accurate estimation of the engine thrust. After the open-cowl PID maneuver, the engine cowl closed, and the vehicle flew a controlled descent over 560 km to “splash-down” in the Pacific Ocean. PID maneuvers were flown at various Mach numbers as the vehicle slowed and descended.

The third flight (F3) trajectory was somewhat different. The B-52 flight conditions were the same. However, the launch vehicle executed a 2.5g pull-up to a flight path angle of over 30 degrees, followed by a 0.5g push over to achieve nearly level flight at 33.5 km altitude. Following burnout, stage separation, and stabilization of the X-43 vehicle, the engine cowl was opened for about 20 seconds: 3 seconds of fuel-off tare, 11 seconds of powered flight (at about Mach 9.68 and dynamic pressure of 0.439 atm.), and another 6-seconds of un-powered steady tare. (No cowl open parameter identification maneuvers were performed due to cowl survival concerns that necessitated closing the cowl immediately following the cowl open tare.) The engine cowl closed, and the vehicle flew a controlled descent over 1600 km to a “splash-down” in the Pacific Ocean. During the descent PID maneuvers were successfully performed [56] at successive Mach number as the vehicle slowed down.

5.3 Instrumentation, Measurements and Data

The X-43 vehicles were well instrumented. Instrumentation included over 200 measurements of surface pressure, over 100 thermocouples to measure surface, structural and environmental temperatures, and discrete local strain measurements on the hot wing and tail structures. The flight management unit included accurate 3-axis measurements of translational acceleration and angular velocity, along with Global Positioning System and control surface deflection measurements. Instrumentation density is illustrated in figure 8 by external and internal wall pressure and temperature on the lower body surface. Internal engine instrumentation, within the cowl on the body side is denser to capture internal flow details (shock waves) within the engine.

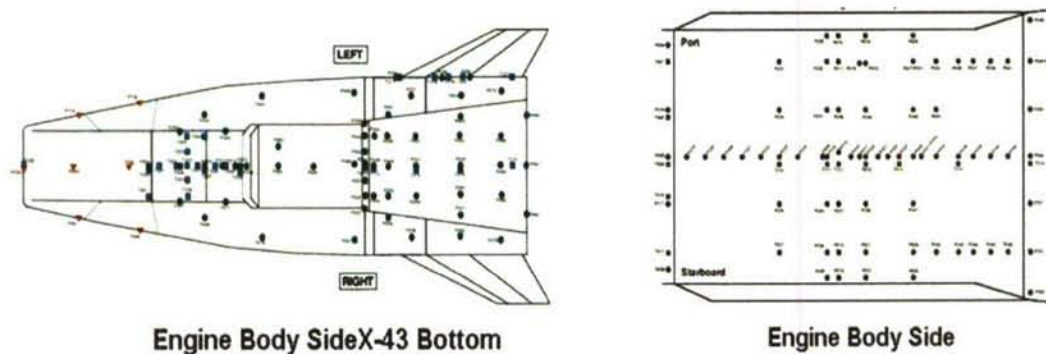


Figure 8. X-43 Instrumentation and Measurements (Circle – pressure; Square – Temperature)

All of the data from the X-43 flights were successfully telemetered and captured by multiple air and ground stations. The instrumentation health and performance were excellent: very few lost

instruments/parameters; very low noise content; no significant calibration issues; no significant delay or time lag issues; and extremely limited telemetry stream drop outs. Accuracy of these measurements benefited from day-of-flight atmospheric measurements by weather balloons. These measurements were used in flight trajectory reconstruction [57], and resulted in a small change in calculated Mach number and dynamic pressure vis-à-vis real time values determined from atmospheric tables and winds from historical atmospheric tables. Flight 2 best estimated trajectories (BET) resulted in higher dynamic pressure and Mach, but only a trivial change in AOA. Flight 3 BET resulted in lower dynamic pressure and higher Mach and AOA. The flight test data from both flights F2 and F3 fully satisfied the Hyper-X Program objective to validate experimental, analytical and computational design methods, plus demonstration of positive acceleration under scramjet power.

5.4 Stage Separation

Following the rocket motor burnout, the launch vehicle targeted flight conditions for stage separation: 0° angle of attack (AOA-alpha) and yaw (Beta); zero pitch, yaw and roll rates; and dynamic pressure of 0.47 atm. The indicated Mach was slightly low for flight 2. Post test analysis indicates that off-nominal rocket motor propellant temperature was the major factor affecting burnout and hence the reduced Mach number at F2 stage separation. The research vehicle separation from the booster was executed cleanly [57]. The X-43 attitude was within less than 1-sigma uncertainty from the predicted nominal by pre-flight Monte Carlo analysis.

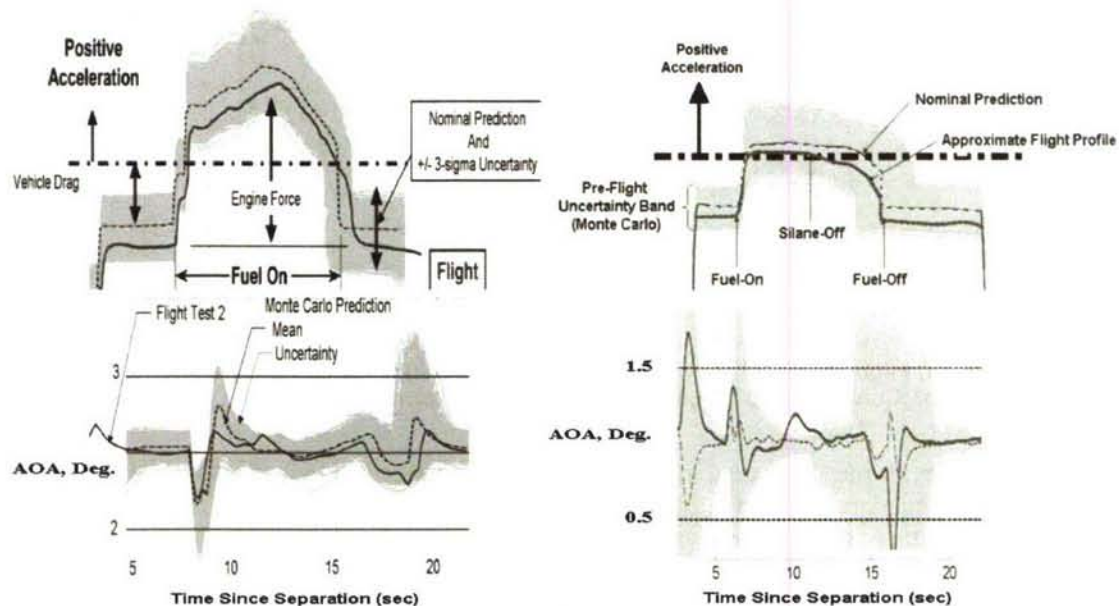
5.5 Scramjet Powered Flight Control

For flight 2, the X-43 was commanded to fly at 2.5° angle of attack during the cowl-open portion of the flight. However, as the fuel was turned-on/off, and throttle adjusted, the engine pitching moment changed significantly. Figure 9a illustrates the measured angle of attack—from cowl open to fuel off and the start of the Mach 7 PIDs. During the scramjet-powered segment, the AOA was maintained at $2.5^\circ \pm 0.2^\circ$, except during flameout, which occurred as the fuel was shut off. (The flight control system included some feed-forward control). For flight 3, the vehicle was commanded to fly 1.0° angle of attack during the cowl open segment. The vehicle control was about the same, as illustrated in figure 9b. For both F2 and F3 the fuel sequencing for powered flight started with a silane/hydrogen mixture to assure ignition, then transition to pure hydrogen fuel. The ignition sequence for F2 required about 1.5 seconds. With transition to pure hydrogen fuel, the engine control was designed to ramp the throttle up (increase fuel mass flow) to either a predetermined or controlled maximum value (limited by inlet unstart monitor), and then decreased as the fuel was depleted. The resulting vehicle performance is characterized by vehicle acceleration, as shown in figure 9. The ignition sequence for F3 was different—the silane remained on for the first two fueled conditions, requiring 5 seconds of silane pilot. Then the same fuel equivalence ratio conditions were tested with only hydrogen. This cautious approach was taken because it was not possible to transition from piloted to unpiloted operation in the short test time available in shock tunnels, and some unpiloted wind tunnel data had poor combustion.

5.6 Scramjet Engine Performance

Gray bands in figure 9 illustrate pre-test Monte Carlo predictions of acceleration and angle of attack about the nominal prediction (dashed line). The heavy solid line depicts flight data trends. The vehicle deceleration is greater than predicted [58], both with cowl closed and open. This is because of two factors: actual flight conditions (2/3 of the difference); and vehicle drag was higher than predicted (1/3 of the difference). However, the drag was within the uncertainty associated with the aerodynamic database. The uncertainty was not resolved before flight because it did not threaten the

outcome of the engine tests. Under scramjet power the F2 vehicle acceleration was positive, and varied with throttle position. The increment in acceleration is about as predicted, which confirms

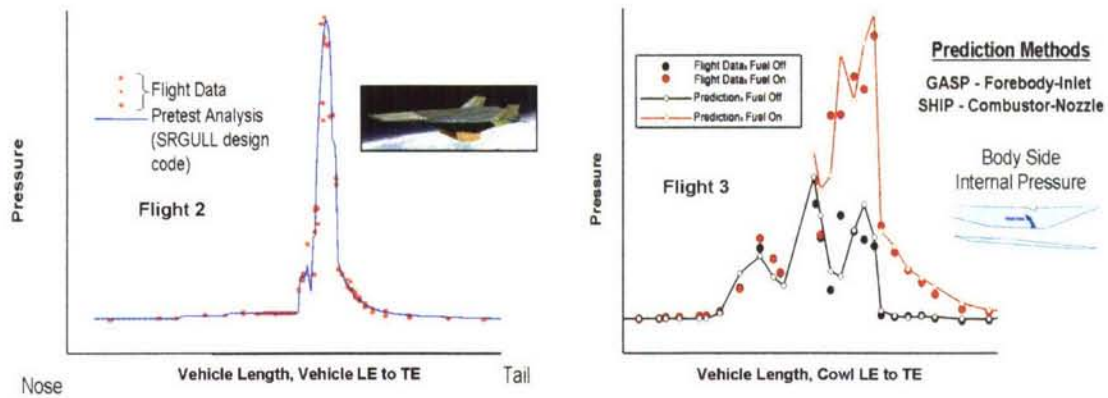


A) Flight 2 at Mach 7
b) Flight 3 at Mach 9.7
Figure 9. X-43 vehicle acceleration and angle of attack (AOA)

the predicted engine thrust to within less than 2% (ref. 5 and 6). It should be noted that the engine throttle was varied over a large range without incurring engine “un-start” or “blow-out.” Under scramjet power the F3 vehicle cruised (thrust = drag) at the reference fuel equivalence ratio with 2% silane pilot, and the engine force was in agreement with predictions [58].

5.7 Validation of Scramjet Design Analysis

Predicted scramjet performance is also confirmed by the excellent comparison of pre-test predicted and flight scramjet flowpath wall pressure (fig. 10). Data are presented from vehicle nose to tail for F2 (fig. 10(a)), and from cowl leading edge to cowl trailing edge for F3 (fig. 10(b)). Mach 7 data showed the scramjet operating in “dual mode,” with sonic flow in the isolator dissipating the inlet shocks at the design throttle position. Mach 10 data exhibits classical pure supersonic combustion mode, i.e. the combustor pressure is shock dominated. The pre-test prediction for Mach 7 was made using the coupled CFD-cycle code SRGULL [59-61], with combustion efficiency determined by analysis of multiple wind tunnel tests, most notably the 2.5 meter diameter test section of the *8-Foot High Temperature Tunnel* (HTT) test [46] of the Hyper-X Flight Engine (HXFE) on the Full Vehicle Simulator (FVS). The Mach 10 pretest prediction was performed using a combination of CFD tools, with the SHIP code [62] used for the combustor. The SHIP code is space marching with uncoupled reaction modelling – both to reduce solution times and allow very fine grid resolution for the complex shock structure. The reaction efficiency used in the SHIP code was derived from analysis of engine tests conducted in the HYPULSE and LENS reflected shock tunnels. Storch [59, 63] and Ferlemann [64] present a detailed discussion of these codes and the pretest predictions for F2 and F3 respectively



a) Flight 2 at Mach 7

b) Flight 3 at Mach 9.7

Figure 10. Comparison of engine body side wall pressure with pre-flight predictions

Post test analyses of the flight data model the “as flown” trajectory to assess thermal loads, inlet mass capture, boundary layer state for boundary layer transition assessment, and to assess the overall vehicle drag, engine force, and vehicle acceleration at exact flight conditions/control positions. Complete nose-to-tail CFD solutions for the actual F2 flight condition include solutions for closed cowl, cowl open, and powered operation, (fig. 11). These solutions show excellent agreement with flight acceleration data.

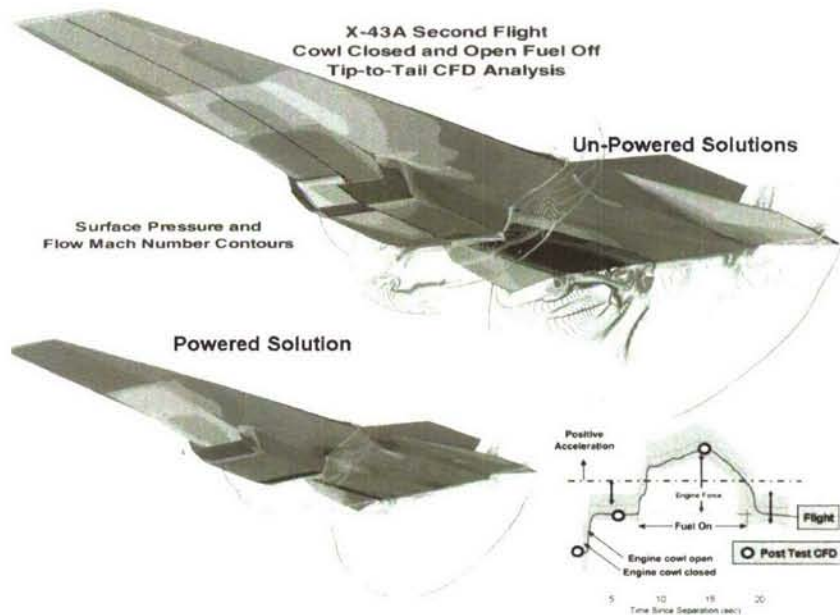


Figure 11. Post Test CFD Analysis

5.8 Validation of Scramjet Experimental Methods

Flight 2 (F2) data compare favorably with measurements made in four separate wind tunnel tests [63] and F3 flight data compare favourably with results from both the HyPulse and LENS shock tunnel tests [64]. Tests with nearly identical values of fuel equivalence ratio were selected for

comparison. Wind tunnel wall pressure measurements were scaled by air mass capture ratio to flight conditions. Flight air mass capture is calculated by 3-D CFD analysis of the forebody. Figure 12 illustrates the resulting comparison of internal wall pressure for the 8-Foot High Temperature Tunnel test of the Hyper-X Flight Engine (HXFE) on the Full Flight Vehicle Simulator (FFS). Similar agreement was noted between flight data and data produced using semi-free jet engine module tests in shock heated, combustion heated and electric arc heated wind tunnels. Storch [59] discusses the implication of this agreement, and the impact on observed combustor performance.

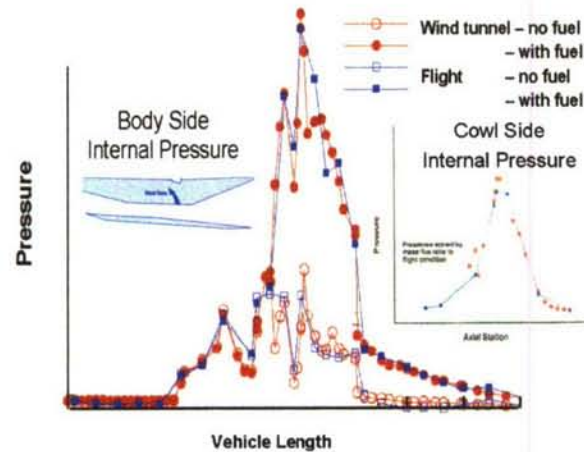


Figure 12. Comparison of flight and Wind Tunnel Data.

Rogers [65] reported a similar trend for the Mach 10, flight 3 data. Results show that ground tests are representative of flight when careful attention is paid to modeling the important flow phenomena. The most significant issues identified for shock tunnel testing are cold wall temperature limitation and attention to correct shock position entering the combustor for the shock-dominated “pure” scramjet operation. This means that the vehicle/engine geometry may have to be changed for tests in typically non-uniform shock tunnel flow fields to truly represent important flight features. This was successfully demonstrated by Rogers [65].

5.9 Hypersonic Boundary Layer Transition

Design of the X-43 research vehicle structure and thermal protection system depended greatly on accurate estimation of the aerothermal environment, which required understanding of the boundary layer state during the entire flight. For good engine operation, boundary layer flow entering the inlet cannot be laminar. For the X-43, boundary layer trips were required to insure the inlet boundary layer was turbulent to limit flow separations due to adverse pressure gradients. A substantial research and design effort [45] was executed to ensure proper sizing of boundary layer trips with minimum induced trip drag, excess vorticity and induced heating. The vehicle upper surface, however, was predicted to be laminar during the scramjet test, based on a pre-flight trajectory, using a classical transition methodology (momentum thickness Reynolds number over the boundary layer edge Mach number of $R_{c,\theta}/M_e = 305$). Figure 13 provides upper surface temperature time histories during the first 350 seconds of flight 2 trajectory from the point of release from the B-52. The three upper surface thermocouples were evenly spaced along the vehicle centerline starting about midpoint for T/C#19 and ending near the trailing edge for T/C#21. Note that by the time the cowl opens and the scramjet is ignited, the entire upper surface appears to be laminar, as indicated by the dramatic temperature decrease that begins at about 70 sec. Likewise, at about 240 seconds the

boundary layer transitions from laminar to turbulent as the vehicle slows. The pre-flight predictions, using the classical approach, were accurate (300 ± 12) in estimating these latter transition points along the flight trajectory. However, the transition from turbulent to laminar earlier in the flight

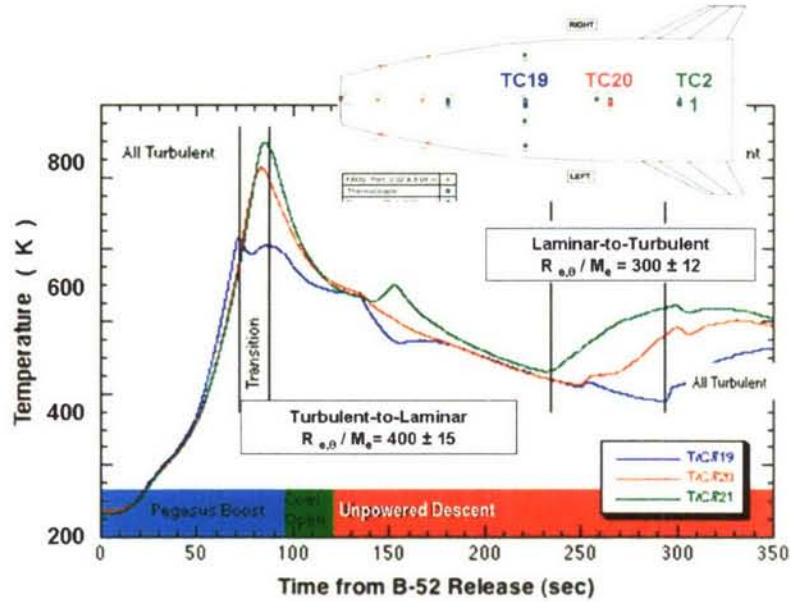


Figure 13 – Natural Boundary Layer Transition

occurred at a local $R_{e,0} / M_e = 400$. Thus the laminar to turbulent and turbulent to laminar transition criteria are not the same, and the X-43 measurements provide flight data that quantify the hysteresis effect [66]. The first transition, from turbulent to laminar, represents the condition for which the transition model was developed - the high heating condition encountered as the hypersonic vehicle accelerates within the high dynamic pressure airbreathing corridor. These results show that the classical boundary layer transition model was not appropriate for application to the boost trajectory. It is hoped that the new, more advanced “physics – based” methods for boundary layer transition can be applied correctly to this problem.

Post test analysis determined the engine efficiency (specific impulse) achieved in the X-43 flights, and “scaled” that value to a vision vehicle performance, by removing effects of small physical (viscous dominated) scale, cold fuel, cold engine wall temperature, off-nominal fuel equivalence ratio, operating dynamic pressure, etc. The scaled specific impulse is within the capability band projected for scramjet engines, as indicated by the square symbols in figure 1. The specific and effective impulse demonstrated by the X-43 has set the bar for follow-on vehicle configurations.

5.10 Validation of Vehicle System Analysis

As discussed herein and in [67], most of the measurements and performance results from the two successful flight tests confirm the design methods, test methodologies, and capabilities of proposed hypersonic air vehicles. Most of the measured performance values were within predicted uncertainties. This included propulsion performance and operability, aerodynamic forces and moments, stability and control, aero thermal heating, structural responses, and the complex mechanics of high Mach, high dynamic pressure, non-symmetric stage separation. Included in this hypersonic environment are many physics challenges, discussed in section 3.1. Most of these phenomena were modeled in the design tools. Others were avoided by application of a large

uncertainty. Success of the X-43 demonstrates an engineering level understanding of the hypersonic physics. A better understanding of the physics might be beneficial for reducing the uncertainty in optimization of vehicle performance—but the current understanding is clearly adequate to continue higher-level technology development and integration. Design and analysis tools demonstrated in the Hyper-X program are clearly adequate for hypersonic vehicle development.

5.11 Technology Achievements

Technology achievements [67] of the X-43 include the first ever test of a scramjet-powered vehicle in a wind tunnel and in flight. The flight also proved the performance, operability and control of an airframe integrated engine – vehicle system. In addition, these results provide information which will allow higher fidelity (i.e. reduced uncertainty) in future system studies. Data and performance from the flight test verified engineering application of the NASA – Industry – University hypersonic vehicle design tools. To support this development, NASA’s HyPulse facility at GASL was modified to be the first facility capable of operation in both reflected and expansion tunnel mode, allowing scramjet testing from Mach 7 to Mach 15 plus in a single wind tunnel.

5.12 Lessons Learned

Lessons learned from the Hyper-X Program’s X-43 flight are infinite and remain a permanent part of the experience base of each participant. From a management perspective several lessons should be noted. First, a lesson handed down over generations – build on the shoulders of Giants, not babies (the “not invented here” approach). This includes selecting the team to execute the program, as well as selecting the configuration and approach to minimize new technology development requirements. Second, plan the program to fit budget and schedule, with a healthy reserve of both. Next, fight requirements creep. Fourth, utilize a small team of ‘hands-on’ experts, and empower them, but maintain good communication (even co-location) with and between them. Finally, beware of outside experts and strap hangers, carefully consider recommendation before including them in program changes.

From a technology perspective the major lesson is that a scramjet powered vehicle performs as advertised. A close second was that going to flight required all disciplines to sharpen their pencils. For example, early NASA predictions for scramjet pitching moment were off by over 25%, and the first prediction of stagnation heating did not include real gas effects. Regarding scramjet technology, flight performance was better than obtained in reflected shock tunnels – probably due to the higher wall temperature in flight. Combustor isolator pressure rise was slightly greater in wind tunnel than in flight. The biggest surprise came from the most mature technology – boundary layer transition. Hysteresis effects had not been considered in the classical boundary layer transition modelling. So, in effect, the boundary layer transition models developed over the past 40 years for the server ascent flight of airbreathing hypersonic vehicles were shown to be only appropriate for re-entry vehicles, not the airbreathing hypersonic vehicle flight corridor. A similar lesson was learned from the CIAM/NASA scramjet flight test [68, 69]. Analysis at the design Mach 6 flight test condition (top and left side of figure 14) predicted excellent inlet flow despite rather strong internal shock waves. Flight data and post test analysis showed that the inlet starting process created a large separation bubble (right side of figure 14) at lower flight Mach number, and the separated flow remained at the design point.

6.0 FUTURE NEEDS AND CHALLENGES

This section addresses the question: “After the successful flight test of the X-43 scramjet-powered vehicle, what is the TRL for a near term hypersonic vehicle, and what needs to be done next?”

Technology status for the Mach 7 first stage vehicle of a TSTO system is summarized in figure 15. Clearly the technology set for a Mach 7 vehicle is less challenging than for the SSTO or higher Mach air-breathing first stage of a two-stage-to-orbit concept. For example, all of the airframe

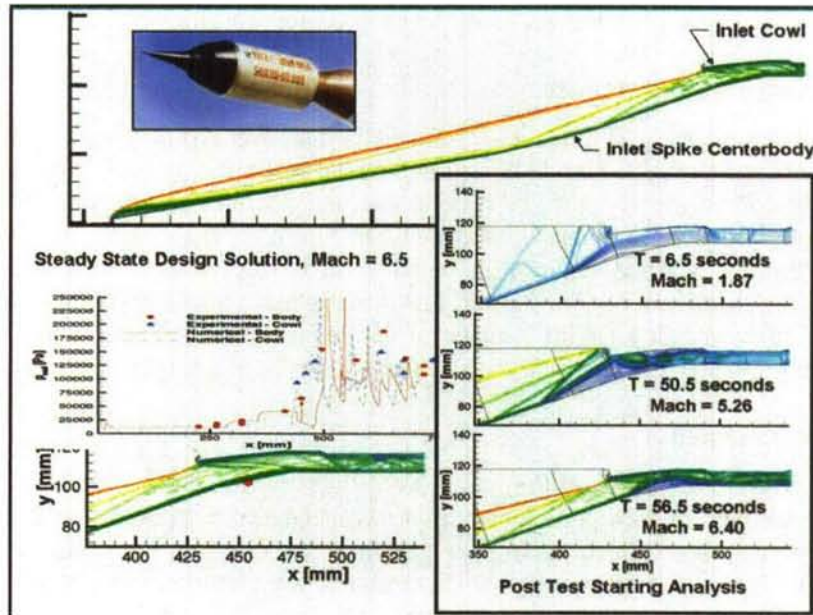


Figure 14. – CIAM Inlet Solutions: Pre and Post Test.

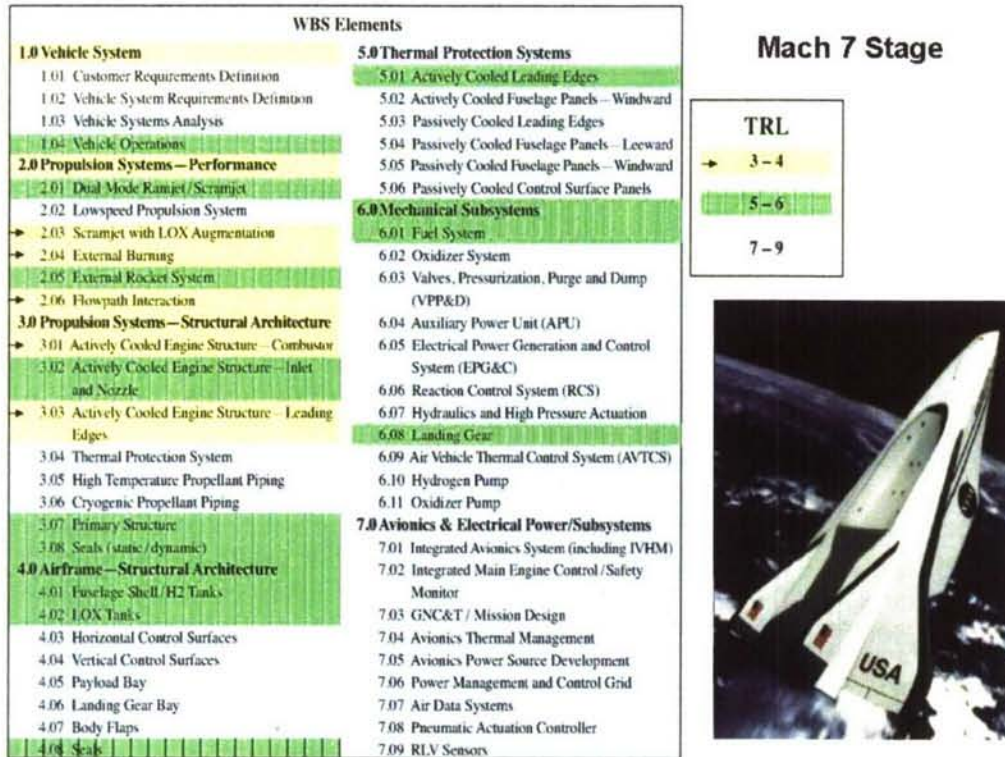


Figure 15. - Technology Status for First Stage of a TSTO Airbreathing Launch System

technologies are at least TRL 5-6 and required propulsion performance is at least TRL 5-6. Programs to complete the technology to TRL 6 were recently estimated by a NASA planning activity for the Hyper-X Phase 2 Program. Details of the airbreathing propulsion technology shortfalls (TRL < 6) for the first stage Mach 0-7 vehicle are discussed in the following sub-sections. Other technology short falls not included herein - High Temperature Materials and Thermal Protection System (TPS); Propellant Tanks; Integrated Vehicle Design and MDO Tools; and Expander Cycle Linear Aero-spike Rocket - are discussed in reference [31, 67].

This propulsion discussion continues to assume that the first application space access vehicle will incorporate the turbine-based combination cycle engine system – i.e. a two-flowpath engine in either an “over-under” arrangement or separately integrated into the airframe. The low-speed engine is assumed to be the NASA/GE Revolutionary Turbine Accelerator (RTA) [70] or equivalent hydrocarbon-fueled turbo-ramjet engine, with uninstalled thrust-to-weight (T/W) of about 10. This engine must dash to Mach 4, with about 2-minute full power operation required above Mach 2.

The high-speed engine is a quasi two dimensional hydrogen-fueled and cooled dual-mode scramjet. Extensive databases exist for flowpath designs for good engine performance and operability, from Mach 4 to 7. Key technical challenges for the dual-mode scramjet are low Mach number ($M < 4$) performance and operability (TRL 4-5); demonstration of durable fixed or variable geometry metallic structure and seals (TRL 5); development and demonstration of robust engine controls for large operating range; optimization of aero-propulsion integration, and development of a 2000 psi expander cycle hydrogen fuel pump. The limited vehicle flight envelope may allow fixed geometry within the ram/scram flowpath, but variable geometry approaches are at reasonable levels (TRL 4-5) if needed. A hydrogen fuel-cooled flight-weight engine must be tested to verify engineering prediction of system durability. These experiments will provide a test bed for instrumentation to support future integrated vehicle health management. This development testing should be possible at small scale in an existing wind tunnel. Based on lessons learned in these systems tests, methods of testing critical flight-weight components at large or full scale using existing facilities must be developed. This will likely be direct-connect tests of the integrated isolator, combustor and nozzle, because the inlet shock structure is not critical to thermal loads and combustor performance at these lower Mach numbers. By limiting the maximum Mach number, this approach may be possible with existing facilities, whereas it will not be possible for Mach 10-15 concepts. By limiting the Mach number to 7, existing ground test facilities may be used to bring durable scramjet engine component technology toward TRL 6. Life cycle can be demonstrated at modest scale in combustion-heated facilities (like the 8ft. HTT), which allow sufficient test time for the structure to reach near equilibrium Mach 7 temperature. Flight mission-length duration tests can be performed at smaller scale. If the flight engine is broken into small enough segments it may be possible to actually do these full-mission simulations in wind tunnel tests.

Two additional propulsion technical challenges must also be addressed. Integration of the turbojet and scramjet into a TBCC engine system (WBS 2.06) is a significant technical challenge (TRL 3-4). Integrated propulsion-airframe design/performance evaluation and thermal management (WBS 1.03) are also at a low TRL. This integration should be verified by tests in wind tunnels—a “relevant environment.” Wind tunnel tests of turbojet engines are acceptable system demonstration for TRL 6. The Mach 7 flight of the X-43 demonstrated that wind tunnels are a relevant environment for scramjet demonstration to TRL 6. Therefore TBCC engine tests in wind tunnels meet the TRL 6 (relevant environment) requirement. However, continual variation of flight Mach number from sea-level-static to Mach 7 can only be performed in flight. Also, flight forces closer attention to details often overlooked by “physics based” analysis and wind tunnel tests. Low cost methods of testing and/or demonstrating these technologies may be possible. The simplest may be

to fly the integrated system on a rocket booster, like the Russian Central Institute of Aviation Motors scramjet flying laboratory. However, a recovery system will be needed due to engine cost.

Integrated TBCC powered hypersonic vehicle TRL level of 6 cannot truly be achieved without a near-full scale flight test vehicle. However, completion of the above technology development provides a strong case to move to a large-scale research or prototype vehicle. Without first completing the above technology development and ground tests, a large scale research or prototype vehicle program may be doable, but it will be high risk.

Flight-testing is a natural evolution of any new aeronautical technology. Flight drives integration of all technologies required to complete a system which are generally developed separately before going to flight. Flight identifies challenges not generally known beforehand (unknown-unknowns). Flight generates customer, political and public interest. When to introduce flight-testing into a technology development program is an issue for thoughtful discussion. If funding is not highly constrained, flight-testing can move technology at a system level forward at a faster rate than possible without flight testing. If funding is constrained (as usual), careful consideration must be given before committing to flight research, or calling a technology development program a flight test program too early in its development. Whatever budget unfolds, flight must be a part of hypersonic air-breathing technology development. The challenges and successes associated with flight-testing will continue to attract bright students into the sciences and engineering. Flight-testing will be required for a few of the technology needs discussed.

7.0 SUMMARY AND CONCLUSIONS

Technology advances within the USA and around the world prove that efficient hypersonic flight is possible. The greatest benefit to mankind will be in space access applications. Development of safe, affordable, reliable, and reusable launch vehicles holds great promise as the key to unlocking the vast potential of space for business exploitation. Only when access to space is assured with a system that provides routine operation with orders-of-magnitude increased safety and at affordable cost will businesses be willing to take the risks and make the investments necessary to realize this great potential. Other applications - to military missions - are inevitable, and may be required to complete the transition from research to the commercial sector, and to convince the remaining sceptics. Exciting challenges remain, both technical and political.

8.0 REFERENCES

- [1] H. Julian Allen, "Hypersonic Flight and the Re-entry Problem," The Twenty-First Wright Brothers Lecture. Journal of the Aerospace Sciences, Vol. 25, No. 4, April 1958.
- [2] Riggins, D.W., McClinton, C.R., and Vitt, P.H., "Thrust Losses in Hypersonic Engines, AIAA Journal of Propulsion and Power," Vol. 13, No. 2, pp. 281-295, 1997.
- [3] Escher, W.J.D, et al., "A Study of Composite Propulsion Systems for Advanced Launch Vehicle Applications". The Marquardt Company Report 25, 194. Final Report, NASA Contract NAS7-337, 7 Volumes, Sept. 1966.
- [4] Daines, R. and Segal, C., "Combined Rocket and Airbreathing Propulsion Systems for Space-Launch Applications," J. of Prop. And Power, vol. 14, no. 5, Sept/Oct 1998.
- [5] Bogar, T.J., Eiswirth, E.A., Couch, L.M., Hunt, J.L., and McClinton, C.R., "Conceptual Design of a Mach 10, Global Reach Reconnaissance Aircraft," AIAA 96-2894, Jul. 1996.
- [6] The Honorable Dr. Ron Sega, "Congressional Report on the National Aerospace Initiative," September 2003. <http://www.dod.mil/ddre/nai>
- [7] Bilardo, V.J., Hunt, J.L., Lovell, N.T., Maggio, G., Wilhite, A.W., and McKinney, L.E., "The Benefits of Hypersonic Airbreathing Launch Systems for Access to Space," AIAA 2003-5265. July 2003, Huntsville, Al.
- [8] Tandy, David, "Architecture C Limited Life Cycle Analysis. SAIC Presentation to NGLT," February 12, 2004.
- [9] Scramjet Propulsion, AIAA Progress in Astronautics and Astronautics, Vol. 189, 2000. Chapter 6, Scramjet Performance Anderson, G.Y., McClinton, C.R., and Weidner, J.P.

- [10] Henry, John R., and Anderson, Griffin Y., "Design Considerations for the Airframe-Integrated Scramjet," Presented at the 1st International Symposium on Airbreathing Engines, Marseille, France, June 1972 (also NASA TM X-2895, 1973).
- [11] Andrews, Earl H., and Mackley, Ernest A., "Review of NASA's Hypersonic Research Engine Project," AIAA Paper 93-2323, June 1993.
- [12] Pinckney, S. Z., "Rectangular Capture Area to Circular Combustor Scramjet Engine," NASA TM 78657, March 1978.
- [13] Jacobs, P.A. and Craddock, C.S. "Simulation and Optimization of Heated, Inviscid Flows in Scramjet Ducts," J. of Propulsion and Power, vol. 15, No. 1, Jan.-Feb. 1999.
- [14] McClinton, C.R., Hunt, J.L., Ricketts, R.H., Reukauf, P., and Peddie, C.L., "Airbreathing Hypersonic Technology Vision Vehicles and Development Dreams," AIAA Paper No. 99-4978, November 1999.
- [15] Hicks, C.R., "Fundamental Concepts in the Design of Experiments", John Wiley and Son, New York, 1982.
- [16] Montgomery, D.C., "Design and Analysis of Experiments", John Wiley and Son, New York, 1991.
- [17] Box, G.E.P. and Draper, N.R., "Empirical Model-Building and Response Surfaces," John Wiley and Son, New York, 1987.
- [18] McClinton, C.R., Ferlemann, S.M., Rock, K.E., Ferlemann, P.G., "The Role of Formal Experiment Design in Hypersonic Flight System Technology Development.," AIAA 2002-0543. Jan. 2002.
- [19] Riggins, D. W., and McClinton, C. R., "A Computational Investigation of Mixing and Reacting Flows in Supersonic Combustors," AIAA 92-0626, Jan. 1992.
- [20] Guy, R.W., et.al., "The NASA Langley Scramjet Test Complex," AIAA 96-3243. 32nd AIAA/ASME/SAE/ASEE Joint Propulsion Conference. Lake Buena Vista, FL, July 1-3, 1996
- [21] Andrews, E.H., "Scramjet Development and Testing in the United State," AIAA 2001-1927. April 24-27, 2001.
- [22] Volland, R.T, et.al., "Hyper-X Engine Design and Ground Test Program," AIAA 98-1532.
- [23] Roudakov, A.S., Y. Schickhman, V. Semenov, Ph. Novelli, and O. Fourt, "Flight Testing an Axisymmetric Scramjet: Russian Recent Advances, in *proceedings of 44th Congress of the International Astronautical Federation*, Oct. 16-22, 1993, Graz, Austria.
- [24] Bittner, R. D., Private Communications, Nyma, Hampton Virginia.
- [25] Rogers, R. C., Weidner, E. H., and Bittner, R. D., "Quantification of Scramjet Mixing in Hypervelocity Flow of a Pulse Facility," AIAA Paper 94-2518, June 1994.
- [26] "NASP Phase 2D Final Scientific and Technical Report," A011 (DI-MISC-08711/T) F33657-91-L-2012, Dec., 94.
- [27] Hunt, J.L., Ricketts, R.H. and McClinton, C.R., "Reference Technology Sets and Readiness Levels for Hypersonic Airbreathing Vehicles," 200 JANNAF CS, APS, PSHS and MSS Joint Meeting. Monterey, CA, Nov.13-17, 2000.
- [28] Brown, R.L., "Assessing Technology Readiness Using a Value Stream Process. Presented at NET Workshop on Processes for Assessing Technology Maturation and Determining Requirements for Successful Infusion into Programs," Marshall Space Flight Center, Sep. 16-18, 2003.
- [29] Committee on National Aerospace Initiative, Air Force Science and Technology Board, Division on Engineering and Physical Sciences, "Evaluation of the National Aerospace Initiative. National Research Council of the National Academies," The National Academies Press, Washington, D.C., April 2004.
- [30] Bowcutt, K.G, and Hatakeyama, S.J., "Challenges, Enabling Technologies and Technology Maturity for Responsive Space," AIAA 2nd Responsive Space Conference. AIAA 2004-6005.
- [31] McClinton, C.R., Rausch, V.L., Shaw, R.J., Metha, U., and Naftel, C., "Hyper-X, Foundation for Future Hypersonic Launch Vehicles," IAC-04-V.8.08. Sept, 2004.
- [32] "Decadal Survey of Civil Aeronautics – Foundation for the Future," National Research Council, The National Academes Press, Washington, D.C. www.nap.edu.
- [33] Curran, E.T., Scramjet Engines: The first Forty Years. J. Propulsion and Power, Vol. 17, No. 6, Nov-Dec 2001.
- [34] Why and Whither: Hypersonics Research in the US Air Force. United States Air Force Scientific Advisory Board. SAB-TR-00-03, Dec. 2000.
- [35] Gibson, C.S., Vess, R.J., and Pegg, R., Low Speed Flight Testing of a X-43A Hypersonic Lifting Body Configuration. AIAA 2003-7086, Dec. 2003.
- [36] Pittman, J.L., NASA Hypersonics Project Overview. Presented at 14th AIAA/AHI International Space Planes and Hypersonic Systems and Technologies Conference. Nov. 2006. <http://www.aiaa.org/pdf/conferences/hypersonics06nasa.pdf>
- [37] Jackson, K.Y., Scramjet Engine Gears up for Flight Tests. *News at AFRL*. http://www.afrl.af.mil/news/mar06/features/flight_tests.pdf
- [38] Rausch, V.L., "NASA Scramjet Flights to Breath New Life into Hypersonics," *Aerospace America*, vol 35, No 7, pp 40-46, July 1997.
- [39] Englund, W.C., Hyper-X Aerodynamics, "The X-43A Airframe-Integrated Scramjet Propulsion Flight Test Experiments," *Journal of Spacecraft and Rockets*, Vol 38, No. 6, Nov-Dec 2001. pg. 801-802

- [40] Engelund, W.C., et al., "Aerodynamic Database Development for the Hyper-X Airframe-Integrated Scramjet Propulsion Experiments," *Journal of Spacecraft and Rockets*, Vol 38, No. 6, Nov-Dec 2001. pg. 803-810.
- [41] Reubush, D.E., "Hyper-X Stage Separation-Background and Status," AIAA Paper 99-4818, Nov. 1999.
- [42] Woods, W.C., Holland, S.D., and DiFulvio, M., "Hyper-X Stage Separation Wind Tunnel Test Program," *Journal of Spacecraft and Rockets*, Vol 38, No. 6, Nov-Dec 2001. pg. 811-819.
- [43] Buning, P.G., Wong, T., Dilley, A.D., and Pao, J.L., "Computational Fluid Dynamics Predictions of Hyper-X Stage Separation Aerodynamics," *Journal of Spacecraft and Rockets*, Vol 38, No. 6, Nov-Dec 2001. pg. 820-827.
- [44] Holland, S.D., Woods, W.C., and Engelund, W.C., "Hyper-X Research Vehicle Experimental Aerodynamics Test Program Overview," *Journal of Spacecraft and Rockets*, Vol 38, No. 6, Nov-Dec 2001. pg. 828-835.
- [45] Berry, S.A., Auslender, A.H., Dilley, A.D., and Calleja, J.F., "Hypersonic Boundary Layer Trip Development for Hyper-X," *Journal of Spacecraft and Rockets*, Vol 38, No. 6, Nov-Dec 2001.
- [46] Huebner, L.D., et al. "Hyper-X Flight Engine Ground Testing for Flight Risk Reduction," *Journal of Spacecraft and Rockets*, Vol 38, No. 6, Nov-Dec 2001. pp 844-852. pg. 853-864.
- [47] Cockrell, C.E., et al., "Integrated Aeropropulsive Computational Fluid Dynamics Methodology for the Hyper-X Flight Experiment," *Journal of Spacecraft and Rockets*, Vol 38, No. 6, Nov-Dec 2001. pp 844-852. pg. 836-843.
- [48] Keel, L.C., "X-43 Research Vehicle Design and Manufacture," AIAA 2005-3334.
- [49] Harsha, P.T., Keel, L.C., Castrogiovanni, A., and Sherrill, R.T., "X-43 Vehicle Design and Manufacture," 13th International Space Planes and Hypersonic Systems and Technology Conference, Capua, Italy. May 2005.)
- [50] Redifer, M.E., Lin, Y., Kelly, J., Hodge, M., and Barklow, C., "The Hyper-X Flight System Validation Program," Hyper-X Program Office Report, HX-849. 2003.
- [51] Joyce, P.J., and Pomroy, J.B., "Launch Vehicle Design Challenges for Hypersonic Flight Testing (Mach 7 and 10)," 28th JANNAF Air-breathing Propulsion Subcommittee Meeting. Charleston, SC. June 13-17, 2005
- [52] Corpening, G., Marshall, L., Sherrill, R., and Nguyen, L., "A Chief Engineer's View of NASA's X-43 Scramjet Flight Test," AIAA 2005-3332, Capua, Italy. May 2005.
- [53] Marshall, L., Bahm, C., Corpening, G., and Sherrill, R., "X-43 Flight 3 Preparation and Results," AIAA 2005-3336, Capua, Italy. May 2005.
- [54] Bahm, C., Stovers, B., Baumann, E., Beck, R., Bose, D., "X-43 Guidance, Navigation and Control Challenges," AIAA-2005-3275, Capua, Italy. May 2005.)
- [55] Morrelli, E.A., "Aerodynamic Parameter Estimation for the X-43A from Flight Data," AIAA 2005-5921
- [56] Karlgaard, C.D., Hyper-X Post-Flight Trajectory Reconstruction. AIAA 2004-4829, Aug. 2004
- [57] Blocker, W, et al., "X-43 Stage Separation Analysis – A Flight Data Evaluation," AIAA 2005-3335. May 2005.
- [58] Engelund, W.C., "Aerodynamics, Results from the Mach 7 & Mach 10 Scramjet Flight Tests," AIAA 2005-3405,
- [59] Storch, A.R., Ferlemann, S.M., Bittner, R.D., "Hyper-X, Mach 7 Scramjet Preflight Predictions versus Flight Results," 28th JANNAF Air-breathing Propulsion Subcommittee Meeting. Charleston, SC. June 13-17, 2005.
- [60] Pinckney, S.Z., Ferlemann, S.M., Mills, J.C., and Bass, L.S., "Program Manual for SRGULL," HX-829.1, Dec. 04.
- [61] Lockwood, M.K., et al., "Design and Analysis of a Two-Stage-to Orbit Airbreathing Hypersonic Vehicle Concept," AIAA 96-2890. July 1-3, 1996.
- [62] Ferlemann, P.G., "Improvements to the SHIP Computer Code and Predictions of Vorticity Enhanced Turbulent Supersonic Mixing," M.S. Thesis. School of Engineering and Applied Sciences. GWU, Washington, D.C.
- [63] Ferlemann, S.M., Volland, R.T., Cabell, K., Whitte, D., and Ruf, E., "Hyper-X Mach 7 Scramjet Pretest Predictions and Ground to Flight Comparison," AIAA 2005-3322Capua, Italy. May 2005.
- [64] Ferlemann, P.G., "Hyper-X Mach 10 Scramjet Preflight Predictions vs. Flight Data," AIAA 2005-3352. Presented at 13th International Space Planes and Hypersonic Systems and Technology Conference, Capua, Italy. May 2005.
- [65] Rogers, R.C., "Scramjet Engine Flowpath Development for the Hyper-X Mach 10 Flight Test," ISABE 2005-1025.
- [66] Berry, S.A., Boundary Layer Transition on the X-43A Flight 2. 28th JANNAF ABPS Meeting, June 2005.
- [67] McClinton, C.R., X-43 – "Scramjet Power Breaks the Hypersonic Barrier," The AIAA Dryden Lectureship in Research for 2006. AIAA 2006-0001. Jan. 2006.
- [68] Roudakov, A.S., et al., "Recent Flight Tests of the Joint CIAM/NASA Mach 6.5 Scramjet Flight Program," NASA TM-1998-206548, April, 1998.
- [69] Volland, R.T., et al., "CIAM/NASA Mach 6.5 Scramjet Flight Test," AIAA 1999-4848, Nov. 1999.
- [70] McNelis, N. and Bartolotta, P., "Revolutionary Turbine Accelerator (RTA) Demonstrator," AIAA 2005-3250. AIAA 13th HyTASP Conference. 2005.

von Karman Institute for Fluid Dynamics

RTO-AVT-VKI Lecture Series 2007

**ADVANCES ON PROPULSION TECHNOLOGY
FOR HIGH-SPEED AIRCRAFT**

March 12-15, 2007

HIGH SPEED PROPULSION CYCLES

V. Balepin
ATK GASL, USA

HIGH SPEED PROPULSION CYCLES

Dr. Vladimir Balepin
ATK GASL, Ronkonkoma, NY, USA

Vladimir.Balepin@ATK.com

ACRONYMS

ALS - air liquefaction system	MIPCC - mass injection precompressor cooling
AspiRE - aspirating rocket engine	MTB - MIPCC test bench
ATRDC - deeply cooled air turbo rocket	NEPP - NASA Engine Performance Program
ATREX - expander air turbo ramjet	RASCAL- Responsive Access, Small Cargo, Affordable Launch
CIAM - Central Institute of Aviation Motors	RBCC - rocket based combined cycle
DC - direct cooling	SC - staged combustion
DCTJ - deeply cooled turbojet	SFC - second fluid cooling
GG - gas generator	SLS - sea level static
GTOW - gross takeoff weight	SSTO - single stage to orbit
ISAS - Institute of Space and Astronautical Science (Japan)	T/W - thrust-to-weight ratio
KLIN - thermally integrated deeply cooled turbojet and rocket engine	TBCC - turbine based combined cycle
LRE - liquid rocket engine	TFC - third fluid cooling
LRE - liquid rocket engine	TJ - turbojet
	TRL - technology readiness level
	TSTO - two stage to orbit

1.0 INTRODUCTION : OPPORTUNITIES PROVIDED BY DIFFERENT CYCLES

The present lecture relates to high-speed aircraft and space-launch vehicle propulsion, specifically to methods of the performance and thrust enhancement of turbojet engines and combined-cycle engines (when they are used in such vehicles). Methods for enabling these engines to operate effectively at higher speeds and higher altitudes will be examined.

Missions for trans-atmospheric vehicle include high-speed, long-range transports, military strike and reconnaissance aircraft, as well as orbital space transports, Reference 1. These extreme missions place severe demands on propulsion systems. They must deliver very high performance to efficiently achieve high velocities. They must also function from very low velocity during takeoff at sea level, to orbital velocities beyond the atmosphere.

Trans-atmospheric vehicles generally use a combination of air-breathing and rocket propulsion. Air-breathing systems are valuable since they gather a significant fraction of their propellant from the atmosphere. This reduces the quantity of propellant that must be stored onboard and increases overall vehicle efficiency. Consequently, air-breathing propulsion is often used to the maximum extent possible before exiting the atmosphere, where acceleration to final velocity is under rocket power.

Turbojet engines are attractive for such applications due to their high efficiency, as well as their operational flexibility. They are particularly valuable during takeoff and landing where their high efficiency at low speeds is critical. However, conventional turbojets are limited in their ability to operate at the high speeds and altitudes associated with trans-atmospheric flight. To extend the velocity and altitude that can be reached using air-breathing engines, a series of combined-cycle

approaches have been suggested. These cycles combine the positive attributes of turbojet engines with rocket engines or other air-breathing cycles, including ramjets and scramjets. Some of these cycles are considered in this lecture.

Usually, air-breathing cycles are characterized by relatively low thrust-to-weight ratios. This is acceptable for missions where propellant economy during long periods of atmospheric cruise is important. However, trans-atmospheric and space-launch missions are generally dominated by acceleration requirements where high thrust is often more advantageous than specific impulse. This is due to the increase in gravity and drag losses during extended acceleration periods. Consequently, an increase in engine thrust, even at relatively low specific impulse, can result in decreased overall propellant consumption since acceleration time decreases out of proportion to the increase in propellant flow.

To address the problem of low engine thrust-to-weight, several concepts have been proposed which utilize pre-cooling to increase the density of the inlet air. This increases the engine's power density and permits it to operate at higher Mach numbers. These engines generally use liquefied hydrogen for fuel. Before entering the engine, the cold hydrogen is circulated through heat exchangers ahead of the turbojet inlet to cool the incoming air. A broad class of propulsion systems utilizing air precooling in air/hydrogen precoolers is presented in this lecture.

The propulsion systems addressed in the previous paragraph are those generally using liquid hydrogen fuel. On the other hand, turbine engines based on hydrocarbon fuels can utilize very efficient thrust augmentation concepts which do not require significant modifications of the basic turbomachines, such as MIPCC and rocket-augmented turbine engines.

This lecture also covers examples of other synergetic cycles, namely, second fluid-cooled scramjet engines and third fluid-cooled liquid rocket engines. The common feature of all these synergetic cycles is that the working fluids do more than one job and/or hardware is adjustable for more than one operating mode.

The next section gives a brief overview of eight different synergistic cycles and Section 3 provides greater details of the MIPCC engine.

2.0 OVERVIEW : SYNERGISTIC PROPULSION CYCLES

This lecture covers eight original synergetic cycles including four TBCCs (ATREX, ATRDC, MIPCC, rocket augmented turbine), two RBCCs (KLIN, AspiRE), scramjets and rocket engines. Four of these cycles must have liquid hydrogen as a fuel (ATREX, ATRDC, KLIN, AspiRE), while the others are intended for hydrocarbon fuels or are not specific to the fuel option. Six cycles have been invented or introduced by the author (ATRDC, KLIN, AspiRE, MIPCC, SFC, TFC). The author has been also involved in ATREX cycle development.

2.1 ATREX Cycle

The ATREX cycle was introduced in Japan by Prof. N. Tanatsugu in the 1980s as a propulsion system for the TSTO space plane. ATREX is an original combined cycle, performing like a turbojet at low speed and like a fan-boosted ramjet at hypersonic flight. The ATREX engine is intended as the propulsion system of the fly-back booster of a TSTO space plane. ATREX works as an expander cycle utilizing in turbomachinery the thermal energy regeneratively extracted in both the precooler installed behind the air inlet and the heat exchanger in the combustor. The engine is able to produce effective thrust at flight conditions from SLS up to Mach 6 at 35 km altitude, Reference 2. When the

fan inlet temperature is lowered to 160K with a pressure recovery factor of 0.9 in the precooler, the thrust and specific impulse of the ATREX engine increase by factors of 2 and 1.5, respectively, at SLS conditions compared to the non-precooled engine.

ATREX employs a tip turbine configuration in order to reduce turbomachinery weight and size. Figure 1 shows an engine schematic.

Turbomachinery with the combustor incorporating a hydrogen heater and upstream pre-cooler were successfully demonstrated in various assembled configurations, as well as in separate units, such as air inlet and plug nozzle. Results have been reported in numerous papers. Figure 2 shows a precooled ATREX engine on the test stand.

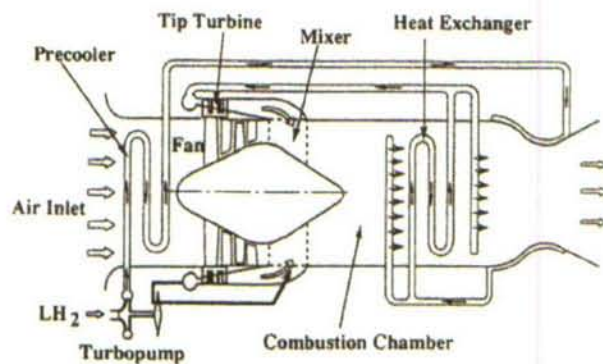


Figure 1: Schematic of the precooled ATREX engine, Ref. 2.

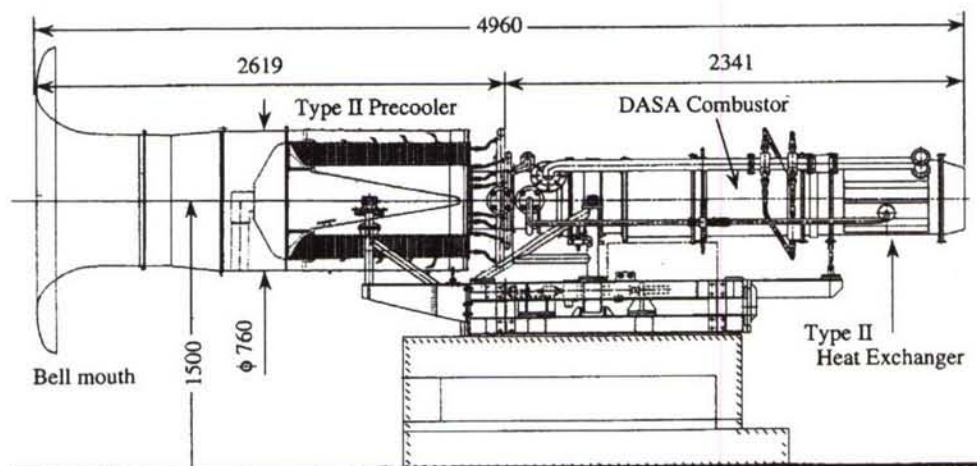


Figure 2: ATREX engine at the test stand, Ref.2.

The effect of air precooling on the engine's flight performance is shown in Figure 3 as a comparison of two levels of air precooling at SLS conditions, namely, $T_2=220K$ and $T_2=160K$. Performance of the ground tested ATREX-500 engine without inlet air precooling is also shown.

The ATREX engine air/hydrogen pre-cooler is a unique component which was built for the first time on this project. One of the early configurations is shown in Figure 4. One of the issues specific to precooled cycles is pre-cooler icing prevention. Reference 2 provides a discussion of the subject and Reference 3 describes measures the design team successfully demonstrated to prevent icing, namely, spraying a small amount of alcohol in front of the pre-cooler.

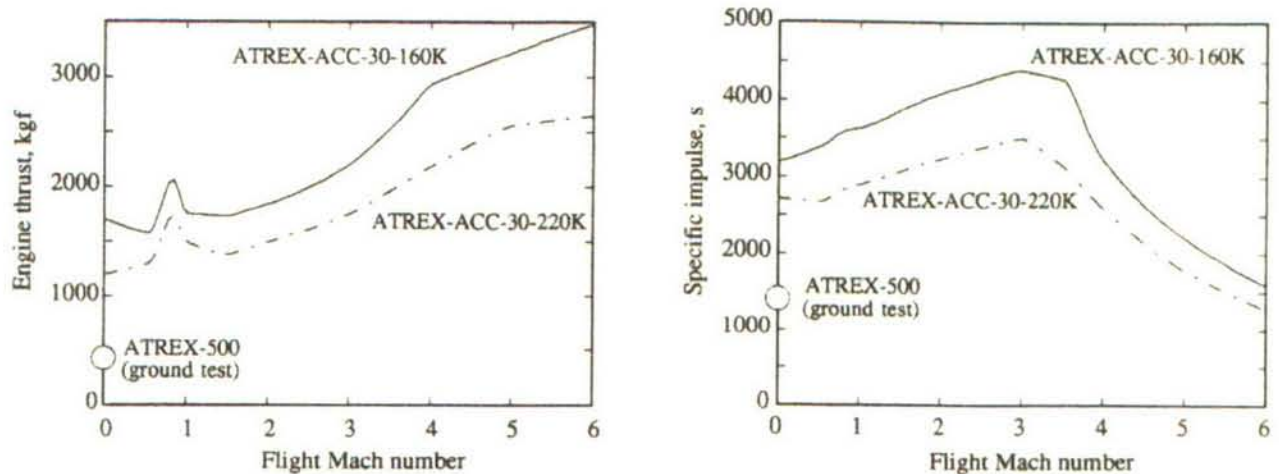


Figure 3: Flight performance of the precooled ATREX engine, Ref. 2. ATREX-ACC-30-160K – advanced ATREX engine using carbon-carbon as a fan structural material, fan diameter 30 cm, precooled to 160K at SLS conditions; ATREX-ACC-30-220K – engine precooled to 220K; ATREX-500 – non-precooled, engine with nominal thrust of 500 kgf.



Figure 4: Assembly of the quarter of the BARABAN-type precooler. (Picture acquired from the ISAS website <http://atrex.isas.ac.jp/>).

Major features of the ATREX engine as well as other cycles are summarized in Table 3 in the concluding Section 4.

2.2 ATRDC Cycle

Air precooling permits a significantly higher compression ratio than that utilized in the ATREX cycle, especially if the overall cycle is fuel rich. A good example of such a cycle was examined in CIAM, Russia, Reference 4. This is a deeply cooled air turborocket engine (ATRDC), Figure 5. The engine employs deep air precooling by the use of hydrogen fuel. In addition to its use as a fuel, hydrogen is performing two other jobs, namely, it precools the air and it drives the turbine. Hydrogen is used in an amount significantly higher than required for stoichiometric combustion, characterized by an

equivalence ratio $\varepsilon \cong 2$. This permits much greater air cooling than in other precooled cycles and much easier air compression (typical equivalence ratios for ATREX cycle is $\varepsilon=1.3-1.5$). The combustion chamber of the engine operates near stoichiometric since nearly half of the hydrogen flow rate is used to drive the turbine and is then exhausted without combustion.

The ATRDC engine consists of two units which may be located in different parts of the vehicle. The first unit includes the inlet air pre-cooler and turbocompressor, the second includes a double-duct combustion chamber with a two-position bell nozzle and a hydrogen heater located between the two combustion zones. The inner chamber duct operates in airbreathing mode, and the external duct in rocket mode.

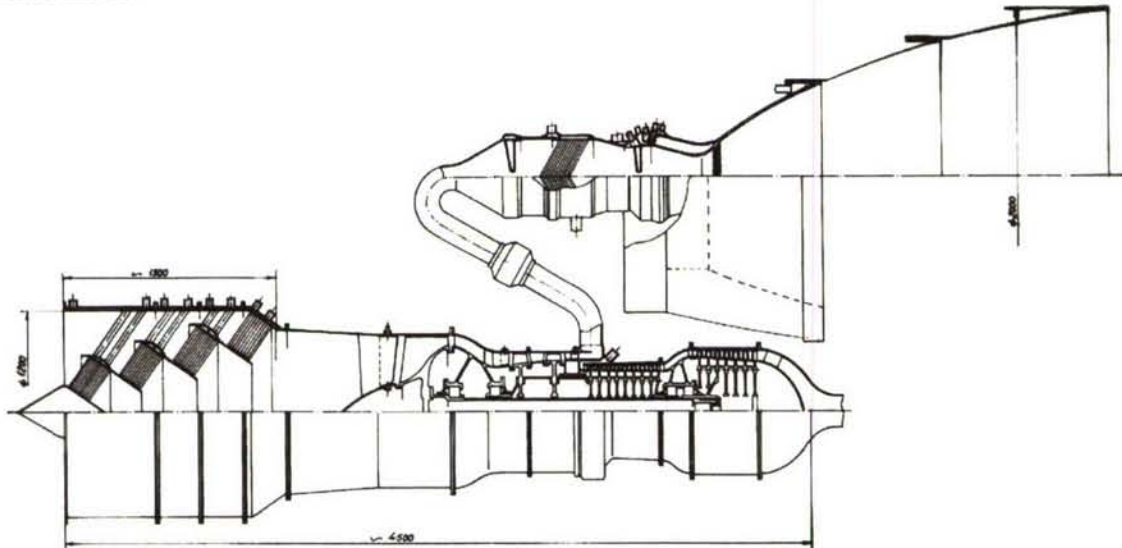


Figure 5: ATRDC engine of 30 ton thrust class, Ref.4.

At an air temperature upstream of the compressor of $T_2=98-112K$, the achievable compressor pressure ratio is $\pi_c=20-40$. At a pressure ratio of $\pi_c=40$, ATRDC provides an average specific impulse in the range of Mach=0 to 6 of $I_{SP}=2500$ s. T/W ratio for the engine constructed with advanced materials has been estimated as high as 18-22. The air pre-cooler is the bulkiest component of the ATRDC cycle accounting for 40% of the total engine weight (without the air inlet).

Since the turbine exhaust is pure hydrogen, the ATRDC engine can be integrated with a ram/scramjet for hydrogen utilization. Such a system is a good example of a synergistic cycle where the hydrogen does four jobs, namely, air pre-cooling in the ATRDC, turbine driving, combustion in the ATRDC chamber, and combustion in the ramjet chamber. Such a propulsion system has better performance as a whole in terms of I_{SP} than the individual components separately. The total specific impulse of the ATRDC and ramjet running simultaneously but which are not thermodynamically connected is :

$$I_{SP} = (1 - \xi)I_{SP}^{ATRDC} + \xi I_{SP}^{RAM}, \quad (1)$$

where I_{SP}^{ATRDC} and I_{SP}^{RAM} are values of ATR and ramjet I_{SP} ;

ξ - fraction of the fuel feeding ramjet.

In the case where ramjet fuel is used for air cooling before the ATRDC engine compressor and to drive the turbine, the total specific impulse is :

$$I_{SP} = I_{SP}^{ATRDC} + \xi I_{SP}^{RAM} - \Delta I, \quad (2)$$

where ΔI is a value of turbine exhaust specific impulse in the case where it is separately exhausted. Depending on flight altitude and speed, the value of ΔI has been estimated to be 2.5-9% of the total ATRDC specific impulse.

When the integrated ATRDC and ramjet are running simultaneously, the total enthalpy of the turbine exhaust is transferred in full to the ramjet flow and $\Delta I=0$. The thrust of the integrated propulsion system is characterized by an equation of the same structure as Eq.2.

Figure 6 shows performance of the separately running ATRDC and ramjet, simultaneously running ATRDC and ramjet without thermodynamic integration as given by Eq.1 at $\xi=0.5$ and of the propulsion system consisting of the thermodynamically integrated cycles per Eq.2. Total specific impulse of the latter is higher than ramjet I_{SP} by 15-30%.

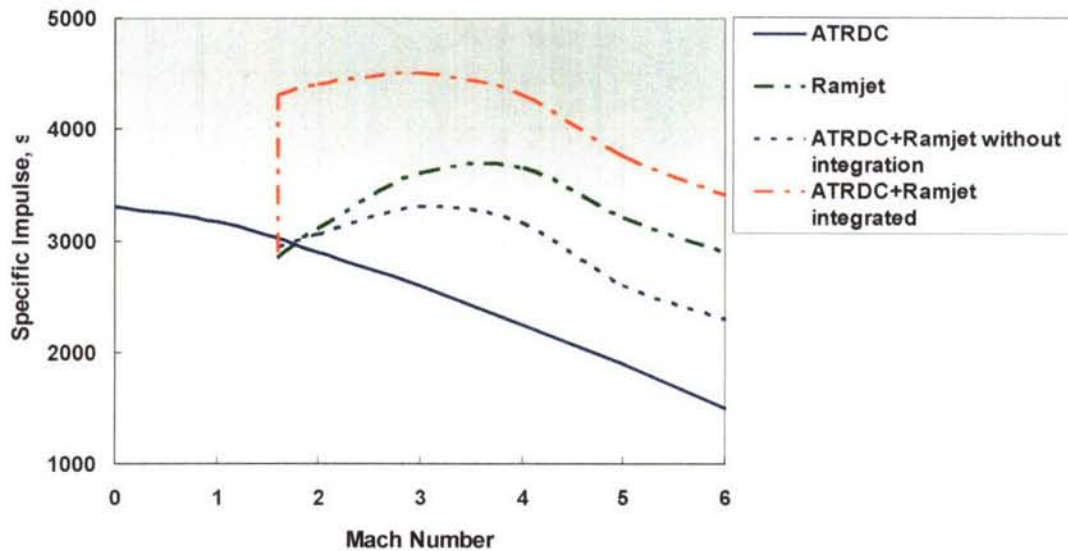


Figure 6: Performance of the separately and simultaneously running engines, Ref.4.

Cycle similar to ATRDC was intended for the British SSTO HOTOL back in 1980s.

2.3 KLIN Cycle

The KLIN cycle is a **thermally integrated**, deeply cooled turbojet (DCTJ) and liquid rocket engine, Reference 5. Thermal integration means that liquid hydrogen fuel for the rocket and turbojet engines is used to deep cool inlet air to 110K at SL and 200-250K at Mach 6. High pressure ratio is attainable with simple and lightweight turbomachinery. This results in high performance and exceptional thrust-to-weight ratio, Reference 6. Schematic of the KLIN cycle is shown in Figure 7.

The KLIN cycle incorporates several rocket and DCTJ units. All DCTJ units and all or part of rocket units operate from take off. The rocket units may be throttled or even cut off after initial acceleration, returning to full usage when the DCTJ are cut at Mach 6. The DCTJ units will be newly designed turbomachines incorporating a lightweight compressor optimized for low-temperature operation.

For a small launcher, the high performance reliable family of RL10 rocket engines is an appropriate choice. Lowcycle pressure and some features of configuration make the RL10 an ideal candidate for integration into the KLIN Cycle. The RL10 engine uses an expander cycle; therefore, it can be naturally integrated into the KLIN Cycle benefiting from additional hydrogen heating in the DCTJ.

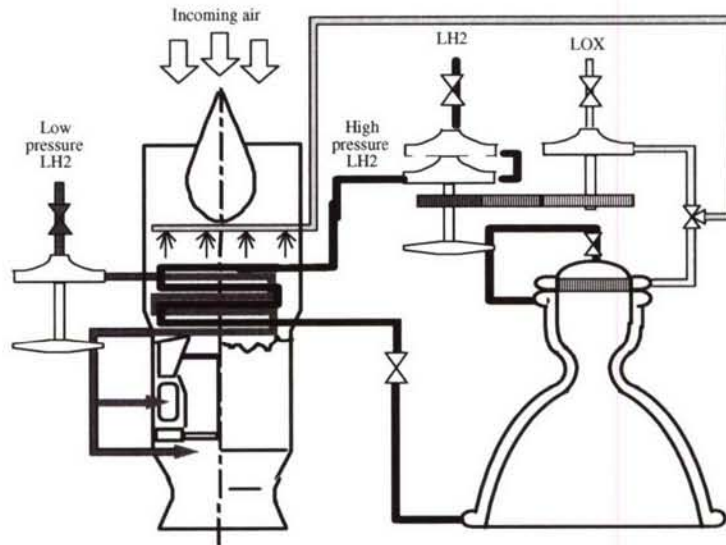


Figure 7: Basic configuration of the KLIN cycle, Ref.6.

The KLIN Cycle offers very flexible performance characteristics and represents a unique compromise between engine weight and fuel efficiency that provides a high payload capability for the vertical takeoff launcher.

Major parameters characterizing the KLIN cycle are :

KA - the ratio of the airflow and total hydrogen flow ($KA=4-12$), **KA₀** corresponds to KA at SLS conditions;

ξ - the ratio of the TJ's hydrogen and total hydrogen flow, the hydrogen distribution factor ($\xi =0.15-0.4$)

DOL₀ - fraction of the TJ thrust in total thrust at SLS ($DOL_0=0.25-0.65$)

With the KLIN Cycle, various launchers (e.g., SSTO, TSTO with fly back booster), as well as different takeoff and landing scenarios (horizontal or vertical, including a powered descent and landing), are possible.

Advantages of the KLIN Cycle can be summarized as follows:

- simple configuration—ideas such as an air/oxygen heat exchanger for additional air cooling, helium closed loop, or the bypass turbojet were rejected from the beginning of the concept analysis in order to maintain a simple design. Turbomachinery of the simplest possible configuration was considered, and a single spool design with no variable geometry for the compressor was employed. The addition of these features may improve turbojet parameters, but they will also add mass and complexity;
- light weight structure due to the high efficiency of air processing (high specific thrust), “excess” of cooling hydrogen and a low temperature compact compressor;
- high engine thrust-to-weight ratio;
- two to three times higher I_{SP} than for an LRE depending on the mission; and
- known solution for icing problem (LOX injection in front of precooler).

A small reusable vertical takeoff/horizontal landing SSTO launcher that delivers a 330 lb payload to a 220 nmi, 28.5-degree inclination orbit was selected as the reference launcher in the Reference 6 study. The launcher was sized at TGOW 62 tons and a dry weight of 12 tons. The propulsion system

configuration for the launcher was defined. It includes seven RL10-type engines with 7.7 tons SLS thrust each and four DCTJs with 6.5 tons SLS thrust each.

The optimum KLIN Cycle corresponds to an initial air-to-hydrogen ratio of $K_{AO}=6$. The thrust-to-weight ratio of this engine was estimated at 33.1, if it is based on an LRE with $T/W=43.6$. The most simple LRE control law (with full thrust) is proven to be the most efficient for the reference KLIN Cycle, as it provides the highest profile of effective specific impulse for $K_{AO}=6$.

Figure 8 shows how parameters of the optimized KLIN cycle change along the trajectory and optimum mode sequence. There are three operational modes indicated by circled numbers in Figure 8a :

Mode 1 (from takeoff to Mach=0.8) corresponds to simultaneous operation of all DCTJ units with oxygen augmentation and all the LRE units;

Mode 2 (in the range of Mach=0.8–6.5) begins after oxygen injection is cut off;

Mode 3 (from Mach 6.5 to orbital speed) a pure rocket mode begins after DCTJ cutoff, and LRE sole operation continues.

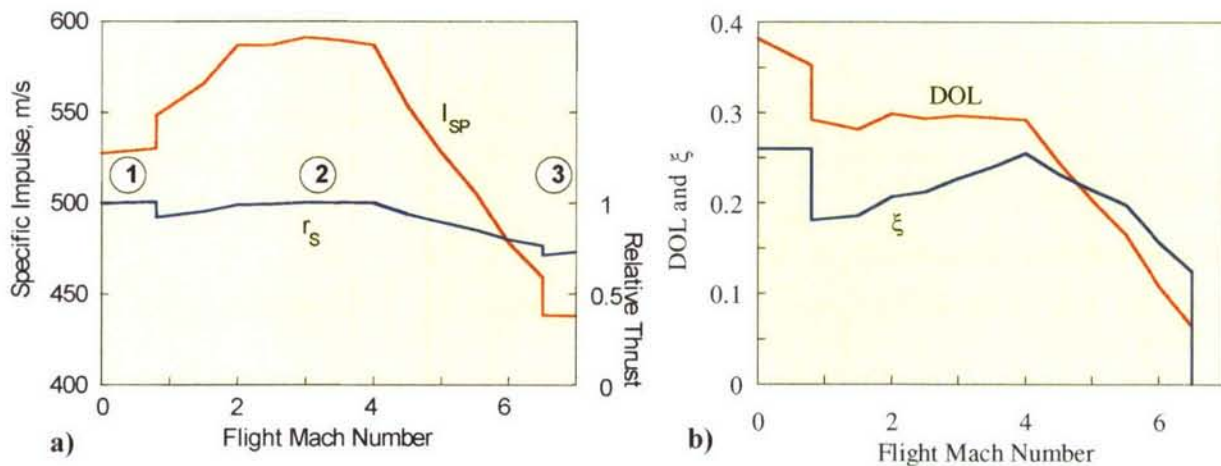


Figure 8. Performance of the reference KLIN cycle, Ref.6.

Optimized operation and performance are shown in Figure 8 where optimization of the launch vehicle is assumed; i.e., minimum GTOW and dry weight at a given payload. A summary of results is shown in Figure 9.

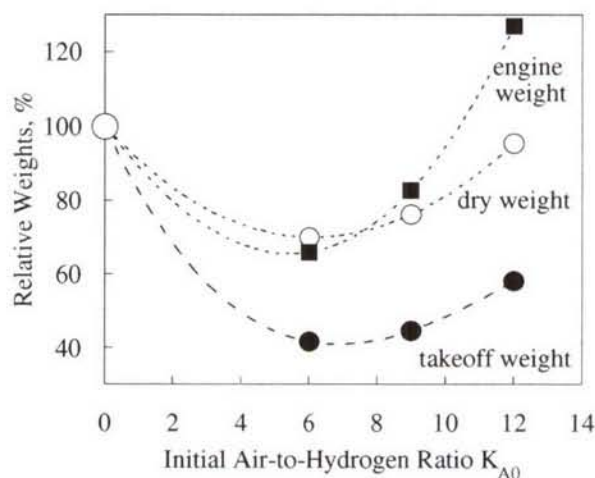


Figure 9. Comparison of the weights of all-rocket launcher and the KLIN Cycle launcher as a functions of the air-to-hydrogen ratio.

The relative GTOW, dry weight, and propulsion system weight are plotted vs. air-to-hydrogen ratio. Corresponding weights of the all-rocket launcher are taken as 100%. As Figure 9 shows, the minimum GTOW would be approximately 40%, and the dry weight and engine weight would be 70% of the corresponding weights of an all-rocket system. These minimums are rather gentle, and one may see that in the range of $K_{AO} = 5-8$, the KLIN Cycle launcher masses do not change much. The minimum launcher dry weight corresponds to the DCTJ contribution in SLS thrust, $DOL=30\%-45\%$.

Figure 10 is a schematic of the DCTJ sized for the optimized KLIN cycle. It is a dimensional scheme with major units sized for an SLS thrust of 7 tons. Table 1 gives DCTJ parameters in the main stations as shown in Figure 10, Reference 6.

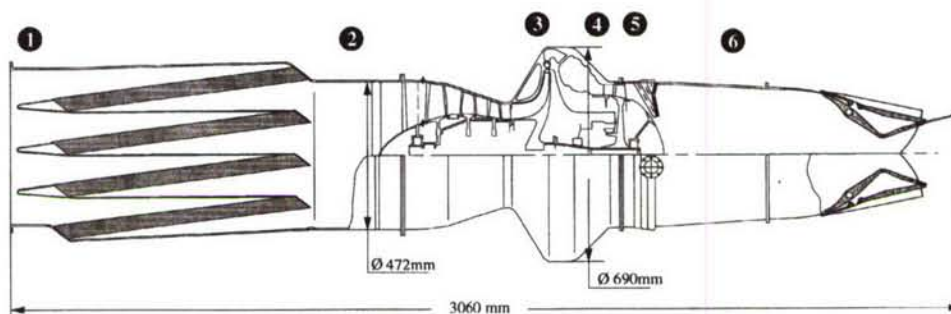


Figure 10. Dimensional scheme of the 7-ton thrust DCTJ, Ref.6.

Table 1. DCTJ parameters at SLS.

Station in Figure 10	Temperature, K	Pressure, bar
1	243	0.92
2	110	0.782
3	331	23.5
4	1451	22.3
5	1229	12.2
6	2505	11.8

2.4 ASPIRE CYCLE

The KLIN cycle requires development of a new turbocompressor that is a costly and long-duration effort. The next cycle is a logical extension of the KLIN cycle which does not require a turbocompressor. The AspiRE is an original combined cycle, Reference 7, that is capable of operating in two different propulsive modes. For the first air-breathing mode, part of the onboard oxygen is replaced by liquefied intake air prepared in an air/hydrogen heat exchanger/condenser and air/oxygen mixer. At a high Mach number, the engine changes to the second mode, which is a conventional oxygen/hydrogen rocket engine. Both modes use common hardware, namely the fuel and oxidizer turbopumps and the combustor/nozzle assembly. The air inlet and air liquefaction system (ALS) are the only attributes of the airbreather. This synergy is possible because in the combined-cycle mode, three fluids (LH_2 , LOX, and $Lair$) are used in a combination that provides sonic flow in the throat of the nozzle, which is designed for the rocket mode when two fluids (LH_2 and LOX) are used. This results in high cycle performance and an extremely high thrust-to-weight ratio for the combined cycle. Figure 11 shows the AspiRE cycle based on the expander rocket engine.

The AspiRE approach inherits some features of the KLIN cycle and has an even higher degree of cycle "rocketization." In fact, the AspiRE is a more rocket dominated cycle than any other RBCC.

The main issue with operating a combustor/nozzle in two different modes is the matching of the gas flows through the nozzle critical section (throat) and fluid flows through the pumps. References 7 and 8 show how it can be done for the AspiRE cycle. All devices providing high pressure (pumps and their drivers) are used in both the AspiRE and all-rocket modes and this results in a significant increase of the engine thrust-to-weight ratio compared to prior art concepts.

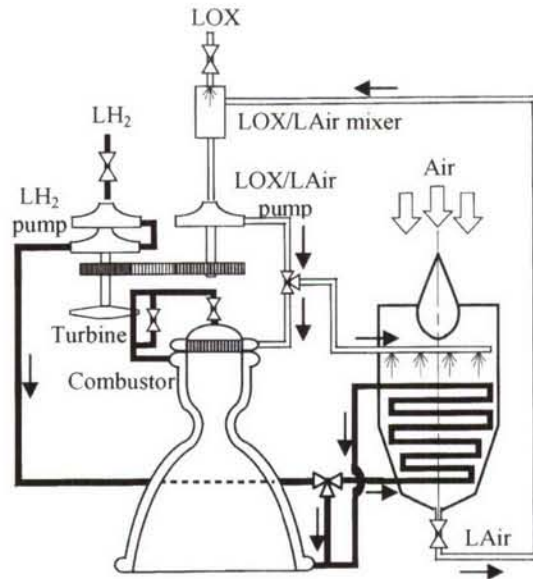


Figure 11. AspiRE cycle schematic.

Figures 12 and 13 show a comparison of the I_{sp} and relative thrust for the AspiRE cycle with different initial air liquefaction ratios KA_0 (air liquefaction ratio goes down during acceleration) and pure rocket propulsion. It is seen that the AspiRE cycle I_{sp} is always higher (in sea level conditions, it is 30% higher) than that of a rocket engine until it is switched to the pure rocket mode at Mach 6.5. Substantial thrust deterioration along the trajectory is a typical weakness of the air-breathing accelerators, which results in engine oversize. In the case of the AspiRE cycle, thrust is high at sea level conditions and always higher and nearly constant during acceleration (Figure 13). A combination of these two parameters provides a very favorable effective I_{sp} , which along with an exceptional engine thrust-to-weight ratio, explains the high launcher efficiency. These simulations were conducted with real RL10 engine constraints.

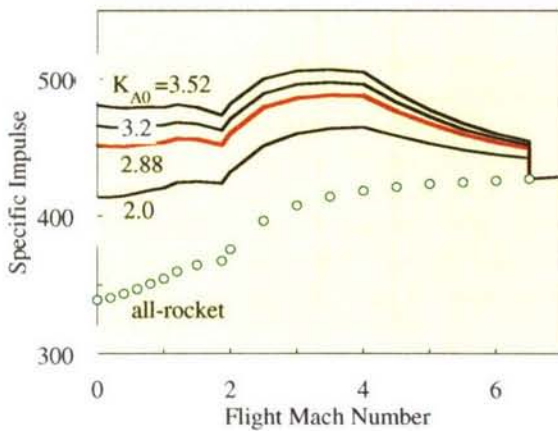


Figure 12. I_{sp} comparison, Ref. 8.

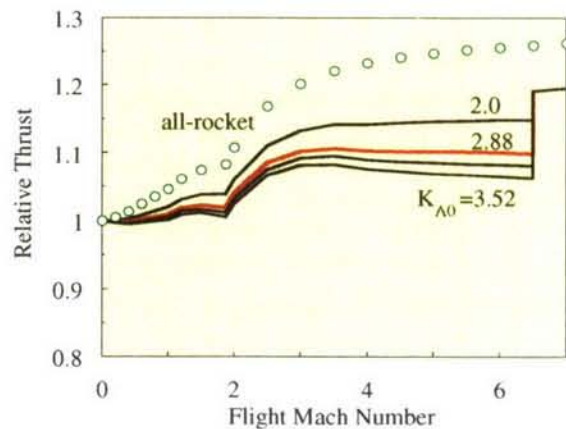


Figure 13. Relative thrust comparison, Ref.8.

The AspiRE cycle makes feasible systems that are not feasible with all-rocket propulsion (small or mid-size reusable SSTO launchers). Small military spacecraft and also quick response suborbital vehicles having global-reach capability are feasible with this technology. In the commercial arena, an AspiRE cycle-based launcher can create a new capability for on-demand, small payload launch services similar to Federal Express® or United Parcel Service®. The AspiRE cycle is also an attractive propulsion option for an International Space Station (ISS) resupply vehicle, Ref.8.

Figure 14 shows a comparison between an AspiRE cycle launcher and an all-rocket launcher in terms of relative GTOW and dry weight (corresponding parameters of the all-rocket launcher are taken as 100%), as a function of the initial air liquefaction ratio K_{A0} .

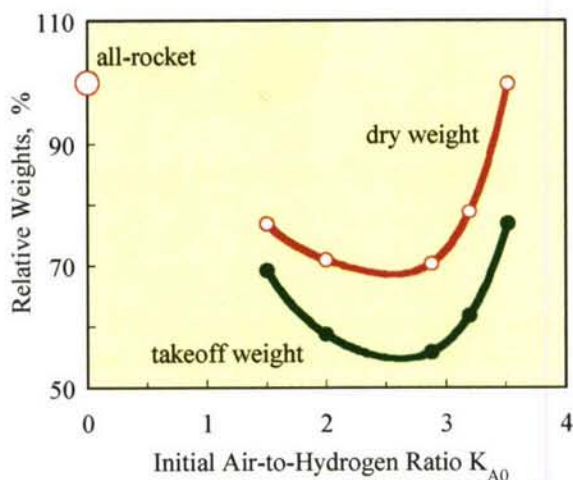


Figure 14. Comparison of the weights of an all-rocket launcher and the AspiRE launcher, Ref.8.

According to Figure 14, the GTOW and dry weight of a small launcher (330-lb payload to 220 nmi orbit) using the AspiRE cycle could be reduced by 45% and 30%, respectively, as compared to the all-rocket launcher. The best launcher efficiency corresponds to an initial air liquefaction ratio $K_{A0}=2.0-3.0$. At smaller K_{A0} , I_{SP} improvement allows only insignificant system improvement. With K_{A0} increase beyond the indicated range, the disadvantage of the bulky ALS cannot be mitigated by better I_{SP} . Due to low optimal K_{A0} , the ALS/air inlet system is expected to be rather compact.

The lightweight, moderate I_{sp} /high thrust AspiRE cycle provides exceptional efficiency for both vertical and horizontal takeoff small SSTO launchers. Other attractive features include:

- The AspiRE cycle is fully within the current manufacturing capability of the aerospace industry;
- The AspiRE cycle can be based upon existing expander rocket engines of the RL10 class. Incorporation of these engines and their derivatives into the AspiRE cycle can allow them to be used as boosters for small launchers;
- SLS operation of the AspiRE cycle is the most important mode, therefore, feasibility and efficiency of the technology can be proven in the ground demonstration;
- The ALS and triple mixture (air/oxygen/hydrogen) combustor/turbopump assembly can be separately developed and demonstrated.

Figure 15 shows an AspiRE cycle based on the RL50 engine (RL50 configuration from Pratt&Whitney web site).



Figure 15. AspiRE cycle based on RL50 engine, Ref.8.

2.5 MIPCC Engine

The main feature of the previously-discussed cycles is precooling of the incoming air using the heat sink capability of the liquid hydrogen fuel. Recently, hydrogen-fueled propulsion concepts are not as popular as they were back in 80s and 90s, especially for the booster stages of launch vehicles. The next cycle does not require hydrogen fuel. Moreover, this technique is readily applicable to existing turbine engines.

Mass Injected Pre-Compression Cooling (MIPCC) propulsion systems feature a conventional turbojet or turbofan engine as their core propulsion unit with a specially designed fluid injection system that sprays water and/or liquid oxidizer into the engine inlet, Reference 9. MIPCC reduces the incoming air stream temperature and delivers additional mass to the system. It results in an increase in the density of the air stream, permitting more capture. It allows operation at higher than core engine design Mach number and provides enhanced thrust levels at elevated Mach numbers. When properly scheduled, MIPCC allows the engine to operate within its normal operating envelope and use its existing control systems.

Water is an excellent coolant due to its high latent heat of vaporization, therefore, it was chosen for the baseline MIPCC concept. The main purpose of the oxidizer injection is to avoid afterburner blowout at depleted oxygen concentration due to water addition and high altitude. Cryogenic LOX and LAir as well as stable N_2O_4 may also serve as additional coolants. H_2O_2 and N_2O are subject to the exothermic reaction of decomposition which will add enthalpy in the AB, but is not appropriate in front of compressor. A MIPCC engine schematic with all listed injectants is depicted in Figure 16, Reference 8.

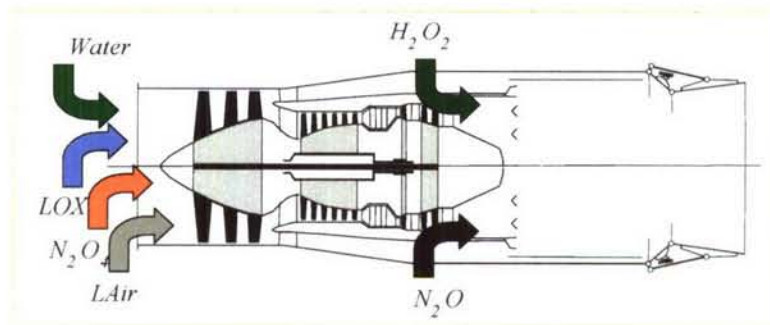


Figure 16. Injection of the different coolants/oxidizers in the MIPCC engine, Reference 8.

Reference 1 emphasizes use of the oxidizer as a coolant in front of turbine engine. The addition of oxygen to the inlet air flow allows the engine to operate at higher altitudes by preventing flameout due to decreasing oxygen.

If liquid air is used as a coolant, inlet temperature in front of the fan/compressor of the regular turbine engine can be kept rather low without any changes in gas composition, which provides comfortable conditions not only for compressor components but also for combustion devices. In addition, cryogenic fluid is easier to evaporate. However, use of the cryogenic oxidizer as a sole coolant leads to rather low I_{SP} at high Mach numbers.

Greater details of the MIPCC cycle as well as a progress in engine development and demonstration are discussed in Section 3.

2.6 Rocket Augmentation for Turboaccelerator

Further turbine engine thrust increase can be provided by oxidizer addition to the afterburner. It provides direct mass addition and also, if hardware permits, can be used for temperature increase in the AB. In this case more fuel will also be consumed. This type of turbine engine modification has been discussed in Reference 8 (see Figure 16). Reference 10 provides further details, Figure 17.

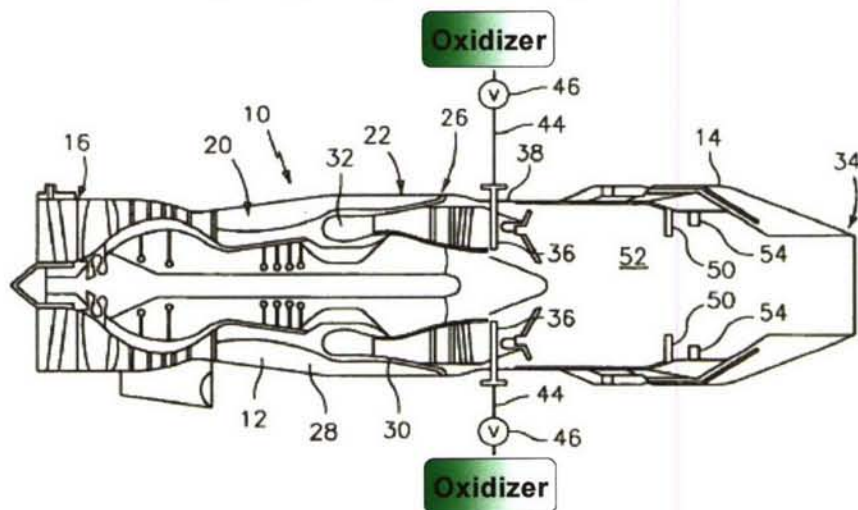


Figure 17. Rocket augmentation for turbine engine, Ref. 10.

According to Reference 10, advanced reusable hypersonic vehicles have a number of challenges to overcome in order to achieve their mission objectives. One of the most significant is the ability to meet the vehicle thrust requirements while also achieving aggressive size/weight/volume goals for the propulsion system. The combination of meeting propulsion thrust requirements while meeting severe packaging restrictions has contributed to the failure of earlier hypersonic vehicle designs. The propulsion system is especially tasked at the transonic pinch point. The transonic pinch is caused by the steep increase in vehicle drag as it transitions from subsonic to supersonic flight. Thus, what is needed is a way to increase engine thrust while holding engine size so that the vehicle could then reach closure ((i.e. complete the mission). One of the means of such thrust increase is rocket augmentation of the turbine engine, i.e., injecting oxidizer into hot gases in the augmenter so as to significantly increase the oxygen available for combustion resulting in a significant increase in the thrust force generated by the engine. Hydrogen peroxide is a preferred oxidizer of the authors of Reference 10.

Figure 18 illustrates the impact on the engine thrust with the injection of hydrogen peroxide into the augmenter of the engine. According to Figure 18, 70% thrust increase using rocket augmentation

requires eight times increase of the consumables through the engine. This results in eight times lower I_{SP} compared to the basic turbine engine.

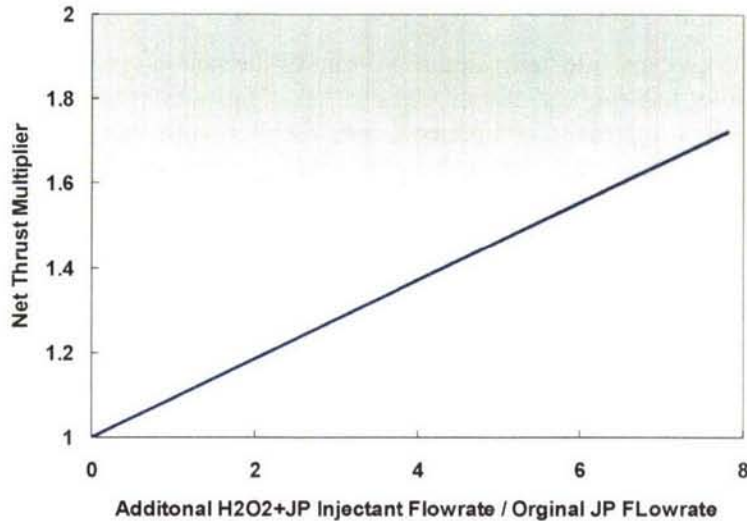


Figure 18. Rocket augmentation impact on the engine thrust, Ref. 10.

2.7 Second Fluid-Cooled Scramjet

A second fluid cooling (SFC) system is the system intended for use in a scramjet engine fueled by heavy hydrocarbons (US Patent pending). Hot elements are cooled with a second non-reactive fluid (N_2 , He, etc.), that permits a much higher hot wall temperature, resulting in reduced heat flux to the coolant. This permits an extension of coke-free engine operation to higher Mach numbers. Less heat is transferred to the fuel leading to comfortable and controllable thermal conditions in the SF/fuel heat exchanger. The SF forms a closed-loop Brayton cycle pumping the second fluid through the system, along with pumping of the main fuel and additional optional power generation, Reference 11.

Major advantages of the SF system over a direct cooling (DC) system are extended Mach number, higher I_{SP} (no overfueling) and/or higher thermal margins.

The second fluid of the cooling system travels in a closed Brayton loop. A compressor pumps the second fluid which enters the combustor wall. Within the combustor wall, the second fluid absorbs the heat generated by the combustion process. The heated second fluid exits the combustor wall and is expanded in a turbine which is used to drive the compressor and a fuel pump and provides additional power for the high-speed vehicle. The second fluid then enters a heat exchanger wherein heat is transferred from the second fluid to the fuel. The second fluid then returns to the compressor, closing the Brayton loop. The heated fuel travels from the heat exchanger to the combustor, where it utilized to propel the high-speed vehicle. A high temperature material combustor wall is essential for the SFC concept. Figure 19 shows SFC scramjet architecture.

In both conventional, direct-cooling techniques and in the SFC technique, fuel ultimately acts as the end heat sink. The ability of the fuel to absorb heat may be described by the "heat sink margin". Before the bulk fuel temperature reaches the coking limit and the wall temperature reaches its limit, the heat sink margin indicates how far the fuel heat sink is from the maximum possible heat sink at the coking limit.

If the fuel temperature at stoichiometric condition reaches the fuel coking limit, or if the wall reaches its material limit, extra fuel should be added for cooling purposes, even if it is excessive for the combustion process. The heat sink margin will be negative to reflect the

need for engine overfueling. Without engine overfueling, engine operation is not permitted for long periods of time, as fuel coking will occur. With the use of overfueling, operation is possible at the expense of engine fuel efficiency.

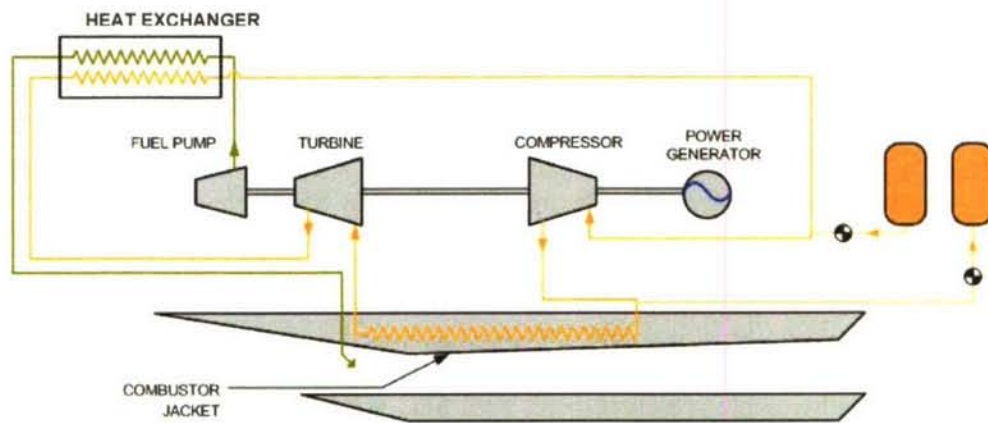


Figure 19. SFC cycle architecture, Ref. 11

Thus, fuel heat sink margin may be presented in two forms:

- before temperatures hit their limits at stoichiometric fuel/air ratio, fuel heat sink margin is

$$\delta = 1 - \frac{Q_x}{Q_{max}} \varepsilon \quad (\delta \geq 0) \quad (3)$$

- after temperatures exceed their limits at stoichiometric conditions

$$\delta = 1 - \varepsilon \quad (\delta < 0) \quad (4)$$

where δ - fuel heat sink margin;
 Q_x - heat absorbed by the fuel;
 Q_{max} - maximum heat to be absorbed by the fuel at coking limit;
 ε - equivalence mixture ratio.

As an illustrative example, Figure 20 shows a comparison of the fuel heat sink margin for direct cooling with endothermic hydrocarbon fuel and for second fluid cooling, where the same fuel is the end heat sink but nitrogen is used as a second fluid.

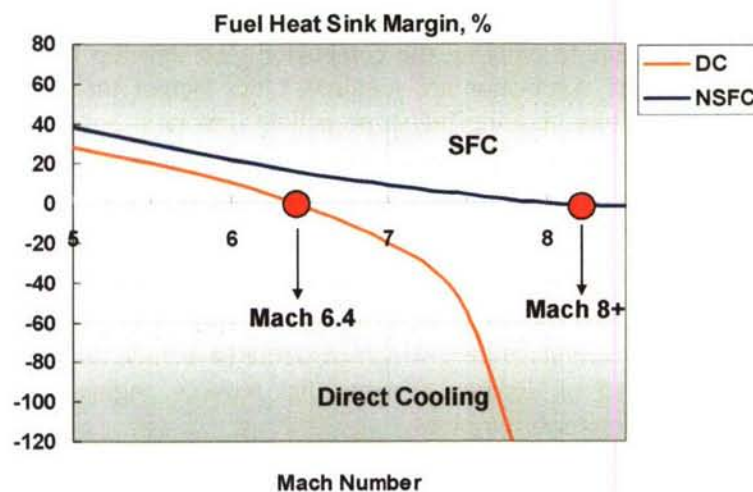


Figure 20. Fuel heat sink margins for DC and SFC methods, Ref. 11.

It is seen that direct cooling can provide scramjet operation up to Mach 6.4 with positive heat sink margin, i.e., without overfueling. Prohibitive overfueling, characterized by a negative fuel heat sink margin of less than minus 100%, is required to reach Mach 8. An SFC system extends the stoichiometric operation to Mach 8+ and narrow positive fuel heat sink margin is still available at Mach 8, as shown. The gentle slope of the second fluid cooling curve, as compared to the direct cooling curve, shown in Figure 20, enables further flight velocity increase to speeds over Mach 8.0 with moderate engine overfueling.

In this manner, efficient cruise flight engine operation at Mach 8, where the fuel flow rate required for combustion is lower than during acceleration, may be enabled by SFC technology.

2.8 TFC Rocket Engine

The TFC cycle is a logical extension of the SFC cycle approach on rocket engines, which also utilizes fluid other than fuel and oxidizer (third fluid) to cool the combustion chamber and drive the turbopump. Unlike other cycle presented here, both SFC and TFC cycles minimize the amount of work done by engine consumables through the introduction of the special fluid which is doing all internal work while forming a closed loop.

The TFC concept is a novel expander rocket engine that uses a third fluid as the combustor coolant and the turbine driver, Reference 12. The third fluid forms a closed-loop Rankine cycle permitting much higher available turbine expansion ratios than other closed rocket engine cycles.

The TFC rocket engine combines advantages of all three major pump-fed cycles: high available turbine pressure ratio of the gas generator cycle, full flow through the chamber typical for the staged combustion and expander cycles, high chamber pressure typical for the staged combustion cycle, and no preburner as with the expander cycle.

This unique set of the features permits the TFC cycle to be more efficient compared to the gas-generator and expander cycles in terms of I_{sp} and thrust-to-weight ratio, to exceed or match the staged combustion cycle in terms of thrust-to-weight ratio and to be more reliable than the staged combustion cycle due to significantly lower maximum cycle pressure.

The TFC cycle is applicable to both LOX/LH2 and LOX/HC rocket engines. Here, LOX/LH2 engine will be briefly discussed. More details can be found in Reference 13.

In modern LOX/LH2 rocket engines, hydrogen serves as the combustor coolant and sole turbine driving fluid (in the expander cycle) or part of the turbine gas (in gas generator, tap-off, and staged combustion topping cycles) prior to entering the combustor. To develop higher thrust in a rocket engine, higher pressures in the combustor are required, since output thrust is directly related to combustor pressure and this, in turn, requires higher propellant flow rate.

In both coolant and turbine driver applications, the hydrogen flow loses a significant amount of the pressure generated by the pump. In both the staged combustion SSME and expander RL10 engines, hydrogen pressure downstream of the pump is more than two-fold higher than the pressure in the combustor. However, hydrogen is the most difficult liquid to pump due to its very low density (approximately 70 kg/m³). This leads to lower than desired combustor pressures and explains the complexity of liquid hydrogen turbomachines, which particularly include the number of pump stages and very high mechanical load on feeding systems that reduces engine reliability and, finally, prevent the development of truly reusable engines.

The problem of oversized LH2 turbopumps can be resolved when a third fluid is employed as a coolant and turbine driver.

The TFC configuration, per Reference 12 and Figure 21, includes a typical engine assembly constructed of an injector 1, combustor 2, and nozzle 3. The combustor 2 and nozzle 3 form a nozzle and combustor assembly 4. Fuel, such as liquid hydrogen, and an oxidizer, such as liquid oxygen, are fed from supply tanks 5 and 6, respectively, to the injector 1. These fuel and oxidizer components, referred to as propellants, are mixed and fed to the combustor 2 wherein they are burned to produce hot gas which is ejected from the nozzle 3 to propel the vehicle. The fuel is fed to the injector 1 by a turbine-driven fuel pump 7, while the oxidizer is fed to the injector 1 by a turbine-driven oxidizer pump 8.

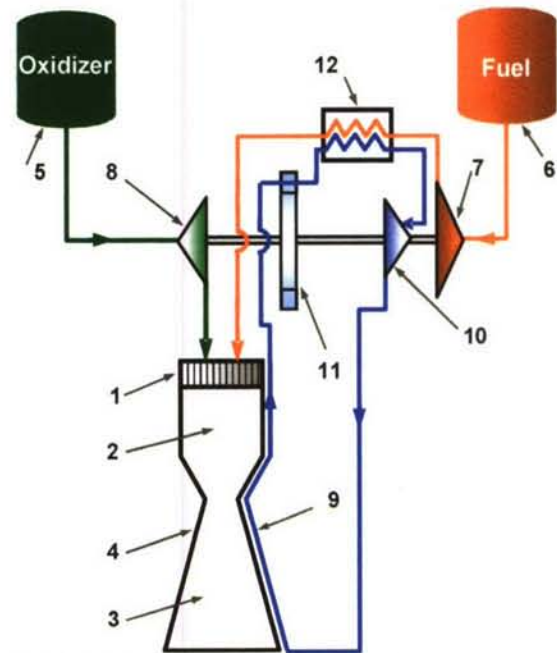


Figure 21. TFC engine flow diagram, Ref.12.

In the TFC engine, the nozzle and combustor assembly 4 is cooled by a circulating coolant such as water, methanol, ethanol, or liquid having equivalent properties, or mixtures thereof. The coolant is circulated through a jacket 9 enclosing the nozzle and combustor assembly 4 by a turbine-driven coolant pump 10. As the coolant circulates through the jacket 9, it is heated and vaporized forming steam or a vapor or gaseous-phase fluid. This vapor or gaseous-phase fluid is fed to the turbine 11 for driving the oxidizer pump 8, coolant pump 10, and the fuel pump 7.

The coolant vapor expands and is partially condensed in the turbine 11 and the turbine temperatures are reduced. The work of driving the turbines is produced by the expansion, temperature reduction, and partial condensation of the coolant vapors. The condensation process is completed in a heat exchanger 12 for exchanging heat between the coolant vapor and the incoming propellant, such as the liquid fuel or oxidizer or both. The coolant vapor condenses to heat the propellant, thereby returning the heat removed by the coolant from the combustor to the propellant fed to the injector 1. The fuel pump, oxidizer pump, water pump and turbine are mounted on one shaft in the particular case shown in Figure 21.

A third-fluid closed loop comprising turbomachinery, combustor jacket (shown as a heat exchanger), and third fluid/fuel heat exchanger is shown in Figure 22.

A well-known thermodynamic cycle, the Rankine cycle, for the flow of coolant such as water, is shown in Figure 23. The diagram shows the stations of the water flow path shown previously in Figure 22; namely water pump inlet 0, water pump exit 1, combustor jacket exit 2, turbine exit 3, heat exchanger exit 4 with the same parameters as in pump inlet 0. Line S defines the water saturation line. Points a and b correspond to intermediate stages of the water heating; point a corresponds to the beginning of the water evaporation in the combustor jacket, point b corresponds to the complete water evaporation in the combustor jacket. Point 3s corresponds to the ideal process of isentropic steam expansion ($S=\text{const}$) in the turbine. The solid lines in Figure 23 correspond to the following stages in the

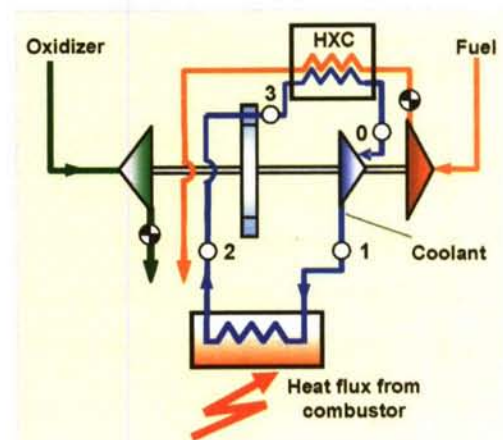


Figure 22. Closed-loop Rankine cycle.

process:

0-1 - water pumping;

1-a-b-2 - water heating, evaporation, and steam heating in the combustor jacket;

2-3 - steam expansion in the turbine (2-3s - ideal expansion);

3-0 - steam condensation in the heat exchanger.

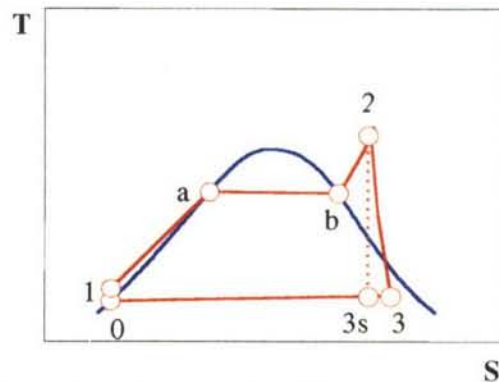
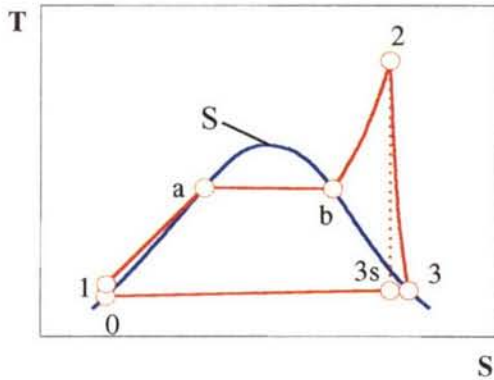


Figure 23. Rankine cycle T-S diagram (dry steam).

Figure 24. Rankine cycle T-S diagram (wet steam).

In order to reduce the size of the heat exchanger, steam or vapor can be partially condensed in the turbine. The more steam or vapor that is condensed in the turbine, the smaller the heat exchanger required. The literature on steam power generation turbines, for example Reference 14, recommends moisture content in the turbine be no more than 12%, since higher values cause turbine blade erosion. This recommendation is valid for steam power turbines with projected lifetimes of tens of thousands of hours. The expected lifetime for even reusable rocket engines is not likely to exceed tens of hours; therefore, appropriate amounts of moisture in the turbine exit can be expected to be significantly higher than 12%. A T-S diagram for the process with wet steam at the turbine exit is shown in Figure 24.

Major benefits of the TFC technology applied to the LOX/LH₂ engines are significantly higher (50-65%) engine thrust-to-weight ratio and feasibility of higher combustor pressures. A preliminary comparison with SSME shows that at the same combustor pressure, 34% of the structural weight saving can be expected. Due to significantly lower cycle pressures, TFC technology may be a key to rocket engine reusability.

Other significant advantages include the fact that compared to the staged combustion cycles of the SSME type, which utilize 3 combustion devices (2 preburners and a main combustor), the TFC eliminates 2 of these 3 combustion devices with an accompanying weight savings and no loss in performance. As a result, development cost and time savings can be expected. This is also true for the LOX/HC rocket engines.

The TFC configuration is a promising choice for the LOX/HC engine because it permits:

- The elimination of the preburner and associated systems
- Low turbine temperature
- Low maximum cycle pressure (on the level of the chamber pressure).

The TFC engine can be used for both booster rocket and upper stage rocket applications.

3.0 MASS INJECTION PRECOMPRESSOR COOLED TURBINE ENGINE

The MIPCC engine is listed among the cycles presented as an example of the efficient accelerator engine. Section 2.5 provides initial cycle information. This section is devoted entirely to the MIPCC cycle and shows the status of its development according to Reference 15.

3.1 Baseline Flight Trajectory

MIPCC engines can be utilized for launchers of different size and configuration. The basic operational concept developed for the small reusable launcher called RASCAL is depicted in Figure 25. This figure shows an airbreathing vehicle (either manned or unmanned) taking off from a conventional runway. The vehicle climbs to its loiter altitude, using a conventional airbreathing turbofan propulsion system. At this point, the vehicle begins a “zoom maneuver”, taking advantage of liquid injection ahead of the first-stage turbofan compressor. The liquid injection allows the vehicle to go to a much higher altitude and velocity than would be possible with an unmodified turbofan. At an appropriate point in the trajectory, the upper stages are released from the first stage. Once the upper stages of the vehicle have safely cleared the first stage, the first stage can return to the Earth for reuse.

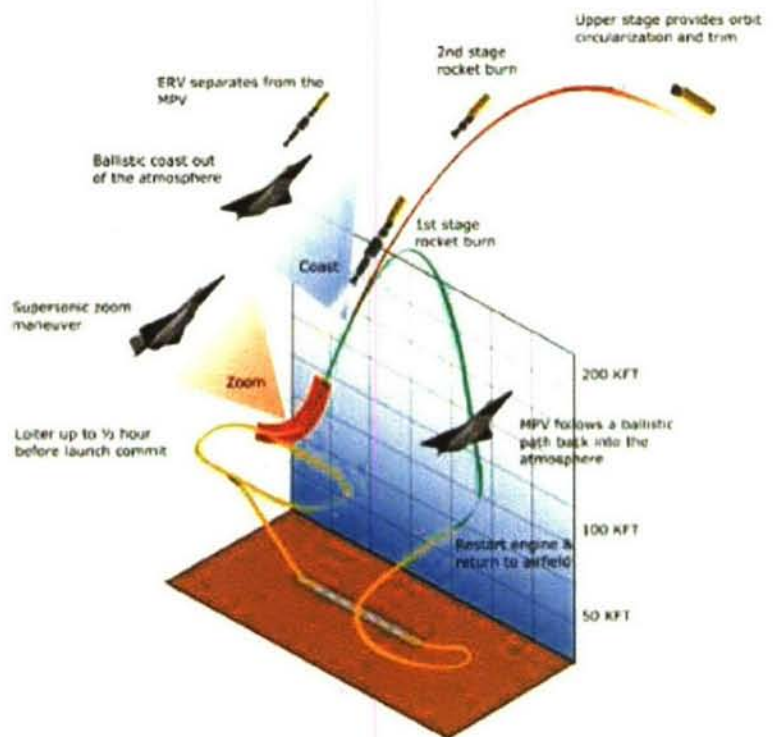


Figure 25. Baseline operational concept, Ref. 15.

3.2 Baseline MIPCC Concept

MIPCC is intended to offset performance losses incurred as an aircraft accelerates and the density of the air flowing into the inlet decreases. The engine subsystem adds water and liquid oxygen to the airflow in the inlet, reducing its temperature hundreds of degrees. The result is twofold: First, it places less stress on the engine and increases its durability because of the lowered temperatures. Second, and from a performance perspective the more important, mass flow is increased due to the increased density.

The baseline MIPCC configuration is shown in Figure 26. The following are the major principles applied by the MIPCC concept:

- The existing turbofan engine is utilized with water and LOX injection ahead of the fan. No modifications of the basic TF engine are planned, except for minor upgrades and adjustments of the control system;
- The inlet capture area is designed to allow the air flow rate required for turbomachinery to generate the maximum thrust. Only at the end of zoom at high altitude inlet limits the thrust restricting the air flow to the amount less than maximum allowed by turbomachinery;

- Injection is initiated in the transonic region;
- During the acceleration mode, the MIPCC engine develops maximum possible thrust. It reaches approximately 200% of the SLS thrust of the basic TF just before the zoom climb;
- Water is injected in an amount not to exceed saturation content;
- LOX is injected in the amount required to maintain normal molar oxygen concentration of 20.9% in the air/water/oxygen mixture. This concentration may be exceeded when additional thrust is required and small amounts of water are replaced by larger amounts of LOX (OXYBOOST mode);
- All applied pressure, temperature, geometry, and RPM limiters of the basic TF engine have been respected.

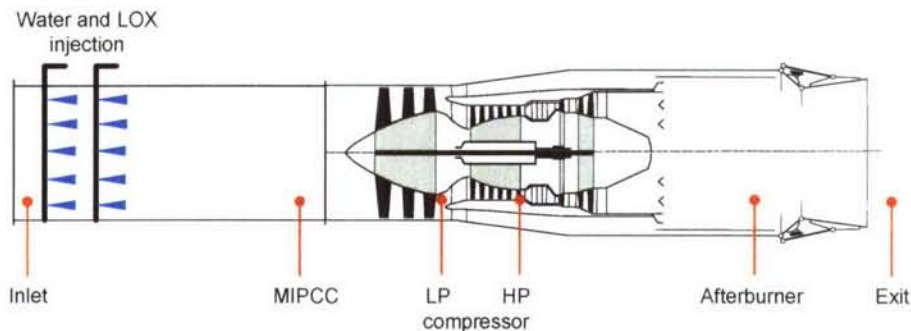


Figure 26. Baseline MIPCC engine configuration.

Water provides the better coolant, but the MIPCC system also is designed to introduce liquid oxygen to maintain combustion stability for the afterburner and for mass addition. Water and LOX injection results in significant thrust increase due to significantly higher mass flow rate and available expansion ratio over the nozzle.

Comparison of the key parameters of the basic F100 engine and the same engine equipped with the MIPCC system at Mach 2.25 are shown in Table 2. Stations are given in Figure 26. Note the difference in flow rates (MIPCC station) and afterburner pressure. The resulting MIPCC engine thrust is more than doubled at this particular point. This difference increases at higher Mach numbers until the basic turbofan becomes non-operable primarily due to temperature limitations.

Table 2. Engine parameters comparison at Mach 2.25, Alt 46000 ft.

Station	Parameter	MIPCC F100 over Basic F100
Inlet	Flow rate	1.66
	Temperature	1.00
	Pressure,	1.00
MIPCC	Flow rate	1.73
	Temperature	0.74
	Pressure	0.98
HP compressor	Temperature	0.92
	Pressure	2.15
Afterburner	Pressure	2.05
Exit	Net Uninstalled Thrust	2.01

3.3 MIPCC Operation

The key to the MIPCC concept is that the engine does not recognize it is flying at extreme Mach numbers and altitudes. Two of the major engine control inputs are total pressure and total temperature

upstream of the fan – P_{t2} and T_{t2} . These parameters indicate the speed and altitude at which the engine is flying. The MIPCC engine fan sees significantly lower temperature compared to the basic TF flying the same Mach number and nearly the same pressure. The solid line in Figure 27 shows the P_{t2} - T_{t2} relationship for the basic TF engine flying a launch trajectory. In the case of a MIPCC engine, this line shows the pressure-temperature relationship upstream of the MIPCC system. The dashed line shows the same relationship upstream of the fan of the MIPCC engine. The latter is entirely within the operating envelope of the basic TF, also shown in Figure 27a.

Figure 27b shows actual flight trajectory and apparent trajectory according to P_{t2} and T_{t2} sensor readings upstream of the MIPCC engine fan. The maximum velocity seen by the engine (apparent trajectory) is two times lower than the maximum velocity for the actual trajectory, due to the temperature reduction. The maximum altitude for the apparent trajectory is also twice as low as the maximum altitude for the actual trajectory. Therefore, despite the extreme actual flight conditions, the engine with mass addition upstream of the fan always stays within the Mach/altitude and P_{t2}/T_{t2} envelopes prescribed for the basic turbine engine.

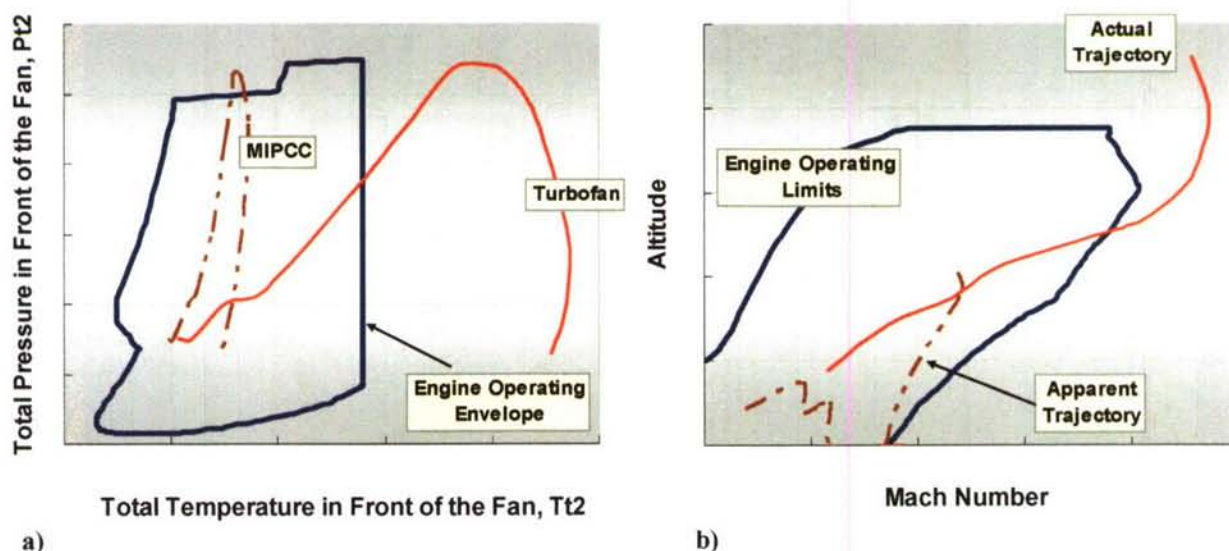


Figure 27. MIPCC engine operating conditions: a) T_{t2} - P_{t2} operating envelope; b) Mach number-Altitude profiles.

The trajectory shown is a result of the interactive MIPCC engine/ vehicle analysis. The goal of this effort was to select the baseline MIPCC engine, size the MIPCC injection system, and identify the required modifications to the basic engine control system. The engine thrust, fuel efficiency characteristics and schedules for all required internal engine parameters were obtained in this analysis.

3.4 MIPCC Configuration

Figure 28 shows the MIPCC system integrated with an engine of F100 size. The configuration shown was sized after accomplishing the first series of MIPCC engine tests and was coordinated with the airframe integrator. The MIPCC system includes one LOX injection plane and two water injection planes. The distance between the last water injection plane and the engine face was defined as the minimum required for evaporation of the substantial amounts of water.

For the MIPCC system demonstration and verification of the major principles involved, a MIPCC duct has been designed, built and tested at the MTB. Configuration of the demonstration MIPCC duct is shown in Figure 29. As in the flight version of the duct, there is one plane of LOX injector bars and two planes of water injector bars. Each injector bar could be individually switched on or off.

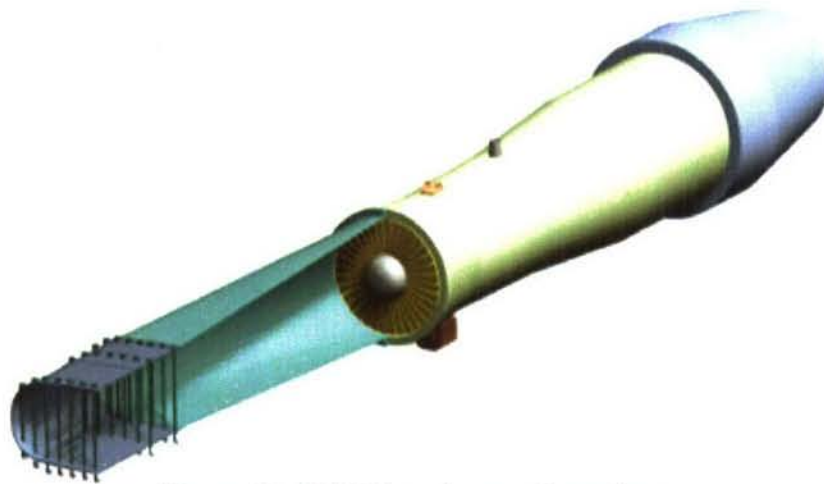


Figure 28. MIPCC engine configuration.



Figure 29. Demonstration MIPCC duct.

3.5 MIPCC Test Bench (MTB)

Ground testing of the MIPCC system was conducted as an early validation of this innovative propulsion cycle. A group of companies under DARPA sponsorship built the MIPCC Test Bench (MTB) at the Mojave Airport, Mojave, CA. The facility is intended to simulate flight environments up to Mach 4 on the ground. A flow diagram of the test setup is shown in Figure 30.

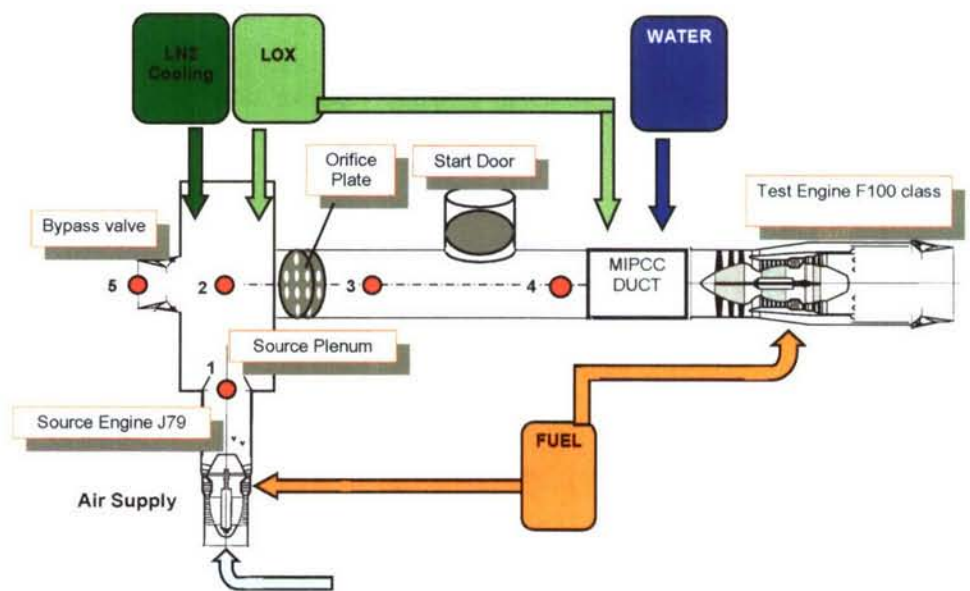


Figure 30. MTB flow diagram.

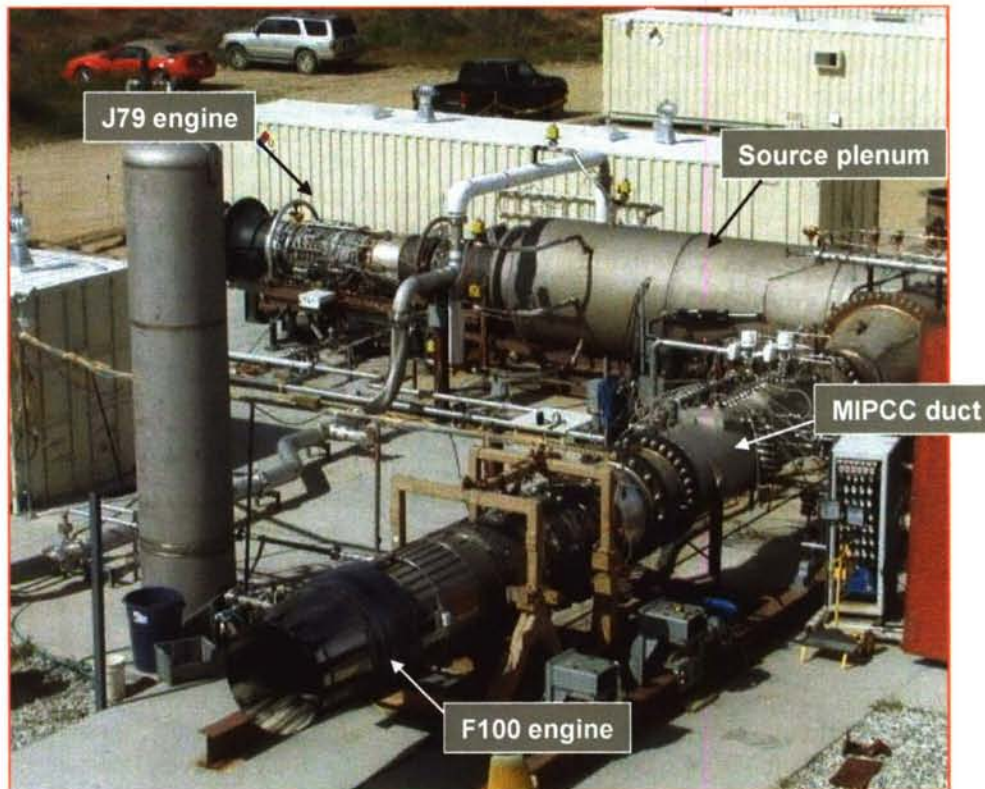


Figure 31. MTB facility.

Heated air is provided by a surplus General Electric J79 turbojet, which exhausts into a source plenum. Air leaving the plenum is conditioned to the proper enthalpy and oxygen level by the addition of liquid nitrogen and liquid oxygen. Air flow through the test engine is controlled by throttling of the J79 source engine, mass addition through LOX injection upstream of the source engine, and source engine exhaust bypass. The air temperature ahead of the test engine is controlled through the J79 engine setting and LN2 injection into the source plenum. The air pressure upstream of the test engine is controlled through LAir injection ahead of the source engine, as well as source engine throttling. The oxygen concentration in the test engine is controlled through makeup LOX injection. A photograph of the facility conveys the scale, Figure 31.

Following facility construction and checkout, testing proceeded in incremental steps. First, a sequence was run with a substitute small J85 turbojet engine in place of the eventual full-scale F100. The testing conducted at a simulated 60,000 ft altitude, served to provide valuable experience in starting and running the test engine. Following completion of this test series, the J85 was removed and the full-sized F100 MIPCC duct was substituted. There followed a series of so-called “hot duct” tests, meaning with just the MIPCC duct installed, prior to installation of the F100 engine. Finally, the entire system was tested with the F100 installed.

3.6 Full Scale MIPCC Engine Demonstration

In the 2004-05 timeframe, a series of F100-200 MIPCC tests was conducted at MTB. MIPCC engine operation in the all the important points of the baseline flight trajectory was demonstrated.

The test series was interrupted by a mishap involving the F100 engine. As of this writing (March 2005), shakedown hot-duct testing of the upgraded MTB has been accomplished and a new F100 has been installed and prepared for another series of full-scale demonstration tests.

Engine operation at two test conditions corresponding to Mach 1.6 is discussed below. Thrust and flow rate data from test 040910 are plotted in Figure 32. These test results clearly show the significant impact that MIPCC has on engine performance. The NEPP model accurately matches both MIPCC and non-MIPCC operation.

Figure 32 shows gross thrust and two flow rates – water and fuel- versus testing time. MIPCC operation corresponds to the time when water flow is non-zero. The fuel flow spike corresponds to initiation of the F100 engine afterburner (AB). This attempt to light AB was not successful. Experience gained from this and subsequent tests shows that AB should be initiated before water injection.

Stable thrust between approximately 420s and 450s corresponds to non-MIPCC engine operation in military mode. Thrust at 447s has been exactly matched with the NEPP code (white circle in Figure 32 at approximately 450 s). Lower than nominal efficiencies have been applied in the model due to the age and usage of the F100 engine at MTB. The NEPP model adjusted to the military non-MIPCC operation point was applied to the MIPCC mode. Estimated thrust matches the thrust measured in the test very closely (white circle in Figure 32 at approximately 470s). Water flow rate at this point was 2.2% of the air flow rate. Injection of this relatively small amount of water led to a 34% increase of gross thrust of the engine operating without the AB.

Results from test 040914 are shown in Figure 33 as thrust and water and fuel flow rate profiles versus test time. Three different engine modes can be found in this plot, namely: 1) AB mode without MIPCC, 2) AB mode with MIPCC, and 3) MIL mode without MIPCC. Several unsuccessful attempts of AB relight can also be seen in Figure 33.

An 11% thrust increase in AB/MIPCC mode compared to AB/no-MIPCC mode was observed. The NEPP model adjusted to exactly match engine thrust on MIL/no-MIPCC mode in the 040910 test, has been applied to MIL/MIPCC mode of the 040910 test and three points of the 040914 test (three white circles in Figure 33). The model closely matches engine thrust. Figure 34 is a comparison of the predicted and observed gross thrust. A maximum disagreement of 5.2% is observed for the “simplest” MIL/no MIPCC mode in the 040914 test. In this case, thrust is underpredicted, meaning that lower thrust is predicted than demonstrated in the test.

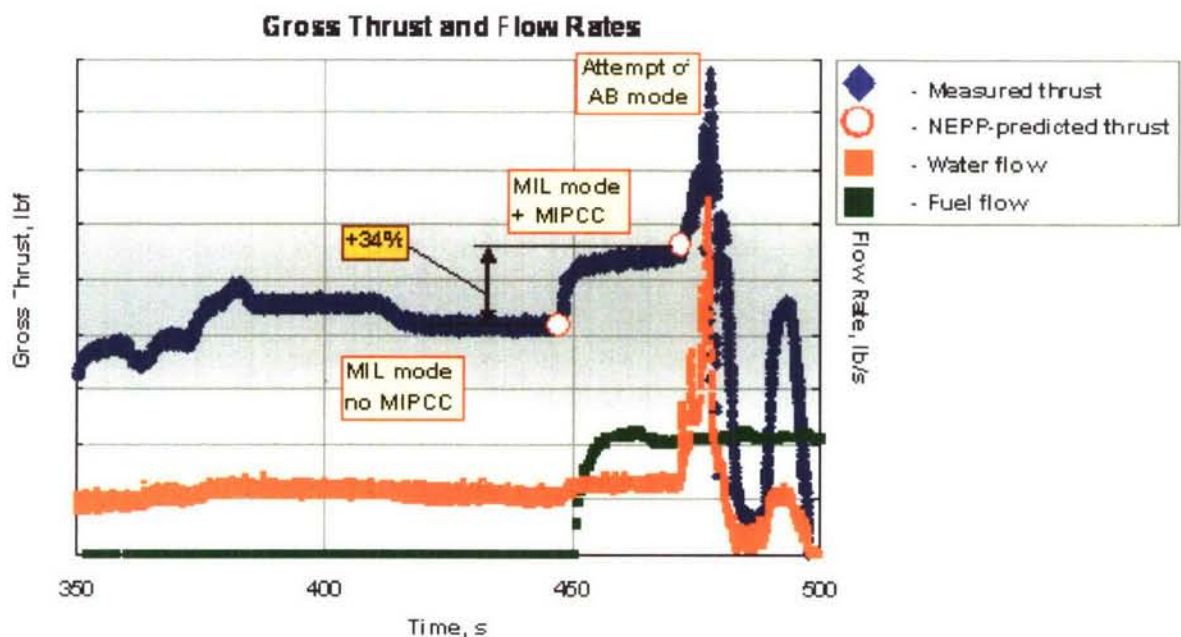


Figure 32. F100-200 MIPCC engine performance in test 040910.

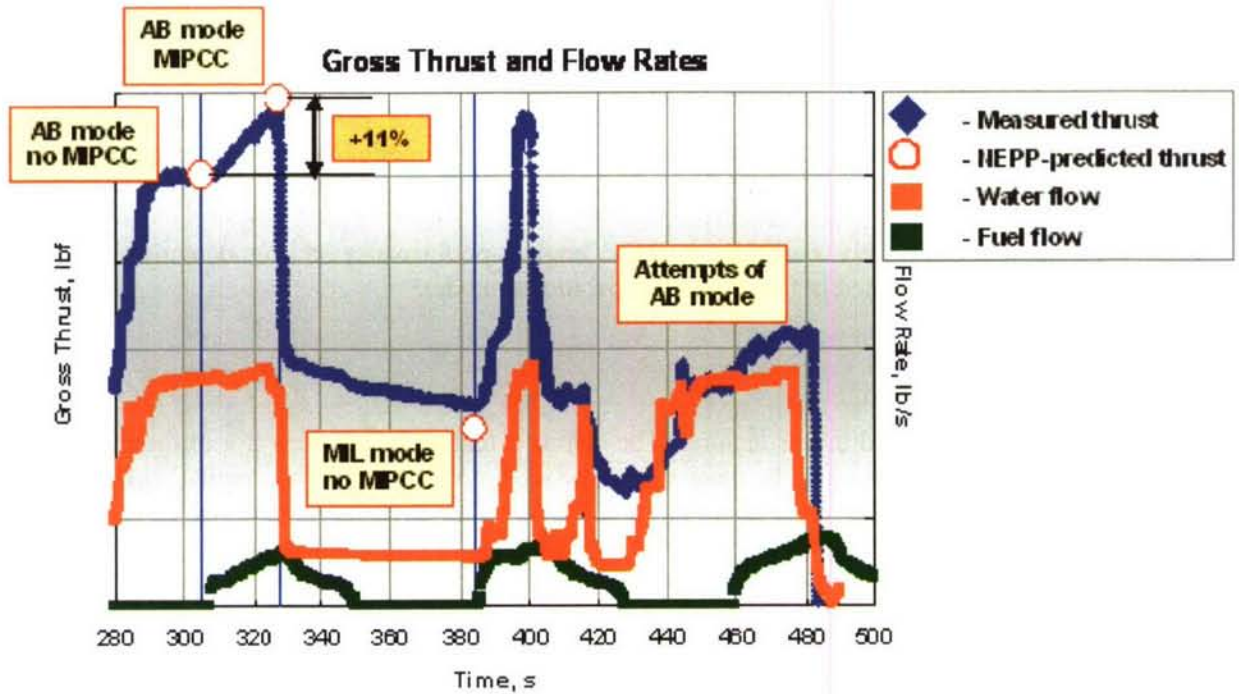


Figure 33. F100-200 MIPCC engine performance in test 040914.

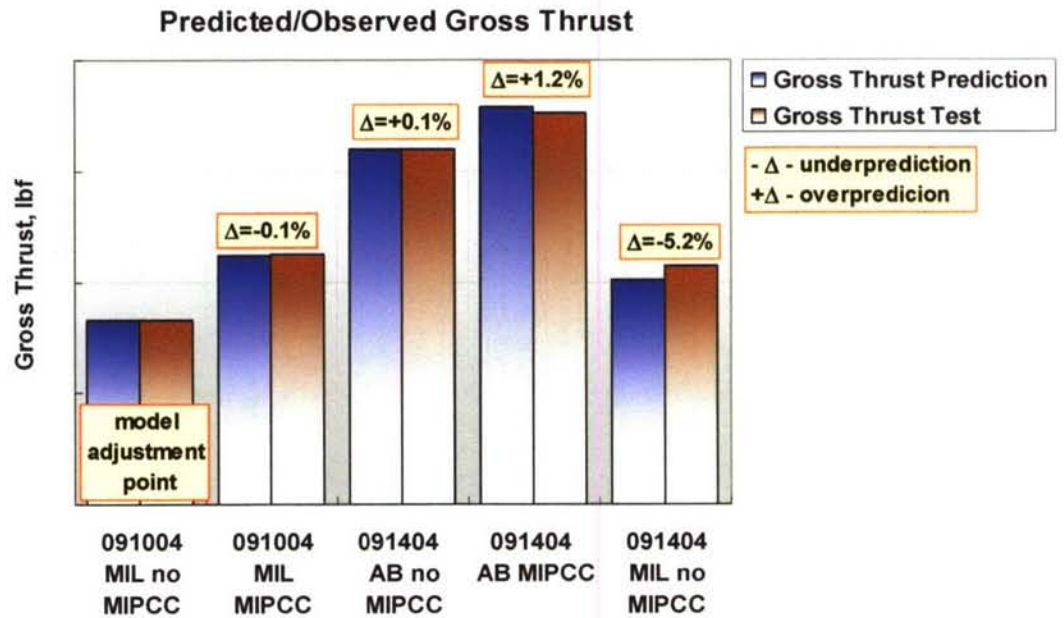


Figure 34. Comparison of the predicted and observed MIPCC engine thrust.

3.7 Concluding Remarks on MIPCC

The feasibility of a launch system using MIPCC as the primary propulsion system of the reusable first stage has been proven in numerous analytical, design, and experimental efforts. It is commonly recognized, that MIPCC is a key enabling technology for such launch system types. Flying at high Mach number and altitude, the engine works within conventional operating envelopes due to the judicious use of coolant injection. This permits limited technology demonstration prior to a flight test program. For this demonstration, MTB has been developed and proven to provide high Mach

number/high altitude conditions at the engine entrance. The highest Mach number of 3.5 at an altitude 81,000 ft has been simulated to date with full- scale air flow rate.

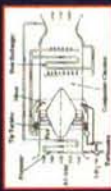





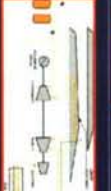

An F100 engine with MIPCC installed generates thrust as predicted at Mach 1.63 and an altitude of 35,000 ft trajectory point . 34% gross thrust improvement at MIL mode has been observed at MTB for Mach 1.6 engine inlet conditions (water/air ratio 2.2%).

The NEPP model adequately describes MIPCC engine performance at the demonstrated MTB conditions. It has been verified in five different operational modes.

4.0 CONCLUSION

Eight cycles were considered in this lecture. The common feature is judicious use of thermodynamic properties of the working fluids. In most cases (ATREX, ATRDC, KLIN, AspiRE, MIPCC) this permits performance enhancement and/or flight envelope expansion compared to the basic cycles. In other cases (SFC, TFC) it permits enhancement of the internal cycle thermal management and either operational range extension (SFC) or enhancement of the engine reliability and weight characteristics (TFC). A summary of the cycles considered is presented in Table 4.

Table 3. Summary of the synergistic cycles.

Cycle	Application	Pros/Advantages	Cons/Challenges	Synergistic Features
 <p>ATREX – expander air turbo ramjet</p>	<ul style="list-style-type: none"> • First stage of the TSTO • Mach 0-6 	<ul style="list-style-type: none"> • High I_{sp} • Low development and production cost • High TRL 	<ul style="list-style-type: none"> • Low T/W ratio • Low specific thrust • Only LH_2 fuel 	<p>LH_2 works as a :</p> <ul style="list-style-type: none"> • Coolant • Turbine gas • Fuel
 <p>ATRDC – deeply cooled air turbo rocket</p>	<ul style="list-style-type: none"> • SSTO • First stage of the TSTO • Mach 0-6 	<ul style="list-style-type: none"> • High T/W ratio • High specific thrust • Can be integrated with ramjet 	<ul style="list-style-type: none"> • Moderate I_{sp} • Complexity • Only LH_2 fuel • Low TRL 	<p>LH_2 works as a :</p> <ul style="list-style-type: none"> • Coolant • Turbine gas • ATRDC fuel (Ramjet fuel)
 <p>KLLN cycle – thermally integrated T.J and LRE</p>	<ul style="list-style-type: none"> • SSTO • First stage of the TSTO • Mach 0-6 	<ul style="list-style-type: none"> • Balance between I_{sp} and T/W • Promising launcher performance 	<ul style="list-style-type: none"> • Complexity • Only LH_2 fuel • Low TRL 	<p>LH_2 works as a :</p> <ul style="list-style-type: none"> • Coolant • Rocket turbine gas • Rocket fuel • Turbine fuel
 <p>AspiRE cycle – rocket engine utilizing liquefied air on the “low speed” mode</p>	<ul style="list-style-type: none"> • SSTO • First stage of the TSTO • Mach 0-6 	<ul style="list-style-type: none"> • Balance between I_{sp} and T/W • Promising launcher performance • Simplicity compared to KLLN cycle 	<ul style="list-style-type: none"> • Only LH_2 fuel • Low TRL 	<p>LH_2 works as a :</p> <ul style="list-style-type: none"> • Coolant • Rocket turbine gas • Fuel
 <p>MIPCC engine – conventional turbine with coolant injection prior to compression</p>	<ul style="list-style-type: none"> • SSTO • First stage of TSTO • Other accelerators • Mach 0-4.5 	<ul style="list-style-type: none"> • High thrust • Extended flight envelope • High TRL, applicable to existing turbines 	<ul style="list-style-type: none"> • Reduced I_{sp} • Increased length for water evaporation 	<p>Water injection provides:</p> <ul style="list-style-type: none"> • Lower air inlet temperature • Higher air compression • Higher air flow
 <p>Turbine engine with rocket augmentation</p>	<ul style="list-style-type: none"> • SSTO • First stage of TSTO • Other accelerators • Mach 0-4.5 (with MIPCC) 	<ul style="list-style-type: none"> • High thrust • May reduce airflow reqs. • Flexible operation • Applicable to existing turbines 	<ul style="list-style-type: none"> • Low I_{sp} • Requires AB redesign 	<p>Oxidizer injection provides:</p> <ul style="list-style-type: none"> • Higher engine mass flow • Higher AB temperature
 <p>SFC scramjet – scramjet with closed loop second fluid cooling</p>	<ul style="list-style-type: none"> • Launch vehicle • High speed cruise vehicle • Mach 4-8+ 	<ul style="list-style-type: none"> • Extended flight Mach numbers for HC fuels • Higher I_{sp} at high Mach • Higher thermal margin 	<ul style="list-style-type: none"> • Complexity • Low TRL 	<p>Second fluid is used to :</p> <ul style="list-style-type: none"> • Cool engine • Drive turbopump • Generate power (optional)
 <p>TEC rocket engine – cycle with closed loop third fluid cooling</p>	<ul style="list-style-type: none"> • Booster rocket engine • Upper stage rocket engine 	<ul style="list-style-type: none"> • High I_{sp} compared to GG cycle • 2-3 times lower max cycle pressure compared to SC cycle • Flexible fuel 	<ul style="list-style-type: none"> • Additional unit – heat exchanger/condenser • Start up/shut down issues 	<p>Third fluid is doing job usually done by fuel or hot gas from preburner. This allows lower max cycle pressure and turbine loads</p>

ACKNOWLEDGEMENT

The author worked on the propulsion cycles described in this lecture during his employment/scholarships with six different organizations/companies in four different countries : CIAM (Russia), NAL and ISAS (currently JAXA, Japan), Techspace Aero (Belgium), MSE (USA), and ATK GASL (USA). He would like to thank the managers and engineers of these organizations as well as the government organizations who inspired his thinking and supported his efforts.

REFERENCE

- [1] B. McKinney, "Turbojet with precompressor injected oxidizer," United States Patent 6,644,015, Nov. 11, 2003.
- [2] N. Tanatsugu, T. Sato, V. Balepin, et al., "Development Study on ATREX Engine," *Acta Astronautica* Vol.41, No. 12, pp.851-862, Pergamon, 1997.
- [3] N. Tanatsugu, "Method for Improving the Performance of a Cryogenic Heat Exchanger under Frosting Conditions," United States Patent No. US 6,301,928, Oct 16, 2001.
- [4] A. Rudakov and V. Balepin, "Propulsion Systems with Air Precooling for Aerospaceplane," SAE Technical Paper Series 911182, 1991.
- [5] V. Balepin, "Propulsion System for Earth-to-Orbit Vehicle," United States Patent No. US 6,227,486, May 8, 2001.
- [6] V. Balepin, P. Czysz, R. Moszee, "Combined Engine for a Reusable Launch Vehicle (KLIN Cycle)," *Journal of Propulsion and Power*, Volume 17, Number 6, Nov-Dec 2001, pp.1239-1246.
- [7] V. Balepin, "Multi-Mode Multi-Propellant Liquid Rocket Engine," United States Patent No. US 6,619,031, Sept 16, 2003.
- [8] V. Balepin, G. Liston, R. Moszee, "Combined Cycle Engines with Inlet Air Conditioning," AIAA-2002-5148, 2002.
- [9] V. Balepin, "Method and Apparatus for Reducing the Temperature of Air Entering a Compressor of a Turbojet Engine by Variably Injecting Fluid into the Incoming Air," United States Patent No. US 6,202,404, Mat. 20, 2001.
- [10] R. Freese, J. Wazyniak, "Rocket Augmentation for Combined Cycle Turboaccelerator Jet Engine," United States Patent Application Publication No. US 2006/0032230, Feb16,2006.
- [11] V. Balepin, "Concept of the Second Fluid-Cooled Scramjet", to be presented at ISABE-2007.
- [12] V. Balepin, "Rocket Engine," United States Patent No. US 6,769,242, Aug 3, 2004.
- [13] V. Balepin, "Concept of the Third Fluid Cooled Liquid Rocket Engine," AIAA-2006-4695, 2006.
- [14] El-Wakil, M.M., "Powerplant Technology," McGraw-Hill, Inc., 1984.
- [15] V. Balepin, R. Engers, T. Spath, C. Ossello, "MIPCC Technology Development," ISABE-2005-1297, 2005.

von Karman Institute for Fluid Dynamics

RTO-AVT-VKI Lecture Series 2007

**ADVANCES ON PROPULSION TECHNOLOGY
FOR HIGH-SPEED AIRCRAFT**

March 12-15, 2007

PULSED DETONATION PROPULSION

F. Schauer
Wright-Patterson AFB, USA

PULSED DETONATION PROPULSION

March 2007

APPROVED FOR PUBLIC RELEASE; DISTRIBUTION UNLIMITED



The views expressed in this presentation are those of the author and do not reflect the official policy or position of the United States Air Force, Department of Defense, or the U. S. Government.

Dr. Fred Schauer

Head,



Air Force Research Laboratory
Wright-Patterson AFB

Intro to Pulsed Detonation Propulsion

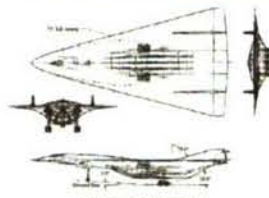


Fig. 1. Reproduced from the article by Schauer, 2006.

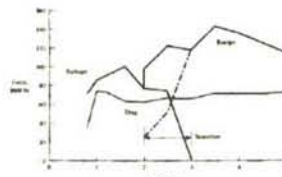


Fig. 2. Reproduced from the article by Schauer and Dring, 2006.

Pulsed Detonation Engine

(PDE): Cheap, simple, high performance engine that is highly scalable and efficient across a broad operating range (Mach 0-4+)

Problems:

- Practical Fuel Initiation
- Performance Data
- Research Capability

What is a PDE / Detonation?

Detonation: Usually avoided solution to combustion equations that takes uncompressed fuel/air to **Mach 5, 6x compression with no moving parts**

Pressure in detonation tube

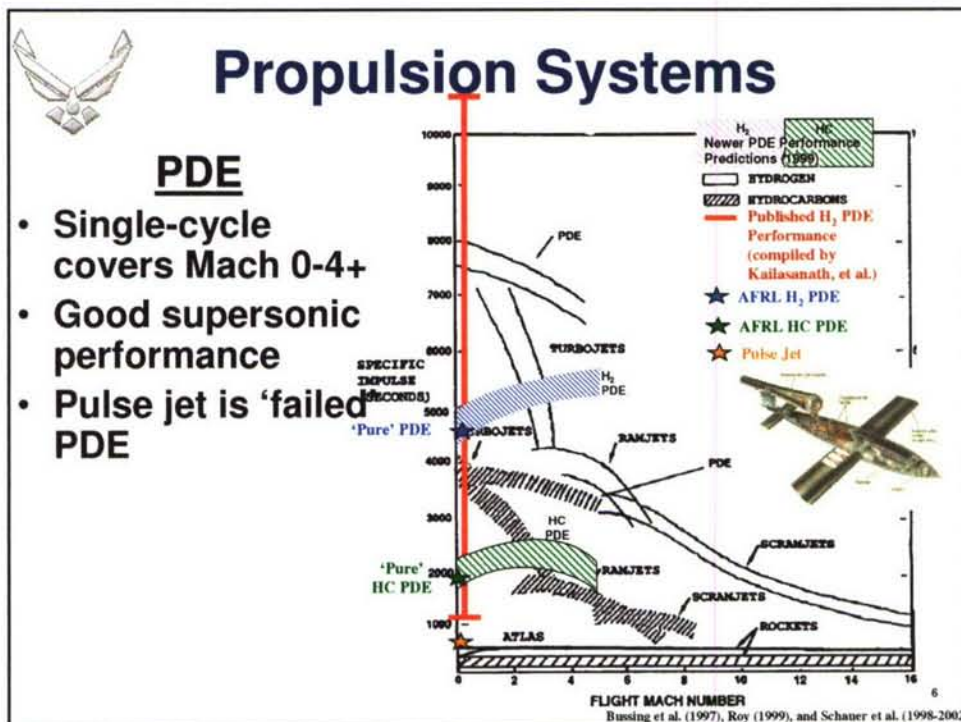
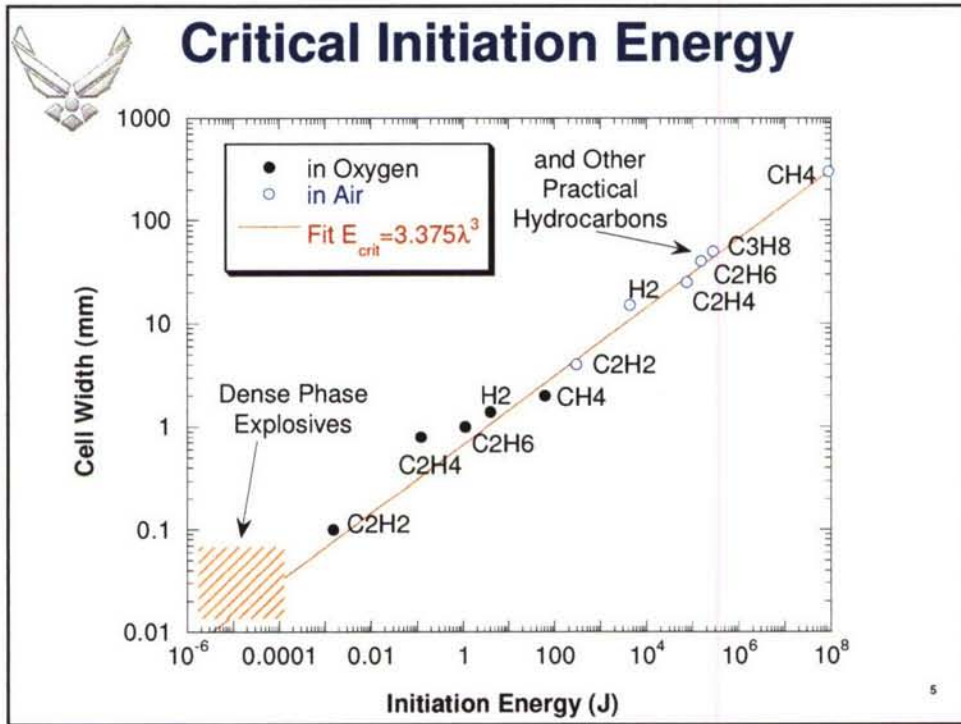
Deflagration vs Detonation

Deflagration (Conventional Combustion)

- Subsonic Flame
- Heat Release => Expansion


Detonation

- Supersonic Flame Propagation
- Heat Release => Pressure Rise
- 20-40% higher temperatures



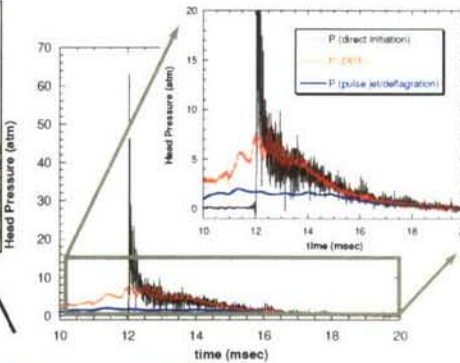
P51D with Pulsejets

Experimental Aircraft at WPAFB post-WWII




North American P-51D
USAF Museum Photo Archive

Detonation versus Pulsejet


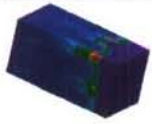


- Ford copy of German Argus AS014 pulsejet
- 8kN (1,800 lb) thrust
- Cost \$1,600



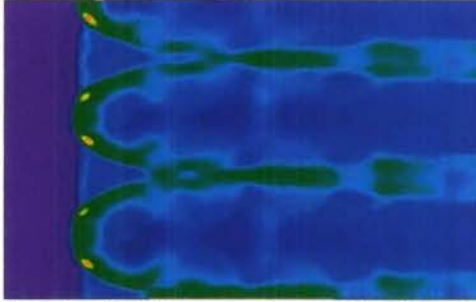
- Rolls-Royce V1650
- 1260kw (1,695 hp)
- Cost \$25,000

Combustion / Detonation Modeling





In House CFD


- 3D Deflagration/ Detonation Modeling
- Initiation and DDT Studies
- Detonation Propagation
- Confinement/ Obstructions
- Shock Reflections
- Chemistry-fluid dynamic interactions




Moving Ref. Frame at Detonation Speed



Peak Pressure or 'Smoke Foil' Traces with Particle Traces




D-Bay: Pulsed Detonation Research Facility




250 kN Thrust Research Facility

Full Scale Explosion Proof Engine Research Facility

- 3 kg/sec 6 atm air supply
- High Capacity Inlet/Exhaust Stacks
- Direct Connection to Liquid Fuel Farm
- Choked Flow Measurements - Fuel and Oxidizer
- Hardened Remote Control Room
- 16 High Frequency DAC Channels, up to 5Mhz
- High-Speed Digital Imaging Systems




Damped Thrust Measurements
10-5000 N capacity




Isolated and Protected


That's a .4m thick steel door in a .7m thick reinforced concrete wall!

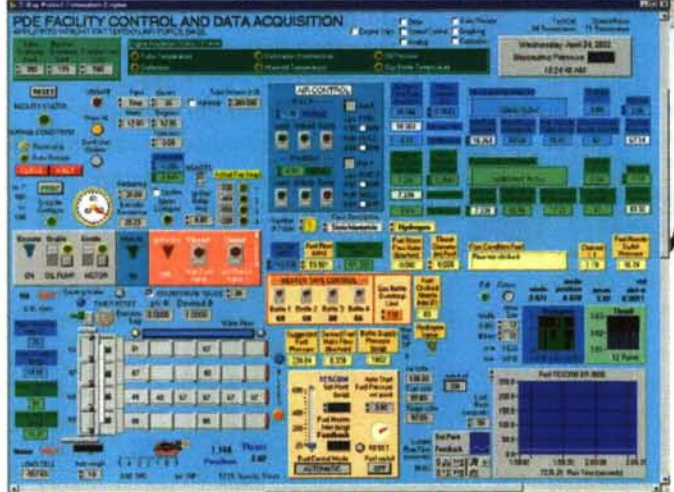


Remote Control and High-Frequency DAC



Integrated Remote Controls for: Facility, Engine, and Data Acquisition



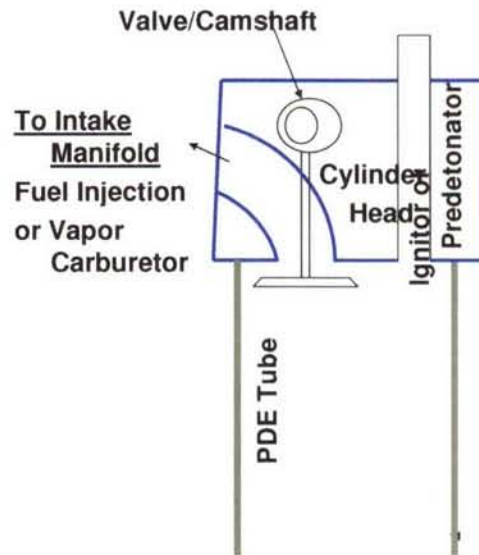


Jeff Stutrud



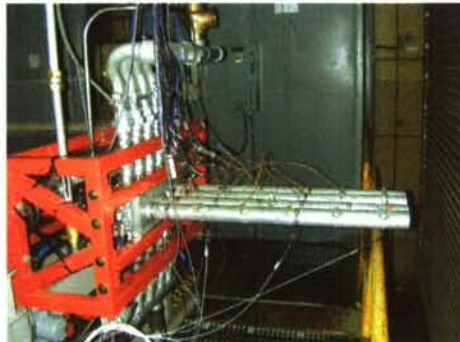
Adapting OHC Cylinder Head to PDE

- Automotive Engines Designed for 8-20 Pressure Ratio
- Provisions for Valving, Fuel Injection, Timing, and Cooling
- Vapor Carburetor Available
- Bolt Flanged PDE Tubes to Cylinder Head
- Multiple Tubes/'Header' Effect
- Extra Valves for Predetonator or Purge Cycles
- Cheap/Mass Produced



In-House PDE Research Engine

GM Quad 4 DOHC, 4 Cylinder Pulsed Detonation Engine



- Lowcost Technology - < \$2,000 Initial Hardware Investment
- Pontiac Grand Am Cylinder head (formerly 150 BHP) converted to research PDE
- Test-bed for PDE Research, Benchmarking Performance
- Predetonator/Initiator Development
- High Frequency Operation
- Multi-tube Effects
- Pulsed Ejector Research

- Modified Automobile IC Engine
- Adapter Plate Mounts Detonation Tubes
 - 1-4 Tubes
- Electric Motor Driven Camshafts
 - 0.5-40+ Hz currently (per tube)
- Vapor Fuels: Hydrogen, Propane, etc.
- Liquid FI: Gasoline, Ethanol, JP, etc.



Stock Intake Manifold with Ball Valve Selection of 1-4 Detonation Tubes
(Purge Manifold Similar)

12

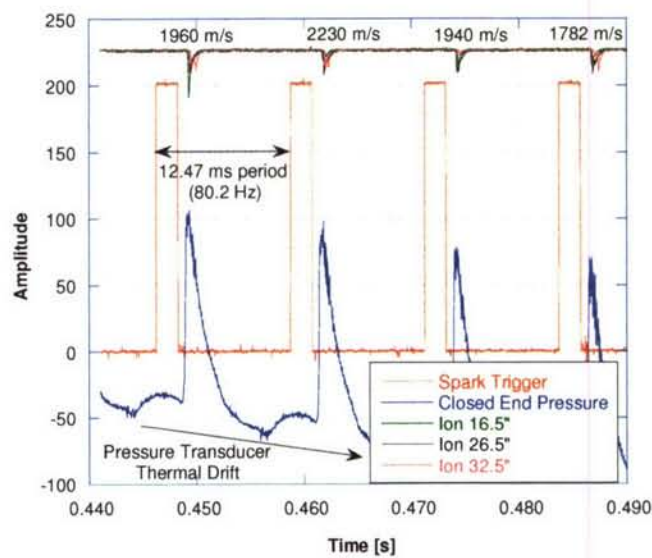


In-House Research 'Quad- 4' PDE




13
Combustion Branch

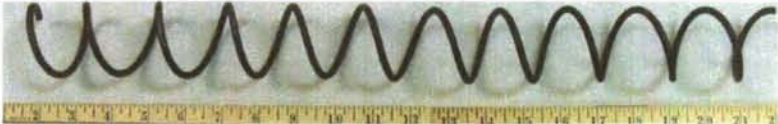
80Hz H₂/air with a Quad 4 Cylinder Head


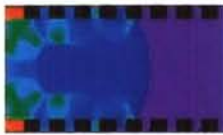


14





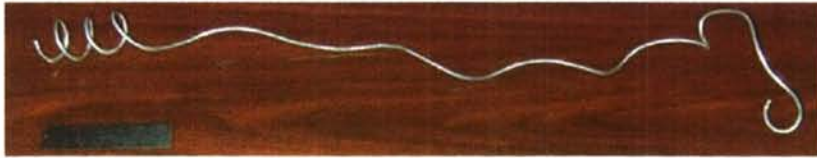
Schelkin Shocking Spirals







DDT through flame acceleration
RESULT: Dramatically increased thrust,
 DDT between 3 and 9" instead of ~36"







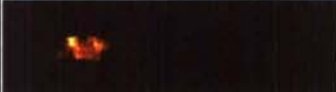
15




Polycarbonate tube with Schelkin Spiral




Formation of hot spot




Propagation of hot spots




Microexplosions



DDT



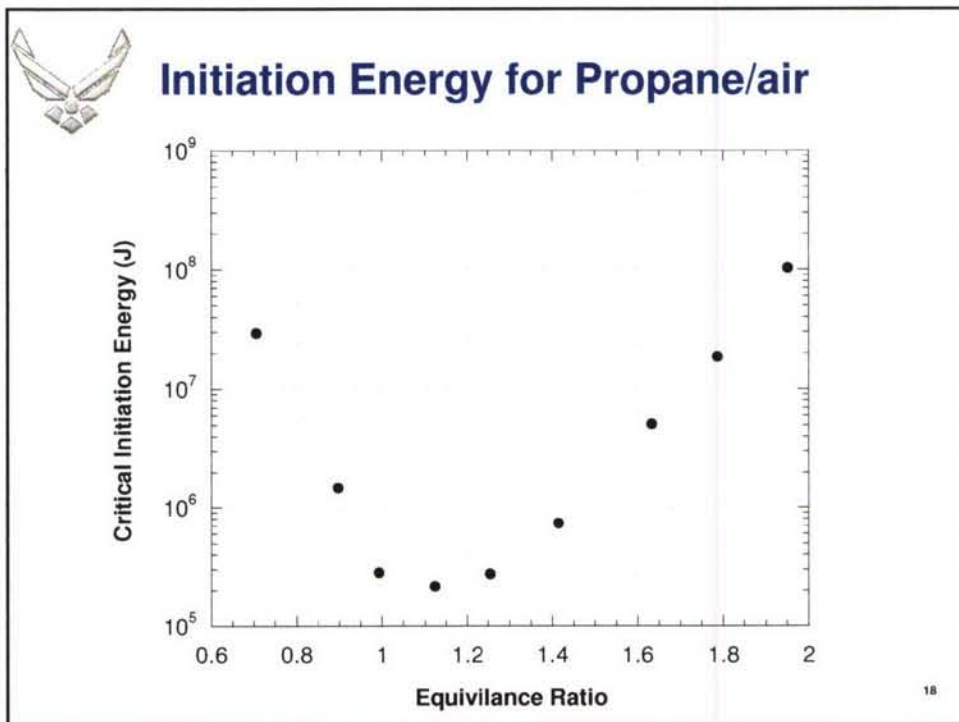
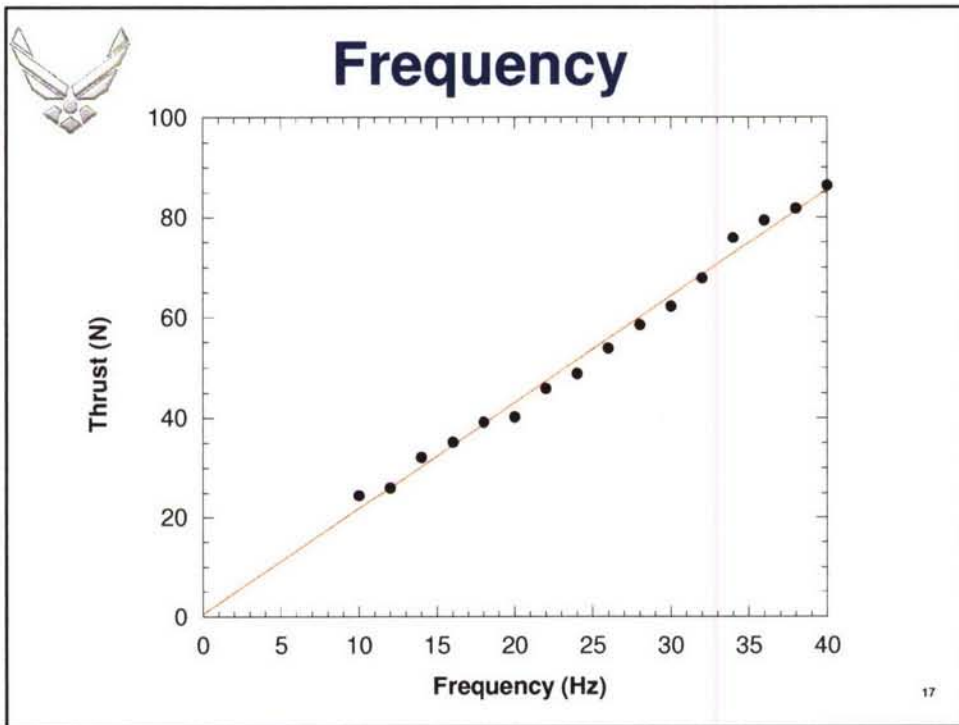
Detonation propagation (to right) & retonation propagation (to left)

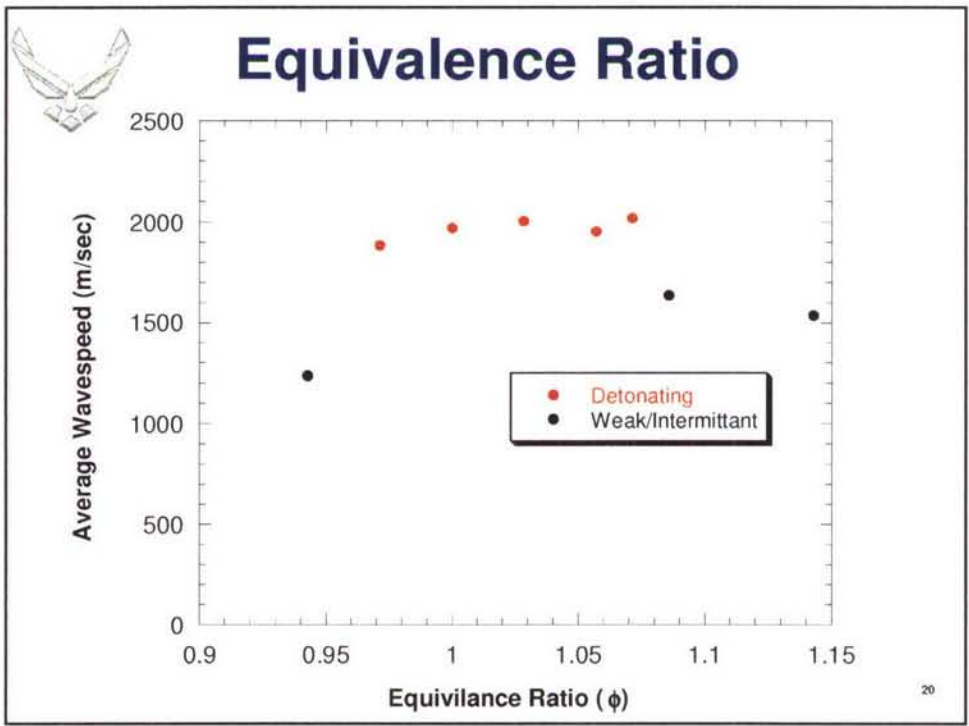
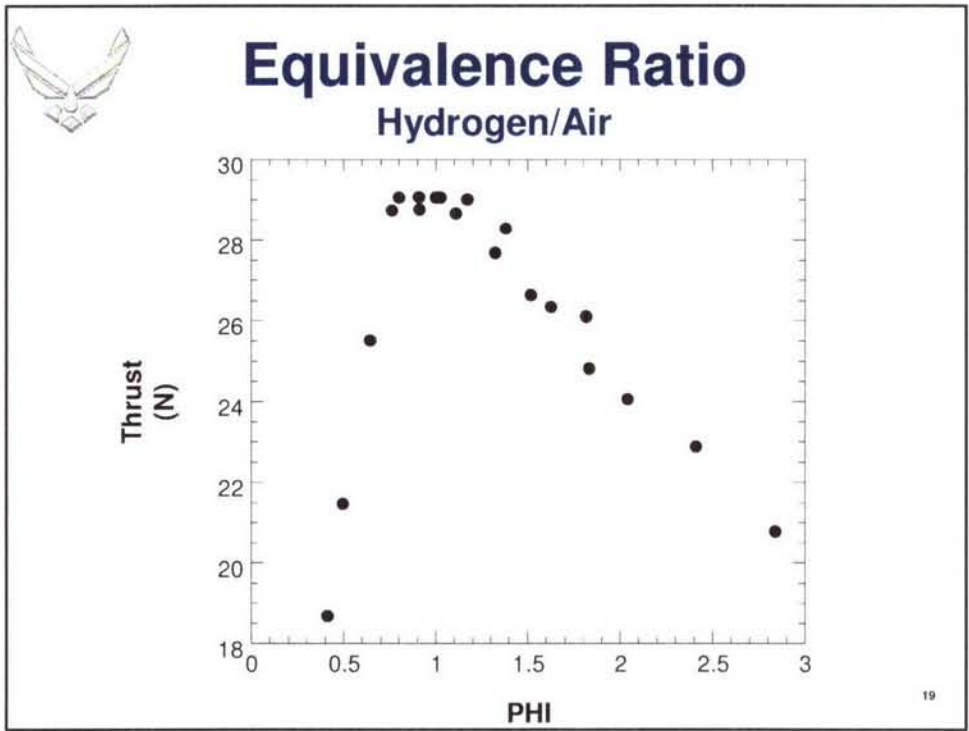


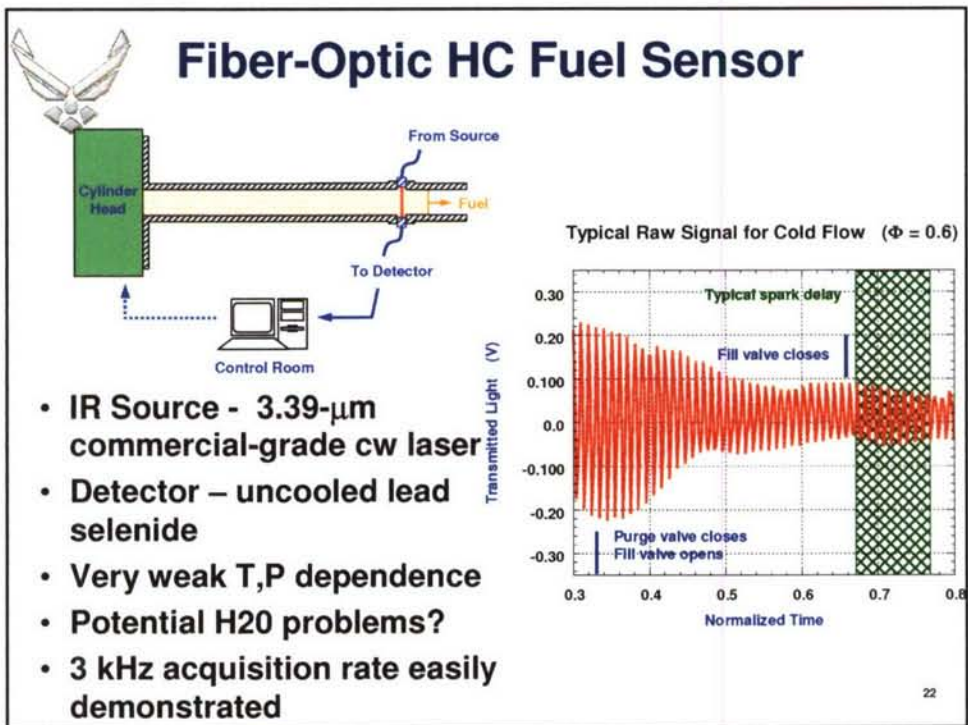
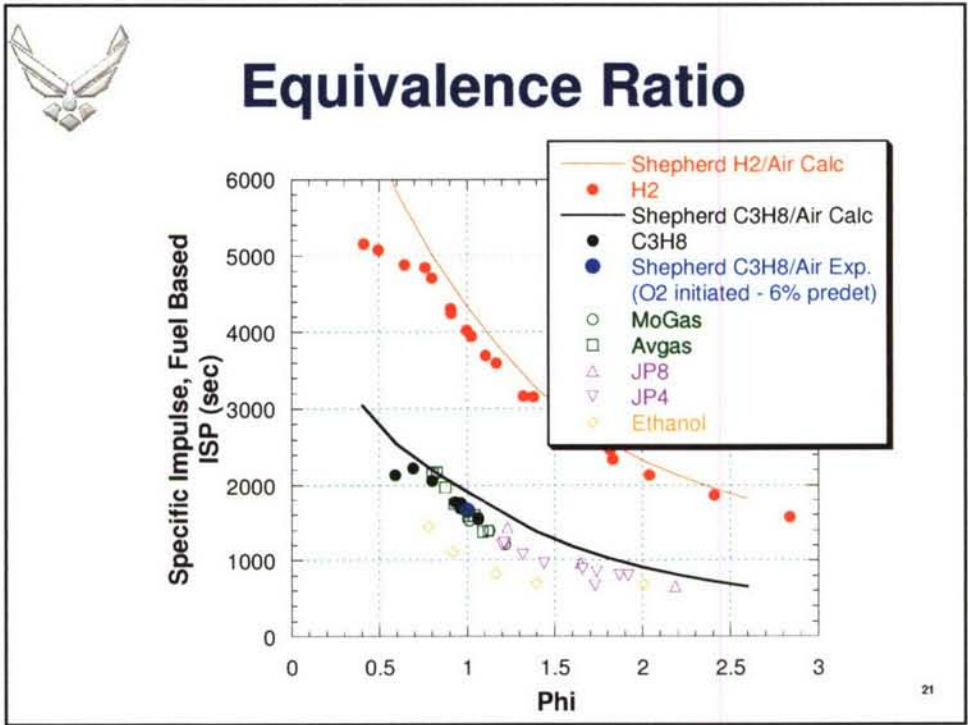
Blow down/expansion propagation (right to left).

Typical Events during DDT

16





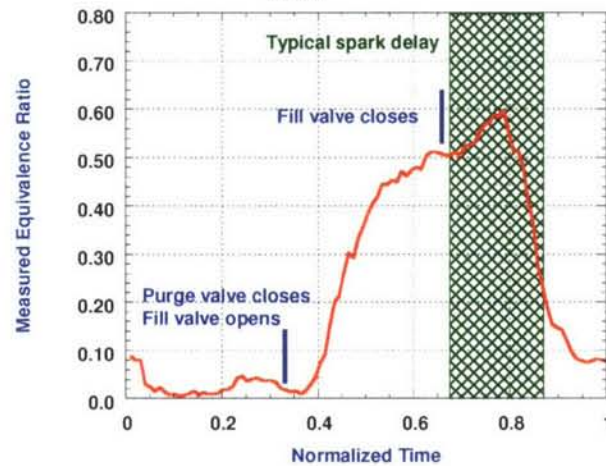




Dynamic Equivalence Ratio

Quantitative Time-Varying Propane Equivalence Ratio Derived From Raw Sensor Signal

Cold Flow: $\Phi_{\text{desired}} = 0.6$, fill frac. = 1, 20 Hz

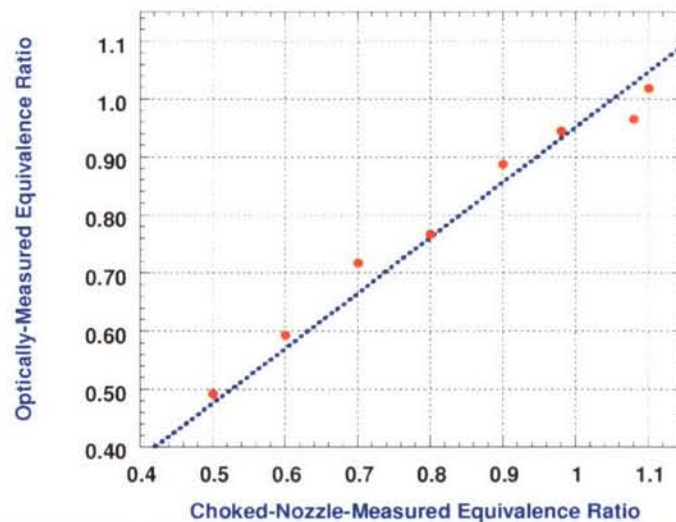


23

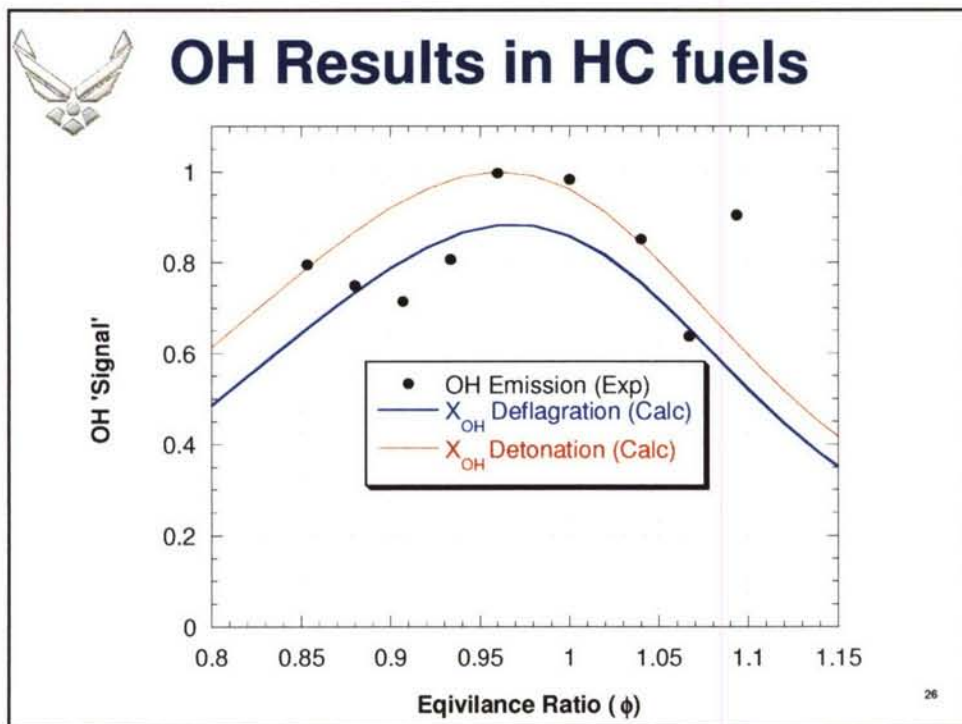
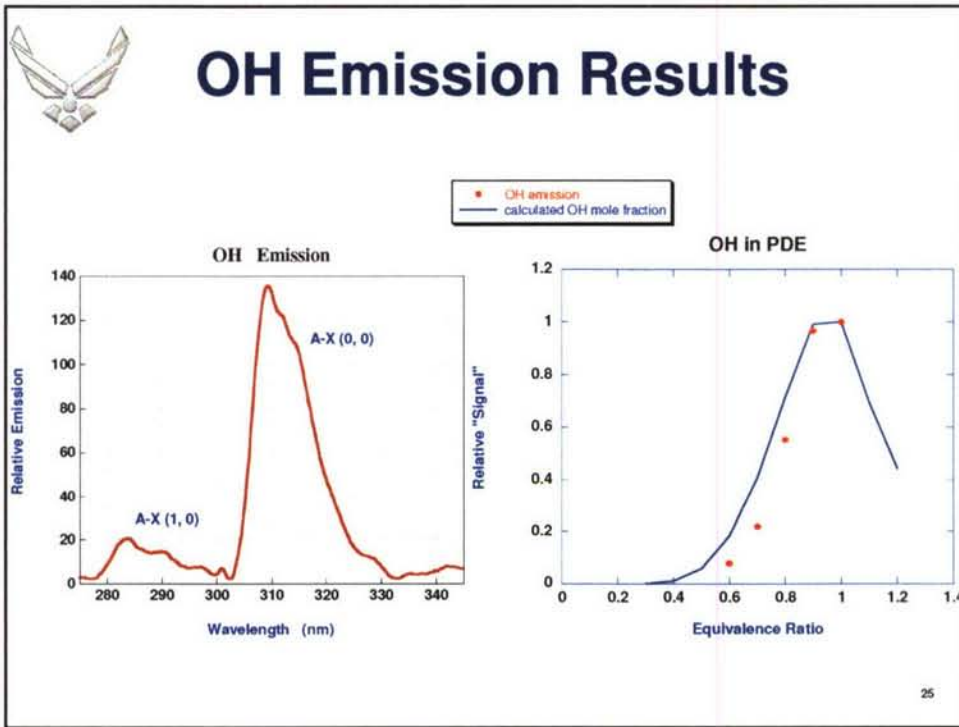


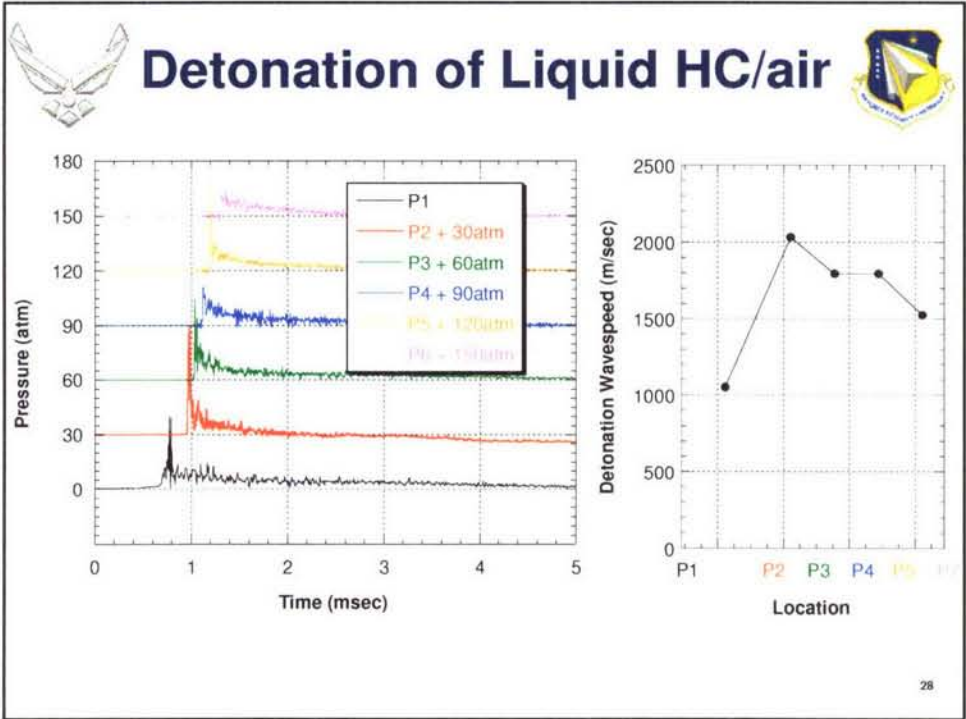
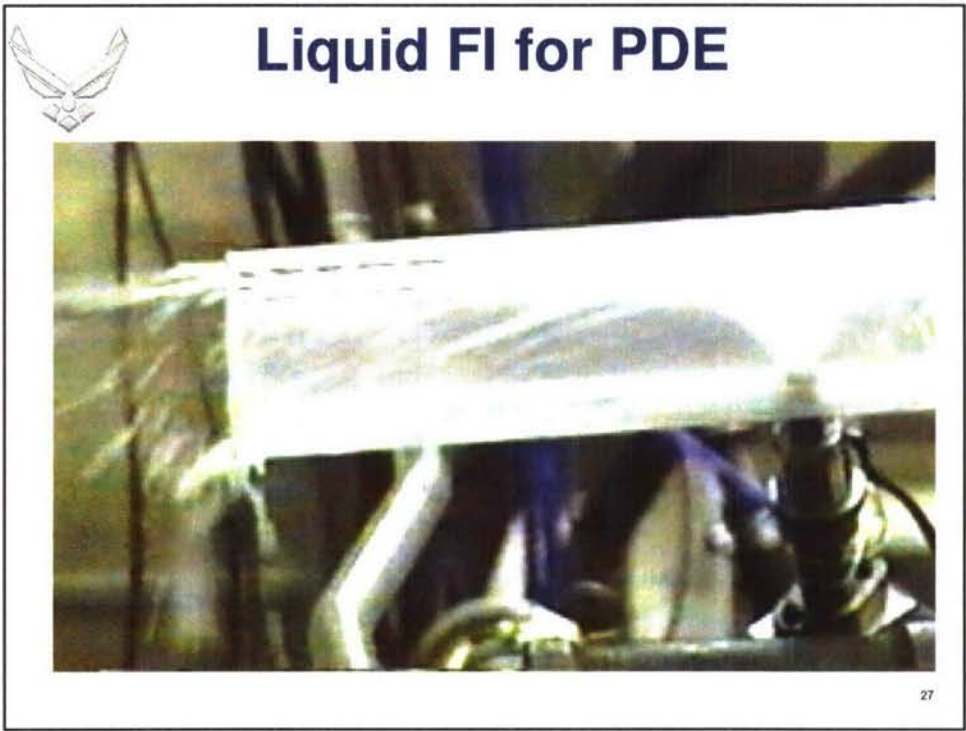
Propane Sensor Results

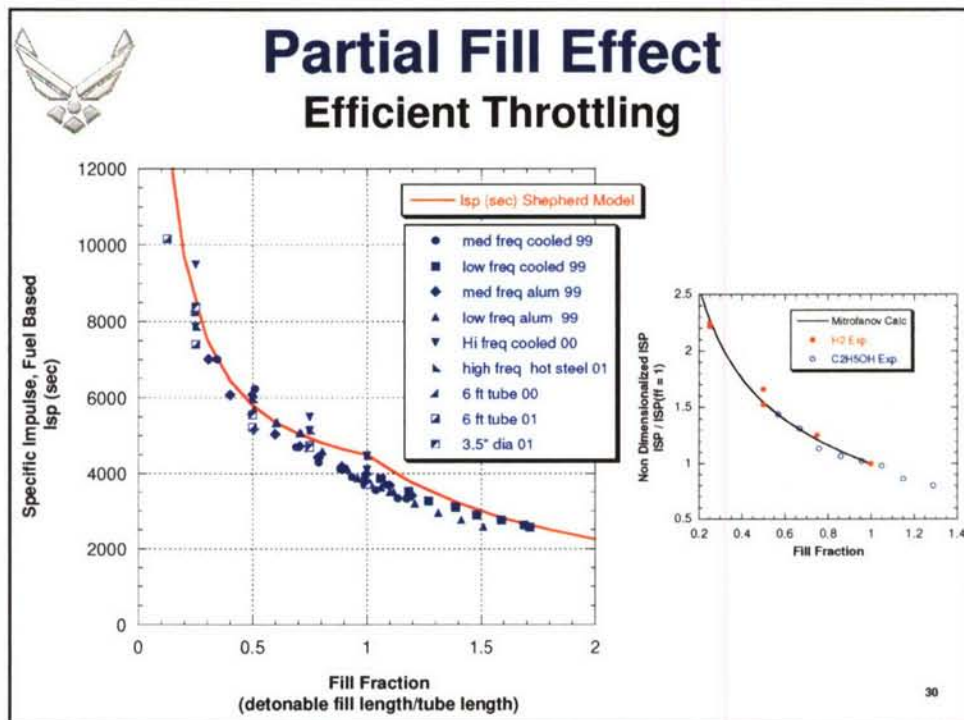
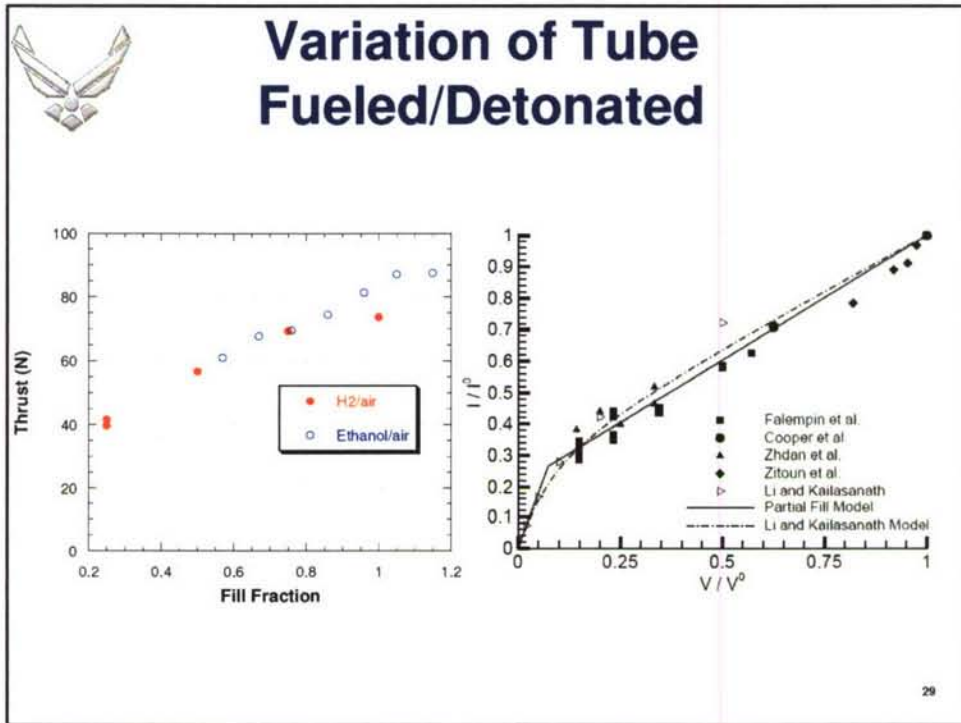
Measured Φ Versus Mass Flow Φ

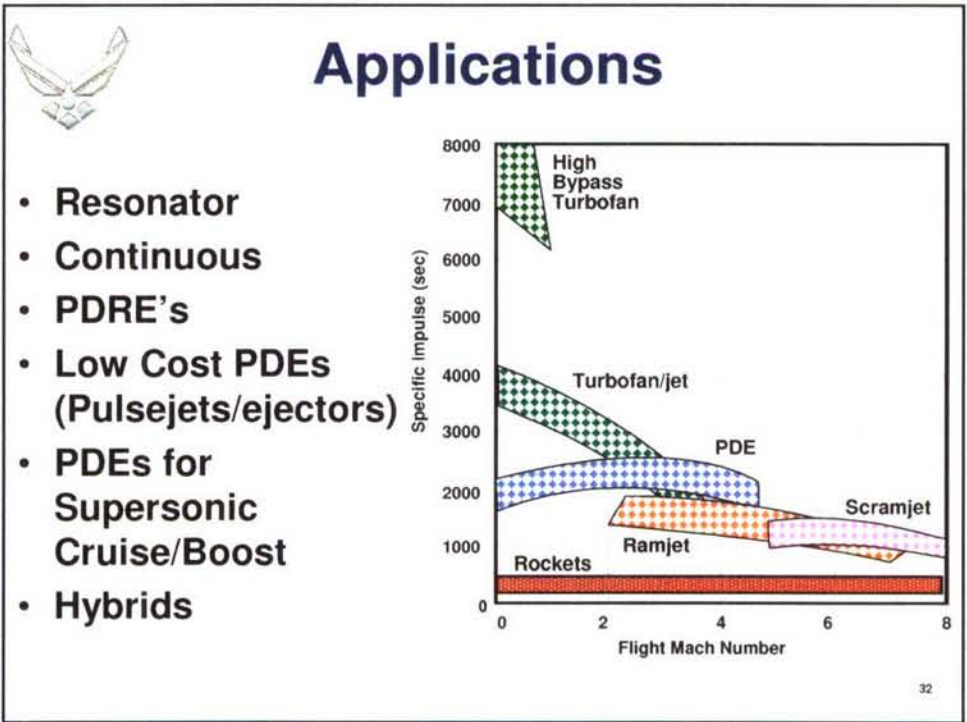
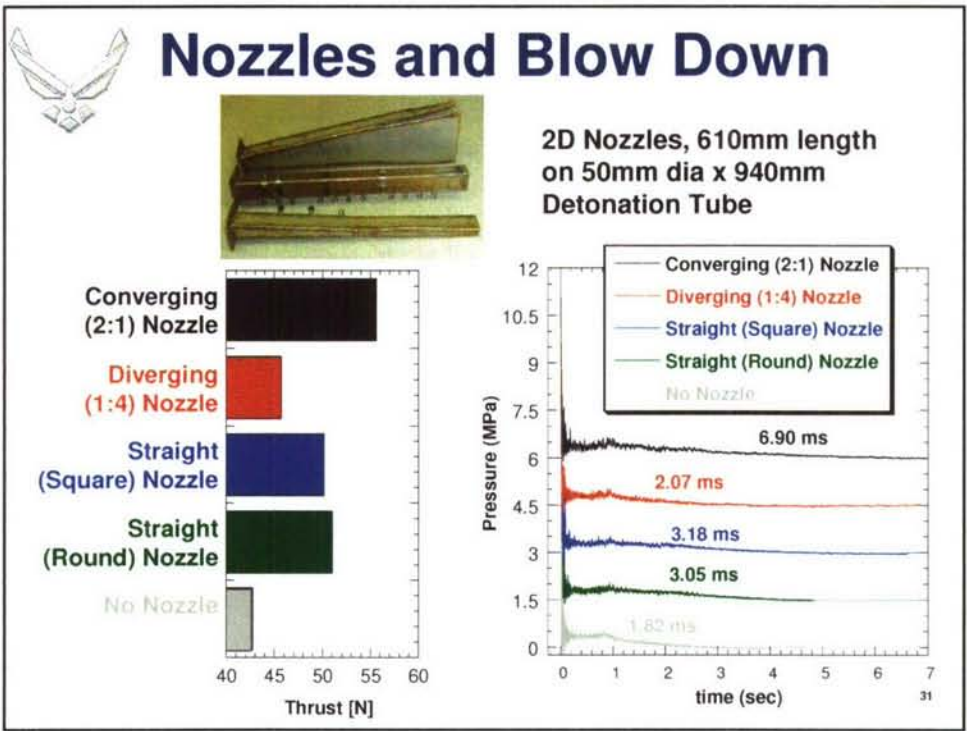


24








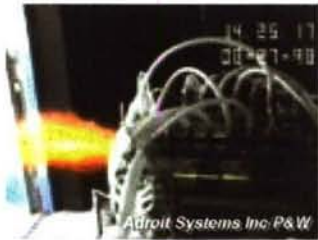


PDREs (Pulsed Detonation Rocket Engines)


- Same benefits as increased chamber pressure, but reduced feed system requirements
- Throttling @ operating frequency
- Unsteady nozzles/valving



AFRL




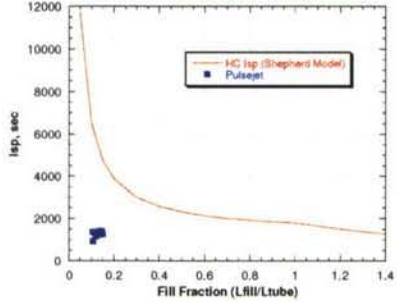
Adroit Systems, Inc. P&W



Adroit Systems Inc P&W

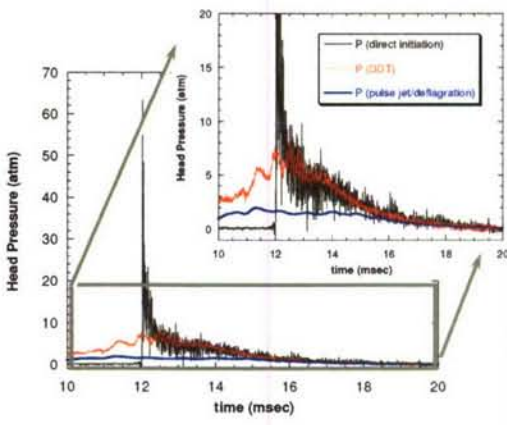
33

Pulsejet Performance

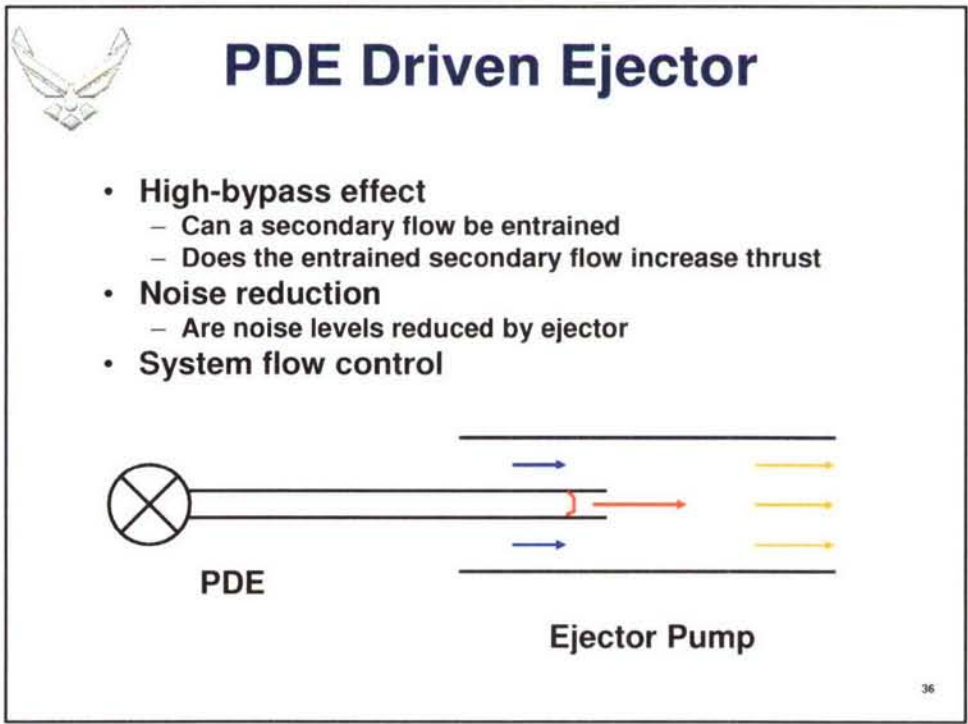
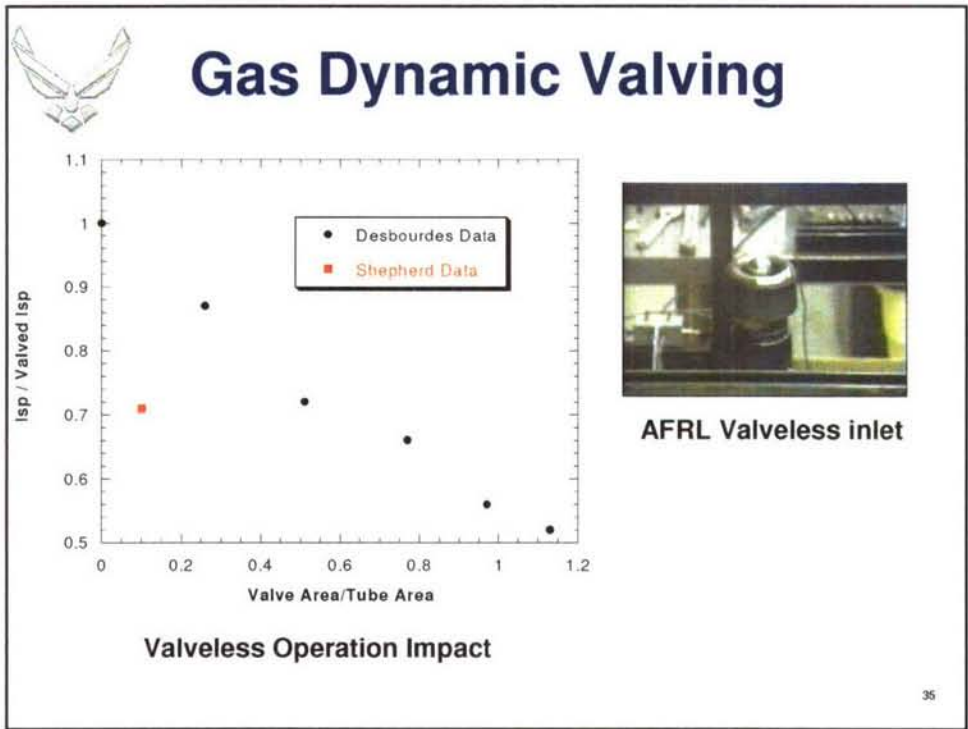



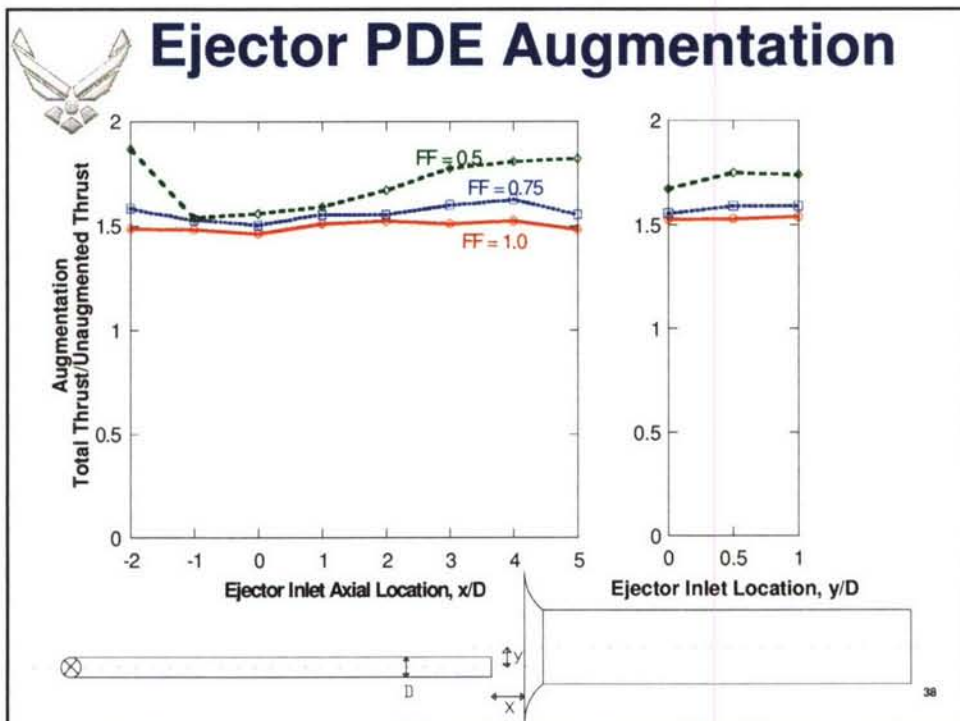
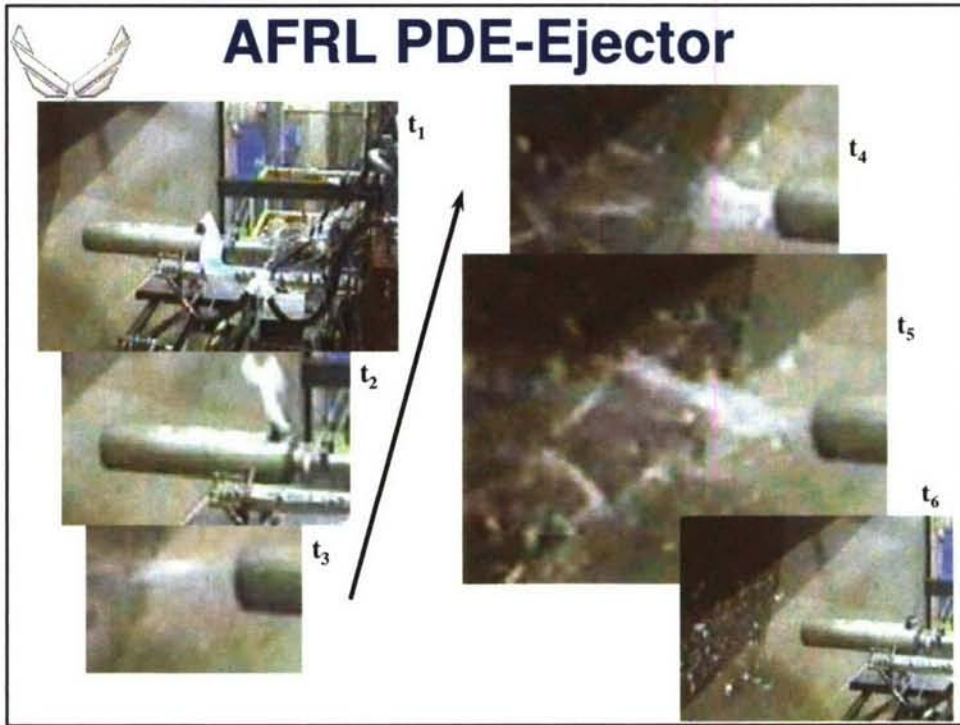
Detonation versus Pulsejet

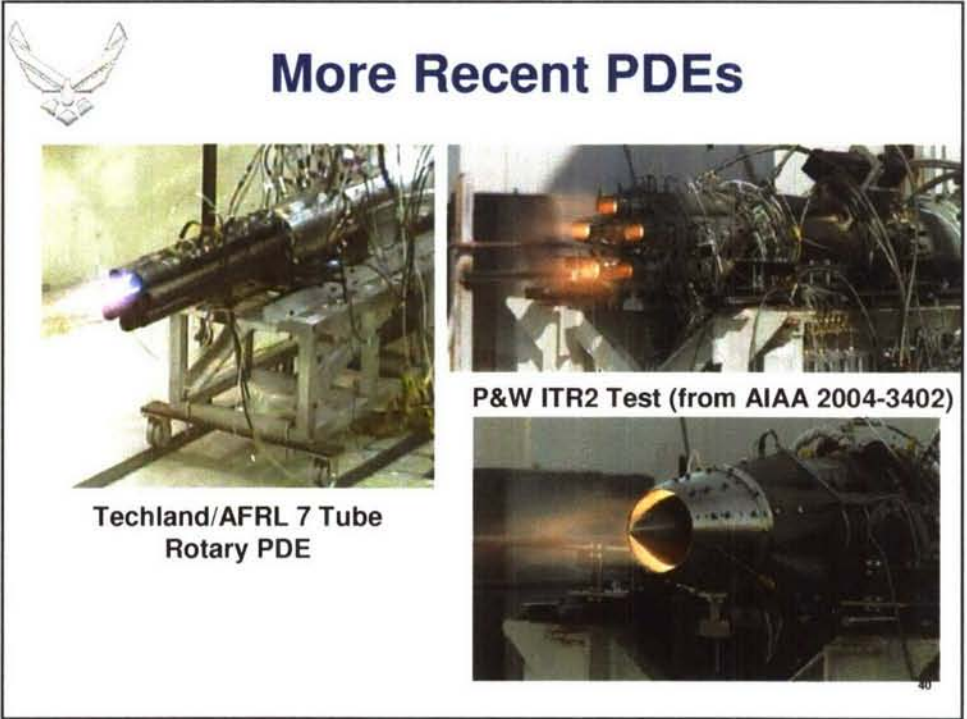
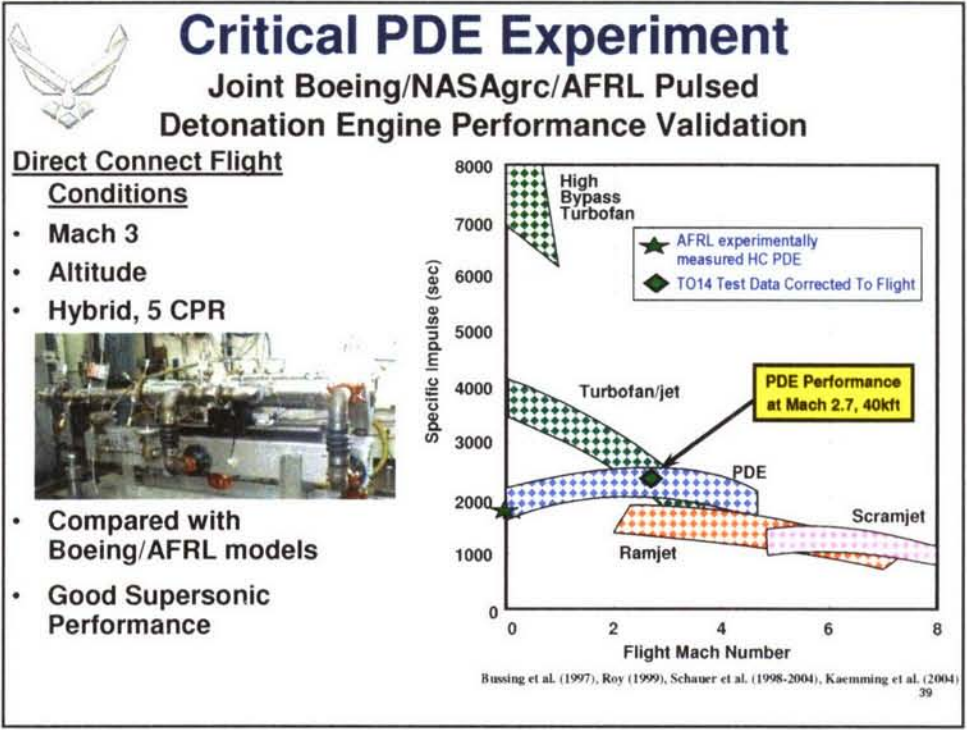
Detonation versus Pulsejet

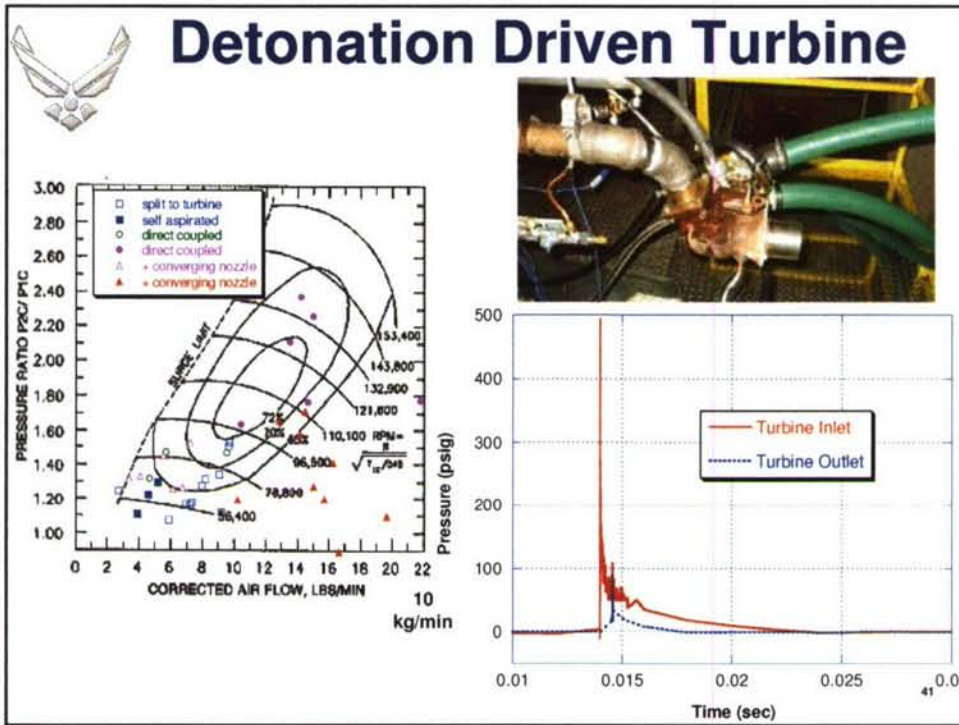


34









Detonation Driven Turbines

GE 600kW Axial Flow Turbine

AFRL Centrifugal Turbine

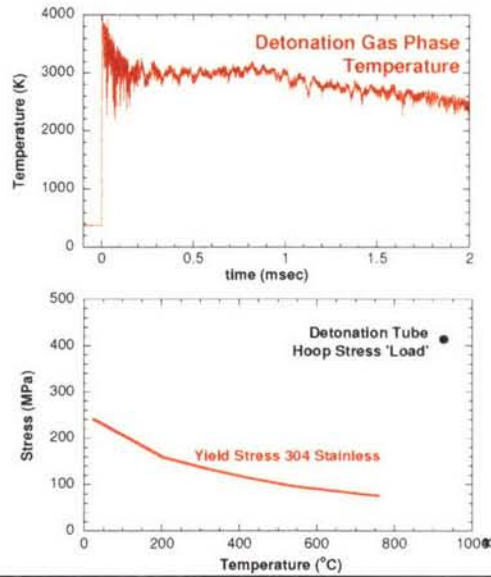
JFS-100-13A Axial Turbine

- Significant Hybrid Turbine Cycle Efficiency Improvement Theoretically Possible (5-30% vs conventional)
- Turbines Surviving
- Turbine Component efficiency is key

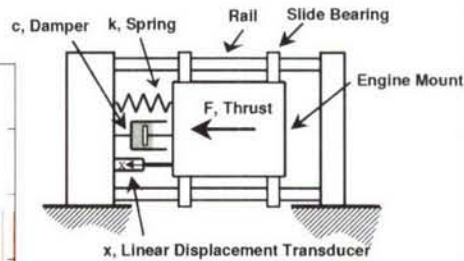
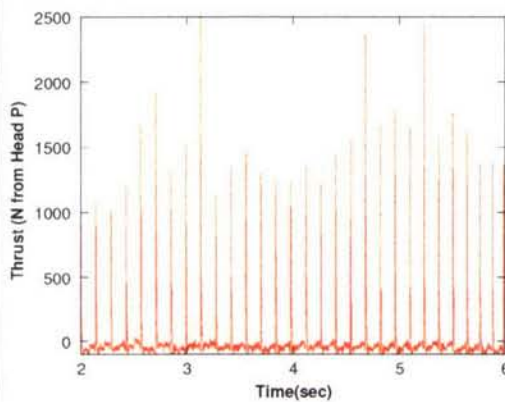


Technical Challenges

- Detonation Initiation of Practical Fuels
- Heat Transfer
- Aspiration
- Unsteady Flows
- Engine Longevity
- Airframe Vibration
- Acoustics



Vibration Loading

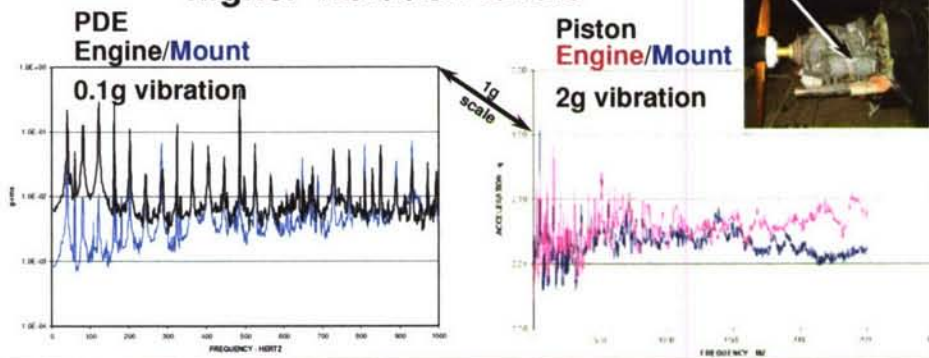


- Pulsed thrust creates oscillating excitation
- Simple frequency/harmonics easy to tune out via spring/damping mounts

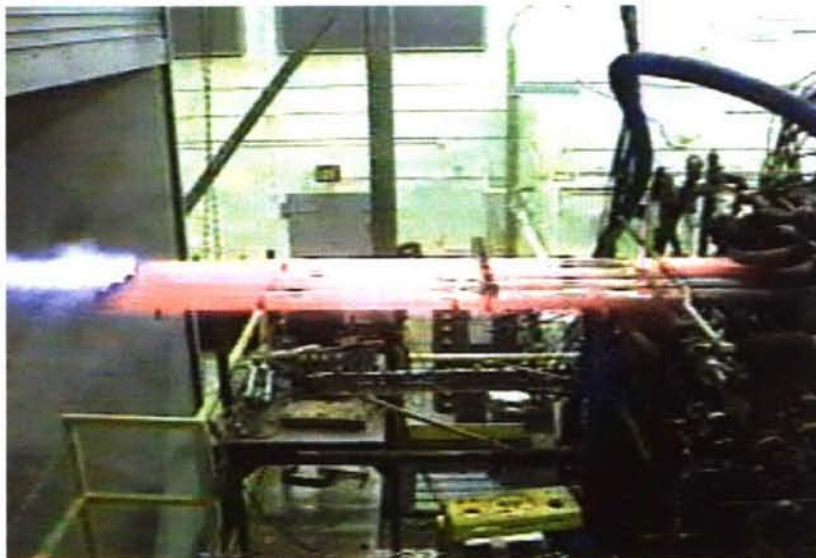


Vibration Measurements

- Overall detonation vibration levels considered low
- Conventional IC engines exhibit higher vibration levels



0.6mm Detonation Tube Walls

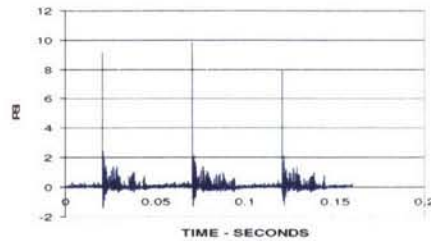
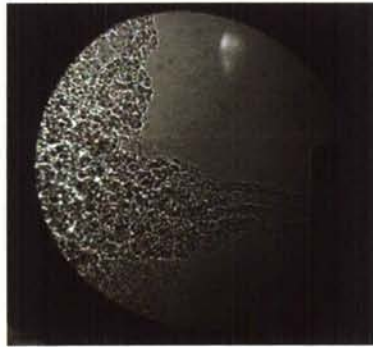


46



PDE Acoustics

TYPICAL TIME HISTORY FOR
20 HERTZ FIRING FREQUENCY,
FILL FRACTION AND
EQUIVALENCY RATIO OF 1.0



Highly Directional
Peak Tone

- 190+ dB
- short duration

RMS

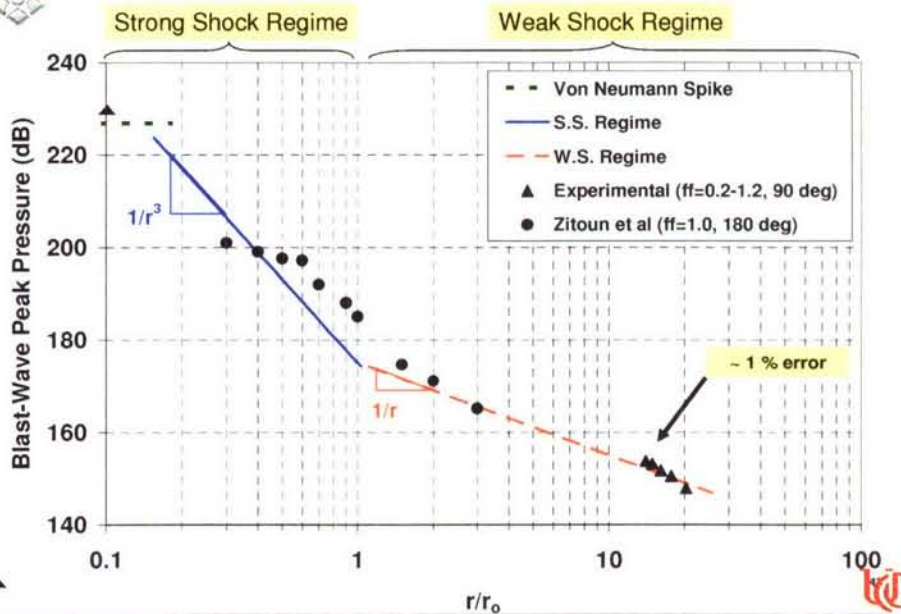
- 170 dB

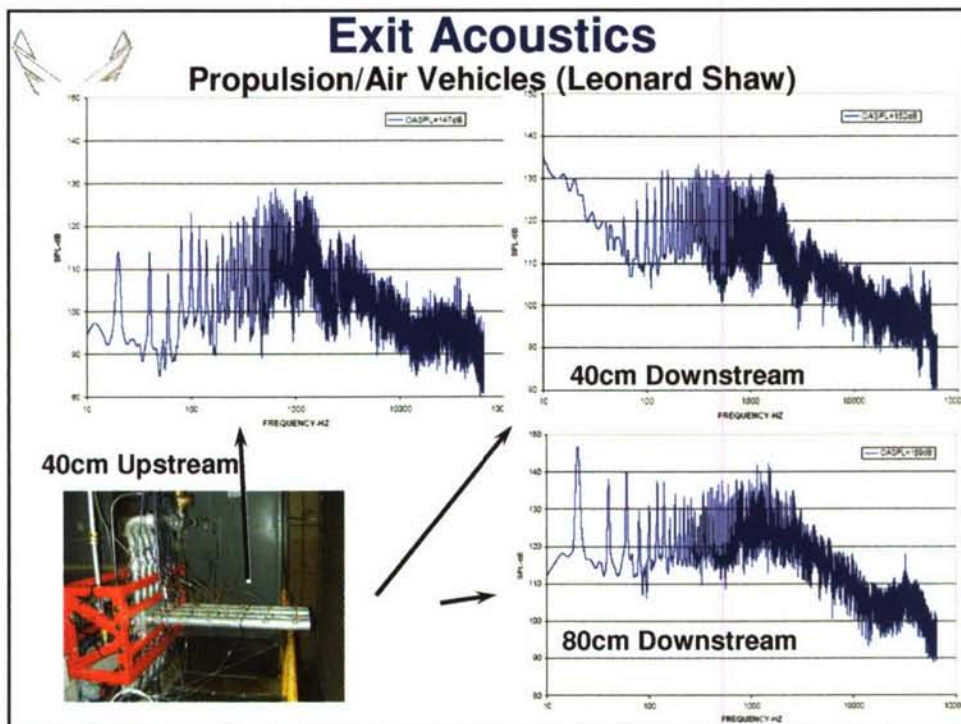
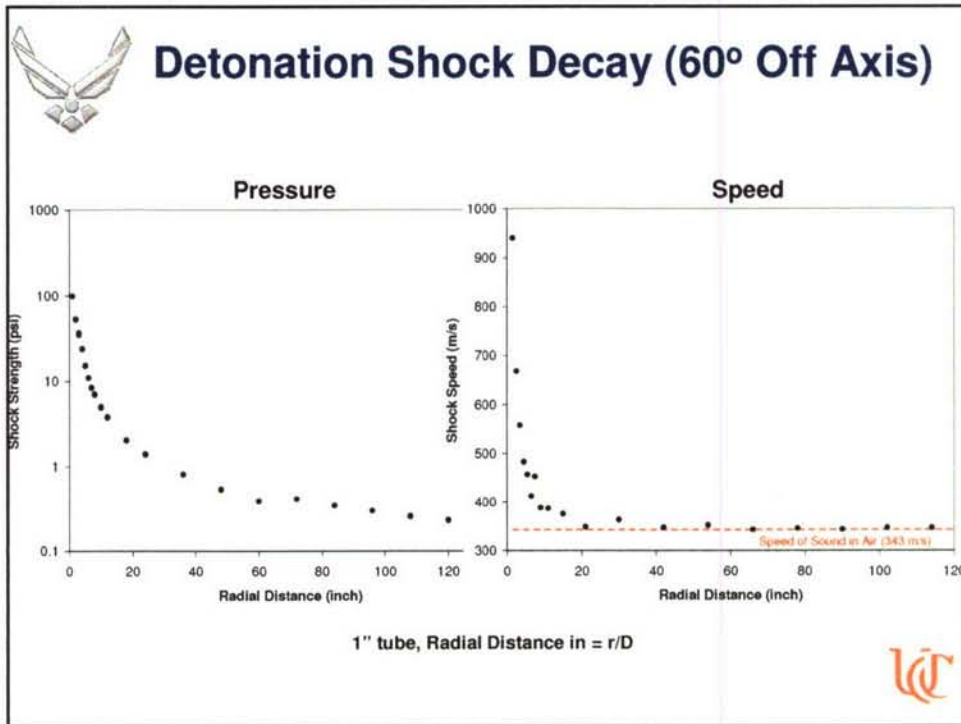


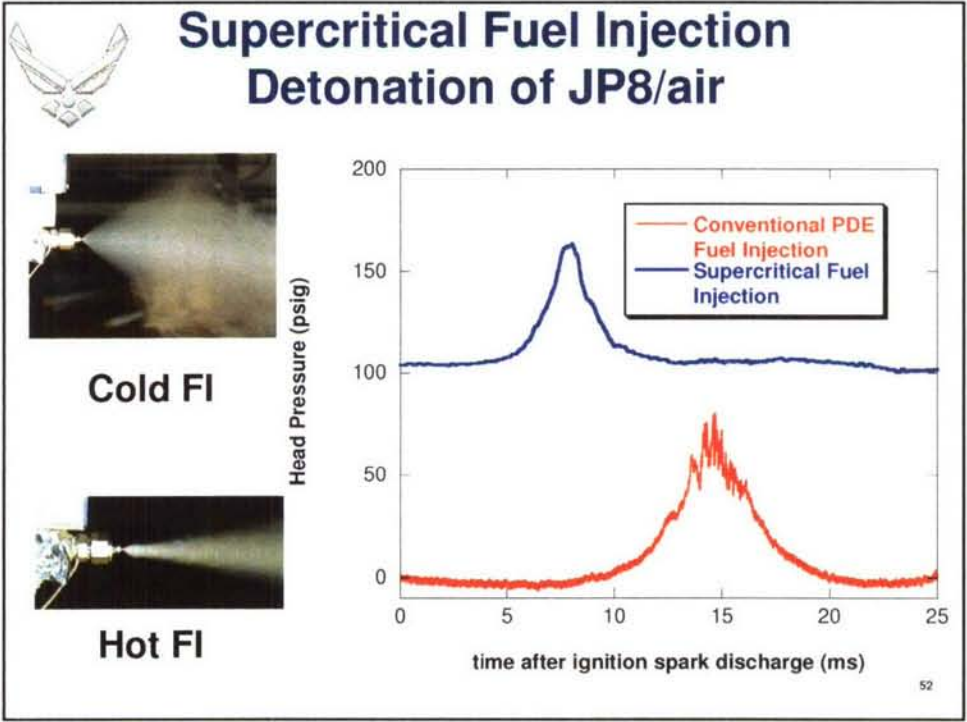
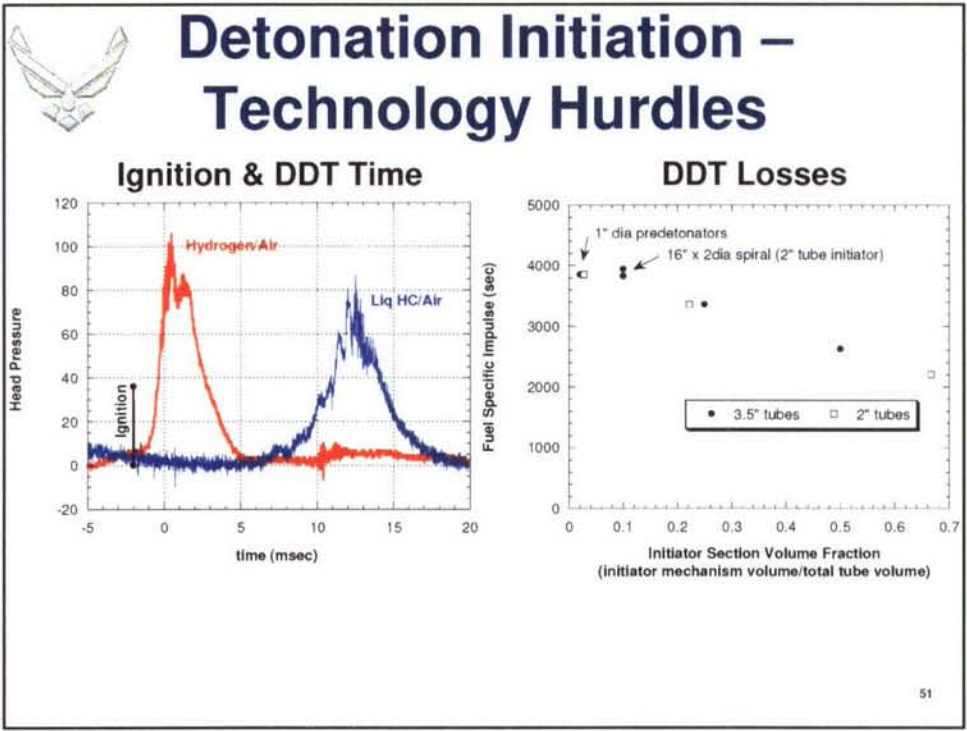
AFRL/PR and AFRL/VA⁴⁷

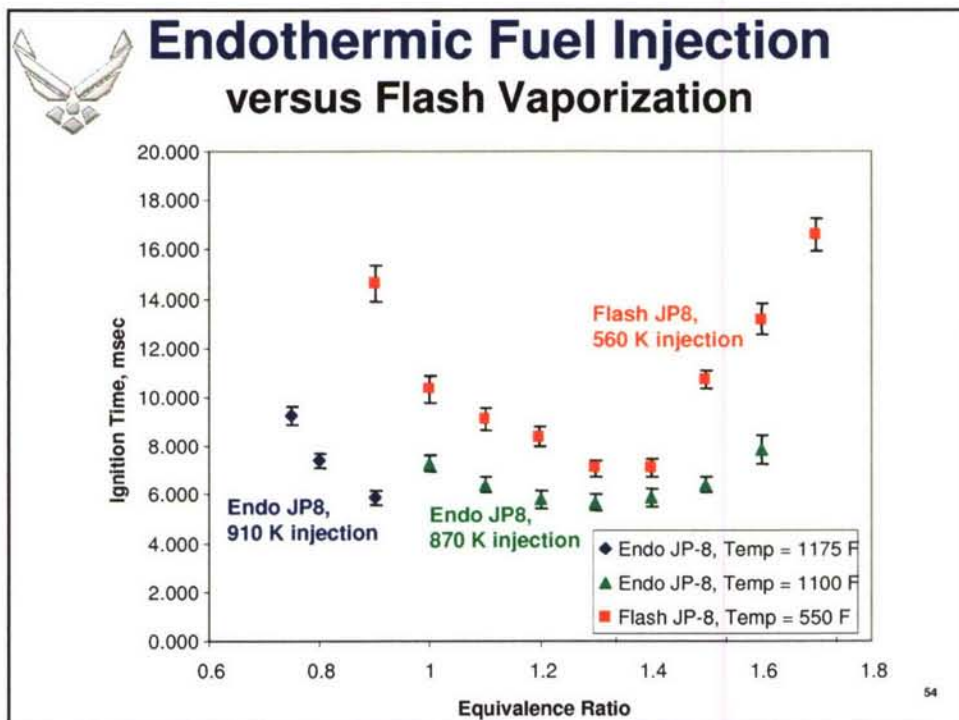
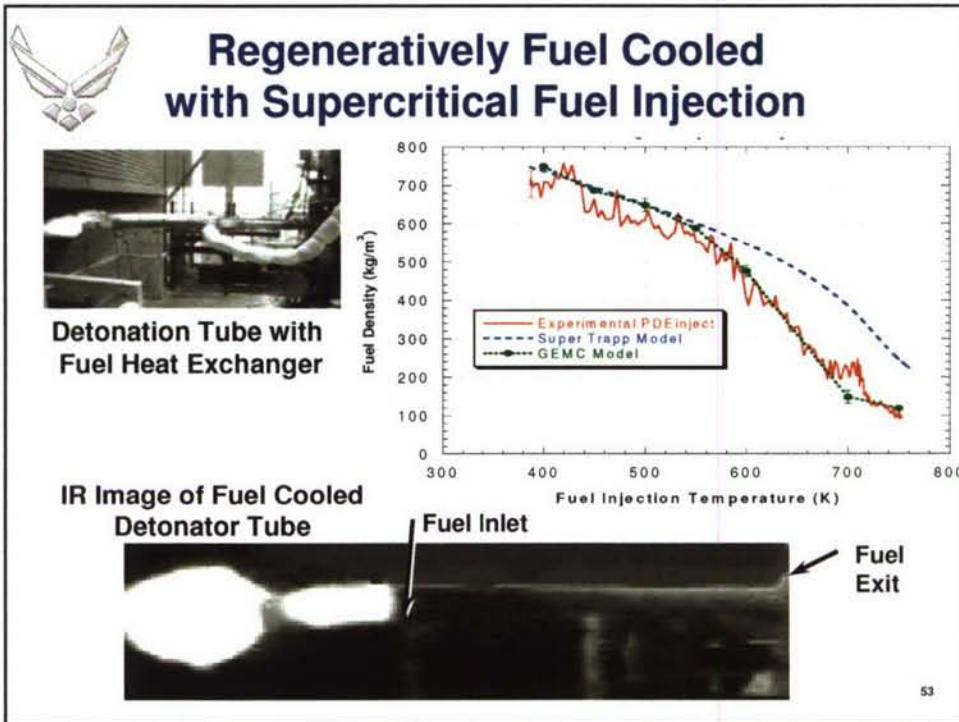


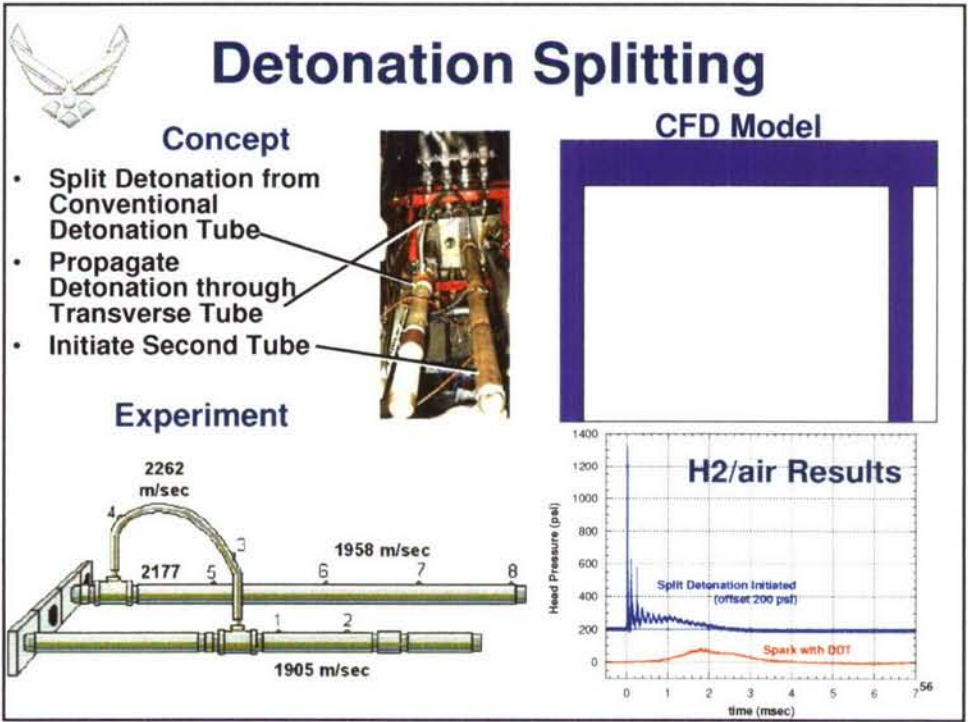
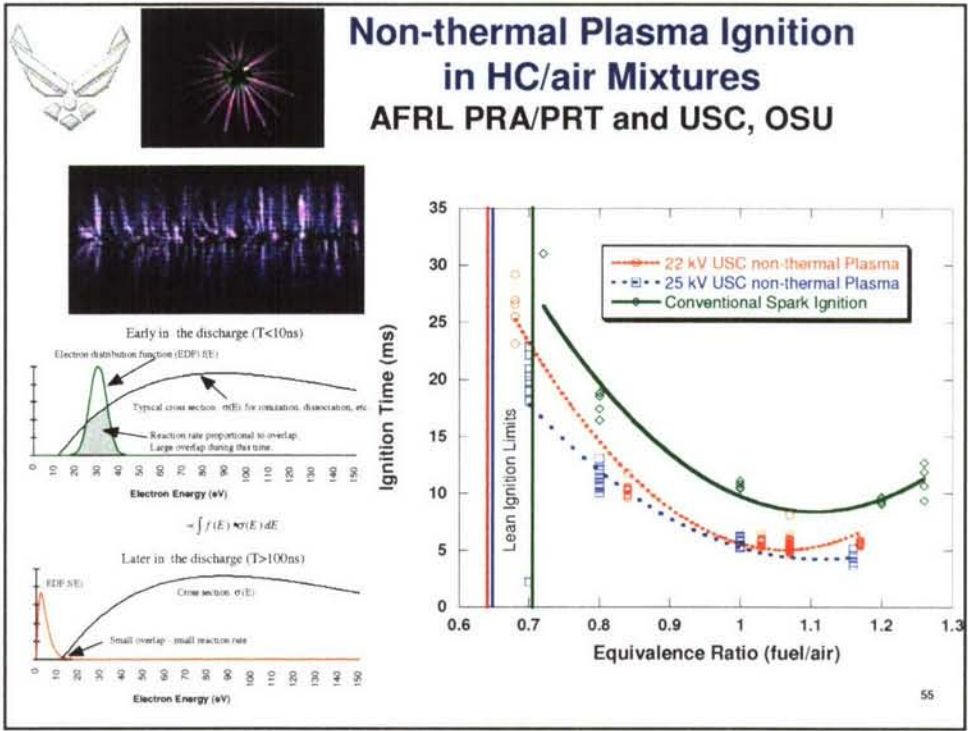
Detonation Shock Decay

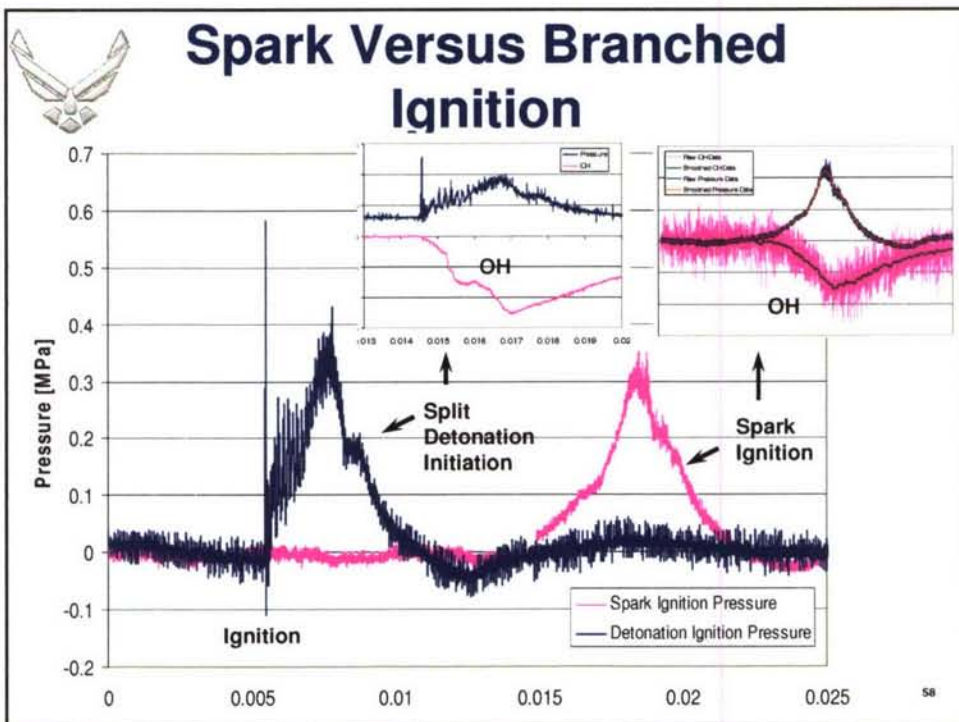
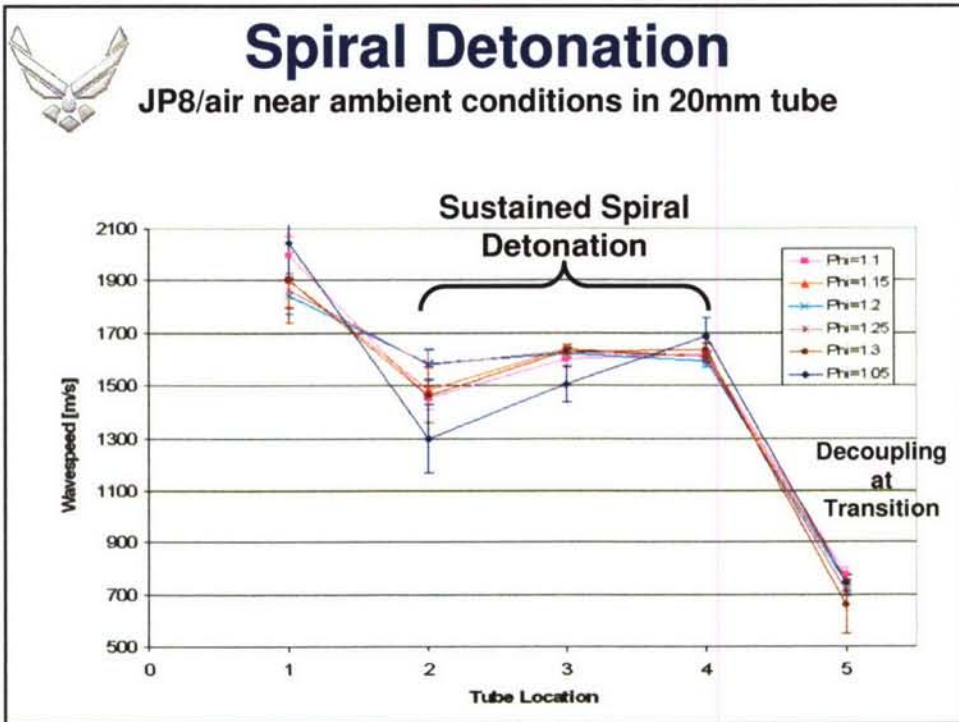


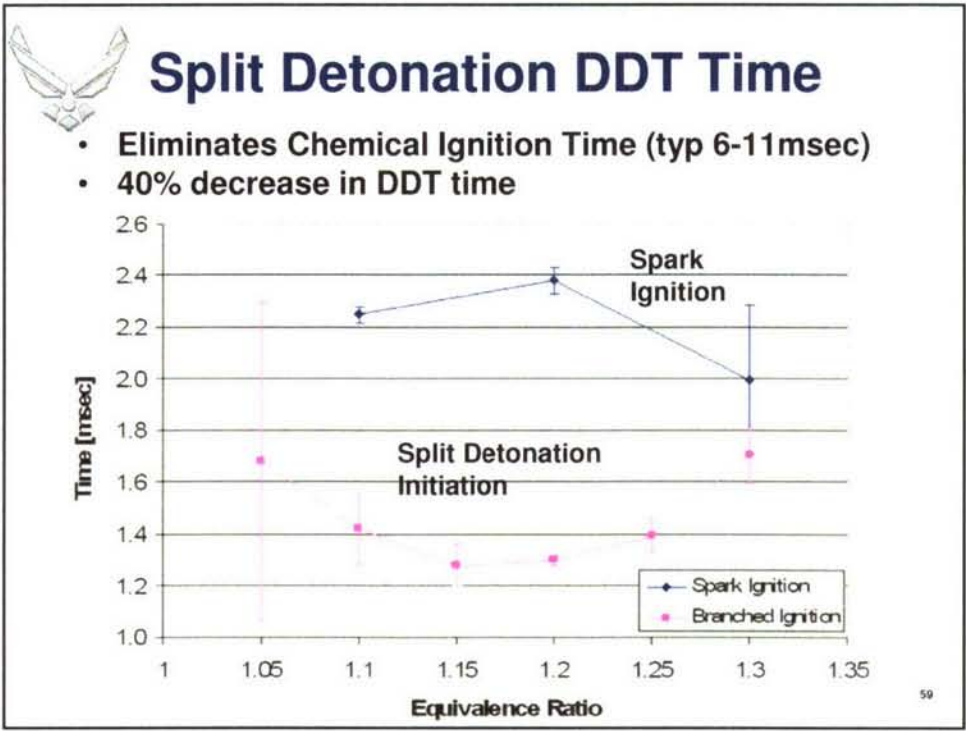














Pulsed Detonation Propulsion Summary

Cheap, simple, high performance propulsion that is highly scalable and efficient across a broad operating range (Mach 0-4+)

Acknowledgements: PDRF team and collaborators, funding by AFRL/PR, VA, AFOSR and industry 60



PDRI
Pulsed Detonation Research Facility

AFRL/PRTC, Bldg 490
1790 Loop Road North
Wright-Patterson AFB 45433
Phone: (937)255-6462
Frederick.Schauer@wpafb.af.mil

61

von Karman Institute for Fluid Dynamics

RTO-AVT-VKI Lecture Series 2007

**ADVANCES ON PROPULSION TECHNOLOGY
FOR HIGH-SPEED AIRCRAFT**

March 12-15, 2007

TURBINE BASED COMBINED CYCLES

A. Bond
Reaction Engines Ltd, United Kingdom

Turbine Based Combined Cycles

Alan Bond

Reaction Engines Ltd

Building D5, Culham Science Centre, Abingdon, OX14 3DB, United Kingdom

1 Summary

The atmosphere both supplies the most massive chemical component (the oxidiser) and over 95% of the reaction mass needed to potentially realise highly effective engines for vehicles flying at all Mach numbers. The development of gas turbine cycles to manipulate this medium from a static start and operate up to around Mach 2.5 has been very successful, delivering high thrust/weight and specific impulse. In deriving propulsion systems which extend the flight regime they therefore seem an obvious technology with which to start.

However, the ability of gas turbines to handle high temperature inlet flows ($\geq 600\text{K}$) is seriously limited by the need to carry out subsequent compression work on the air prior to combustion. It is therefore an obvious step to seek some means of reconfiguring and adding other features to the gas turbine which preserve its best low speed characteristics while adding new capabilities.

In particular we would like the ability to operate at higher cruise conditions (to Mach 5 or so) or to continuously accelerate to orbital velocities (7.8 km/s), while keeping the ability to aspirate from a static take-off. These are the Turbine Based Combined Cycle (TBCC) engines, one early example of which was the Pratt & Whitney J58 turbo-ramjet which successfully powered the SR-71 reconnaissance aircraft at over Mach 3, and another 'species' of which is the subject of this paper.

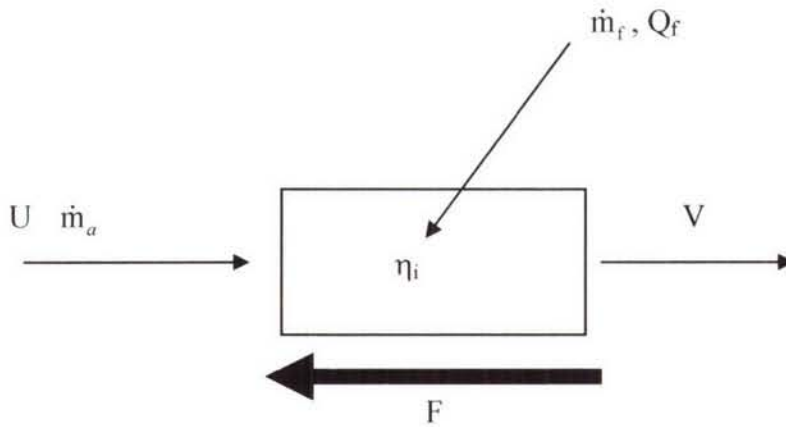
By addition of a precooler in front of the compressor and by driving the compressor with a turbine not in the air loop, it has proved possible to design engines able to meet the cruise and accelerating conditions referred to above for antipodal civil transport and for reusable space transportation applications. These engines use liquid hydrogen as fuel because of its outstanding thermodynamic properties and low storage temperature. However, the fuel is not simply used as a coolant, but as part of a thermodynamic cycle in which work transfer plays as significant a role as does heat transfer and the overarching principle is to minimise the combined entropy rise of the air and fuel together.

In the following, the theory of airbreathing engines is derived first in order to place limits on the theoretical performance of these engines, and then the theory of precooled engines is derived and compared with the ideal case. Two of the engine cycles being examined at Reaction Engines are then described, the Scimitar intended for Mach 5 antipodal cruise and the SABRE intended for accelerating a single stage to orbit (SSTO) reusable spaceplane.

2 Theory

2.1 General Theory of Airbreathing Engines

The conservation of energy and momentum enable a quite accurate estimate to be made of the performance limits of all chemically fuelled airbreathing engines irrespective of their internal machinery or configuration. Consider the following 'engine'.



The vehicle has a velocity relative to the air U . We take a frame of reference at rest relative to the engine. The flow of air entering the engine is \dot{m}_a and the fuel flow is \dot{m}_f which upon combustion releases Q_f joules/kg. The velocity of the exhaust is V . The engine produces thrust F Newtons. The second law of thermodynamics determines that only the kinetic energy of the air and the thermochemical energy of the fuel are available to effect propulsion, the thermal energy of the air being unavailable. The proof of this is not undertaken here. The efficiency of conversion of this total available input energy into exhaust jet kinetic energy is η_i and can range from 0 to 1.0

Hence;

$$F = (\dot{m}_a + \dot{m}_f) \cdot V - \dot{m}_a \cdot U \quad (\text{conservation of momentum})$$

$$(Q_f \cdot \dot{m}_f + \dot{m}_a \cdot \frac{U^2}{2}) \cdot \eta_i = (\dot{m}_a + \dot{m}_f) \cdot \frac{V^2}{2} \quad (\text{conservation of energy})$$

After algebraic manipulation and writing $afr = \frac{\dot{m}_a}{\dot{m}_f}$;

$$V = \sqrt{\left(\frac{2 \cdot Q_f + afr \cdot U^2}{1 + afr} \right) \cdot \eta_i}$$

$$F = \dot{m}_a \left(\sqrt{(1 + afr) \left(\frac{2 \cdot Q_f + afr \cdot U^2}{U^2} + afr \right) \cdot \eta_i} - U \right)$$

We define the thrust per unit fuel flow as effective exhaust velocity, $V_{\text{eff}} = \frac{F}{\dot{m}_f}$ and arrive at;

$$V_{\text{eff}} = U \cdot \left(\sqrt{(afr + 1) \left(\frac{2 \cdot Q_f}{U^2} + afr \right) \cdot \eta_i} - afr \right)$$

This equation is quite generic and contains a great deal of information about the capabilities of airbreathing engines. It can be shown by differentiation that there is an optimum value of afr which maximises V_{eff} so long as the combustion is less than stoichiometric and η_i is constant .

Substituting $a = \frac{2 \cdot Q_f}{U^2}$ for convenience, the optimum afr is given by;

$$afr = \frac{1}{2} \left(\sqrt{\frac{(a-1)^2}{1-\eta_i}} - (a+1) \right)$$

Inserting values for hydrogen, $Q_f = 1.2 \times 10^8$ J/kg, stoichiometric $afr_{min} = 34.029$ and a typical efficiency of $\eta_i = 0.8$ we can examine the variation of parameters with Mach number. It is convention to work with the equivalence ratio $ER = afr_{min}/afr$ and this is plotted against Mach number in fig.1. The corresponding optimum V_{eff} is shown in fig.2.

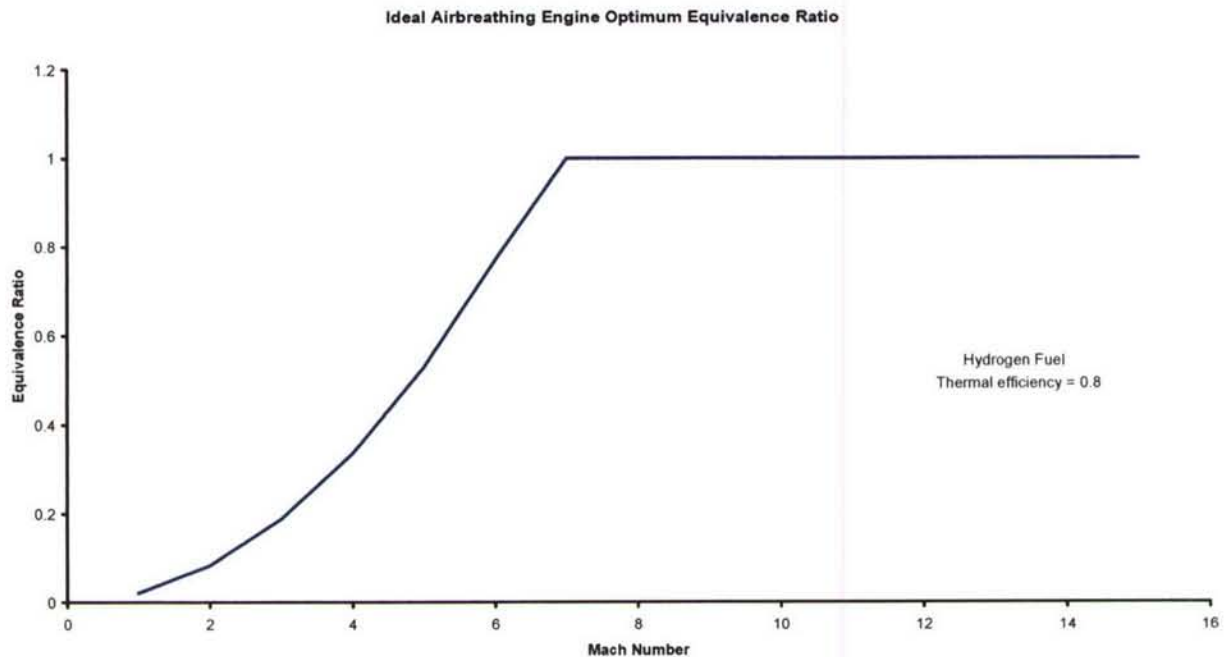


Fig.1. Optimum Equivalence ratio for hydrogen fuelled engines vs Mach Number

Ideal Air Breathing Performance

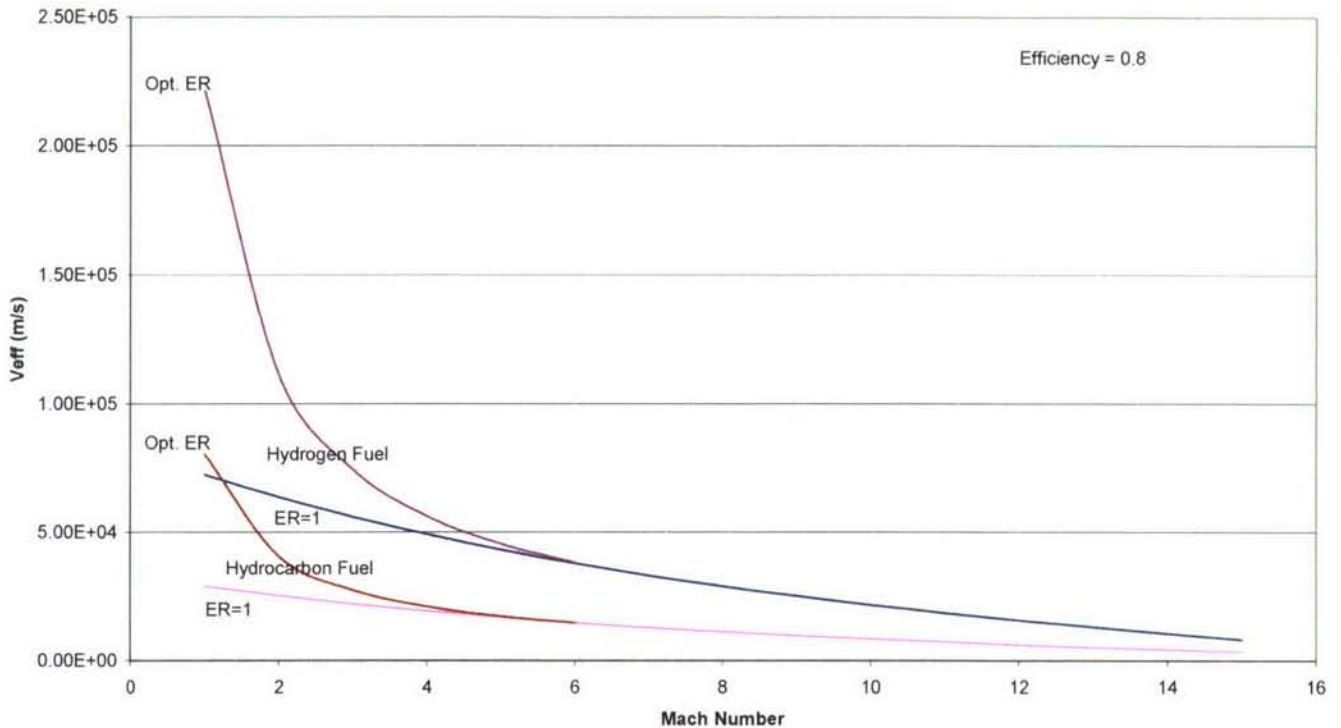


Fig.2. Optimum Effective Exhaust Velocity vs Mach Number

Also plotted on fig.2 is the V_{eff} curve for stoichiometric combustion ($ER = 1$) so that the region between this and the optimum curve correspond to the usual range of equivalence ratio's. It is immediately evident from fig.2 that hydrogen is far superior to hydrocarbons with respect to performance, although the physical characteristics (low temperature and density) raise taxing design issues.

As the $ER \Rightarrow 1.0$ the thrust per unit airflow increases (not derived here) and the size of the engine is therefore reduced. At speeds around Mach 5 it can be seen that there is little performance penalty in operating above the optimum ER and from fig.1 it can be seen that above about Mach 6 the engine will always operate at $ER = 1$.

With current technology the final acceleration of the flow from an airbreathing engine is invariably achieved using a nozzle in which the pressure falls from a plenum value to the ambient static pressure. In the plenum, the total energy of the intake and fuel combustion appears, including the thermal content of the captured ambient air. The total-to-static pressure ratio of the nozzle, treating it as an ideal friction free flow, is given by;

$$\eta_n = \eta_i \cdot \frac{af_r \cdot U^2 + 2 \cdot Q_f}{af_r \cdot (U^2 + 2 \cdot Q_{tha}) + 2 \cdot Q_f} = 1 - \left(\frac{P_n}{P_n} \right)^{\frac{\gamma-1}{\gamma}}$$

This assumes that the whole of η_i is accounted for by the final nozzle performance. This is clearly not the case but we are interested in principles in this paper. The pressure ratio of the nozzle is determined by the intake and internal machinery compression processes. For the intake the compression can be expressed adequately in theoretical studies by;

$$\frac{P_i}{P_i} = \left(1 + \frac{(\gamma-1)}{2} Mn^2\right)^{\frac{\gamma}{\gamma-1}} \cdot \left(1 + (1-\eta_{KE}) \cdot \frac{(\gamma-1)}{2} Mn^2\right)^{\frac{-\gamma}{\gamma-1}}$$

Where γ is the specific heats ratio, η_{KE} is the intake kinetic energy recovery efficiency and Mn is the flight Mach number. If $(P/p)_i \geq (P/p)_n$, the intake recovery pressure ratio is greater than the nozzle expansion pressure ratio and the engine is in the ramjet regime. Internal compression at that Mach number is then unnecessary to achieve the internal energy conversion efficiency stated. However, without internal driven compressors the engine cannot accelerate from rest to this operating condition and some form of combined cycle is needed. An obvious combination of a gas turbine and ramjet is simply to bypass the gas turbine at sufficiently high speed by diverting the air from the common intake into the ramjet. The Pratt & Whitney J58 was this type of engine.

An alternative to bypassing the hot flow round the core engine is to cool the captured air using the hydrogen fuel and to pass it through the core at all flight conditions. This mechanism is described in the next section.

2.2 General Theory of Precooling

At Mach 5 the air stagnation temperature of 'perfect air' is about 1320K (about 1240K with real gas effects) and it is impractical to compress it directly to high pressures due to both the work requirement and because the resulting compressor delivery temperature would be too high to handle. However, more subtle thermodynamic processes are possible when the fuel is liquid hydrogen, possessing high thermal capacity and entering the engine at very low temperature. The possibilities this opens can be examined by considering the air and fuel entering the engine as a single thermodynamic system having enthalpy and entropy which are conserved during the air compression process. The chemical potential is not employed in the first stage of the analysis where we consider an engine operating in cruise conditions at high speed.

We use perfect gas relations to keep the derivations simple and to make the underlying principles clear. The enthalpy balance through the compression process is;

$$(\dot{m}C_p)_{air}(T_1 - T_5) = (\dot{m}C_p)_{H_2}(T_f - T_i)$$

Where T_1 , T_5 are the air entry and exit temperatures from the compression process and T_i , T_f are the hydrogen entry and exit temperatures. $\dot{m}C_p$ is the thermal capacity of the appropriate flow.

The entropy balance, ΔS , through the compression is given by the sum of the well known expressions for the individual fluid streams;

$$\Delta S = \dot{m}_{air} \left(C_{p,air} \cdot \ln \left(\frac{T_5}{T_1} \right) - R_{air} \cdot \ln \left(\frac{P_5}{P_1} \right) \right) + \dot{m}_{H_2} \left(C_{p,H_2} \cdot \ln \left(\frac{T_f}{T_i} \right) - R_{H_2} \cdot \ln \left(\frac{P_f}{P_i} \right) \right)$$

where \dot{m} is the mass flow, C_p the specific heat, P the pressure and R the gas constant for the appropriate fluid. For a perfect cycle $\Delta S = 0$, otherwise $\Delta S > 0$.

Substituting $K_1 = \frac{(\dot{m}C_p)_{H_2}}{(\dot{m}C_p)_{air}}$, $\Delta s = \frac{\Delta S}{\dot{m}_{air}}$, $R = C_p \left(\frac{\gamma - 1}{\gamma} \right)$ with γ_a and γ_h for air and hydrogen respectively where $\gamma = \frac{C_p}{C_v}$, the ratio of heat capacities at constant pressure and constant volume, the above relations become;

$$T_1 - T_5 = K_1 (T_f - T_i)$$

$$\frac{\Delta S}{C_{p,air}} = \left(\text{Ln} \left(\frac{T_5}{T_1} \right) - \frac{(\gamma_a - 1)}{\gamma_a} \cdot \text{Ln} \left(\frac{P_5}{P_1} \right) \right) + K_1 \left(\text{Ln} \left(\frac{T_f}{T_i} \right) - \frac{(\gamma_h - 1)}{\gamma_h} \cdot \text{Ln} \left(\frac{P_f}{P_i} \right) \right)$$

For the moment it may be assumed that $\Delta s = 0$, T_1 is given by the flight condition, T_i is given by the hydrogen storage and pumping conditions, P_i and P_f for the hydrogen are left as a design choice and that K_1 , which is the reciprocal of *af_r* scaled by the relative specific heats, is determined by the general requirements of efficient propulsion as discussed above in 2.1 .

This leaves T_5 and T_f as free variables to maximise the pressure ratio $\frac{P_5}{P_1}$. This optimum can be shown by standard methods of calculus to occur when $T_5 = T_f$. This is also a general consequence of the second law of thermodynamics, for if $T_5 \neq T_f$ it would be possible to derive more work from this temperature difference to drive the compression process. If these are set equal their value can be determined from the enthalpy balance relation. The best attainable pressure ratio is then determined from the entropy equation. Without heat addition by combustion this is the very maximum pressure ratio across the compressor which is thermodynamically allowed.

For example:

Let $\gamma_a = \gamma_h = 1.4$, $T_1 = 1320\text{K}$, $T_i = 35\text{K}$ (following pumping), $\frac{P_f}{P_i} = 1$ (i.e. no pressure changes on the LH₂ side), $K_1 = 0.4188$ (stoichiometric fuel-air ratio).

It then follows that $T_5 = T_f = 940.7\text{K}$ and $\frac{P_5}{P_1} = 38.04$.

This is a very theoretical example and, due to the practical constraints of actual components, the real values which can be achieved for the pressure ratio are very much smaller, by a factor 5 or so. We can also see that for the above example the compressor inlet temperature at Mach 5 would be only 333K for isentropic compression showing that the air will be pre-cooled substantially before entering the compressor.

Using the precooling technique for achieving high speeds, the compressor temperature regime becomes very conventional and the hydrogen fuel exit temperature is relatively low while remaining at the full pump delivery pressure. At the same time, the equivalence ratio remains low (1.0 in the above idealised example) so that the engine can achieve close to the theoretical maximum specific fuel consumption derived in section 2.1. However it remains to determine practical cycles which can deliver the above thermodynamic results but, here, thermodynamic theory proves infuriatingly vague. Having shown us that there is a ‘promised land’, it provides scant clues on how to get there!

As K_1 is increased the pressure ratio attainable also increases, which will increase η_n and hence η_i in section 2.1. However there is clearly an optimum to be struck since the af_r will be increasing beyond the optimum, or even beyond stoichiometric at some point. This effect is modified if heat is added from an auxiliary combustion system so that the work available at the compressor is greater than that from the recovered kinetic energy alone. This is important in designing a combined cycle to operate at low speeds when the inlet kinetic energy rapidly falls to very low values.

In constructing combined cycles we are therefore aware of the following possible features from the theoretical arguments so far.

The engines will have a 'core engine' in which a compressor is preceded by a large heat exchanger, 'the precooler'. The coolant will be part of a thermodynamic cycle containing a turbine to drive the compressor since the delivery pressure of the compressor is only that needed for the propelling nozzle and has no possibility of providing other work. The coolant available will be guided by the af_r derived in section 2.1 (but see the SABRE engine below!). The thermodynamic loop will contain a 'preburner' and a heat exchanger to heat the cycle at low forward speeds. Finally, the waste heat from the cycle will be rejected to the hydrogen, either because it is the cycle working fluid directly, or via yet another heat exchanger to the cycle working fluid. It has become convention in Reaction Engines to call the precooler HX1-2, the preburner top-up heat exchanger, HX3 and the heat rejection heat exchanger, HX4. Their context will become more evident in the engine examples which follow.

3 Example Engines

3.1 The SABRE spaceplane engine

The SABRE engine is designed to propel the SKYLON single stage to orbit reusable spaceplane. It is an accelerating engine, having no cruise phase, and in this case the combined engine has a core engine integrated with a rocket engine which continues the acceleration beyond Mach 5 to orbital speed. The general engine appearance is shown in fig.3.



Fig.3. The SABRE engine installed in its nacelle.

A general feature of these TBCC engines is the bypass duct which is needed to match the intake capture flow to the core engine flow over the flight Mach number range. This component can also be used to add additional propulsion modes to the basic combined engine cycle by incorporating a combustion system in the duct and in this limited respect they resemble the turbo-ramjet concepts described above. However, here the bypass flow falls steadily with rising Mach number reaching zero at Mach 5 rather than the contrary.

In the SABRE engine, the requirement is to minimise engine mass and base drag and the design therefore uses a common combustion system and expansion nozzle for both modes of operation. In order to maximise the rocket engine exhaust velocity the area ratio must be around 100 and the rocket mode combustion pressure approximately 145bar in order to limit the nozzle size. In order to use this same nozzle in airbreathing operation the compressor pressure ratio must be very high, over 140:1 permitting the combustion chamber pressure to reach over 100 bar in this mode. A simplified cycle diagram is shown in fig.4.

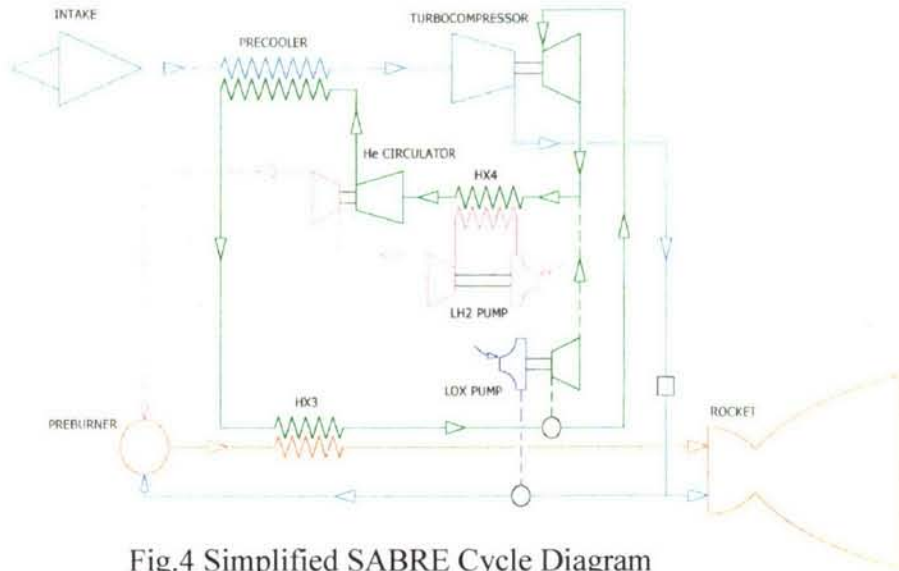


Fig.4 Simplified SABRE Cycle Diagram

In airbreathing operation the air flow (blue) passes from the intake to the pre-cooler which is cooled by cold high pressure (200 bar) helium (green). The cold air (about 140K) is then compressed, part of which is then delivered to the preburner and part to the main combustion chamber.

The high pressure helium is heated to a constant delivery temperature of 1180K in HX3 before being passed to the turbine to drive the compressor. The helium then passes to HX4 where heat is rejected to the hydrogen (red) before being recompressed in the helium circulator.

All of the hydrogen passes to the preburner where in combustion with the air flow it produces a hot hydrogen rich flow (1800K – 1500K) to heat the helium in HX3 before passing to the main combustion chamber to meet the remaining air flow. The preburner temperature is controlled at different flight conditions by adjusting the air flow split between the main combustion chamber and the preburner.

Upon transition to rocket operation the turbo-compressor is taken out of the power loop and the liquid oxygen pump brought in. There is a substantial change in the power demand and the operating conditions of the helium loop (pressure, temperature and flow rate) have to change to accommodate this.

The liquid oxygen is used to cool the combustion chamber and in rocket operation is vaporised to substitute for air in the same injectors. The use of helium in the power loop is dictated by the need to avoid hydrogen embrittlement in the hot pre-cooler and the

convenience of the high specific heats ratio which minimises the pressure range (4.5:1) that the power cycle has to operate over. These are practical constraints which are not relevant to the thermodynamic subject of this paper but are mentioned to clarify the reasons for some of the choices.

In order to achieve this high pressure ratio (140) the SABRE engine operates with a very high fuel flow corresponding to an equivalence ratio of 2.8, i.e. well over stoichiometric. As a consequence the V_{eff} of this engine in airbreathing mode at Mach 5 is only 16,000m/s compared with an optimum value of about 46,000m/s. Even so the combined effect of both modes is to enable a single stage to orbit reusable vehicle to be realised. There is obviously scope for substantial improvements in performance in future engine designs.

3.2 The Scimitar Engine

The Scimitar engine is configured to power a Mach 5 civilian airliner. Although the design requirement is to cruise with high efficiency at Mach 5 it must also fly with acceptable efficiency at Mach 0.9 during overland flight path segments to eliminate sonic boom. In addition the engine must be sufficiently quiet at take-off to satisfy international noise regulations and this can only be achieved if the exhaust jet is subsonic at take-off. The engine configuration is shown in fig.5

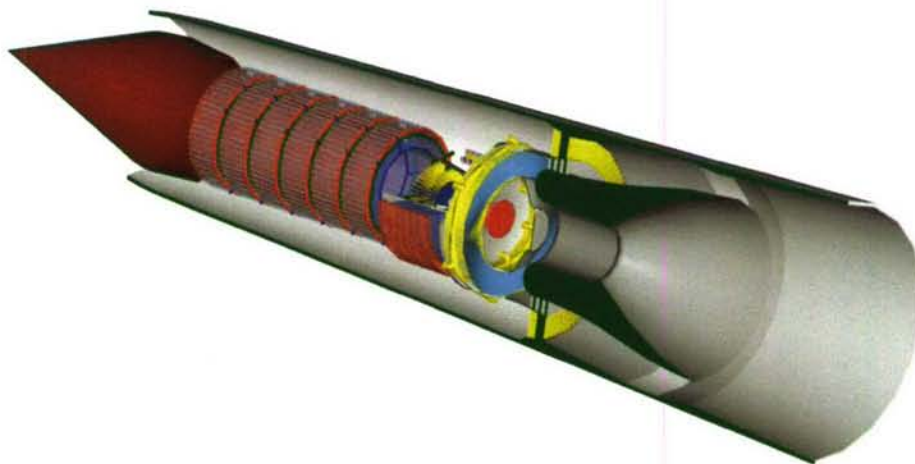


Fig.5 Scimitar Mach 5 Cruise Engine Configuration

The Scimitar engine core is only precooled when the engine is operating above Mach 3 when the compressor inlet temperature reaches 635K. Above this speed the precooler keeps the compressor inlet temperature at this value up to Mach 5. The compressor pressure ratio can be optimised for best cruise performance and is approximately 4:1 at which the Equivalence Ratio is 0.8. At this condition the V_{eff} is 44,000m/s.

In order to fly subsonically the bypass duct has a fan installed with a pressure ratio of 1.8:1. In subsonic mode the fan is driven by a hub turbine by the output of HX3 as shown in fig.6 and the cycle diagram in fig.7, the turbine exhaust discharging into the bypass duct downstream of the fan. For take-off and acceleration the bypass duct contains a burner to reheat the flow and increase the thrust.

At Mach 0.9, $afr = 458$ (ER = 0.07488) and $V_{eff} = 96,000$ m/s. The ideal V_{eff} at this condition would be 245,000m/s from section 2.1. However the achieved value gives the aircraft almost

the same subsonic range as its supersonic range and allows an operator considerable flexibility over his routing strategy. Again there is substantial possibility for future engine performance improvements. A modern subsonic high bypass hydrocarbon engine has a V_{eff} of around 68,000m/s.

The bypass nozzle is annular and is constructed from a series of petals which fold radially inwards at high Mach number to complete the nozzle extension for the core combustion chamber.

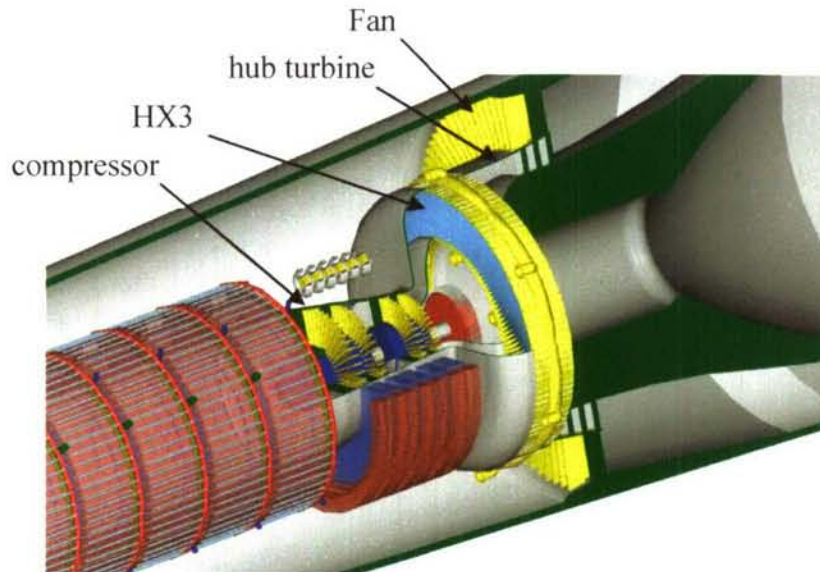


Fig.6 Scimitar Engine bypass fan

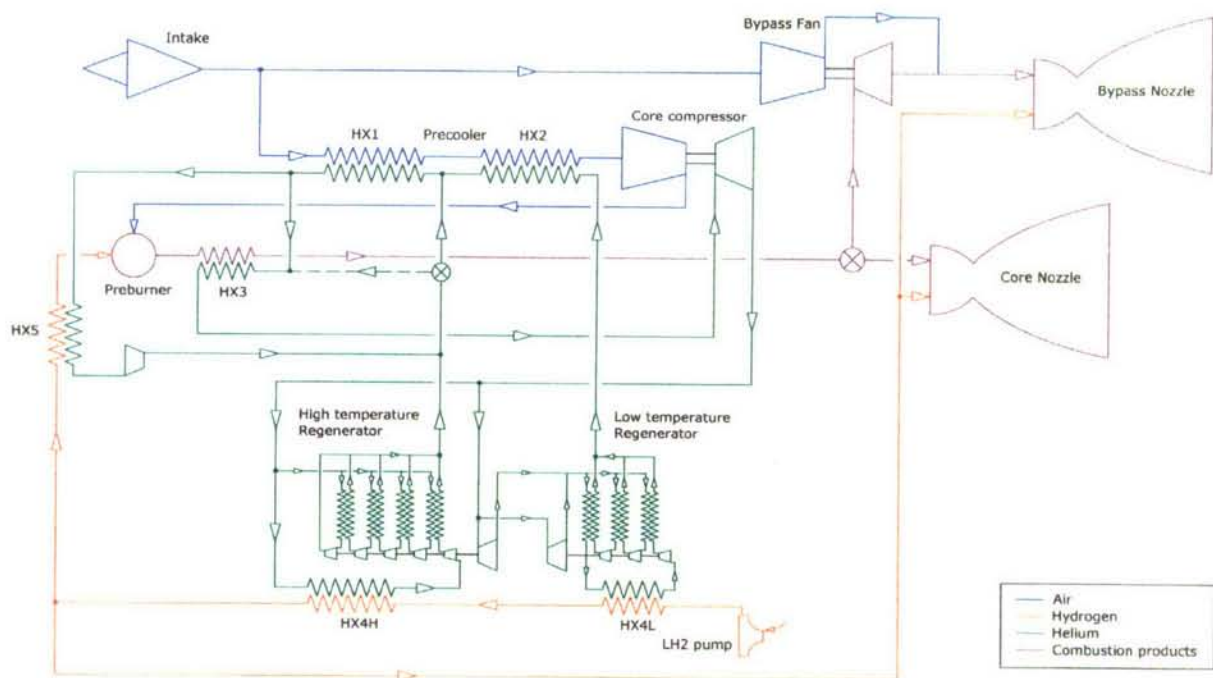


Fig.7 Scimitar Mach 5 Cruise Engine

Unlike the SABRE engine, the Scimitar passes all of the air through its preburner and adjusts the fuel flow to control the temperature rather than *vice versa*. At supersonic speeds the flow from the preburner passes directly to the core nozzle, bypassing the fan hub turbine, where the remaining fuel is added to achieve the correct mixture ratio. At moderate supersonic speeds the bypass duct operates in ramjet mode like the SABRE and the fan is allowed to windmill to limit its pressure losses. The bypass nozzle adjusts to handle the bypass flow depending on its pressure and temperature during the vehicle acceleration.

As can be seen in fig.7, the heat rejection from helium to hydrogen in the Scimitar is more complicated than for the SABRE. This is because at an Equivalence Ratio of 0.8 the capacity ratio K_1 is 3:1 and a flow arrangement has to be devised which will locally exchange heat at a capacity ratio of 1:1 so as not to generate an undesirably high entropy rise, as discussed in section 3.3. This is achieved by splitting the flow into three tandem loops and using a regenerating cascade between them. The principle is clear on examining the low temperature regenerator HX4L.

The high temperature regenerator (HX4H) is a little more complicated. Due to materials limitations it is necessary to increase the coolant flow through the hot part of the precooler (designated HX1) In this the capacity ratio of the helium to air is increased from 1:1 in the cooler part (HX2) to 3:1. This means that the helium to hydrogen capacity ratio increases from 3:1 to 9:1 for the hotter flow. The same regenerator principle applies, requiring 6 extra flow paths, HX4H plus HX5.

It is a feature of these engines that they contain several heat exchangers and therefore appear complicated when first encountered. It is also the case that as the Equivalence Ratio is reduced the number of heat exchangers increases, hence the more complicated appearance of the Scimitar cycle compared with the SABRE cycle.

3.3 Entropy Generation

Entropy generation comes from several sources within the engine cycle;

- compressors & turbines
- duct friction, bends and expansions
- heat exchanger pressure losses
- spontaneous temperature rise in combustion devices
- heat exchanger finite ΔT between fluid streams.

Because of their relative novelty and importance as major contributors to the entropy rise the last of these sources is discussed below.

Material temperature limitation

Fig.8 illustrates the method of heat exchange within the precooler matrix. This illustrates the initial counter-flow heat exchanger (HX1) using an increased capacity rate ratio (K_1) followed by a capacity matched (K_2) counter-flow heat exchanger (HX2).

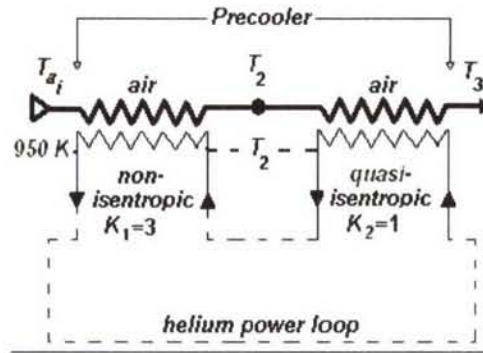


Fig. 8: Pre-cooler thermodynamics; K is the helium to air capacity ratio.

At the assumed Mach 5 design condition air enters the engine at 1240 K (real gas properties). Due to pre-cooler material constraints, however, the helium coolant is limited to around 950 K and the potential entropy generation as a result of this large temperature difference must be controlled by increasing the capacity rate of the coolant flow.

When considering a counter-flow heat exchanger with no imposed temperature limitations the entropy generation can be minimized by matching the capacity rates of both streams. Given the above temperature limitations at entry to the pre-cooler, the entropy generation can be reduced by increasing helium coolant capacity rate; the higher coolant mass flow allows the heat to be transferred at a higher average temperature. Fig.9 illustrates that a capacity ratio (helium/air) of at least 3 is desirable such that the entropy increase in the heat exchanger is considerably reduced. T_2 (fig.8) is the resulting cold end temperature of the non-isentropic counter-flow heat exchanger to counteract the entropy rise due to the hot end temperature limitation of the pre-cooler.

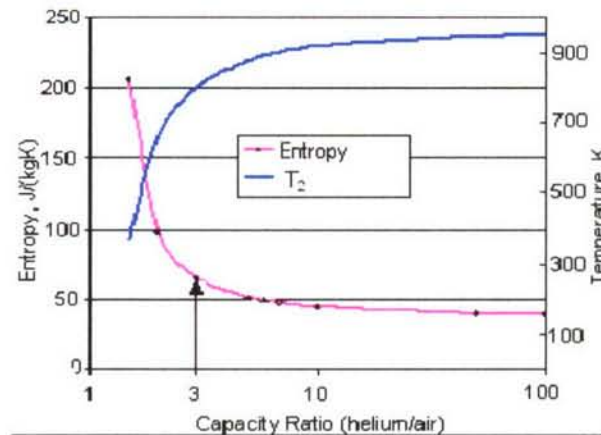


Fig.9: Effect of helium to air capacity ratio on entropy generation in a counter-flow heat exchanger with air inlet temperature of 1240 K and helium exit temperature of 950 K, and where T_2 is the cold end temperature of both streams assuming $\Delta T = 0$ there.

Low temperature heat exchange

The remaining heat in the external air flow can be removed using a low temperature heat exchanger (HX2) that is not constrained by material temperature limitations and can therefore operate closer to isentropic conditions (fig.10). However, the very nature of low temperature heat transfer, constitutes a major source of entropy generation even at the lower ΔT 's

achieved using a capacity matched counter-flow arrangement. Since the low temperature heat exchanger must still remove almost 60 % of the heat from the intake air flow, the performance of this heat exchanger, in terms of minimal ΔT , is critical to the performance of the whole engine cycle.

For HX2, writing $C = \dot{m}c_p$ of either the air or helium stream, the entropy rise per unit capacity rate, $\frac{\Delta S}{C}$, assuming no pressure loss is;

$$\frac{\Delta S}{C} = \ln\left(\frac{T_3}{T_2}\right) + \ln\left(\frac{T_2 - \Delta T}{T_3 - \Delta T}\right)$$

Assuming a $\Delta T \ll T_2, T_3$, this can be approximated to:

$$\frac{\Delta S}{C} \approx \frac{(T_2 - T_3)}{T_2 T_3} \Delta T$$

The entropy increase of HX2 is therefore proportional to the finite temperature difference, ΔT , between the hot air stream and helium coolant stream.

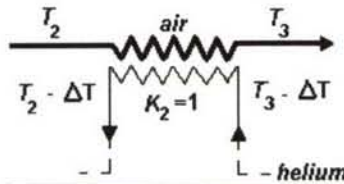


Fig.10. Precooler low temperature heat exchanger.

It is essential therefore to have the highest heat transfer coefficient possible consistent with mass and pressure drop constraints.

4 Technology of Precooled Engines

This paper is mainly aimed at a discussion of cycle features of precooled TBCC engines but these are only of interest if the components they require are technically feasible. The following limited discussion examines the technology status of the major hardware components.

4.1 Turbines, compressors and intakes

Although the configuration of precooled TBCC engines is rather different to gas turbines the technology of the turbo machinery and intake/bypass system is relatively conventional. A particular advantage of helium cycle working fluid is that it is inert and materials which would otherwise suffer either oxidation or hydrogen embrittlement can be used. Examples are the super alloys and carbon-carbon composites. The helium is also used at high pressure (200bar) and as a consequence components tend to be very compact.

With helium turbines driving cold or relatively cool air compressors there is a speed mismatch. However, several design studies of stator-less turbines with contra-rotating rotor stages coupled to a contra-rotating two spool compressor have shown that this can be overcome. The resulting turbines are ultra compact also.

The compressors are very conventional in construction, and for heavily precooled engines like the SABRE can have carbon reinforced plastic early stages and light alloy intermediate stages. The high pressure ratio SABRE compressor has a very limited nondimensional operating range and would probably benefit from some variable inlet guide vanes.

The intakes considered so far at Reaction Engines are axisymmetric and use a single translating centre body to keep shock-on-lip condition while accelerating to cruise conditions or to transition to rocket operation in the case of SABRE. The SABRE intake must also close for re-entry. The SABRE engine only requires low η_{KE} , about 0.8, achieved with a two shock compression while the Scimitar requires a higher value $\eta_i = 0.9$ achieved with a three shock compression. The bypass burners are normal subsonic combustion systems. Both engines require variable geometry bypass nozzles.

4.2 Heat Exchanger Technology

The success or otherwise of precooled TBCC engines pivots on the practical feasibility of low mass, high surface area heat exchangers. The heat exchangers required in this type of engine fall into three main types:

- Super alloy, shell and tubular surface matrix heat exchangers (HX1-2, SABRE HX4) with one high pressure and one low pressure stream and low driving temperature drop.
- Ceramic shell and tube or plate surface heat exchangers (HX3) with two high pressure streams but very large driving temperature drop.
- Metallic micro-channel plate heat exchangers (HX4) with two very high pressure streams with close thermal matching, i.e. low driving temperature drop.

Development programs are in progress at Reaction Engines on all three types of heat exchanger, but is most advanced for the first type. A prototype module and a close view of brazed tube junctions of a tubular surface in Inconel 718 using tubes 0.88mm bore with 40 μ m walls is shown in fig.11a and 11b. It is intended to operate a precooler built from 42 of these modules in conjunction with a Viper jet engine during this development program.



Fig.11a Prototype precooler module

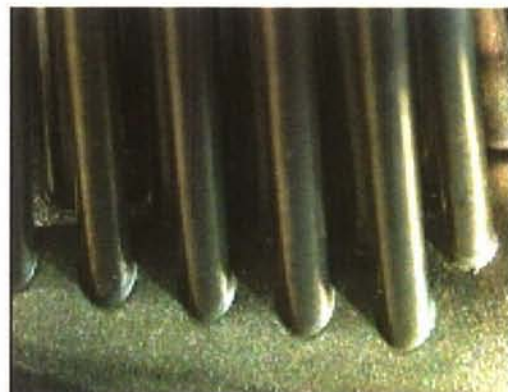


Fig.11b Sample brazed joints

For the second type of heat exchanger silicon carbide tubes of suitable straightness, accuracy and outer diameter have been produced, but they are still not available in the desired wall thickness. These tubes have been successfully joined to a tungsten tube sheet. At present the design of HX3 is severely constrained by manufacturing capabilities in SiC and while the SABRE HX3 is close to achievement there is still not a suitable design for the Scimitar engine.

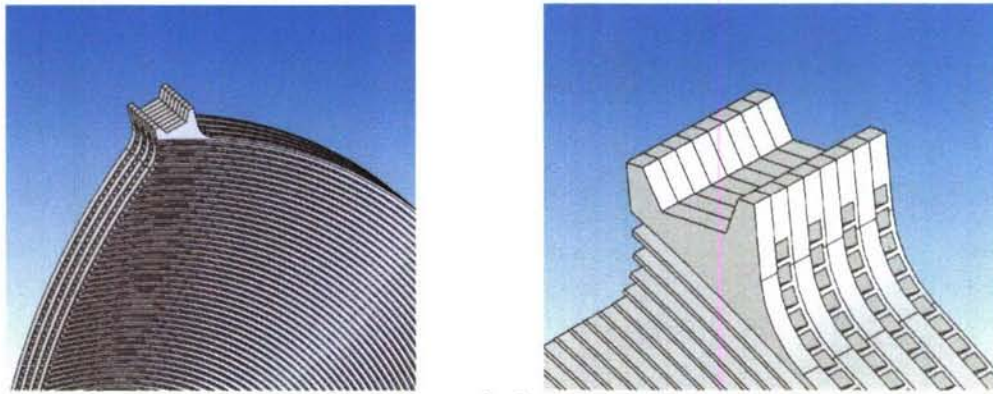


Fig.12. Micro-channel plate assembly

Finally, for the third type shown in fig.12, manufacturing trials of plate heat exchangers with channels of a few tens of microns hydraulic diameter is just beginning.

4.3 Problems remaining

The main problem in the case of realising a Mach 5 cruise engine is the lifetime of the precooler. Here the upper temperature is constrained by the creep strength of oxidation resistant high strength alloys. Work continues to find novel solutions to this problem through design rather than searching for miracle materials.

In all of the heat exchanger types discussed above, the physics of operation, the materials properties and the mechanical integrity of designs are not central questions; we are entirely dependent on the status of manufacturing technology.

5 Conclusions

- Precooled Turbine Based Combined Cycle (TBCC) engines have the potential to achieve close to the ideal performance for airbreathing propulsion over a wide Mach number range up to a limit around Mach 5 with current materials.
- These engines offer the promise of civilian antipodal flight in about 4 ½ hours and single stage to orbit reusable spaceplanes, but only with liquid hydrogen fuel.
- Precooled TBCC engines are configured around well established gas turbine and rocket technology but have heat exchangers which are a new development in flying engines.
- TBCC engines can be developed, at least in a major part, on open test bed facilities since they aspirate at zero forward speed.
- The feasibility of the precooler will be demonstrated over the next couple of years with R&D work currently in progress.
- The development of other heat exchangers is lagging the precooler and in particular, practical ceramic components are not yet close to the promise of their material properties.
- Cycle design innovation continues in order to improve performance and to try to bypass the limitations of current materials.
- This class of engines are the most practical known to the author for accessing the lower hypersonic flight regime (Mach 5)

Acknowledgement

Helen Webber's contribution to the discussion of entropy generation in the precooler in section 3 is gratefully acknowledged.

von Karman Institute for Fluid Dynamics

RTO-AVT-VKI Lecture Series 2007

**ADVANCES ON PROPULSION TECHNOLOGY
FOR HIGH-SPEED AIRCRAFT**

March 12-15, 2007

ROCKET ENGINES: TURBOMACHINERY

H. Mårtensson, S. Andersson, S. Trollheden, S. Brodin
Volvo Aero Corporation, Sweden

ROCKET ENGINES : TURBOMACHINERY

Hans Mårtensson

Sonny Andersson

Stefan Trollheden

Staffan Brodin

VOLVO Aero Corporation
S-461 81 TROLLHÄTTAN
Sweden

1. INTRODUCTION

A turbopump in a rocket engine consists of a pump that delivers fuel or oxidizer to the thrust chamber where the propellants are brought to react and increase in temperature. Since the combustion process takes place under constant pressure, the chamber pressure is the net result of the turbopump system. Turbomachinery for liquid rocket propulsion shares many of the design features and challenges found in gas turbines. To an even greater extent than in jet-engines used for aircraft the emphasis is on delivering very high power in a small machine. Pumps and turbines are classical subjects of engineering and are in wide spread use in many areas. The constraints and requirements of the application is what make the design of turbopumps for liquid rocket engines unique. In this lecture the pumps will be discussed mostly in the context of load on the turbine. The main reason for doing so lies in the background of the authors, working at a company that designs and manufactures turbines for space propulsion. We shall look into what governs the design of turbines for liquid rocket engines. This is done by example following a simplified design loop, discussing as we go.

Many important steps were taken from after the war and to the 70's in the design of turbopumps for rocket engines. A historical review of the development is very enlightening and highly recommended for interested engineers [1]. Following a period of very active development NASA issued a collection of documents that summarizes design experience in terms of rules and criteria [4]-[7]. These are still very valid in terms of providing guide lines to what works and what does not. Also very important is that they provide insight to solutions adopted for several machines and by several different companies. Much of what we will describe in terms of design will be based on these. This provides a coherent basis for the lecture, and does not infringe on proprietary information. In engineering practice each company that develops turbines has in-house practices and experience that strongly affects the final design. Modern computational tools have provided for great changes to engineering work and advancement of machines since the 70's. Much of this is used in detailed design and replaces to some extent testing on component level, and has become indispensable in modern engineering.

New materials and computational tools allow the designer to improve the performance of the machine. With improved tools for design the machine becomes more optimal, which is good. At the same time as the designer approaches the limits of what is physically possible the numbers of failure modes multiply and the accuracy required in verification of the analysis increases. It has always been argued that computational tools such as CFD and FEM reduce development time and cost. It appears more that the actual effect is that as optimization

becomes possible with better tools, the machines get better but the development time and cost is equal, at the best. This is maybe not to surprising after all since new designs are often made in order to deliver better performance. At the end of the day this is still a balance act of risk management, customer input, innovation, economy and hard work.

2. Cycle selection effects on turbopump characteristics

Selection of the engine cycle determines the characteristics of the turbine to a large extent. The cycle a choice made on engine level, balancing complexity with performance for some flight and load. On the development side this is made quite some time before the detailed design of turbomachinery is made. In order to optimize the system the engine designer will need to know what to expect in terms of performance from the different components that make up the engine. The engine designer will want to know in a variety of configurations and cycles what can be achieved in terms of cost, weight and efficiency potentials.

Trying to describe how the cycle selection affects the turbomachinery we will first look at the main performance numbers describing the propulsion system as a hole. This gives some appreciation of what the controlling parameters of the engine means to the turbopump. Since we want to discuss the turbomachinery aspects simplifications are taken as necessary. First of all, the measure of the rocket engine performance can be expressed in the specific impulse I_{sp} :

$$I_{sp} = \frac{F_n}{g \cdot \dot{m}} \quad \begin{array}{l} F_n \text{ is the thrust} \\ g \text{ is the gravitation constant} \\ \dot{m} \text{ is propellant mass flow} \end{array} \quad (1)$$

For our purposes of studying turbomachinery we will accept the notion that the higher the I_{sp} the better the performance is. The first we can notice is that the higher the chamber pressure is the higher the thrust F_n will be. This of course immediately goes back to the pump exit pressure which must be higher than the chamber pressure. The second component that can be discussed is the mass flow. If nothing else is changed we would expect the thrust to be proportional to the mass flow. This is easiest seen in the trivial example of putting 2 engines side by side resulting in twice the thrust for twice the mass flow and I_{sp} equal.

The choice of cycle can be described in 3 main categories, which have great implications for the turbomachines. The main cycles used for larger modern liquid rocket engines are, as shown I figure 1, gas generator, expander and stage combustion.

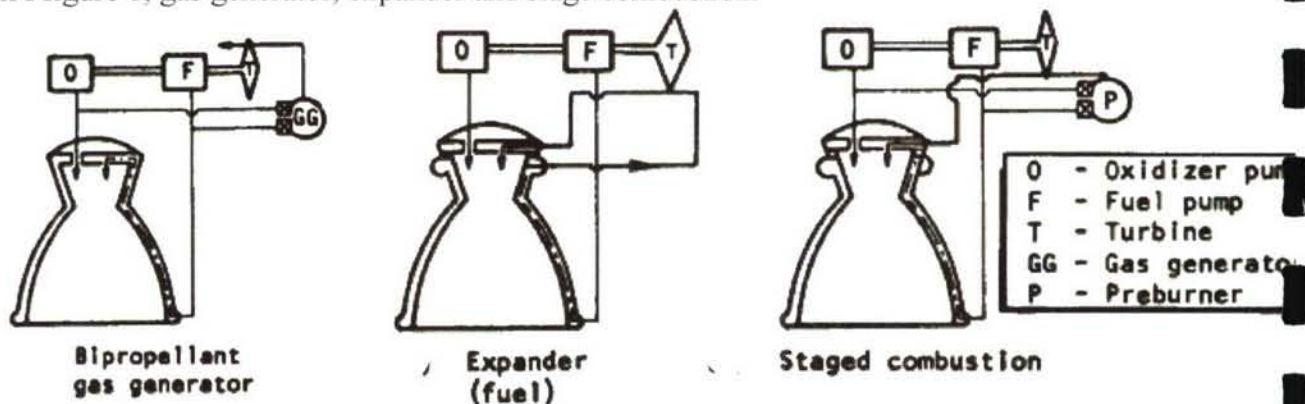


Figure 1 Principle schematics of major liquid bi-propellant rocket engine cycles from NASA SP-8107

Out of these 3 cycles the gas generator cycle is the easiest to control and least sensitive since it works against atmospheric or low pressure not very dependent on the turbine itself. The turbine for this cycle is a low flow high pressure ratio machine. The discharge pressure of the pump is slightly above chamber pressure. For the expander cycle the heat source is the nozzle cooling, which means that the amount of heat is limited by heat transfer processes. All the flow is pass through the turbine, and the available chamber pressure depends directly on the on how much pumping power that can be delivered given the heat input. This makes it sensitive to the turbine efficiency. The discharge pressure is high compared to the chamber pressure, enough to allow expansion through the turbine before being injected to the chamber. A staged combustion cycle allows for extremely high chamber pressures. As a consequence the discharge pressure from the pumps will be needed to be extremely high and multiple pumps are used in some cases. From NASA SP-8107 a summary graph is given in figure 2 for reasonable choices of cycle for different chamber pressures along with the resulting pump discharge pressure.

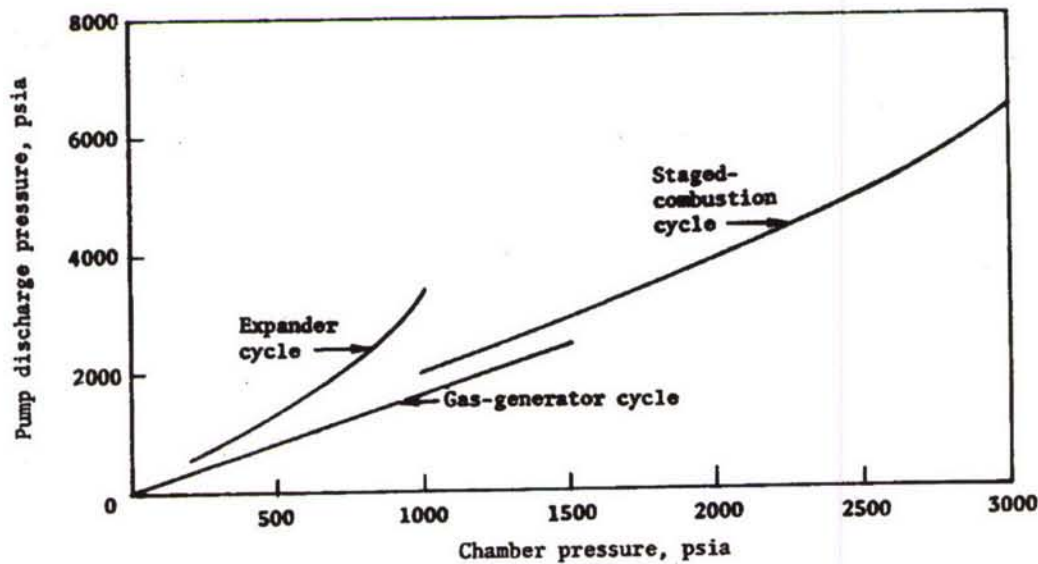


Figure 2 Relation between chamber pressure and pump discharge pressure for the cycles
(1000 psi = 70 bar)

The mass flows of fuel and oxidizer respectively will vary with the choice of propellants. The most important property for the pump is the density of the fuel. We can compare RP-1 with liquid hydrogen LH2 in this respect. For a 100 bar discharge pressure the pump head is for the propellants summarized in table 1. The lower the density therefore the higher the pump power becomes. The differences are large, for the same mass flow of LH2 the pump will take a factor of 10 times the power.

Table 1 Effect of density on pump head

	Density * [kg/m ³]	Pump head at 100 bar [m]
LH2	75	13600
RP-1 (Kerosene)	810	1260
LO2	1200	849

* Approximate numbers. Density varies with temperature and pressure

Notably the pump head for liquid hydrogen is 13.6 km, a huge number that if applied as a fountain would send the water column up above the Mount Everest, and the most extreme discharge pressure would go up to above 600 bar exit pressure from a pump. Other effects to consider are the lubricating and cooling properties for bearings. The burner gases are of very different quality, they are going to be either fuel rich or oxygen rich. For LH2/LO2 the choice is always hydrogen rich, and LH2 is used for cooling with excellent properties. For RP-1/LO2 there is some variation. For Oxygen rich gases means that the partial pressure of oxygen is extremely high with associated fire risk and risk for deterioration of structural surfaces by oxidation. In order to reach 1000K on the rich side an O/F=13 (or equivalence ratio 26) would be needed. Such very rich mixtures may cause problems with residue as the carbon compounds meet surfaces. Using kerosene for cooling can also easily cause coking.

For the turbopump assembly some different arrangements have been used. Gears have been in use early on in the development of American engines. These have been replaced largely by pumps driven directly by the turbine. We shall therefore not discuss geared configurations. There may also be one turbine driving fuel and oxidizer pump on a single shaft. The choice is made as a trade between cost/complexity and efficiency. On the pump side both axial and radial pumps are used in different configurations. The majority would appear to be radial pumps with an inducer fitted to avoid cavitation. An example of an axial pump for LH2 is shown in figure 3 from the J2 engine LH2 fuel pump. Further down examples of centrifugal pumps are shown .

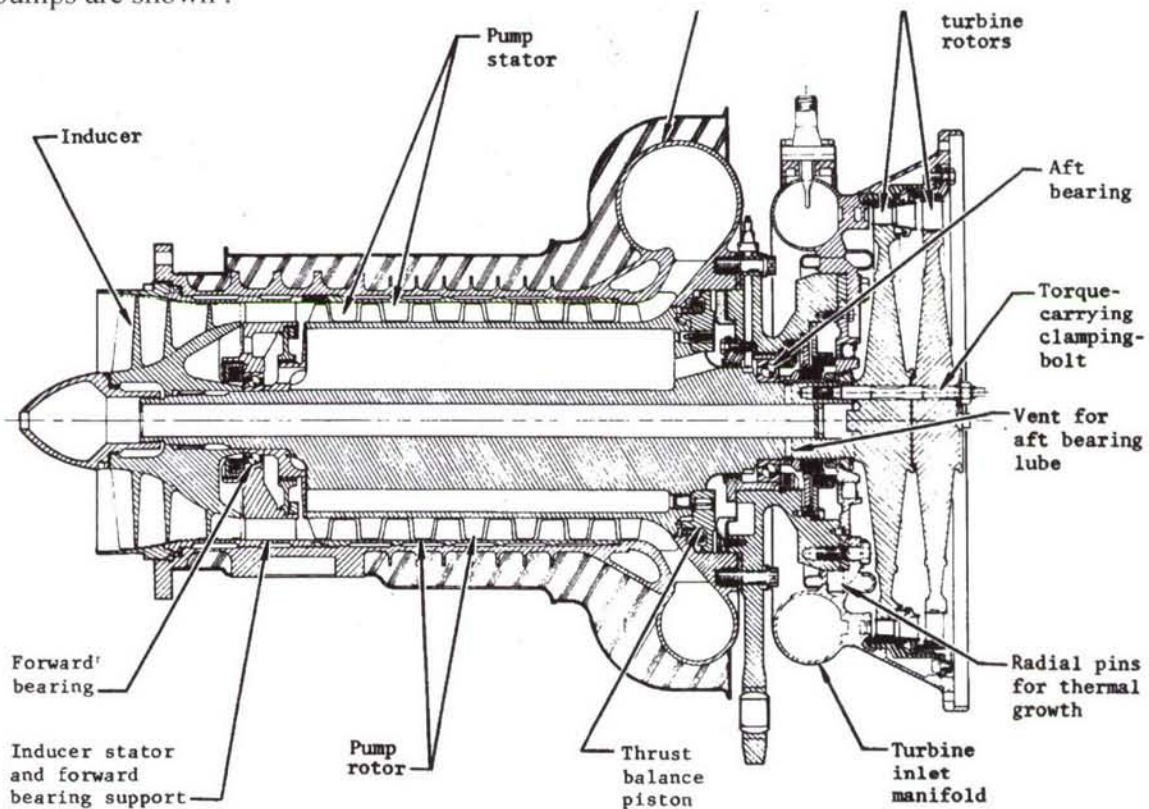
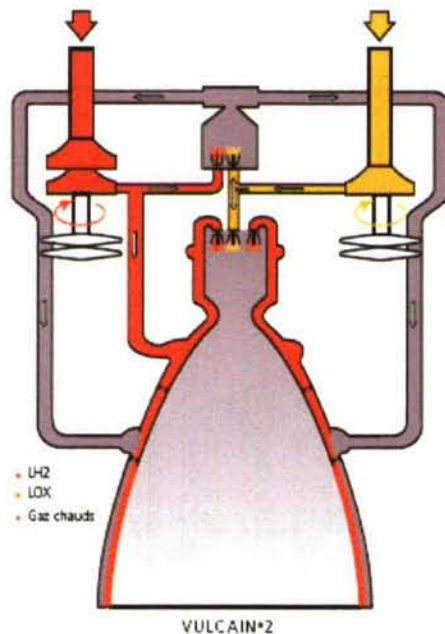


Figure 3 J2 axial fuel turbopump assembly from [3]

1.1. Gas generator

In a gas generator cycle the turbine exhaust is de-coupled from the main flow of propellant thus giving an available pressure ratio that is chamber pressure to atmosphere.

The gas is produced by burning some of the fuel/oxidizer. The first goal is to limit the loss of Isp inherent in expanding some of the gas to lower pressures than the chamber pressure, the mass flow used should be limited. Increasing the inlet temperature beyond $\sim 1000\text{K}$ would mean that the vanes and blades must be cooled. In terms of turbomachinery efficiency it is difficult to use a pressure ratio in the order of 100 efficiently over the single turbine; therefore the gas is exhausted to atmosphere through separate nozzles contributing to the thrust, or possibly introduced in the main nozzle. The latter principle is used on the Vulcain 2 engine, shown in figure 4. This arrangement uses the turbine exhaust gas both to generate thrust and to help in the cooling of nozzle wall by using the turbine exhaust as a film. Weight is then gained by avoiding a large surface that need fuel cooling near the hot flame.



Le moteur cryotechnique Vulcain*2 est dérivé du moteur Vulcain* de l'étage principal d'Ariane 5. Il a été développé dans le cadre du programme Ariane 5 Evolution.

Lancé en octobre 1995, ce programme a permis d'augmenter les performances du lanceur. Ainsi sur une Ariane 5 équipée de l'étage supérieur ESC-A, le moteur Vulcain*2 permet une augmentation de la charge utile en orbite de transfert géostationnaire de 1 150 kg par rapport au moteur Vulcain* qu'il remplace. Snecma est maître d'oeuvre du programme Vulcain*2 et pilote dans ce cadre une coopération d'industriels européens comprenant notamment Techspace Aero, société du groupe SAFRAN, EADS ST GmbH, Avio et Volvo Aero Corporation.

Vulcain*2 a été optimisé en améliorant, en particulier, trois paramètres :

- le rapport de mélange oxygène liquide/hydrogène liquide est passé de 5,2 à 6,1

CARACTÉRISTIQUES

• Poussée dans le vide (kN)	1 340
• Impulsion spécifique (s)	431
• Pression de combustion (bar)	115
• Ergols	LOX- LH2
• Débit d'ergols (kg/s)	320
• Rapport de mélange	6,10
• Vitesse de rotation TP (tr/min)	LOX : 12 300 - LH2 : 35 800
• Puissance turbines (kW)	LOX : 5 - LH2 : 14
• Hauteur (m)	3,45
• Diamètre sortie tuyère (m)	2,10
• Masse du moteur (kg)	2 100

Figure 4 Schematic and main data of Vulcain2 engine developed by SNECMA and used for the European Ariane5 heavy launcher (Source: fichier technique available at www.snecma.com)

The start transients need to be very fast in order not to consume propellants on the ground, in this case a pyrotechnic device is used. This means that a hot gush at high pressure hits the turbine after the start "explosion", the turbine acceleration is completed in seconds giving an

extremely rapid load transient. This start transient is a major challenge to the mechanical design, as it leads to extremely severe thermal gradients and thereby stresses in the material. The stop transients can be as severe a load case on the engine. This may appear strange for a dispensable engine, but the engine is test fired at least once before flight. The hot engine is flushed with cold gases when it shuts down which produces a shock cooling

In order to minimize the mass flow consumed the turbine and pump should operate efficiently. In order to achieve this the blade speed and flow velocities should generally be high. The blade speed is limited by mechanical constraints to the order of 500-600 m/s. For the Oxygen pump the shaft speed may limit the practical mean speed to values lower than this. In the Vulcain 2 engine separate pumps are used for LH2/LOX both with radial pumps. A cross section of the LOX pump in figure 5 shows the arrangement using an inducer on the pump side and an overhung 2-stage axial turbine on the turbine side. The overhung turbine arrangement is generally preferred if it is possible. Outboard bearings cost weight and but allows higher rotor stiffness, and higher rotor speed which is necessary for the LH2 turbopump. Such an arrangement is used for instance on the LH2 turbine for the Vulcain engine.

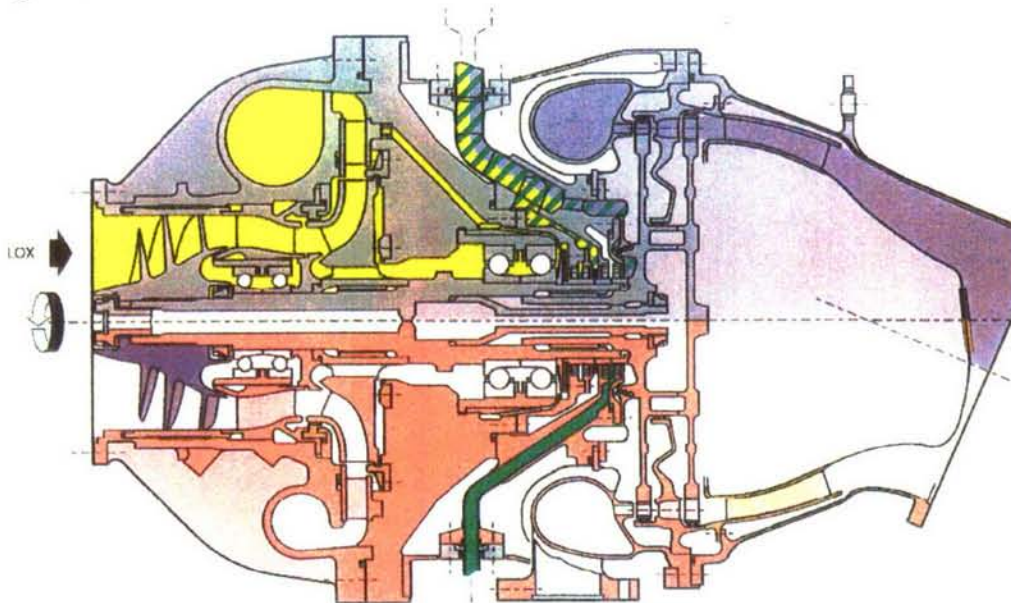
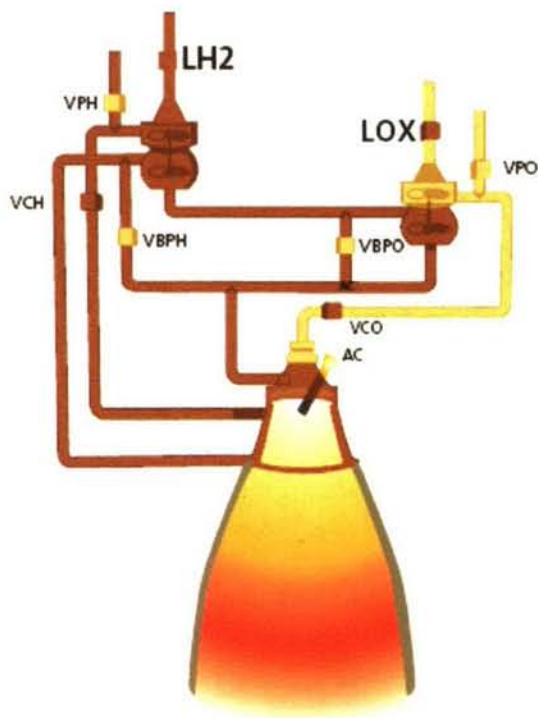


Figure 5 Cross section of LOX pump developed by Avio together with VOLVO Aero for the Vulcain 2 (from [9].)

2.1. Expander cycle

The attainable chamber pressure is immediately affected by the turbomachinery efficiency since the available heating power is limited by the heat exchanger process on the thrust chamber. On the upside for this cycle is the fact that a separate combustor is not needed in this cycle. The efficiency of the turbomachine is critical to operation and the engine system integrator has to work very closely with the component designers. The engine can start from tank overpressure, especially if it is an upper stage engine with vacuum counter pressure. The start produces a very cold dip before the heating of the fuel starts following ignition in the chamber very cold dip on the start transient. The initial LH2 flow is at $\sim 30\text{K}$ from which temperatures rise fast. A modern example of an engine using the expander cycle is the SNECMA VINCI upper stage engine, shown in figure 6.



CARACTERISTIQUES

• Type	Cycle expander
• Poussée dans le vide (kN)	180
• Impulsion spécifique (s)	465
• Pression de combustion (bar)	60
• Rapport de section	240
• Ergol	LOX - LH2
• Débit d'ergols (kg/s)	LOX : 33,70 - LH2 : 5,80
• Rapport de mélange	5,80
• Vitesse de rotation TP (tr/min)	LOX : 18 000 - LH2 : 90 000
• Puissance turbines (kW)	LOX : 350 - LH2 : 2 800
• Hauteur (m)	4,20
• Diamètre sortie tuyère (m)	2,20

Figure 6 Characteristics of the VINCI upper stage expander cycle engine by SNECMA
(Source: fichier technique available at www.snecma.com)

In the expander cycle all the fuel passes the thrust chamber in order to pick up heat. LH2 is the fuel most easily adapted to the cycle. It has a high heat capacity and does not risk to coke or contaminate the pipes. Oxygen is mostly avoided as heat carrier as it is aggressive and easily causes fires. Hydrocarbon fuels have a coking problem and works less well as heat carriers than the hydrogen. Figure 7 shows a cross-section through a VINCI LH2 pump for an expander cycle.

TPH VINCI 180

CARACTERISTIQUES :

Vitesse de rotation	90 000 tr / min
Puissance	2500 kW
Débit entrée pompe	5.8 kg / s
Débit entrée turbine	4.8 kg / s
Pression sortie pompe	225 bar
Pression entrée turbine	180 bar
Pression sortie turbine	90 bar
Température entrée turbine	240 K

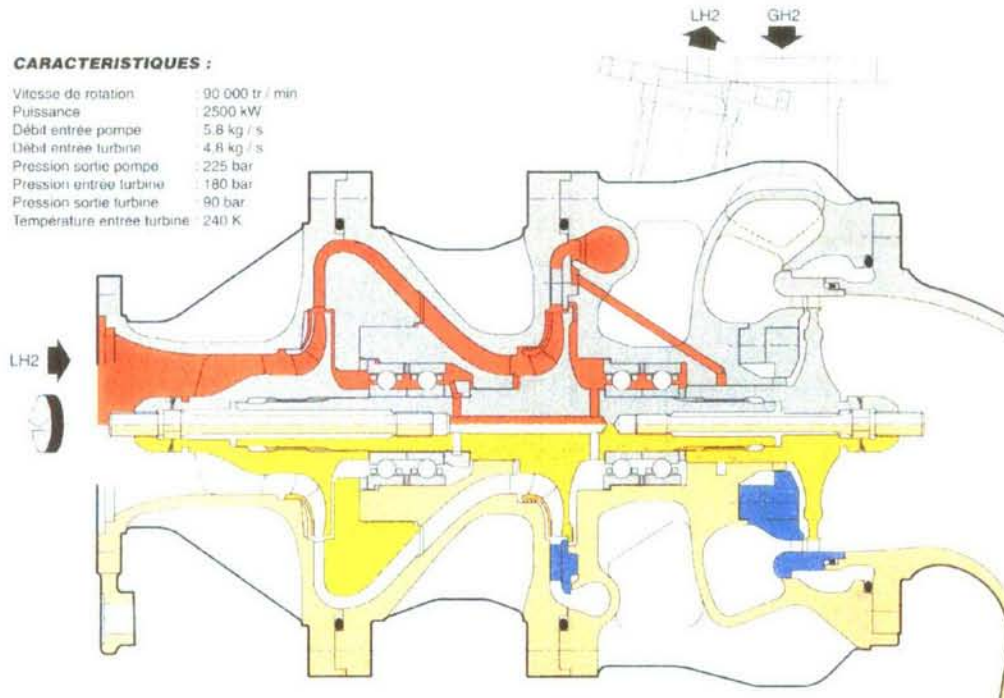


Figure 7 showing the VINCI LH2 turbopump developed by SNECMA with VOLVO aero as responsible for the turbine [13]

3.1. Staged combustion

The most typical feature is the extremely high pump discharge pressure, the SSME (Space Shuttle Main Engine) at 470 bar for a chamber pressure of 223 bar and Russian RD-170 has discharge pressures above 600 bar for a chamber pressure of 250 bar. The SSME has dual turbopumps making the system more complex in number of machines and sensitive to the success of the design of components. Under such extreme pressures the mechanical integrity of the machines becomes the overwhelming issue. This is shown in figure 8 where both low pressure and high pressure turbopumps can be seen.

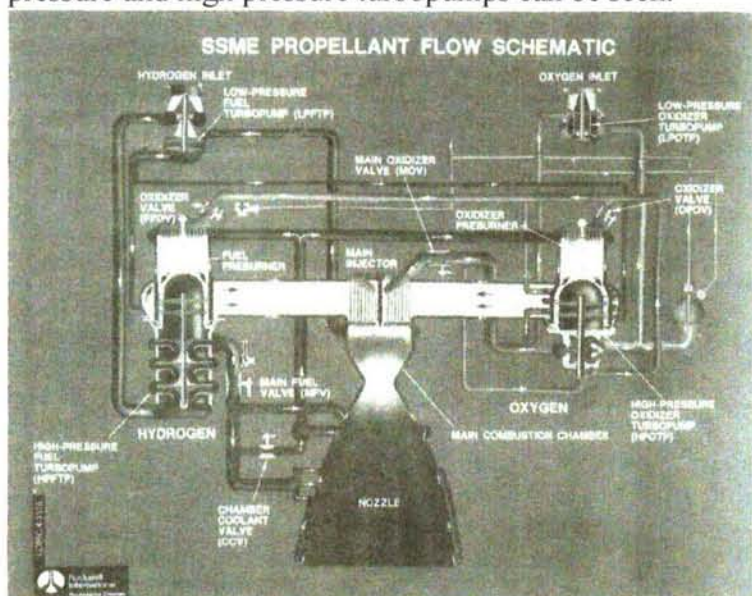


Figure 8 SSME chart showing engine flows

The turbine of the RD-170 feeds all turbopumps, with a total shaft power of and 192 MW over a single stage, the inlet pressure in 519 bar and the flow 2400 kg/s [2]. The pressure ratio over the turbine is 1.92 and inlet temperature 770K. I the engine RP-1/LOX is used with the choice of oxygen rich gas in the turbine. For this engine development a remarkable note is that over 200 development engines was used for testing.

3. Example design of turbopump

The actual development of the turbine starts from the basic architecture and specification of the engine performance parameters. A specification in this context is a set of data and rules agreed with the engine designer. This will set goals on performance, weight and cost. The development phase can span over a decade starting with a specification and ending with a functional product. In this process progressively more people become involved and more money is spent each week. At the same time as time progresses there will be less and less things that can be changed since more details become frozen.

Preliminary Design of pump for an imaginary gas generator cycle

In order to provide some understanding of how design features relate we will go through a sample design loop using relatively simple tools. The example will be a design for a gas generator cycle using LH2 and LO2. The basic cycle parameters for the cycle that are of relevance to the turbomachinery are picked arbitrarily:

Propellant mass flow rate 300 kg/s at O/F=6, Pchamber 100 bar, Pinlet 1 bar.

Table 2 Summary of Pump flow data for example turbopump

Pinlet	Pexit LH2	Massflow LH2	Pexit LO2	Mass flow LO2
1 bar	132 bar	42.9 kg/s	120	257.1 kg/s

In order to start the design we begin with the sizing of the pump. The efficiency potential of the pump will be maximized for the engine and the sizes and speed are selected. These numbers hen form the primary requirements on the turbine. As the turbine is designed it could happen that it is difficult to find a good solution which could force us back one step and re-design the pump. The main tools for selecting the pump size are 2 non-dimensional numbers, classical in turbomachinery:

Specific speed
$$n_s = \frac{\Omega \sqrt{Q_m}}{(gH)^{3/4}}$$

Specific diameter
$$d_s = \frac{D(gH)^{1/4}}{\sqrt{Q_m}}$$

The red circle in figure 9 marks the optimal choice of specific speed and specific diameter. Commonly American literature does not use SI-units and comes out differently in terms of size. Here SI-units will be used, and conversions made when using diagrams or numbers quoted from American literature.

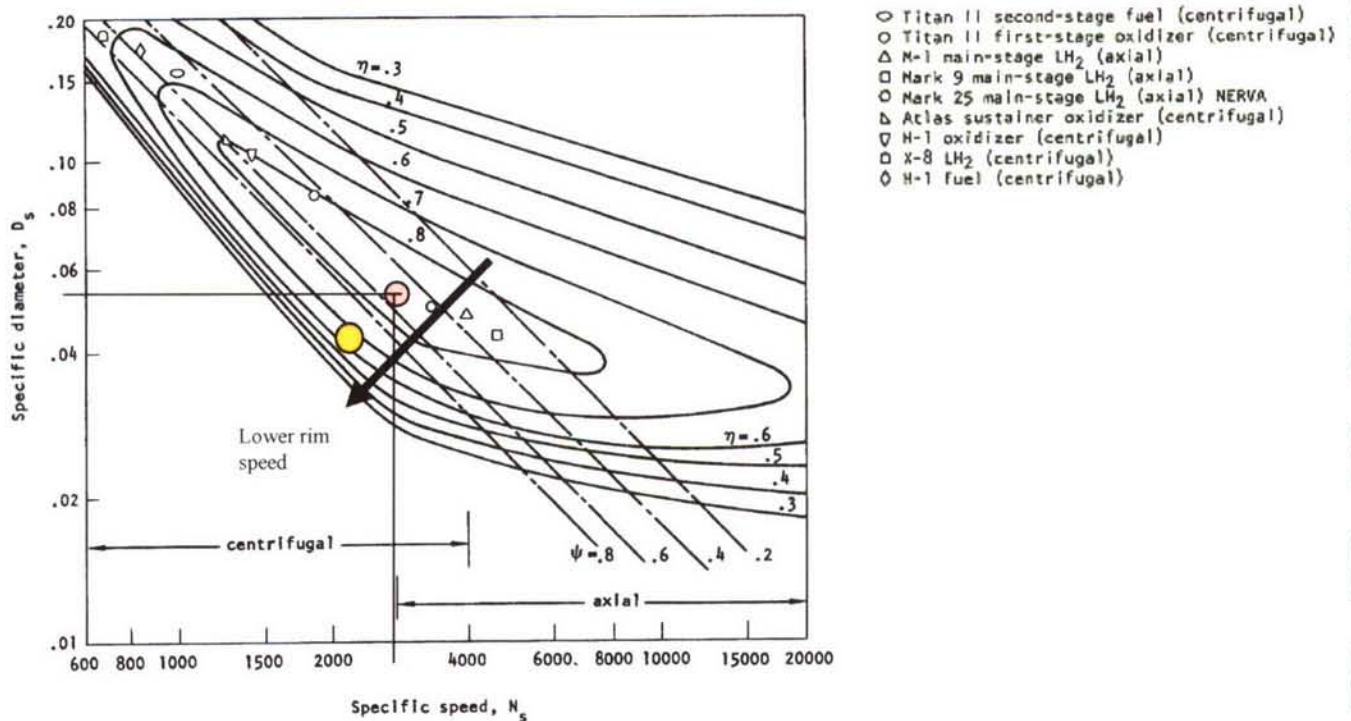


Figure 9 ns-ds diagram with from NASA SP-8109

The selected point at maximum efficiency gives (converted to SI units):

$$\text{Specific diameter } d_s = 0.055 * 50.5 = 2.77$$

$$\text{Specific speed } n_s = 3000 * 3.66 * 10^{-4} = 1.1$$

The design point for a single stage pump the diameter and shaft speed for the machines.

The LO2 pump

The LO2 pump must be chosen with a relatively low tip speed but gets a rather large diameter. The pumped power is about 1/3 of the LH2 pump, and hence it will be less critical to performance of the cycle. In terms of a system trade the weight could be brought down by decreasing the tip diameter and increasing the shaft speed. The weight range of the LO2 pump in this class is 150-200kg. Table 3 compiles the data for the pumps.

The LH2 pump

Trying first with a single stage LH2 pump gives a design that would have a high rim speed, 665 m/s, SP-8107 considers pump rim speeds (unshrouded) above 800 m/s, but here we will take a careful approach. We also have a low inlet pressure that leads to cavitation risks. It is then reasonable to consider this too high and look for other solutions. The options that we have are to reduce rim speed by lowering d_s and/or n_s . The choice indicated by the yellow dot in figure 9 gives a rim speed below 500 m/s, but also a lower efficiency. In the diagram the loss is as much as 10 % a rather large number that must be compensated by turbine shaft power. Another option is to use a second stage and stay on the optimal performance point, table 3 includes those options.

Table 3 Solutions for pumps using design charts

	Shaft speed N [RPM]	Tip diameter D [mm]	Tip speed U _{tip} [m/s]	Efficiency potential η [-]	Power needed P [kW]
LO2	22980	132	158	0.8	3500
LH2 1-stage	122100	104	665	0.8	10200
LH2 1-stage reduced ns,ds	106140	83	462	0.7	11700
LH2 2-stage	72600	124	469	0.8	10200

This example of pump sizing serves to show the effects of constraints and to provide operating conditions that will be used for sizing a turbine. Another constraint is formed by the risk for cavitation in the pump. The pressure ahead of the pump must be large enough so that the lowest pressure on the suction side of the impeller does not fall below a critical value for cavitation. This is usually measured as NPSH (Net Pressure Suction Head) and will often affect the allowable limits of the machine. In [5] these limits are detailed and compared in several ways. Other constraints that may limit the speed is, rotor dynamics and the bearing inner race speed may become limiting as well as the turbine blade stresses in a later stage of the design.

At this point, however, we will be happy for now with the sizing of the pumps so that we can go on with the turbine.

4.1. Turbine performance

The most important performance data can be thought of as a budget for the turbine designer. In order to start working out the details of the turbine these must be known. We shall try to give an example that is non-unique but reasonable way to work through the choices that can be made. The start is made from the basic set of data given on one aerodynamic design point (ADP). When the engine cycle and architecture has been selected and laid out the pump load is known and a suitable turbine can be designed to meet those requirements. The pump size and reduced speed depends on the working media and delivery pressure. The speed on the shaft will be considered governed by the pump, until other limitations must be accepted.

5.1. Turbine duty and assessment of efficiency potential

We are going to use 1000 K as the inlet temperature to the turbine, which can marginally be managed with super alloys with no cooling. By comparison modern aeroengines are at 1900K, using advanced cooling technology. Introducing cooling to the blades would increase complexity of the system, in particular for the relatively small blades and also require bleeds from the pump with increased plumbing as a result. On the oxygen side cooling must be drawn from somewhere else since the turbine is mostly fuel rich. We have a temperature and pressure at the inlet to work with, after allowances for pipe and valve losses and burner. The exit pressure would be selected to be something sufficiently high to allow safe evacuation of the hot exhaust from the aft of the rocket. The higher the exit pressure the more thrust can be generated; on the other hand more gas will be consumed. This trade must be done at engine

level but is probably fixed when the turbine shall be designed. The spouting velocity

$$C_0 = \sqrt{2C_p(T_{00} - T_{is})} = \sqrt{2C_p T_{00} \left(1 - \frac{P_{out}^{\frac{\gamma-1}{\gamma}}}{P_{00}} \right)} = 2655 \text{ m/s}$$

can expect to find in terms of the velocity ratio and the possible turbines that would go with it. For the LH2 turbine we can expect the following: More than 500 m/s in U_m will not be allowed for stress reasons. $U_m/C_0 < 0.2$ results and we can see in diagram, figure 10, that for a single stage machine an impulse design could give 45% efficiency, in diagram figure 10 that a 2 stage design could improve this to 55% 3 stage will probably be too heavy on the rotor dynamics and is not admissible. For the LOX we know that the pump is slow, if we expect to end up at $U_m=300$ m/s then we have $U_m/C_0=0.12$. This gives us 38% for the single stage and 45% for the 2-stage machine. Cost constraints in the wants us to save on hardware so we accept a 38 % efficiency in the spec in order to make allowances for a 1 stage machine.

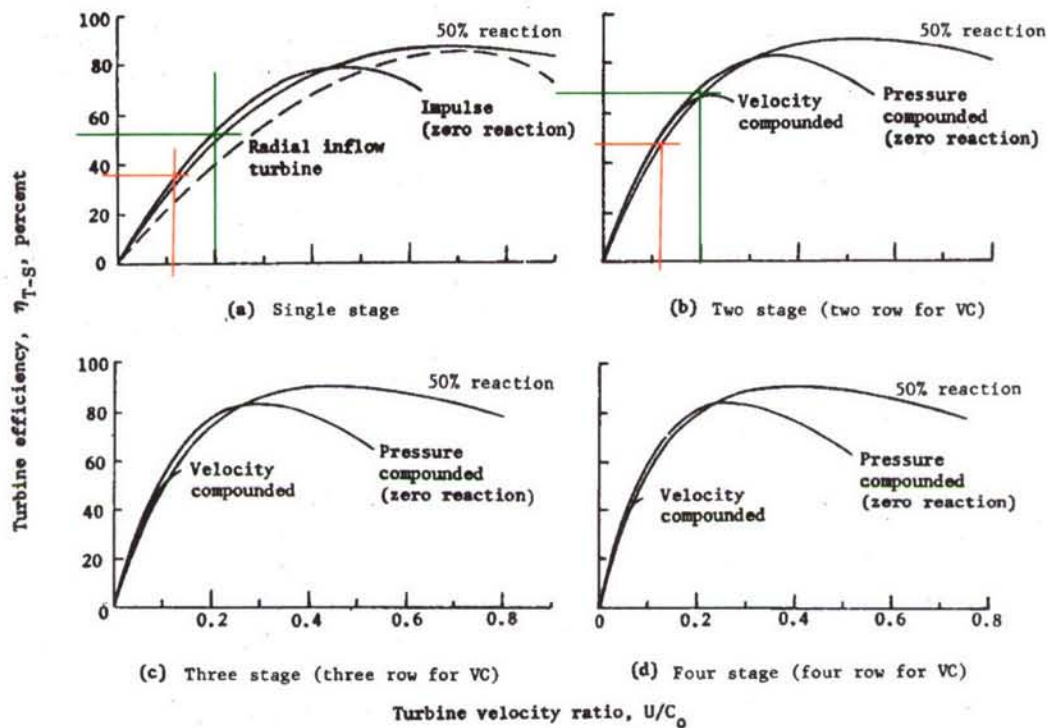


Figure 10 Efficiency potentials for supersonic turbines, red LO2 green LH2 points

As is seen from table 4 the mass flow consumption will still be twice as high for the LH2 turbine, which motivates the choice of saving cost on picking a single stage machine. 8 kg/s is below 3% of the flow to the chamber. Table 4 data will now form the specification that the turbine design will be set to match.

Table 4 Given data to match for the turbine ADP

	P _{tin} [bar]	T _{tin} [K]	Shaft speed [RPM]	Power [MW]	P _{out} [bar]	Massflow* [kg/s]	Efficiency* [-]
	100	1000	72600	10.2	10	5.27	55
	100	1000	22980	3.5	10	2.6	38

* Overdetermined less massflow is "always" better, as well as higher efficiency

This set is over determined in the sense that power can be computed given the other parameters. Efficiency could however be taken as a minimum requirement, the same way as the mass flow could be taken to be a maximum requirement. In a gas generator cycle the engine designer will probably be able to improve his engine if these parameters are better than budget. A temperature of 1000K is reached by burning at an O/F of 1.02, which gives values of $\gamma=1.357$ and a heat capacity $C_p=7757$ that will be used as constants through the turbine.

Selection of diameter and blade height

The first steps in the design are to fix some of the more general parameters for the turbine. The turbine gas paths mean diameter will be the first to be selected. This is done in more or less the same way as for the pump. Figure 10 gave some indications on how stages can be selected for a supersonic design. One of the most general design charts is given in figure 11 from [3]. Optimization of turbine performance in general is described in classical literature, and we will not go through all the possibilities given there. For each product there are unique constraints that affect the design. Applying these will force the designer away from the optimal selection of specific speed and specific diameter in order to satisfy load or mechanical requirements. The goal will be to find the best design considering a combination of weight, cost, efficiency and risk. The turbine parameters are normally given using exit parameters and this is the way they are used in our diagrams, so we will follow that way of presenting data.

Specific speed for the turbine

$$n_s = \frac{\Omega \sqrt{Q_{exit}}}{(gH)^{3/4}}$$

Specific diameter for a turbine

$$d_s = \frac{D(gH)^{1/4}}{\sqrt{Q_{exit}}}$$

We will now take the given shaft speed, which immediately gives the specific speed. The shaft speed was given by the pump, the isentropic enthalpy drop by inlet temperature and pressure ratio and the volume flow by exit density and mass flow.

The LO2 turbine

In figure 11 the red line mark the LO2 turbine choices for a 2 stage and a single stage turbine. In both cases $n_s=0.05$. d_s is 6.37 for the single stage and 8,37 for the 2-stage machine at a diameter D_m of 250 mm.

The diameter for the LO2 turbine was increased compared to the pump in order to increase the specific diameter. The blade height however for the LO2 turbine is becoming small, 1-2% of the diameter giving a blade that is only 5 mm high following the correlation in figure 11. The selection of blade height is probably the most open choice that the designer has to deal with. Reducing the diameter in order to increase the blade height would lower the efficiency again and make the effort useless. The blade height can allow for some blockage in the passage. In Sp-8107 a lower limit of 4mm is given for blade height. This would of course be dependent on whether a tip shroud is used or not, but can serve as a warning sign until it can be shown that the leakage can be handled. The height will have to be negotiated at a later stage in more complete loss analysis, where the aspect ratio of the blade can be calculated.

The LH2 turbine

The green lines in figure 11 shows the LH2 2-stage machine choices, and the black line the LH2 1 stage.

Using an intelligent guess that we will need all speed we can get, and assuming that the max we can have is a blade speed at mean diameter $U_m=500$ m/s. The diameter can be picked out immediately at $D_m=132$ mm. Optimal it would be $d_s=8$, but this takes us to 1000 m/s which is hopeless. In terms of attainable efficiency the 1 stage is at 55% in figure 11. For the LH2 the first check shows that a stage count of 2 for the LH2 turbine in our example gives good improvements in efficiency $>60\%$ and will be worth considering. A blade height of 10-13 mm is perfectly acceptable to start with.

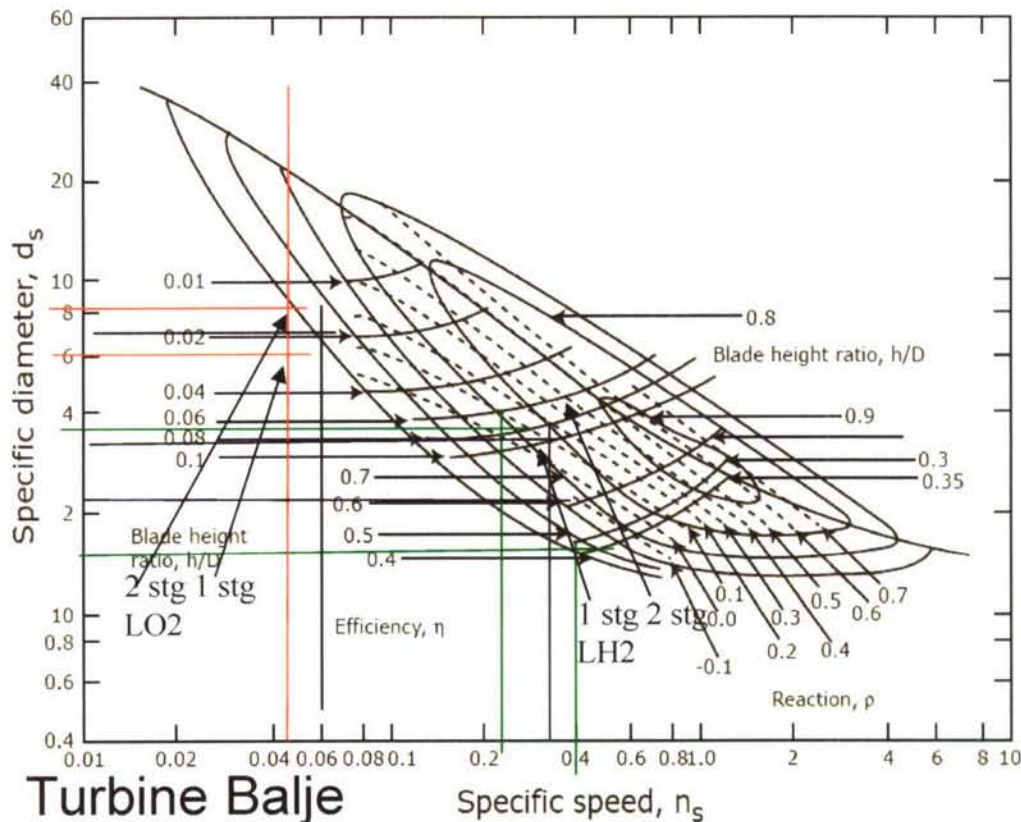


Figure 11 n_s - d_s diagram for turbines with selected points for the LO2 red and LH2 green options

Velocity or pressure compounding

Velocity compounding provides the extreme in obtaining power for a given pressure ratio and mass flow. However in our example we have chosen to fix the pressure ratio over the entire turbine. The reason for doing so practical, the engine designer will have assumed a pressure for designing exhaust of the turbine gas, whether in separate nozzles or if it is introduced in the main nozzle. For the turbine to be efficient at high pressure ratios the tip speed must be high. Here the propellant properties become important, for the LO2 pump the shaft speed will be low, so without a gear the specific speed will have to lower than desirable for turbine performance. The degree of reaction should be low at low isentropic velocity ratios, say lower than 0.25 the degree of reaction should be 0 and increasing to 50% as the isentropic velocity ratio goes to 0.45. This is here settled in the layout step where we look at the velocity triangles.

Layout

At this stage it is appropriate to introduce analysis using the notion of velocity triangles and flow areas. We will use analysis on the mean diameter of the turbine at design point, in order to get a better view of loss distributions and area development. More constraints can be added on structure angles etc. Also we work up to selecting chord and blade count. Some definitions of velocity triangles and notation are given in figure 12 below.

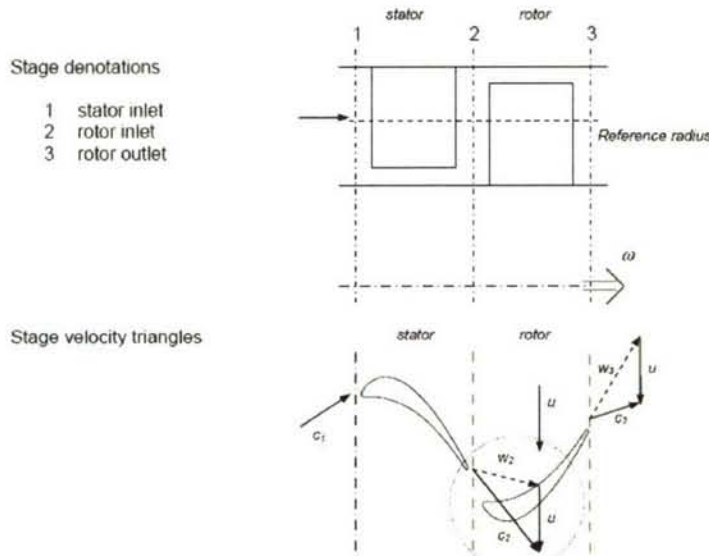


Figure 12 Turbine stage notations

Stress limits are assessed by using the AN2 parameter that relates to blade root mean stress. $AN^2 = \pi(r_o^2 - r_i^2) \cdot \Omega^2$. Figure 13 gives a NASA correlation for the parameter. Notably for INCO 718 for example is that the data falls sharply after 1000K. At that point cooling must be added or the material improved.

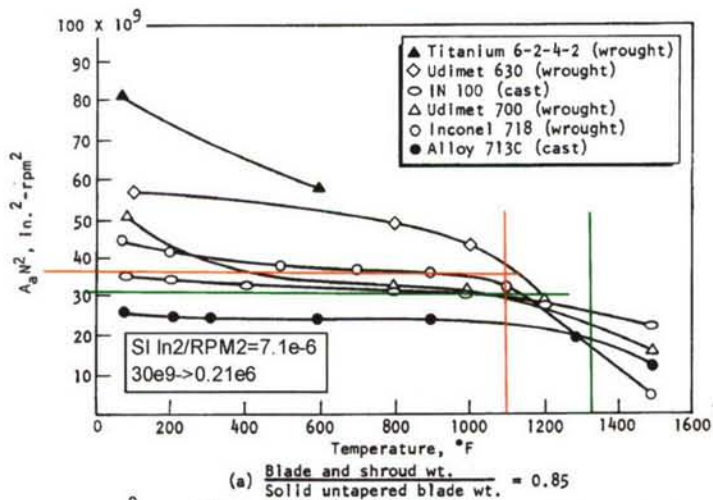


Figure 13 AN2 versus temperature stress limitation from [6]

Now the design points will be given on the mean line in order to show main data that helps to make final decisions on the turbine layout.

LH2 turbine single stage

For the LH2 turbine we first try to get a single stage design to work. Beginning Layout of a single stage turbine for the LH2 will require height substantial height increase through the rotor in order to avoid choking. This piece of information is not found in the ns-ds diagram, but could be vital as the AN2 parameter gets out of admissible range. This can not be seen immediately in the ns-ds diagram. Opening up the gas path means that the blade becomes much longer which first increases the root stress, the AN² parameter goes up above admissible values, in final version 0.635E6 which is above the admissible 0.21E6 (in SI units). In order to improve this situation shaft speed could be reduced, with some implications for the turbine efficiency.

Table 1

LH2	Station	S1 inlet	S1 outlet R1 inlet	S2 inlet R1 outlet
Total pressure (abs)	[bar]	100.0	80.0	16.4
Total pressure (rel)	[bar]		28.6	20.0
Static pressure	[bar]	94.1	12.1	12.5
Total temperature (abs)	[K]	1000	1000	818
Total temperature (rel)	[K]		863	863
Static temperature	[K]	984	608	763
Density	[kg/m ³]	4.69	0.97	0.81
Speed of sound	[m/s]	1651	1298	1453
Mach No. (abs)	-	0.30	1.90	0.64
Mach No. (rel)	-		1.19	0.86
Axial velocity	[m/s]	350	680	816
Tangential velocity (abs)	[m/s]	350	2370	-439
Tangential velocity (rel)	[m/s]		1868	-941
Flow angle (abs)	[deg]	45.0	74.0	-28.3
Flow angle (rel)	[deg]		70.0	-49.1

With these problems reported and that there seems to be little hope to improve the single stage LH2 is abandoned. It is desirable in early design to have some margins to work with later in the detailed design in order to make up for off design points or shifts in design point needed by the engine designer. At this point we are bouncing between choking and stress limits. Increasing the diameter implies reducing shaft speed, which can be done but preferably not.

LH2 turbine 2-stage

The 2 stage machine as seen in the ns-ds diagram has a higher efficiency potential to start with. The initial potential estimate has an efficiency of 55% giving a mass flow consumption of 5.27 kg/s. In the layout estimates we arrive at an efficiency of 63% which is comforting. The overall data for this design is compiled and shows good margins. The exception is AN2 for stage 2 which is marginal. Some more work should be added here, possibly trading away some efficiency to gain on robustness. This can be done at pump level now since we have some margins on the turbine.

Station data for the 2 stage LH2

LH2	Station	S1 inlet	S1 outlet R1 inlet	S2 inlet R1 outlet	S2 outlet R2 inlet	S3 inlet R2 outlet
Total pressure (abs)	[bar]	100.0	88.0	44.4	39.1	19.1
Total pressure (rel)	[bar]		59.1	53.1	27.5	24.0
Static pressure	[bar]	94.1	41.8	35.7	14.4	12.7
Total temperature (abs)	[K]	1000	1000	875	875	750
Total temperature (rel)	[K]		917	917	797	0
Static temperature	[K]	984	822	826	672	674
Density	[kg/m ³]	4.69	2.49	2.12	1.05	0.92
Speed of sound	[m/s]	1651	1509	1512	1364	1366
Mach No. (abs)	-	0.30	1.10			
Mach No. (rel)	-		0.73	0.79	1.02	1.01
Axial velocity	[m/s]	350	643	772	1022	971
Tangential velocity (abs)	[m/s]	350	1530	-401	1450	-481
Tangential velocity (rel)	[m/s]		1028	-903	948	-983
Flow angle (abs)	[deg]	45.0	67.2	-27.5	54.8	-26.4
Flow angle (rel)	[deg]		58.0	-49.5	42.9	-45.4

The overall blade data comes out of the analysis so that now we have sufficient data to start drawing the turbine cross section. Figure 14 details a view over the turbine blades the way the profile may look. From left to right we have Stator1 (nozzle) Rotor1 stator 2 rotor2

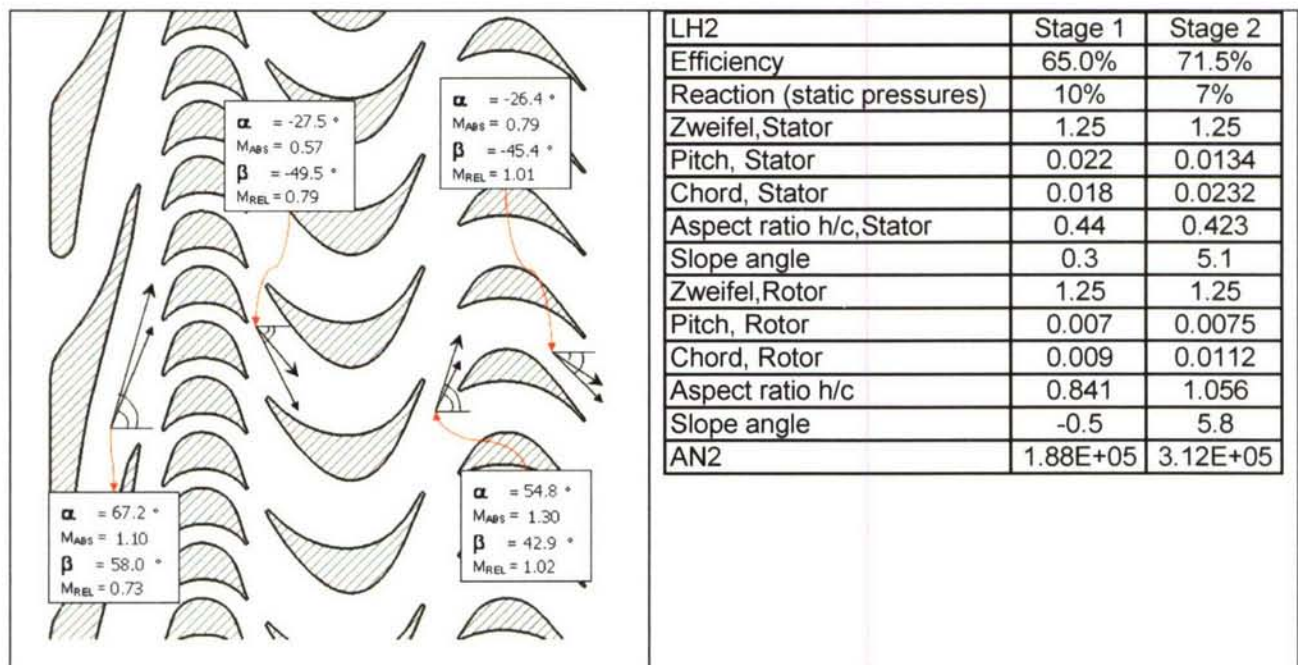


Figure 14 View of the example LH2 turbine with velocity triangles

LO2 turbine single stage

For the LO2 turbine the stress limitation is not a problem. Here the High Mach number is a problem for the efficiency. We find also here that a 2 stage machine would be beneficial to efficiency we shall make the best of a single stage machine, if a robust solution can be found.

Table LO2 single stage main data

LOX	Station	S1 inlet	S1 outlet R1 inlet	S2 inlet R1 outlet
Total pressure (abs)	[bar]	100.0	75.0	13.6
Total pressure (rel)	[bar]		25.7	19.2
Static pressure	[bar]	94.1	8.3	3.1
Total temperature (abs)	[K]	1000	1000	827
Total temperature (rel)	[K]		907	907
Static temperature	[K]	984	560	561
Density	[kg/m ³]	4.69	0.72	0.27
Speed of sound	[m/s]	1651	1245	1246
Mach No. (abs)	-	0.30	2.10	1.63
Mach No. (rel)	-		1.40	1.86
Axial velocity	[m/s]	350	610	701
Tangential velocity (abs)	[m/s]	350	2542	-1909
Tangential velocity (rel)	[m/s]		2241	-2210
Flow angle (abs)	[deg]	45.0	76.5	-69.8
Flow angle (rel)	[deg]		74.8	-72.4

LOX	Stage 1
Efficiency	42.2%
Reaction (static pressures)	6%
Zweifel, Stator	1.25
Pitch, Stator	0.029
Chord, Stator	0.007
Aspect ratio h/c, Stator	0.73
Slope angle	22.8
Zweifel, Rotor	1.25
Pitch, Rotor	0.013
Chord, Rotor	0.007
Aspect ratio h/c	1.009
Slope angle	33.9
AN2	5.68E+04

At this stage the flow angle should be kept below 75 degrees, because above this angle control of the flow area is difficult. We have a lot of margin to stress and rotor exit choke in this design so that it can be redesigned to lower the angle of the start. The degree of reaction would then go up slightly.

Summary of the designs

Now we have a design that has been defined to some level in one pass. There is definitely more work to be done on the example. If a better total design is to be generated there are at least 2 things that we may rework on the turbopump. NPSH criteria should be introduced in order to give realistic cavitation limit behaviour, and some thought should be given to tank pressure in this context. The second step is to check whether we could find better total solutions by increasing the diameters and reducing speed in order to find better efficiency on the turbine side. The efficiency on the pump side is relatively flat around the maximum, whereas the turbine has a larger gradient, so there is good hope to find a decent solution. This could also resolve some of the choking margins that we have on the turbine without increasing stresses.

The preliminary design choices will also affect the pump in terms of the axial thrust force on the shaft. The degree of reaction determines the pressure difference over a rotor disk. In our example we have discussed single stage impulse turbines which nominally do not have an axial thrust on the shaft, as well as weak reaction blades that have a significant pressure difference. In our example a 10-15% reaction gives up to a 2 kN axial thrust. This is important in terms of the system function and must be considered when designing seals as well as it may later affect the aerodynamic design. The total axial force on the bearing is not allowed to change sign, as the bearings will be designed to have the force going one way. This point must be analyzed carefully at off-design conditions.

Secondary flow system

Control of the thermals and leakage flows in the turbopump is an important design task. Provisions must be made for purging the cavities between rotors and stators. In gas turbines and aero engines this amounts to providing cooler compressor air to the turbine rotor stator

cavities in sufficient amount to avoid the penetration of hot gases into the cavity. Also coolant for the turbine blade and shroud are provided for in this way. In the LH2 turbo pump leakage flows of liquid hydrogen can be purged through the turbine cavities and entered to the main gas path. The main particularity of this is that LH2 comes very cold; the temperature can be in the range of 30-40K. LH2 is also used in the system to cool and lubricate the bearings. In the oxidizer pump the situation is very different. If oxygen leaks into the turbine the risk for explosion or failure is large. The turbine is driven by a hot fuel rich mixture together with which the oxygen will react very rapidly. This has caused several failures in development as well described in [1]. It is preferred that hot turbine gas flows down through the cavity, with implications in particular for the disk temperature. Alternative or complementary schemes used involve purging with Helium or other inert gases.

Pitch line or stream line analysis

At this point we have a proposed baseline turbine that should satisfy most constraints and have a good efficiency potential. We can turn this around and start analyzing the performance at design point and at other operating points, as well as start to consider the blade profile shape, angles thickness distributions et.c.. The correlations at this stage will relate the loss in total pressure to the flow velocity or loading. Typically this is given in terms of the total pressure loss over a blade or vane row divided by the exit dynamic pressure. For turbines the common form is:

$$Y_{xx} = \frac{\Delta P_t}{P_{t,out} - P_{s,out}}$$

In the literature and practice a number of different sets of losses are referred in order to describe the losses due to different design features. Ainley-Mathiesen or Kacker-Okapuu are two well known such systems. We shall not go into a detailed discussion on these, only refer to the more important losses in these turbine blades. In [9] a classic text on turbine performance.

- Shock loss – A dominant loss for supersonic turbines such as the LO2 turbine in our example. A normal shock at M=2 relative speed causes a loss of almost 30% of the total pressure. This can increase the total loss dramatically.
- Profile friction loss – The boundary layer friction causes the classical wet surface loss. At high pressures and velocities the Reynolds number is large despite the small size and the wet surface loss therefore relatively small. $Y \propto Re^{-\frac{1}{5}}$
- Trailing edge – The base surface gives a drag that incurs significant losses, in particular for small blades and mechanically challenged where the thickness to chord ratio is large. Normally $Y \propto \frac{t}{c}$ but can be worsened at high exit Mach numbers or when the thickness/throat ratio becomes large. The aerodynamic designer will want to have 0 trailing edge thickness, while the structural designer will want to have a large radius in order to reduce stress concentration and thermal differences, add to this the manufacturing responsible who wants a large radius and allowances for tolerances and the ingredients of a good discussion are all there.
- Tip leakage loss – For unshrouded blades this can be a dominant loss factor. Thermal and speed transients in the start/stop sequences cause uneven growth of the casing and tip diameter. Tangency or rub is not allowed since debris may result or the rotor can be thrown into whirl. The resulting tip gap must be large enough so that tangency

never happens, which may require a tip clearance/blade height. Sealed tip shrouds reduce the problem greatly, especially for low reaction blades where the axial pressure difference driving the leakage is small.

- Secondary flow loss – As the blade aspect ratio becomes low the secondary flows formed when incoming boundary layers roll up or are migrated over the blade surface fills up the passage. Classically the desire has been to stay at h/c 3-4 but at least above 1. This is a very open subject today on how to handle. CFD and 3D design has a large impact on the secondary flow loss.

CFD supported detailed design

Current trends and efforts in design is to draw advantages of CFD methods becoming better and faster. All designs are analyzed in 3D CFD today. The results are most often allowed to affect the design in a sort of cut and try fashion, where solutions are modeled geometrically meshed and the results of the modification analyzed again. One such area is in optimizing the blade profile rather than designing the profile in a family. This way the optimization comes in late and can be used on detailed design decisions, unless large deviations in performance are discovered that leads to re-work of the preliminary design. This is however undesirable as it involves more people and often causes extra work and problems on other places. 3D analyses are systematically used and often still complemented by testing in turbine rig, the accuracy is today good in 3D CFD as used by experienced engineers that use good CFD codes and procedures. Figure 15 shows Mach number plots in 3d from CFD analysis of supersonic blades.

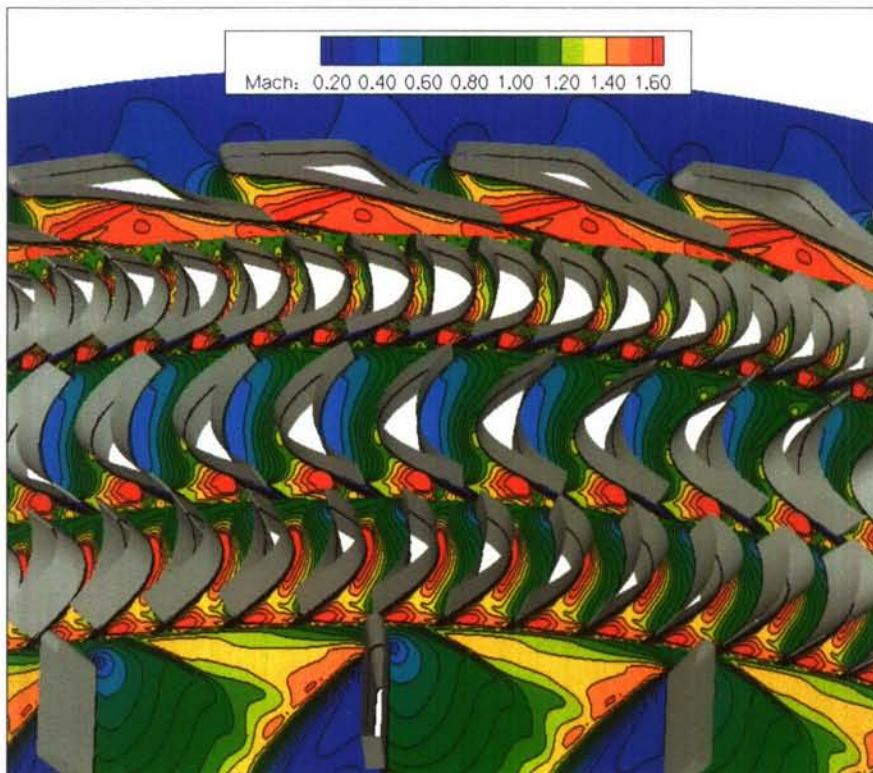


Figure 15 Mach number profiles at mid-span for an LH2 turbine design

The drive is however towards moving the CFD analysis upstream in the design chain so that we can have more parameters open. One such effort has been made in a recent diploma thesis

[12]. Here the blade parametric - CFD analysis chain is automated and then used in an optimization loop such that the efficiency can be maximized under the constraints that power and mass flow are constant. Optimization of the rotor blade was tried with a given nozzle first comparing a single design point at 10% reaction. A comparison of Mach number distributions is provided in figure 16. Clearly, the optimized design could be improved over the old design. The matching of the inlet angle and area is better as evidenced by the strong reduction of the bow shock. Also on the exit side the tendency toward overexpansion vanishes and the matching is better. The improvement in profile loss corresponded to 7% in isentropic efficiency.

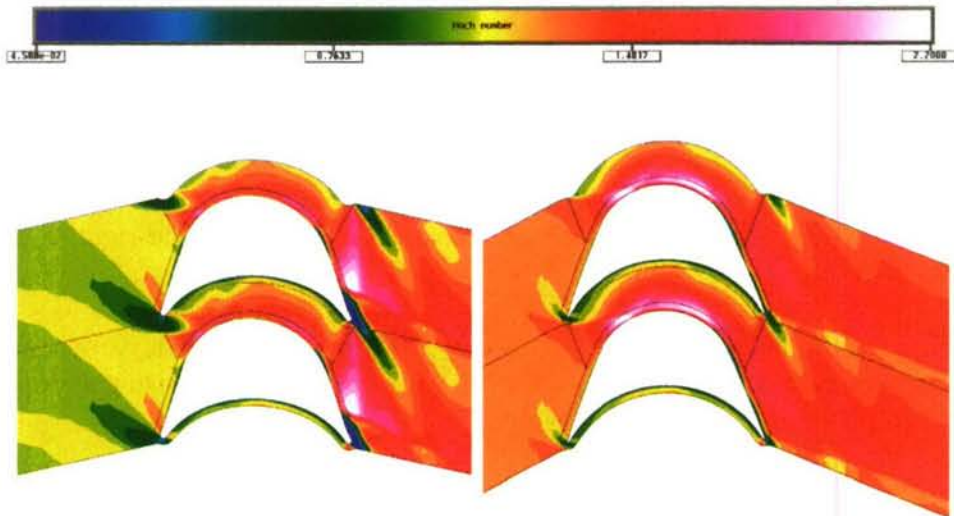


Figure 16 Comparison at 10% reaction. Reference blade left, optimized (Blade 1206) right

Perhaps more challenging is to use a range of operation points representative of an operating envelope and trying to find a design giving both high efficiency and low variability in efficiency under different operating conditions. Also this turned out to be possible; Figure 17 shows the Mach number distributions on a reference operating point and a worst case point. Clearly the blade picked out by optimization is very better adapted both operating conditions.

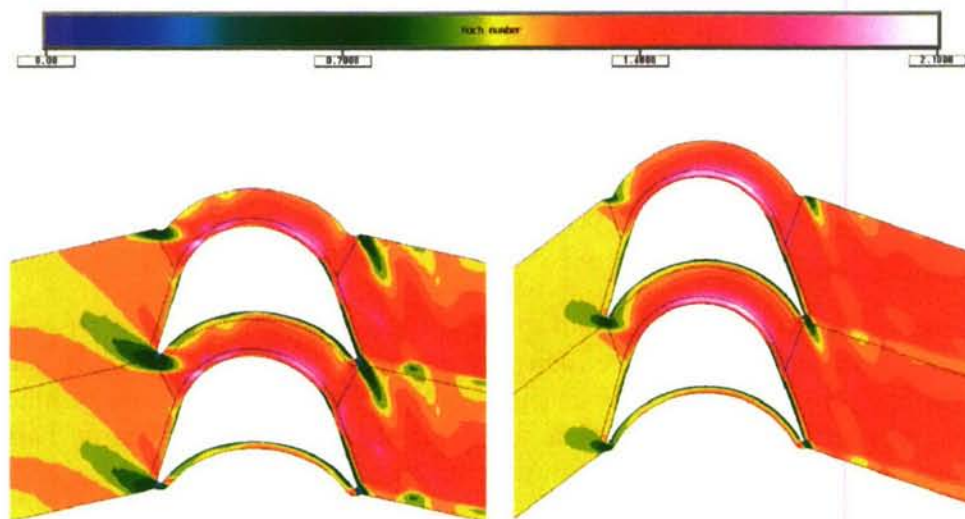


Figure 17 Comparison of Mach numbers at reference blade left optimized blade right, reference operating condition

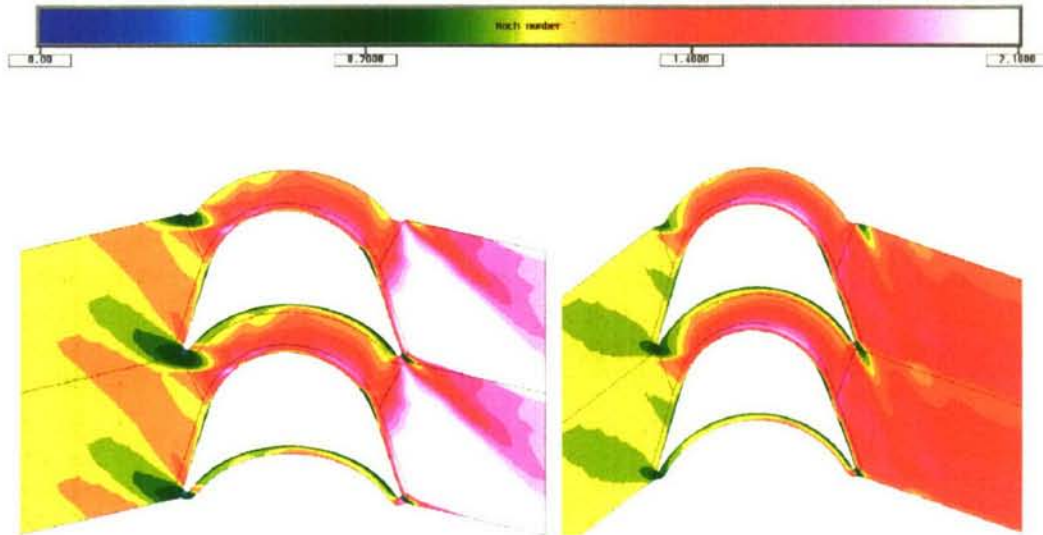


Figure 17 Comparison of Mach numbers at reference blade left optimized blade right, 1206 right off-design point

In fact over 5 operating conditions the variability was very low, and the efficiency improved on all operating points over the reference blade, figure 18. This provides a promising start for a hopefully very good engineering design methodology.

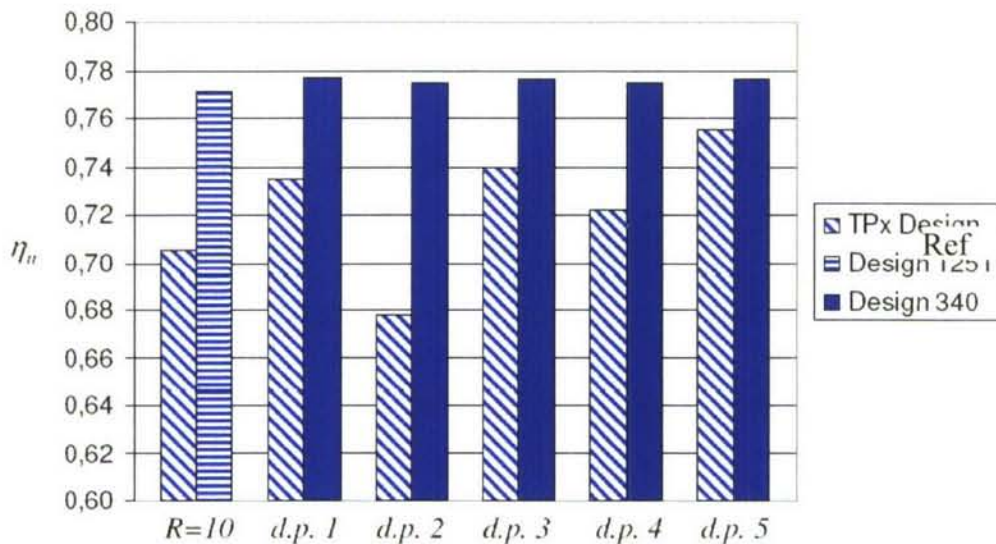


Figure 18 Efficiencies (2D CFD) for optimized profiles

Experience input and robustness

Minimizing development risk factors are important to the success of a project. These are less intuitive to an engineering student but influence industrial design in the common attitude that we do things the same way as last time. This can lead to the selection of an axial turbine where a radial turbine may appear more appropriate following standard selection charts. This occurs relatively often and is a principal reason why machines tend to look alike with stepwise improvements.

In terms of robustness to tolerances the design should be able to function predictably and not show a large scatter within the manufacturing tolerances. This is a very general statement but often machined processes become difficult if they require better than 0.1 mm accuracy. This

could be thought of as form tolerance, thickness of a blade leading edge radius, blade height etc.. The use of such a measure is very arbitrary but to the designer it could help to think in terms of:

“If this thickness is 0.1 mm larger what is the effect on the flow area?” If the answer is worrying then maybe the solution should be considered once again. A blade with pitch 5 mm and at an angle of 70° will have a gap less than 1.7 mm; with 0.1 mm error this changes the area by more than 5%. A 5% critical area is a rather large perturbation that should be considered carefully. The outcome may shift the design point in order to optimize cost or provide the manufacturing responsible with stricter tolerances and affect the process selection. In this area as well CFD/FE computations are and will become important tools coupled with statistical methods such as six sigma. An example of this is given in [15] where sensitivities of due to a number of parameterized departures from nominal drawing are analyzed. The relation between tolerances that can be generated in an EDM process and the resulting efficiency can be given.

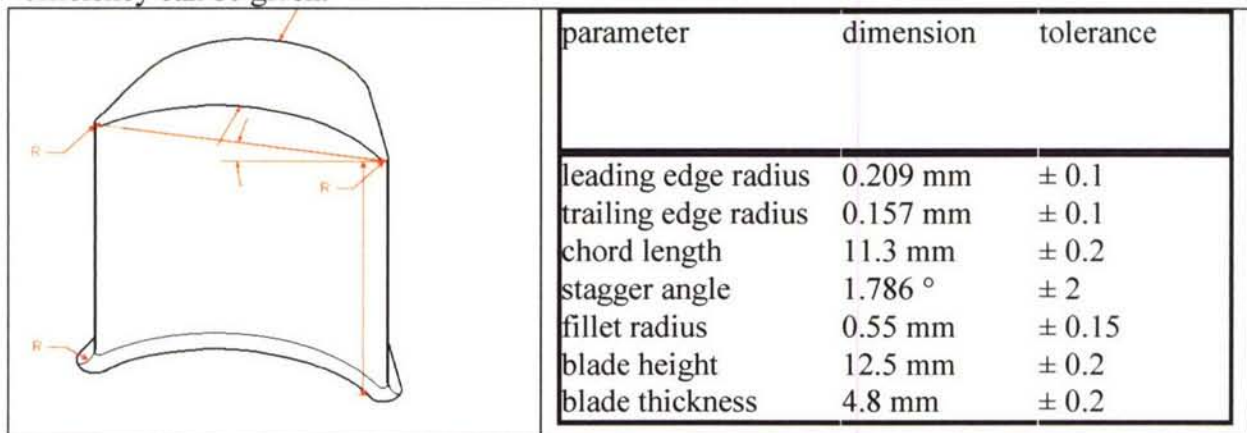


Figure 19 Geometric sensitivity parameters studied

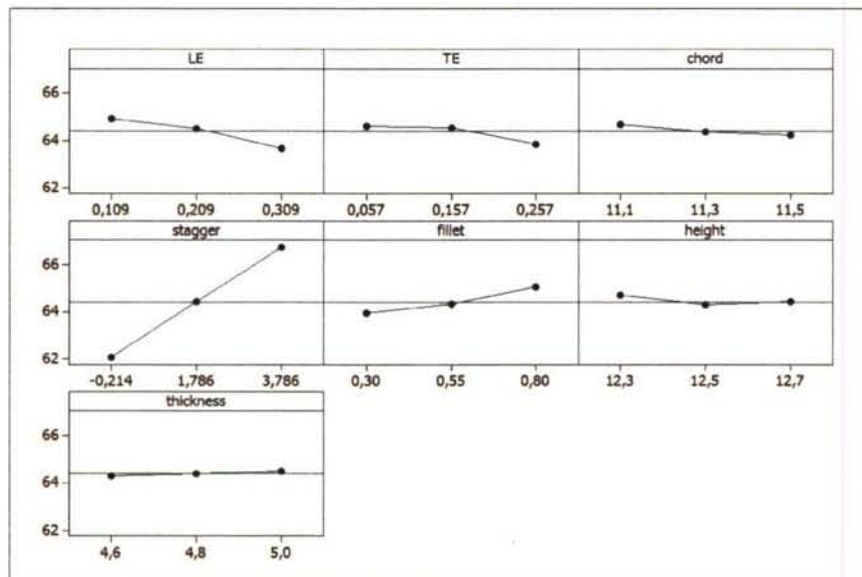


Figure 20 Sensitivity plots for the efficiency due to tolerances

In another application to manufacturing tolerances [10] shows how this is used in order to give allowances for steps in the blade profile and ensuring that the unsteady loads do not increase due to this.

Mechanics

The mechanical design is highly complex both in static and rotating parts. The main difficulty in the static parts is the severe thermal transients encountered on start and stop transients. Parts designed for burst become thick walled due to high pressures suffer from the thermal gradients encountered during transients. This causes a conflict in the designs that are hard to solve and demands a lot of work and design experience. The environment is more aggressive than in normal atmosphere due to hydrogen embrittlement in the hydrogen rich environment. The demands on specific materials data are great in highly loaded machines. Especially data in hydrogen rich atmosphere or other difficult environments require special equipment and is expensive to acquire.

In order to be efficient and have high power output the blades must move at high speed, as was described in the performance design paragraphs. Limitations in tip speed come from the mechanical strength of the blade, expressed as a burst speed in tip speed. Having chosen the tip speed as near to the experience limit as possible the detailed mechanical design can start. All details must sustain the number of load cycles prescribed for the engine. This is for the rocket engine in comparison to an aero engine is relatively few.

Order of magnitude comparison of cycles for turbomachines

	Number of cycles	Operating time
Power generation gas turbine / Steam turbine		1E5-1E6
Commercial jet aero engine	10000-50000	30000-100000 hours
Fighter engine	1000-10000	1000-10000 hours
Rocket	4-10	1-10 hours

The significance of the difference in cycle count and operating time is relatively large in terms of stress limits allowed and how material data can be used. In an aero engine and gas turbine maintenance cycles are defined from the start and inspections are made that allows identification of possible fatigue problems. Fleet leaders, engines with the highest operating time, can be used in order to find and correct problems. In rocket engines this is not an option as in almost every case the engine only flies once, (the Space Shuttle excepted).

Blade vibration

Blade vibration is most definitely one of the major design concerns for the turbine. Blade vibration problems in general constitute the probably largest source of difficult problems late in the design project. Both flutter and forced response concerns are difficult issues for the turbine design. The turbine blade will be exposed to high level excitation from the stator wakes and shocks in the aerodynamic system. Figure 21 shows the highly unsteady flow pattern in a supersonic turbine. The level of the forcing at the principal stator passing frequency $\Omega \cdot m$ can be of the same order of magnitude as the steady state load.

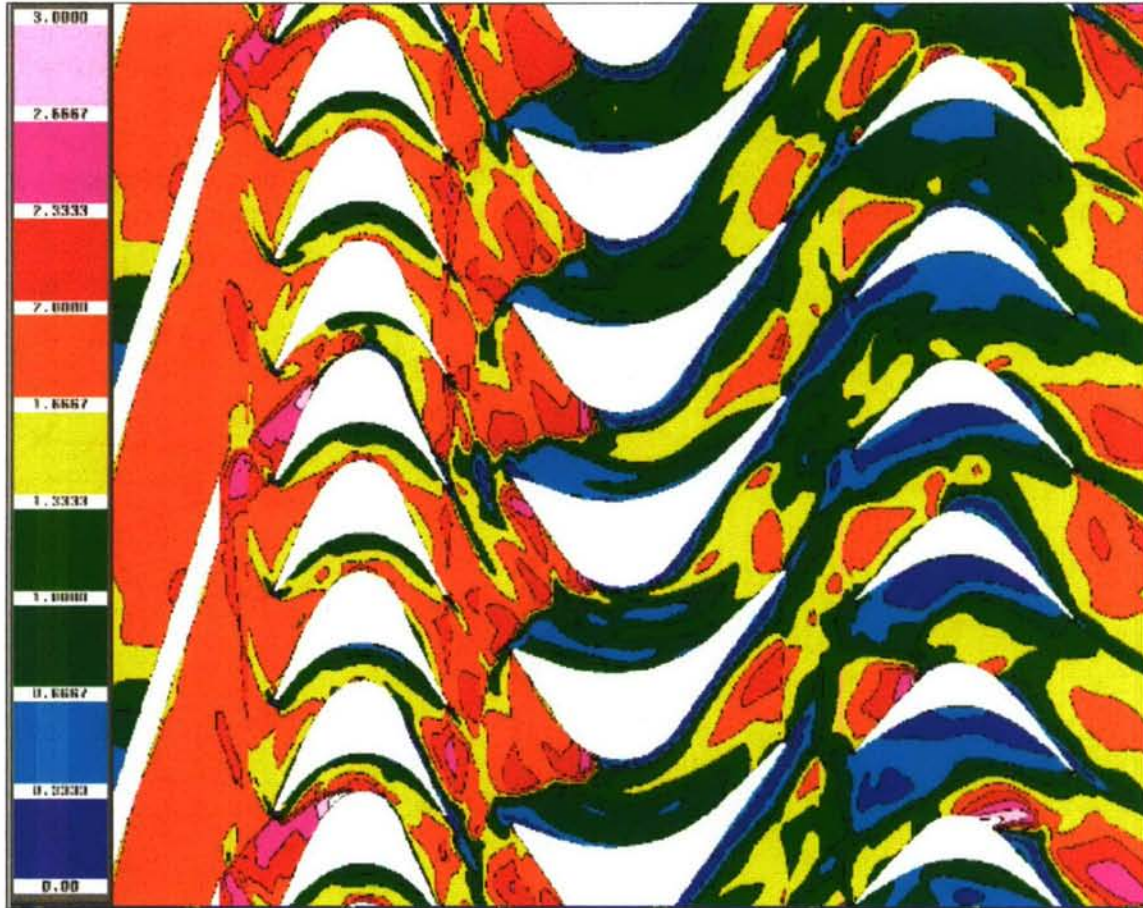


Figure 21: Snapshot from unsteady CFD showing the instantaneous Mach numbers in a supersonic turbine

Forced response is mainly caused by the varying load imposed by flow imperfections leaving the stator and causing a harmonic load onto the rotor. In order to avoid problems the resonances where flow imperfections will excite blade or disk modes the first approach is to work with the Campbell diagrams. For our sample design these are constructed and shown in figure 22

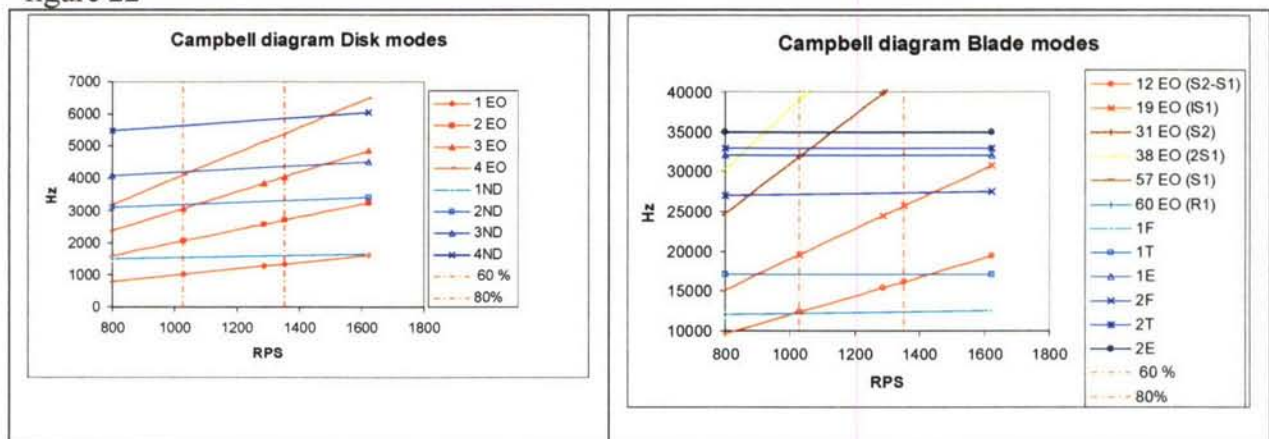


Figure 22 Campbell diagrams for the Rotor 1 blade of the example turbine

The Campbell diagram should be used to identify possible problems. Here experience is of very high importance. There will probably be some crossings where possible excitation

sources cross the mode in the operating range. When crossings occur, it is one has to prioritize and use past experience, and then analyze further using a forced response analysis with CFD/FEM. However the possibility that vibrations occur must be taken seriously. Therefore, development programs usually schedules vibrations testing and mostly dampers are developed in the case that high vibrations should occur. An example of damper implementation is given in [11], where a good figure is used, figure 23 to describe the blade platform damper.

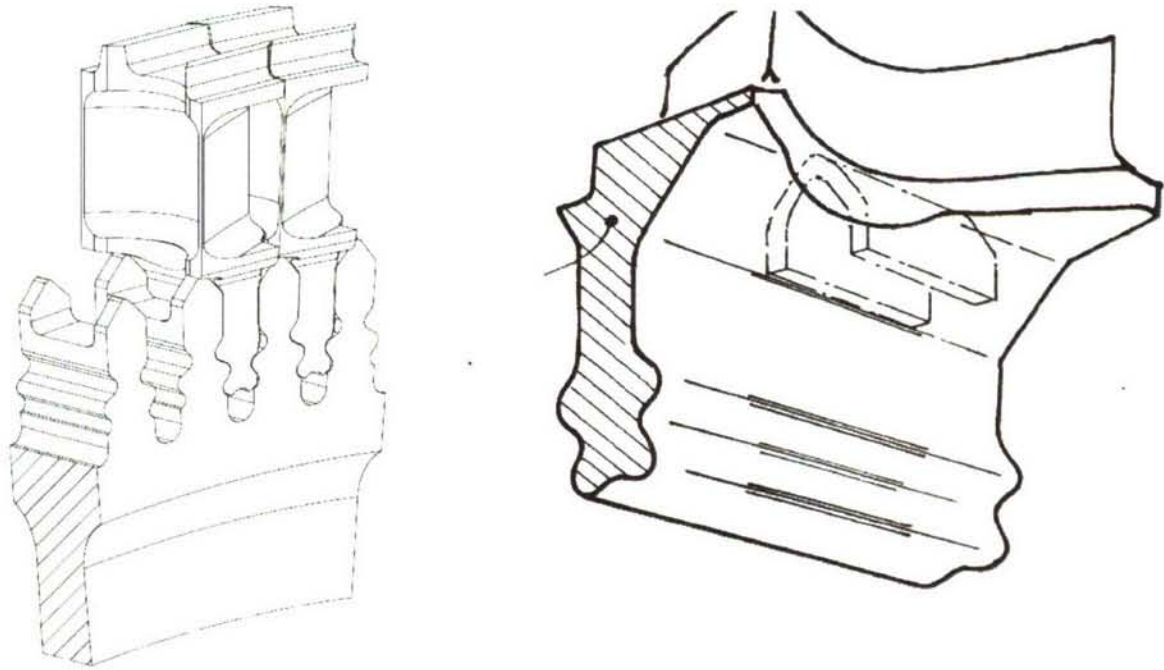


Figure 23 Turbine blade sketch with cottage roof platform damper from [11]

Sometimes dampers are designed for a variety of modes and later used for contingency in the case that high vibrations are encountered in testing.

Flutter is an aeroelastic instability in which a vibration appears at high aerodynamic load as growing amplitude that can cause a failure in a few seconds. [14] Describes this for supersonic turbines, which is particularly difficult in this aspect due to the very high flow velocities in the machine. The most commonly used dimensionless number is the reduced frequency

$$k = \frac{\pi \cdot \text{Chord} \cdot f}{V_{rel}}$$

For our examples the LH2 turbine would have for the 1st flex mode (1F) $k=0.2$ whereas the LO2 single stage design would have $k=0.08$ which is very low, and must be further considered.

4. REFERENCES

- [1] Doyle S., History of liquid rocket engine development in the united states 1955-1980., AAS history series, volume 13, 1992, ISBN 0-97703-349-8
- [2] Sutton G., Rocket propulsion elements, 1992, John Wiley and Sons, ISBN 0-471-52938-9

- [3] Balje O., A guide to design selection and theory, 1981, John Wiley and Sons, ISBN 0-471-06036-4
- [4] NASA SP-8107
- [5] NASA SP-8109
- [6] NASA SP-8110
- [7] NASA SP-8125
- [8] Brennen C., Hydrodynamics of pumps, 1994, Oxford University Press ISBN 0-19-856442-2
- [9] Horlock J., Axial Flow Turbines, 1866, Butterworths
- [10] Bogdan Marcu, Ken Tran , Brad Wright , “Prediction of Unsteady Loads and Analysis of Flow Changes due to Turbine Blade Manufacturing Variations during the Development of Turbines for the MB-XX Advanced Upper Stage Engine” , AIAA-2002-4162, 38th AIAA/ASME/SAE/ASEE Joint Propulsion Conference & Exhibit, 7-10 July 2002, Indianapolis, Indiana
- [11] K. Holmedahl , ANALYSIS AND TESTING OF THE VULCAIN 2 LOX TURBINE BLADES FOR PREDICTION OF HIGH CYCLE FATIGUE LIFE , AIAA-2000-3680, AIAA/ASME/SAE/ASEE Joint Propulsion Conference and Exhibit, 36th, Huntsville, AL, July 16-19, 2000
- [12] Abellsson, C (2007) Parametric Turbine Blade Design for Supersonic Applications, Diploma thesis from School of Engineering Sciences, Aerospace Engineering, University of Southampton, UK.
- [13] S. Brodin J. Steen, I. Ljungkrona, N. Edin, B. Laumert, Vinci Engine Development Testing, a Summary of Turbine Testing Results, AIAA-2005-3949, 2005
- [14] Mårtensson H, Flutter Free Design of Aerodynamically Unstable Supersonic Turbines , AIAA joint propulsion conference, Sacramento CA, 2006
- [15] Török, A, Analysis of manufacturing tolerances for a supersonic blade, 2006, M.Sc. Thesis from VAC and Institute for aero engines (ILA), Univ. Stuttgart, Germany.

von Karman Institute for Fluid Dynamics

RTO-AVT-VKI Lecture Series 2007

**ADVANCES ON PROPULSION TECHNOLOGY
FOR HIGH-SPEED AIRCRAFT**

March 12-15, 2007

ADVANCED ROCKET ENGINES

O.J. Haind
DLR, Germany

ADVANCED ROCKET ENGINES

Oskar J. Haidn

Institute of Space Propulsion, German Aerospace Center (DLR),
74239 Lampoldshausen, Germany

oskar.haidn@dlr.de

Summary

Starting with some basics about space transportation systems such as the thrust equation and some mission requirements, the paper explains the underlying physical and technical challenges every rocket engine design engineer faces at the beginning of a project. A brief overview about the main subsystems of a liquid rocket engine such as turbopumps and gas generators is followed by a more detailed description of the thrust chamber assembly, the injector head, the ignition system and the combustion chamber liner which includes the first part of the nozzle and finally the nozzle extension. The technological challenges of these components are presented which result from the severe operating conditions and their current design principles and production technologies.

Finally, a series of new concepts and techniques for propellant injection, ignition, combustion chamber liners and nozzles are proposed. The major challenges of new materials and production technologies lay in the still missing detailed knowledge about the behaviour of these materials under operating conditions, material-related crack initiation and propagation laws and reliable life prediction tools.

1. Introduction

Rocket engines may either work with solid or liquid propellants or as a combination of both, hybrid propulsion systems, such as the one for the SpaceShipOne project. Liquid rocket engines can be subdivided into mono-propellant or bi-propellant systems. Mono-propellant engines operate either as a simple cold gas system or apply a catalyst for an exothermal decomposition of the propellant, such as hydrazine (N_2H_4) or laughing gas (N_2O). Generally these type of engines are only in use for low thrust satellite propulsion systems. Typical bi-propellant engines use either earth storable propellants, generally combinations of nitric acid or its anhydride with derivatives of hydrazine, i.e. asymmetric di-methyl-hydrazine (UDMH) or mono-methyl-hydrazine (MMH), mixtures of storable and cryogenic propellants, liquid oxygen and kerosene or fully cryogenic, liquid oxygen and liquid hydrogen. Although rocket engines show large differences depending on mission profile and staging of the launcher it is possible useful to separate them in four major classes. Booster, main stage and upper stage engines and satellite propulsion and attitude control systems [1,2].

Rocket engines are energy conversions systems with a heat release in the combustion chamber which exceed by far typical values of nuclear power plants ($\sim 3-4$ GW). While solid rocket engines may even reach power levels of more than 30 GW, the most powerful liquid rocket engines have peak power values of up to 20 GW but the majority works with values of less than 10 GW. Obviously such power levels are only possible with high combustion chamber pressures and even higher propellant mass flow rates which may exceed 1000 kg/s.

1. Chemical Propulsion System Basics

The basic concept of a rocket engine relies on the release of the internal energy of the propellant molecules in the combustion chamber, the acceleration of the reaction product and finally the release of the hot gases at the highest possible velocity in the convergent/divergent nozzle.

1.1 Thrust equation

The thrust equation which describes the basic relations of a chemical rocket was first given in 1903 by the Russian Konstantin Tsiolkovski. Assuming a frictionless, 1-D flow of an ideal gas with negligible entry velocity and the heat release in the combustion chamber at constant pressure with adiabatic walls, see Fig. 1, the thrust equation can be written as:

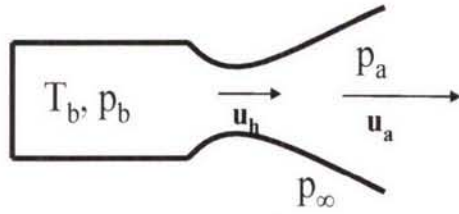


Figure 1: Schematic of an ideal rocket engine

$$F = \dot{m} u_e + (p_e - p_\infty) A_e \quad (1)$$

u_e , the exhaust gas velocity at the exit area A_e , p_e , the exit and p_∞ the ambient pressure, respectively. The first term in eqn. (1) is the momentum and the second, the pressure part of the thrust and replacing $c = u_e + (p_e - p_\infty) A_e / \dot{m}$ or $c = C_F c^*$ finally yields:

$$F = \dot{m} c \quad \text{or} \quad F = \dot{m} C_F c^* \quad (2)$$

C_F is commonly known as the thrust coefficient, c , the effective exit velocity and c^* the characteristic velocity. It is useful to examine these coefficients in more detail since they give valuable hints about the relevance of fluid properties and operational parameters. The characteristic velocity relates the combustion chamber pressure to the burned propellants and thus represents the energy content of the propellant and the combustion efficiency. The widely used term "specific impulse" is available with the gravitational constant g_0 .

$$c^* = \left[\frac{1}{\kappa} \left(\frac{\kappa+1}{2} \right)^{\frac{\kappa+1}{\kappa-1}} \frac{RT_c}{M} \right]^{\frac{1}{2}}; \quad C_F = \left\{ \frac{2\kappa^2}{\kappa-1} \left(\frac{2}{\kappa+1} \right)^{\frac{\kappa+1}{\kappa-1}} \left[1 - \left(\frac{p_e}{p_c} \right)^{\frac{\kappa-1}{\kappa}} \right] \right\}^{\frac{1}{2}} + \left(\frac{p_e - p_\infty}{p_c - p_c} \right) \varepsilon; \quad I_{sp,0} = \frac{c}{g_0}; \quad (3)$$

with ε , the ratio of cross section of nozzle exit and combustion chamber throat.

As equation (3) shows, the characteristic velocity increases with increasing combustion temperature T_b , but decreases with growing molecular weight M and isentropic coefficient k of the exhaust gases. This dependency on the isentropic coefficient holds also for the thrust coefficient but of much greater impact is the ratio between exit pressure and chamber pressure and, in the second term the difference of exit and ambient pressure. Although large exit velocities are quite favourable, the corresponding expansion in the nozzle may depending of the height during ascent result in exit pressures smaller than the ambient pressure which finally yields a smaller thrust coefficient. Typical values of these characteristic properties for a wide range of rocket engines are summarized in the following table 1 [3].

T_c [K]	P_c [MPa]	M [kmol/kg]	c^* [m/s]	\mathcal{E} [-]	K [-]	C_F [-]	I_{sp} [-]
2000-3900	1-26	2-30	900-2500	15-280	1,1-1,6	1,3-2,9	150-480

Table 1: Typical values of characteristic properties of rocket engines

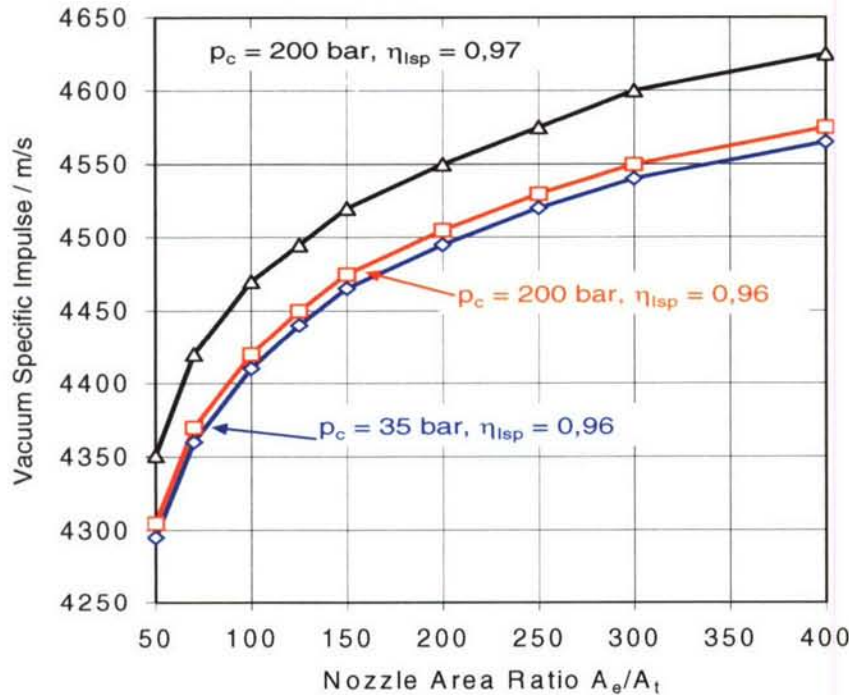


Figure 2: Vacuum specific impulse as a function of the area ratio with chamber pressure and combustion efficiency

1.2 Propellants

Following the previous chapter on characteristic properties allows a classification of typical propellants for rocket engines. Key requirements are high combustion chamber temperatures, usually achievable with a high energy content of the molecules, a small isentropic coefficient and the smallest possible molecular weight of the exhaust gas mixture. Depending on the specific launcher system, rocket engine cycle or mission requirements, values such as propellant density or temperature may become even more important. Generally, the propellant

Oxidizer	Fuel	r_{of} [-]	I_{sp} [s]	ρ [kg/m ³]
LO ₂	kerosene	2,77	358	820
	LH ₂	4,83	455	700
	LCH ₄	3,45	369	430
N ₂ O ₄	UDMH	1,95	342	791
	MMH	2,37	341	880
	UH25	2,15	340	850

Table 2: Characteristic data of typical liquid propellants

combination H₂/O₂ is favourable for upper stage engines while booster engines either apply kerosene / oxygen or solid propellants and as such quite often a combination of ammonia per-chlorate (AP), hydroxy-terminated polybutadien (HTPB) and some ingredients which have the function of either a binder or a moderator to control the heat regression rate and thus the overall booster performance.

In the early days of rocketry hypergolic propellant combinations of nitrogen-tetroxide (N₂O₄) and mixtures of N₂H₄ and UDMH or MMH have been used for almost any engine application although they have a comparatively small specific impulse, are toxic and cause due to their aggressiveness problems during storage and handling but nowadays they are very common only for upper stages and satellite propulsion systems. The main reason for this wide-spread usage is based on their chemical reactivity; they don't require an ignition system and are storable at room temperature. Nowadays booster engines using kerosene / O₂ are

A rather interesting aspect about the impact of the combustion chamber pressure on the performance of the engine is demonstrated in figure 2 which shows the vacuum specific impulse as a function of the area ratio. While variations in the chamber pressure itself have only a minor influence, i.e. an increase by a factor of six yields only a marginal (about 0.1 %) performance increase, an only minor increase of the combustion efficiency (by 1% from 0.96 to 0.97) yields already an increase of the performance of about 1%.

commonly used and the most impressive examples are the Energomash engines of the RD-170 family which power the first stages of the Zenit (RD-171) and the ATLAS (RD-180) launchers. Table 2 shows frequently used propellant combinations, their mixture ratios, specific impulse and densities. For further information see i.e. [3, 4]

The influence of the propellant combination and the mixture ratio on the specific impulse is shown in Figure 3. Three different classes of propellants can easily be detected. H₂/O₂ is by far (~30%) the most efficient propellant pair followed by combinations of O₂ and hydrocarbons and interestingly the specific impulse decreases with increasing carbon content. Fuels which already contain oxygen atoms, alcohols, follow by another 10% margin and have an almost similar specific impulse as storable propellant combinations. For comparison reasons figure 3 includes as well propellant combinations of which use hydrogen-peroxide H₂O₂ as oxidizer.

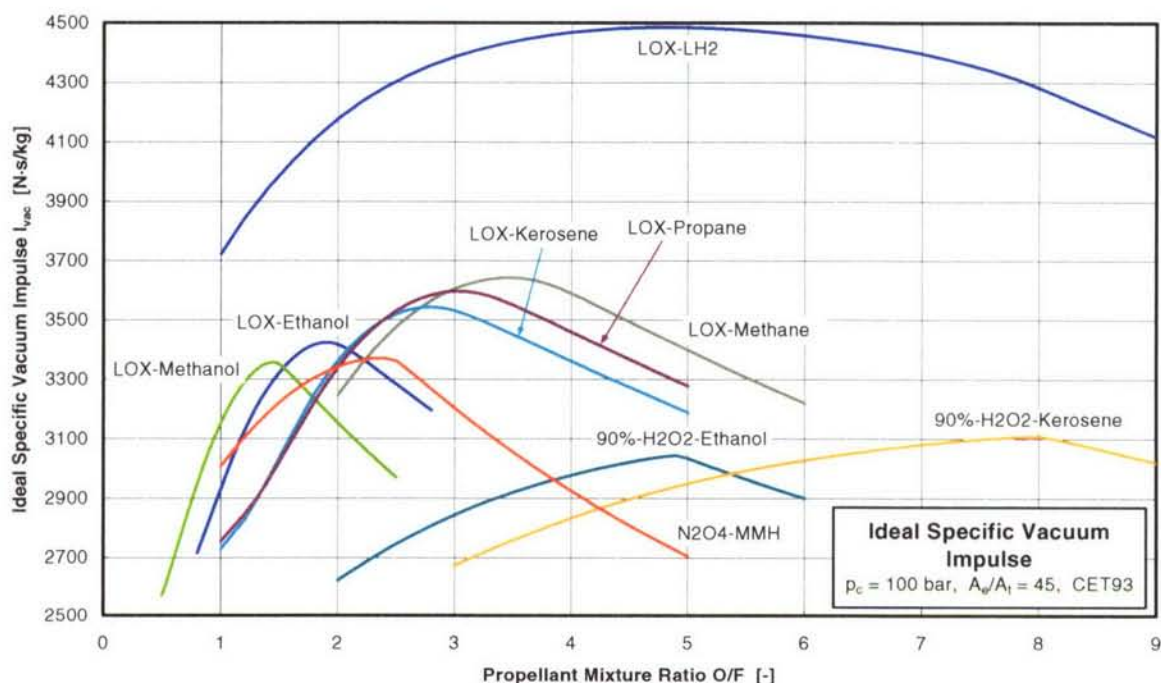


Figure 3: Ideal specific impulse of various propellant combinations

A possibility to combine the advantages of high propellant density at low altitude operation with high specific impulse at high altitudes is a combination of three propellants. So-called tri-propellant combinations of LOX, kerosene, LH₂ or LOX, CH₄, LH₂ burn in the same engine LOX / kerosene at low altitudes and switch to LOX / LH₂ operation at high altitudes have been investigated in the past but have never reached the level of flight hardware. The RD – 701 engine (LOX / kerosene which has been designed for the air-launch MAKS concept reached at least development level [1].

1.3 Engine feed systems

The easiest way to distinguish different engine types is to classify them according to their method of propellant pressurization and transport. While only small and low pressure engines apply pressurized tanks for propellant delivery, the majority uses turbo pumps in order to bring the propellants to the desired pressure level.

1.3.1 Pressure-fed engines

Principally there are two types of pressure-fed systems, self-pressurization and pressurization by foreign high pressure gas. Self-pressurization is typically applied by mono-propellant engines and is achieved either by vaporization of the liquid propellant or thermal decomposi-

tion caused external heat addition or catalytic decomposition. Pressure-fed bi-propellant engines typically apply high pressure (up to 30 MPa) helium bottles. In any case, the thrust level of pressure-fed engines is limited by the available tank technology. An example of such a system is the AESTUS engine of ARIANE 5G. A flow schematic of a pressure-fed engine is shown on the right hand side of figure 3 together with a gas generator cycle and a staged combustion cycle.

Pressure-fed system

Pump-fed systems

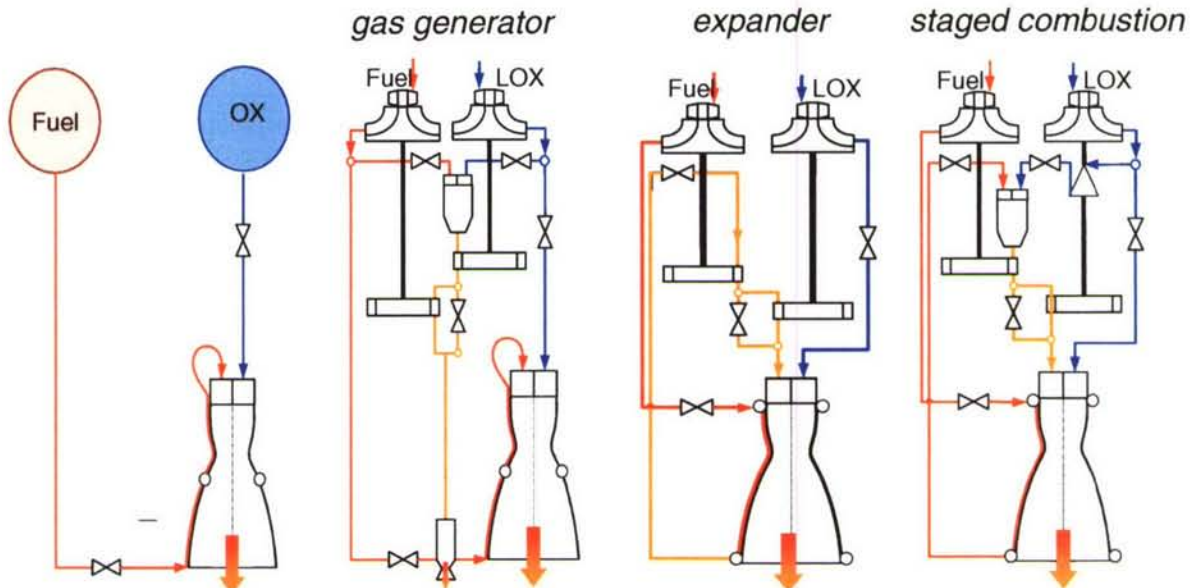


Figure 4: Common Engine Cycles

1.3.1 Pump-fed engines

In contrast to pressure-fed systems, pump-fed engines use the principle of a turbo-charger to pressurize the propellants. Parts of the propellants are fed into a separate combustion chamber called gas generator or pre-burner which usually operates at a sufficiently high pressure level and with a mixture ratio such that the exhaust gas temperature reaches values around 850 K. These gases are then fed to a turbine which drives the propellants pumps. Depending on the pathway of the turbine exhaust gases one distinguishes between different engines cycles. The cycle schematics in figure 3 show that the case characterized by the direct release of the turbine exhaust gases into the ambient is called “Gas Generator Cycle”. In the case that they are fed together with the remainder of the propellants into the main combustion chamber, this cycle is called „Staged Combustion Cycle“. The differences between those two options are first, much higher system pressures since the gas generator has to operate at a pressure sufficiently high to compensate the pressure losses in the turbine, the cooling channels and the injector head and second a better performance since all the propellants go through the main chamber and thus produce both a higher mass flow rate and allow so for a larger nozzle expansion ratio and finally for an equivalent increase in the specific impulse.

With the exception of Russian LOX/kerosene stage combustion engines which run oxygen-rich, all other gas generator or staged combustion systems operate in a fuel-rich mode. As part of the Integrated High Payoff Rocket Propulsion Technology (IHPRP) program [5], the US aims at the development of an integrated power-head which focuses on the most critical sub-components of this cycle, the oxygen-rich pre-burner and turbine as well as the injection system of the main chamber. China as well works towards the development of staged combustion technology [6]. The attractiveness of a full flow cycle engine results from a higher overall system performance and the elimination of critical inter-propellant seals [7]. Nevertheless,

there has been only one rocket engine to date, the Russian RD-270, which had an ox-rich and a fuel-rich pre-burner which made it full scale to the test facility but unfortunately never into flight [1].

1.4 Engine applications

Typically the propulsion systems and thus the rocket engines are tailored to the specific requirements of the launching concept. This has consequences insofar as any improvement or modification of the engine has significant impact on the entire launch system and, even more important, an improvement of the engine, i.e. engine performance, may not necessarily improve the overall efficiency of the launcher. The currently operational space transportation systems can be divided into two major types: Launchers with large strap-on boosters with core and upper stages such as the European ARIANE, the Japanese HII, the Russian Soyuz or the American Space Shuttle and launchers with a booster, an optional sustainer and an upper stage such as the American ATLAS and Delta, the Russian PROTON, the Chinese Long March or the international Sea Launch Vehicle [2].

Typical booster engines provide a high lift-off thrust (i.e. 3000 – 8000 kN) over a short burning time (i.e. < 150 s). Table 3 above shows characteristic values of booster engines. Engines with a thrust level smaller than 3 MN are clustered together to provide the necessary lift-off thrust. For example, the Soyuz boost system consists of an ensemble of four RD-107 engines, the YF-21 boost stage comes with 4 YF-20 engines and the ARIANE 4 L40 configuration was made up by 4 Viking 6 engines. Core engines provide a comparable lower lift-off thrust (i.e. 1000 - 2000 kN) but with a higher specific impulse and with operating times in the range of about 600 sec. The thrust levels of upper stage engines vary between 30 – 150 kN with operating times varying between 600 – 1100 sec. Typical representatives of booster, main stage and upper stage engines are summarized in table 3, table 4 and table 5. Unsurprisingly, almost all of the booster engines shown in table 3 are fueled with relatively high density propellants and only one, the RS-68 operates with the unfavorable density combination LOX/LH₂.

Rocket Engine	Engine Cycle	Propellant combination	Thrust [MN]	spec. impulse (sl) [s]	Chamber pressure [MPa]	Burn time [s]
RD-170	SC	LO ₂ /Kerosene	7,65	310	25,1	150
RD-180	SC	LO ₂ /Kerosene	3,82	311	25,5	150
RD-107	SC	LO ₂ /Kerosene	0,81	257	5,9	119
F-1	GG	LO ₂ /RP1	6,91	264	6,6	161
MA-5A	GG	LO ₂ /RP1	1,84	263	4,4	263
RS-27	GG	LO ₂ /RP1	0,91	263	4,8	265
RD-253	SC	N ₂ O ₄ /UDMH	1,47	285	15,2	130
YF-20	GG	N ₂ O ₄ /UDMH	0,76	259	7,4	170
Viking 6	GG	N ₂ O ₄ /UH25	0,68	249	5,9	142
RS-68	GG	LO ₂ /LH ₂	2,89	360	9,7	249

Table 3: Characteristic data of liquid booster engines [2, 8]

Main stage engines operate as booster engines right from the start and generally have thrust levels similar to clustered booster engines somewhere in the range between 800 kN to 2000 kN. The burn times however are much longer and may reach 400 s to 600 s. An analysis of the data presented in table 4 in more detail reveals some interesting features. Similar thrust levels and burning times of the SSME and the RD-0120 are no longer surprising, knowing that engines were developed to serve a similar purpose: provision of sufficient thrust for a

manned vehicle in low earth orbit. The LOX/LH2 fired LE-7A and Vulcain 2, show comparable thrust levels and operating times and are applied as core engines in a launchers with two large thrust boosters each, the HII and the ARIANE 5, respectively. A comparison of the data for the RD-108, Viking 5C, and YF-20B reveals similar parameters and again, these engines are all applied as clusters of engines in the first stage of launcher without large boosters.

Rocket Engine	Engine Cycle	Propellant combination	Thrust (sl) [MN]	Thrust (vac.) [MN]	Spec. impulse (sl) [s]	Spec. impulse (vac.) [s]	Chamber pressure [MPa]	Burn Time [s]
RD-108	SC	LO ₂ /Kerosene	0.78	1.01	252	319	5.1	290
Viking 5C	GG	N ₂ O ₄ /UH25	0.68	0.75	249	278	5.9	142
YF-20B	GG	N ₂ O ₄ /UDMH	0.73	0.81	259	289	7.4	170
RS-68	GG	LO ₂ /LH ₂	2.89	3.31	360	420	9.7	249
SSME	SC	LO ₂ /LH ₂	1.82	2.28	364	453	20.5	480
RD-0120	SC	LO ₂ /LH ₂	1.51	1.96	359	455	21.8	600
LE-7A	SC	LO ₂ /LH ₂	0.84	1.10	338	438	121	390
Vulcain 2	GG	LO ₂ /LH ₂	0.94	1.35	320	434	11.6	600

Table 4: Characteristic data of core and main stage engines [2, 8]

The key characteristic feature of an upper stage engine is the vacuum ignition capability. The broad differences in propellant combination, engine cycle, and thrust level are explainable only by the different applications. The main mission of the J-2, the second and third stage engine of the Saturn V, was to enable the spacecraft to leave the earth for the moon. The engine with the second-largest thrust level, the RD-0210, has a considerably shorter burn time and brings the Block M of the Proton into GTO. All the other engines have thrust values below 200 kN and operating times between roughly 500s and up to 1100s.

The thrust requirement for apogee engines and satellite thrusters for attitude control is much smaller than for any other engine. While the thrust levels of the first may reach up to 600 N, the latter first may have peak values in the order of less than 100 N. Generally, attitude control thrusters are monopropellant engines with tens of N. The key characteristics of a satellite engine are extremely long (more than 10 years) and reliable functioning and the very high cyclic loads due to the pulse operation mode. Hence, a satellite engines is optimized towards aspects of long-life valve operation such as seals and leakage and corrosion.

Rocket Engine	Engine Cycle	Propellant combination	Thrust (vac.) [kN]	Spec. impulse (vac.) [s]	Chamber pressure [MPa]	Burn Time [s]
11D58M	SC	LO ₂ /Kerosene	79.5	353	7,6	680
RD-0210	SC	N ₂ O ₄ /UDMH	582	327	14.8	230
AESTUS	PF	N ₂ O ₄ /MMH	30	325	1,0	1100
J-2	GG	LO ₂ /LH ₂	890	426	4.4	
YF-75	GG	LO ₂ /LH ₂	79	440	3.7	470
LE-5B	EC	LO ₂ /LH ₂	137	447	3.6	534
HM7-B	GG	LO ₂ /LH ₂	70	447	3.5	731
VINCI	EC	LO ₂ /LH ₂	180	465	6.1	
RL-10B	EC	LO ₂ /LH ₂	110	462	4.3	700

Table 5: Characteristic data of upper stage engines [2, 8]

2. Components of Liquid Rocket Engines

The key components of a liquid propellant rocket engine are the devices for propellant delivery, the turbines and pumps as well as the generators of the driving gases, i.e. gas generator or pre-burner, the propellant injection system, the thrust chamber which combines the combustion chamber and a short part of the diverging section of the nozzle which typically ends with a distribution manifold for the propellants used as coolant for the thrust chamber liner, and, finally the thrust nozzle. Each of these devices has its own design problems and criteria and the optimum of one component not necessarily leads to the optimum of the entire system. The following section will touch briefly the key issues of each of the components but will finally focus on the thrust chamber.

2.1 Gas generator and preburner

The main requirement for any gas generator or preburner is the delivery of a sufficient amount of driver gas at a designed pressure and temperature which guarantees a continuous propellant supply of the thrust chamber. A quick glance at equation (4), yields that the necessary turbine power depends aside of the desired the ratio of exit to entry pressure and the mass flow rate of the gases, solely on thermodynamic properties, temperature, heat capacity and isentropic coefficient, and, of course the efficiency of the device.

$$P = \eta \dot{m} c_p T_1 \left(1 - \left(\frac{p_2}{p_1} \right)^{\frac{\kappa-1}{\kappa}} \right) \quad (4)$$

As already mentioned previously, the turbine exit pressure in gas generator cycle engine is independent of the pressure in the thrust chamber. This is entirely different for staged combustion engines where the exhaust gases are fed to the chamber. While the combustion pressure in the gas generator lay frequently below the one in the thrust chamber, the pressures in the pre-burners are typically a factor of two or three higher, see table 6 which summarizes characteristic data of sample gas generators and pre-burners. A high turbine power may be achieved by appropriate mass flow rates and pre-burner exhaust gas temperatures. Due to the extremely high dynamic loads of the turbines, the entry temperature of the gas is limited to about 850 K to ensure sufficient turbine life which leaves only gas generator mass flow rate and pressure to adjust to the power needs. Extremely important is a homogenous temperature distribution at the entrance to the turbine to avoid local overheat at the turbine blades through hot spots.

An analysis of all the gas generator engines shows that cryogenic engines such as SSME, LE-7, RD-0120, Vulcain 2, operate independently of the cycle, the gas generator or pre-burner in a fuel-rich mode. Taking into account that all liquid rocket engines operate fuel-rich and that the stoichiometric mixture is for any propellant combination always larger than 2, reveals that the amount of oxidizer outnumbers that of the fuel significantly. Hence, oxidizer-rich operation allows for a sufficient reduction of the turbine entry temperature since the mass flow rates are available. Although there has been considerable effort in the US to develop an oxidizer-rich cycle, only Russia seems to have mastered the problem of material compatibility of pre-burner, piping system and turbine as well as the injector head with high temperature ($T > 800$ K) oxygen-rich turbine gas since all Russian LOX/Kerosene engines operate oxygen-rich [9]. None of the American LOX/Kerosene engines, neither the old F1, nor the RS-27 and the MA-5A which are all gas generator cycle engines are running oxygen-rich although a fuel-rich operation will have problems with soot formation in the gas generator and subsequently soot deposition along the flow lines [1]. The only explanation might be that for the relatively short operation times of less than 200 s and rather small pressures in the gas generator soot deposition in the turbine might still be tolerable while for even shorter times of 150 s

or shorter, either soot formation and deposition in the turbine is increased drastically or the key problem is soot deposition in the injection system and especially in the injectors.

	Vulcain 2	SSME	LE-7	RD-0120	RF-1	RD-180
Propellant Combination	LOX/H ₂	LOX/H ₂	LOX/H ₂	LOX/H ₂	LOX/RP1	LOX/RP1
T [K]	875	940 / 870	810	846	816	820
p_{GG} [MPa]	10.1	35 / 36	21.0	42.4		55.6
r_{of} [-]	0.9	0.89 / 0.8	0.55	0.81	~55	54
m [kg/s]	9.7	80 / 30	53	78.6	?	887
P [MW]	5 / 14	56 / 21	4.5 / 19	62	44	93.5
p_c [MPa]	11.6	20.6	12.7	21.8	6.6	25.7

Table 5: Characteristic data of sample gas generators and pre-burners [10]

In order to emphasize the difference between LOX/H₂ and LOX/Kerosene as well as gas generator cycle and staged combustion cycle engines, table 5 summarizes typical data such as operating temperature, pressure and mixture ratio of the gas generator or pre-burner, the propellant mass flow rate, the power requirement of the turbine and the pressure in the thrust chamber. For comparison reasons an American, European, Japanese and Russian LOX/H₂ engine are shown together with two, American and Russian LOX/Kerosene engine. Typically all cryogenic engines have for each propellant a turbine and a pump. Only the RD-180 has one single preburner which delivers the necessary driving gas to a one single stage turbine which again provides for the thrust requirements of the two propellant pumps, a single stage oxygen pump and a two stage fuel pump.

2.2 Turbopumps

The function of the turbopump system of a rocket engine is to receive the liquid propellants from the vehicle tanks at low pressure and supply them to the combustion chamber at the required flow rate and injection pressure. The energy to power the turbine itself is provided by the expansion of high pressure gases, which are usually mixtures of the propellants being pumped. Radial pumps and axial turbines are of common use. Figure 5 basic elements of a turbopump and their main function as well as the flow passages.

2.2.1 Turbopump design considerations

Turbomachinery design is an iterative process which requires the interaction of many disciplines, such as hydrodynamics, aerodynamics, mechanics, materials and processes, structural mechanics and analysis, rotor dynamics, thermodynamics and last but not least instrumentation and testing. The set of requirements, pump discharge pressure and flow rate, pump suction pressure, turbine drive cycle and efficiency, fluid properties, throttling range, life, reliability, weight and size, and cost are often contradictory and the final design is at best a compromise optimum for a specific application. The SSME powerhead shown in Figure 6 demonstrates the compact design of a liquid rocket engine.

2.2.2 Pumps

Pumps for engines with similar density fuel and oxidizer propellants such as RP-1/LOX and similar discharge pressure requirements will typically be optimum at approximately the same speed. This permits the fuel and oxidizer pumps to be placed on a common shaft and driven by a common turbine which is the case for the F1, RS-27 or the RD-180. Maximum pump speed is generally limited by the suction performance requirements to avoid cavitation to occur. Due to the large density difference between liquid hydrogen and liquid oxygen and

Basic Turbopump Elements

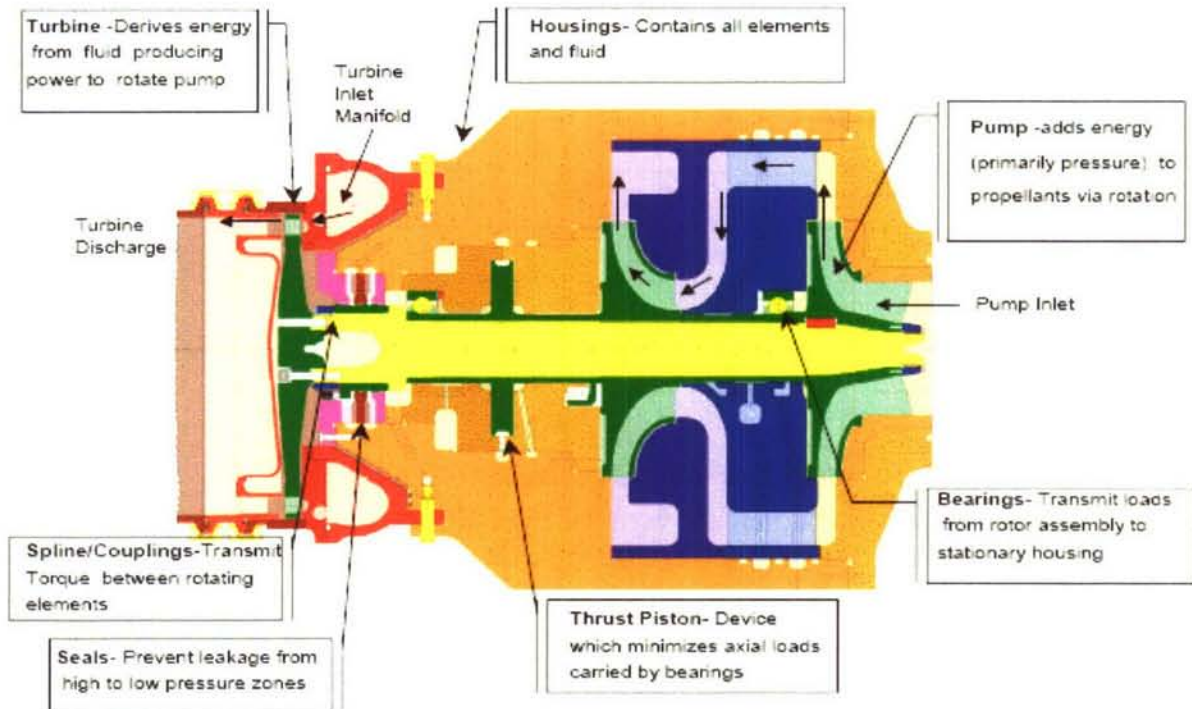


Figure 5: Basic elements of a turbopump and their functional description [11]

the pressure drop required for regenerative cooling cryogenic engines usually have two separate pumps since the hydrogen pump has to operate at much higher speed to provide the necessary high exit pressures.

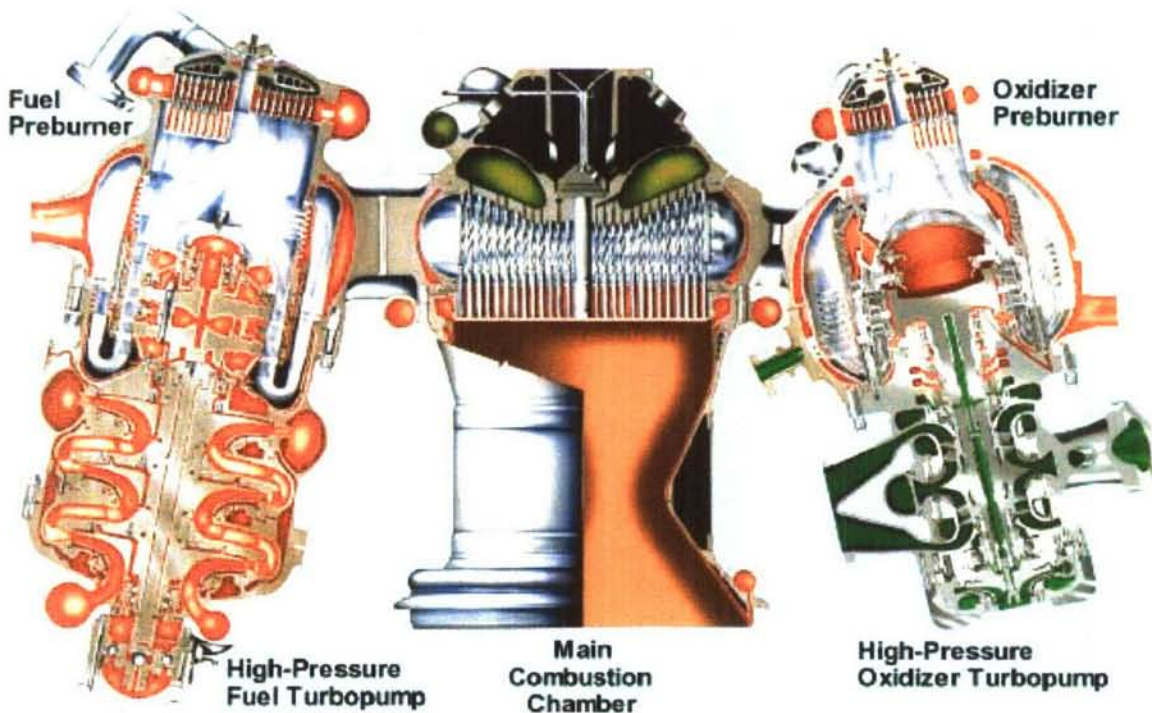


Figure 6: SSME Powerhead with preburners, turbopumps and thrust chamber assembly [11]

Vehicle weight reductions achieved by thinner propellant tank walls result in lower pump inlet pressures and as a consequence the pump speed has to be reduced. Lower fluid velocities

would in turn result in a larger inlet diameter and increased size and weight of the pump. Furthermore, typical high performance staged combustion engines require very high pump discharge pressures. A typical way to overcome these weight and size constraints of the power pack and still maintain sufficient margin for a safe operation are additional low pressure boost pumps which are applied in the SSME or RD-180 engine.

The inducer diameter (inlet area) is selected to limit the fluid velocity so that the available inlet pressure is considerably higher than the dynamic pressure of the fluid, typically 200% for LOX and 100% for LH2. Once the inlet conditions are fixed, the shaft speed will be set such that cavitation at the blade tips is avoided. Increasing blade thickness to react pressure and centrifugal forces sets another constraint for tip speed since it decreases flow passage area and thus reduces the suction performance. Small flow rate pumps are generally less efficient than large flow rate pumps because the clearance and surface finish related losses cannot be scaled with size.

2.2.3 Turbines

Optimum turbine efficiency requires a certain pitchline velocity which is a product of the shaft speed and the turbine diameter. The minimum weight turbine has the highest speed and smallest diameter within the structural and mechanical arrangement limitations.

There are two types of turbines, impulse and reaction turbines which in rocketry may have one or more stages. Each stage consists of a stator part where the flow expands and accelerates and a rotor part where the impulse on the blades sets the rotor in motion thus transforming kinetic in mechanic energy. The impulse turbine is a constant pressure device since the area ratio between the blades is constant and ideally the only the direction of the flow changes. This type is usually applied in cases characterized by a high pressure drop and a small mass flow rate, i.e, gas generator cycle engine. Turbines with more stages may be further distinguished in velocity compound, expansion only the first stator, or pressure compound, expansion in every stator stage.

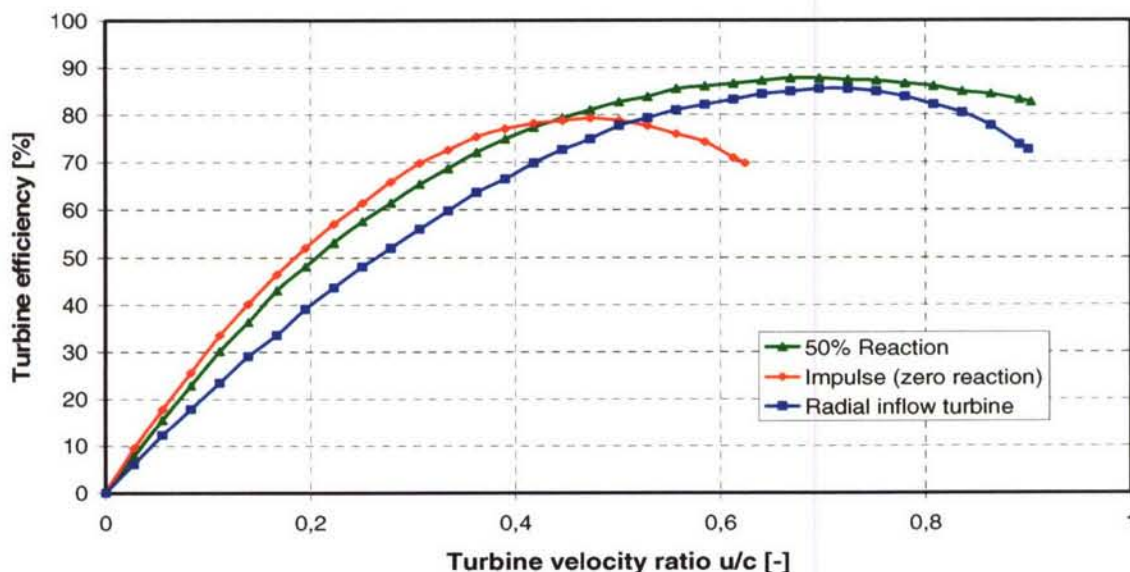


Figure7: Single stage turbine efficiency [12]

Reaction turbines distribute the expansion between stator and rotor and hence, the fluid passages between the blades have a converging cross section. This type of turbine is usually applied in expander or staged combustion cycle systems, typical reaction grade of 50% meaning half of the power of comes from the expansion, where a minimum pressure loss between

pump and combustion chamber is almost mandatory. The efficiency of a turbine is a function of number of stages n and the velocity ratio u/c_0 , which relates circumferential velocity at the mean diameter to the fluid velocity for an isentropic expansion between turbine entry and exit pressure.

$$\eta = f\left(\frac{u}{c_0}\right) \quad \text{with} \quad \frac{u}{c_0} = \frac{\sqrt{\sum_1^n u_i^2}}{c_0} \quad (5)$$

Figure 7 shows the turbine efficiency as a function of the velocity ratio and reveals that the type of turbine too has an impact on the efficiency. Practical turbines have an about 5 and 10% smaller efficiency since the relations given above do not account for losses due to tip clearance.

2.2.4 Materials for turbomachinery components

In the design of turbomachinery various materials, Aluminium alloys, stainless steels, high strength steels, nickel base alloys, cobalt base alloys and titanium alloys are in use. Low pressure components are typically cast from Aluminium to avoid welds. Nickel-base superalloys such as Inconel 718

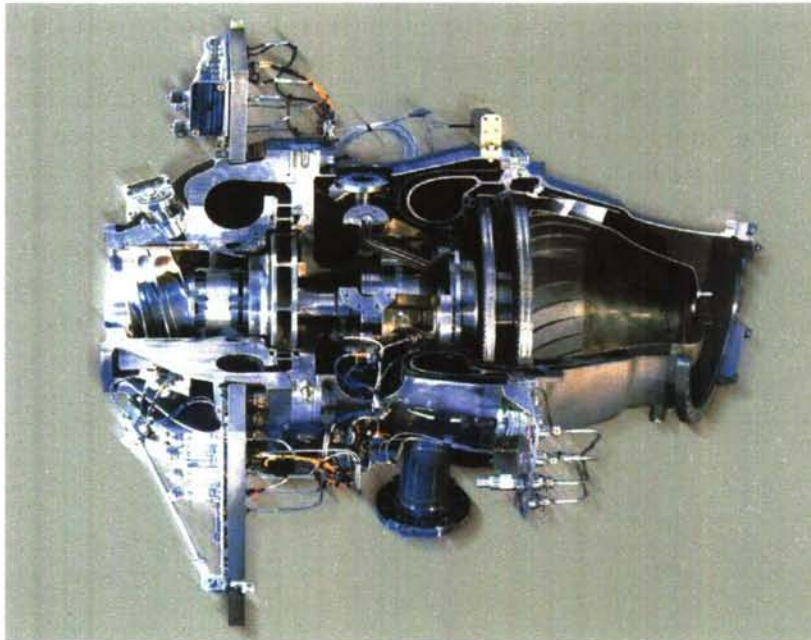


Figure 8: LOX turbopump of the Vulcain 2 engine [12]

are applied used to cast pressure vessels where higher strength is required. The high strength-to-weight ratio of titanium is utilized to obtain the high tip speeds required for LH2 impellers and inducers. The high pressure high temperature hydrogen-rich steam may cause hydrogen embrittlement and thus requires the protection of high-strength superalloys with appropriate copper or gold plating. Turbine blades are often directionally solidified and thermally coated to cope with the extremely high heat fluxes. LO2 pumps where contact with the inducer or impeller could result in ignition are coated i.e. with silver. Similar materials and techniques are also used for potential contact with titanium impellers to preclude the formation of titanium hydrides due to heat generation. The LOX turbopump of the Vulcain 2 engine shown in figure 8 is a rather new example of an entire turbopump set, turbine plus pump, which demonstrates again the compactness of the design

2.2.5 Bearings and seals

Aside pump and turbine any turbopump requires components such as bearings, seals, gears and the suction and discharge ducts. There are two kind of bearings, rolling elements and fluid film ones and they have to perform three primary functions, radial control of the rotor to prevent rubs and to maintain clearance, axial control of the rotor to maintain rotor control during transient mechanic and thermal loads and to react residual thrust loads and third, control of rotordynamics to provide for adequate radial stiffness and damping. They are

usually cooled by the fluid which quite often doesn't provide for lubrication, operate at high speeds and are exposed to high transient radial and axial loads. While static seal design in rocketry generally doesn't exceed standard procedures, dynamic seals which separate stationary and rotating parts are critical. Dynamic seals just must not fail. There are different types of seals, labyrinth, face contact or shaft contacting, floating ring or hydrodynamic face seals. Major design problems are fluid compatibility, thermal gradients and dynamic loads.

2.3 Thrust chamber assembly

In a liquid propellant rocket engine, the function of the thrust chamber assembly is to generate thrust by efficiently converting the propellant chemical energy into hot gas kinetic energy. That conversion is accomplished by the combustion of the propellants in the combustion chamber, followed by acceleration of the hot gas through a convergent/divergent nozzle to achieve high gas velocities and thrust. The basic elements of the thrust chamber assembly of a rocket engine consists of the following components which are closely coupled in their functioning and therefore have to be designed in parallel: the cardan, welded to the injector head

which is which holds the propellant distribution manifolds and the ignition system and the combustion chamber liner including the throat section and the first part of the nozzle to which the inlet manifold for the coolant is welded. Looking at figure 9, a sketch of the Vulcain thrust chamber, simplifies the explanation of these parts.

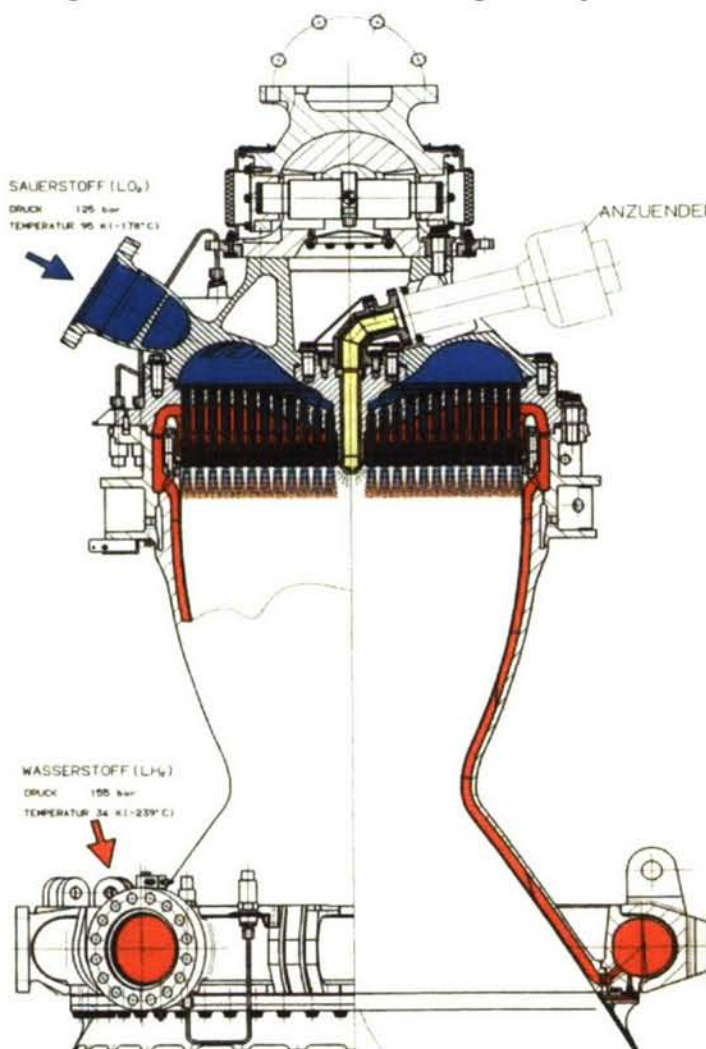


Figure 9: Cut through the Vulcain thrust chamber [12]

2.3.1 Ignition system

A successful ignition is the outcome of matching conditions of propellant mass flow rates and mixture ratio and initiation energy in time and in space. However, the ignition of a rocket engine has also to be smooth with negligible pressure peaks to reduce the risk of triggering combustion instabilities or damaging the cooling channels. Combustion chamber pressure

peaks may cause a partial blockage of the propellant flow inside the chamber yielding extinction or damage the turbopumps. Hence, exact timing of ignition initiation and propellants valve opening is essential. Furthermore, the local mixture ratio of the propellants has to be sufficiently far inside the flammability limits, the energy provided by the ignition system has to be high enough to vaporize and preheat the gaseous propellants above the ignition temperature. Once a chemical reaction has started, the local heat release has to be sufficiently high to overcome the losses. With propellant temperatures below 100 K the process of vaporization and heating especially during the start-up transient may exceed a couple of milliseconds and hence flame extinction may occur locally. In combination with the high propellant mass flow rates even a few milliseconds may locally yield a sufficient amount of premixed propellants which may have catastrophic consequences. Therefore a coupled development of injection and ignition system is mandatory for a successful design. There are quite a large number of ignition devices which either use pyrotechnical propellant charges, hypergolic lead or a torch ignition system with gaseous propellants. An example of a solid propellant based system, the pyrotechnical ignitor of the Vulcain engine is shown in Figure 10.



Figure 10: Pyrotechnic ignition system of the Vulcain engine

The methodology aims at a prediction of the propellant mass flow rates in order to establish a mixture ratio map. Second, the hot exhaust gases from the ignition system are injected and mixed with the propellants without a prediction of the chemical reaction. The main aim is to establish a temperature map inside the combustion chamber. Based on the results of mixture ratio and temperature distributions a map of local ignition probabilities is predicted and successful ignition is assumed when the area where ignition probability exceed a predefined limit is sufficiently high.

2.3.2 Injector head

As part of the thrust chamber assembly, the essential function of the injector head assembly is to uniformly inject liquid propellants into the combustion chamber at the proper oxidizer/fuel mixture ratio. The geometry of the propellant distribution manifolds should dampen secondary flows resulting from the turbopump or piping systems. Injector heads in engines which work with storable or very cold cryogenic propellants are frequently equipped with baffles or cavities which work as damping devices. Furthermore, injection elements have a significant pressure loss, about 15-20% of the combustion pressure, work as damping elements and at least partially decouple dynamically the propellant feed system from the combustion chamber.

There are four different basic concepts of propellant injection: impinging injection, swirl injection, parallel injection in form of a showerhead, and shear coax injection and combinations of these concepts, i.e. a swirl coax injector which can be found in the HM-7B engines or a swirl and impinging as in the AESTUS engine. Any injector has to introduce the propellants into the combustion chamber in a manner to promote propellant mixing and droplet atomization by either impinging propellant streams, swirling, shear mixing or other mechanical means of achieving maximum atomization. Within the combustion chamber, ignition is achieved and vaporization of the atomized droplet is initiated by heat transfer from the surrounding 3500 K

hot gas. The size and velocity of the droplets change continuously during their entrainment and acceleration in the hot gas combustion flow. As the combustion process progresses, the vaporized propellants are mixed rapidly, heated and react, thereby increasing the gas phase flow rate within the combustion chamber. Typically, a well-designed injector atomizes a large population of propellant droplets to less than 100 microns in diameter. Therefore, with proper injector and combustion chamber design, all droplet vaporization and combustion is completed before the combustion gas enters the chamber's narrow throat area.

A major concern of any injector is the injector/wall interaction. In the vicinity of the face plate where propellant mixing is poor oxidizer-rich gases mixed with cryogenic droplets may get in contact with the combustion chamber walls.

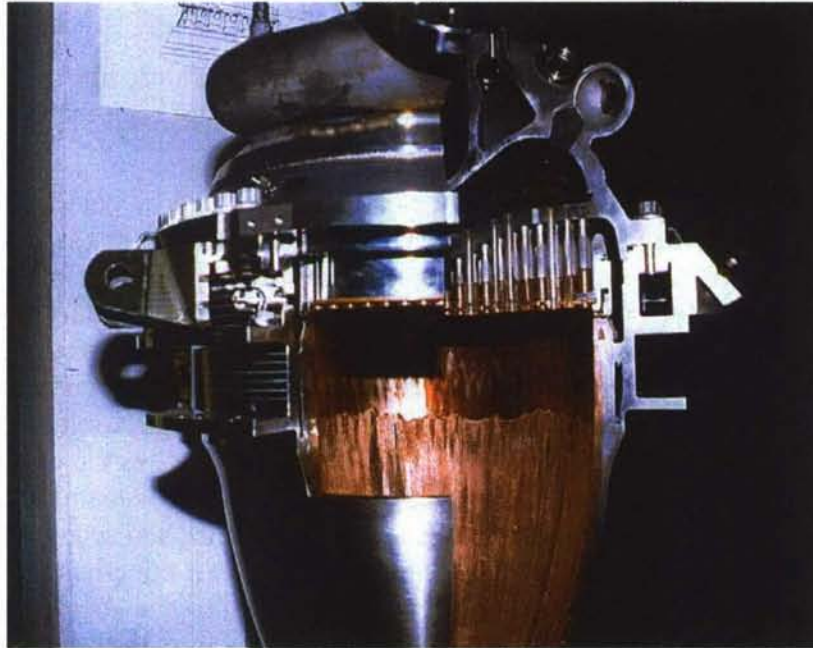


Figure 11: Footprint of "Injector/Wall Interaction" on the combustion chamber liner of the Vulcain engine

The result of this process, a combined physical and chemical attack, clearly visible on the wall of the combustion chamber liner of the Vulcain engine shown in figure 11, is called "blanching". There are two methods to cope with this problem, first, injector trimming where the outmost row of the injectors operates with a smaller mixture ratio to reduce gas temperature and avoid oxidizer-rich gas hit the surface, and, second, injection of a coolant film which has a similar effect.

In cases where both propellants enter the injector in a liquid state the injector of choice would be anyone of a kind of an impinging injector. An injector is called like-on-like if propellants of the same kind impinge on one another and like-on-unlike if fuel and oxidizer jets impinge. The working principle of an impinging injector is as follows: once the jets impinge on one another they form a liquid sheet which either decomposes into smaller fragments and atomizes and, in case of hypergolic propellants, reacts simultaneously (like-on-unlike) or interacts with another liquid sheet and the atomizes and reacts (like-on-like). The establishment of a lifted flame and a considerably large volume of partially premixed propellants is a major drawback of any impinging injector. The typical high mass flow rates establish within milliseconds a large enough amount of propellants which when they react suddenly may lead to pressure peaks which in turn may trigger combustion instabilities.

Swirl injectors which introduce a tangential velocity component to both propellants are typical for small thrusters are often some type of coax injector. They usually create due to the numerous small recirculation zones in the vicinity of the face plate a very good mixing and combustion performance and allow as well for a simple establishment of a cooling film. The major drawbacks are the comparatively large pressure drop, the coupling between performance and thermal loads to the chamber walls and the very stringent precision requirements for production. Nevertheless, there are large engine applications as well such as the RD-170 engine family where this kind of elements are used among others to actively control combustion stability by locally introducing via a this different kind of atomization a different proplet size

distribution of the liquid thus altering the propellant mixing and breaking any symmetry established in the combustion chamber otherwise.

Shear coax injectors with or without swirl are the element of choice when one of the propellant is in its liquid phase. The dominating physical phenomena in a shear injector are the destabilizing aerodynamic forces which act on the liquid jet which may be characterized by dimensionless numbers such as velocity ratio of the propellants, the appropriate Reynolds and Weber numbers, and, finally the momentum flux ratio.

$$V = \frac{w_g}{w_l} \quad \text{Re} = \frac{\mu d w}{\rho}; \quad \text{We} = \rho_g \frac{(w_g - w_l)^2}{\sigma_l}; \quad J = \frac{(\rho w^2)_g}{(\rho w^2)_l} \quad (6)$$

It is important to note that the liquid oxygen is injected below its critical temperature but above its critical pressure, and, as a consequence, atomization in the near injector region is additionally influenced by thermodynamic effects.

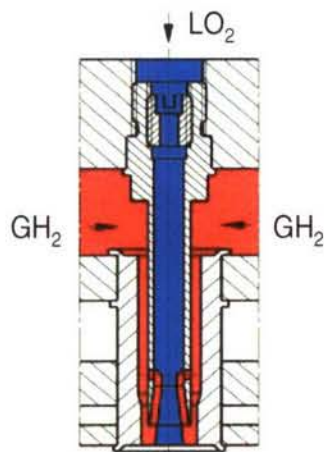


Figure 12: Schematic of a shear coax injector element

The gaseous hydrogen enters the injector and is finally accelerated at the edge to velocities in the range of 250 m/s – 350 m/s.

The basic functional principles of a shear coax injector can be explained using figure 12. The area constriction at the entrance of the liquid oxygen guarantees a homogenous mass flow rate for every element and is the main decoupling mechanism. The restriction and the expansion afterwards introduce large scale turbulences in the liquid which support the atomization. Prior to the exit some of the gaseous hydrogen is injected into the liquid which has two effects. First, it increases the pressure drop and thus introduces engine throttling capabilities without jeopardizing the combustion performance and second it improves atomization and mixing. The final exit cone has two further specifics, a tapering angle which lays somewhere between 5 and 10° and a recess of a few millimetres. Both measures will again support atomization and mixing. Typical exit velocities of liquid propellants range between 10 m/s – 20 m/s.

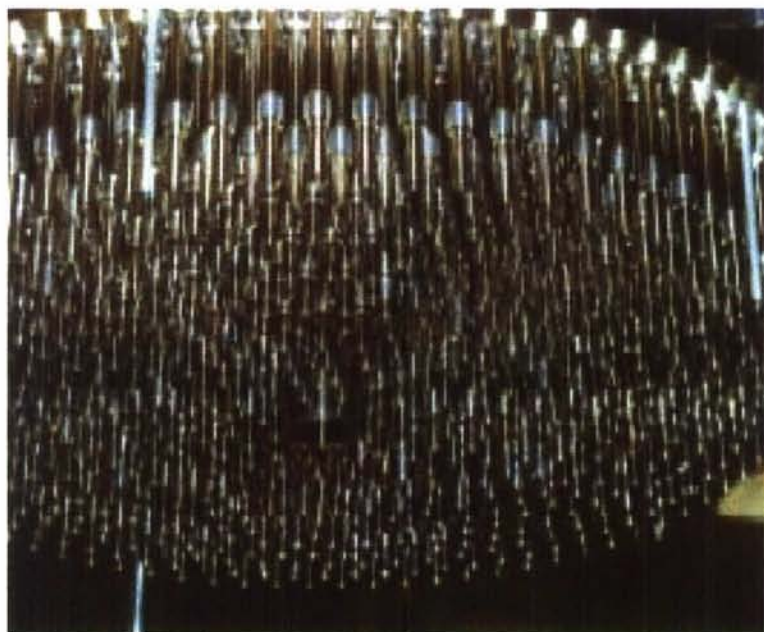


Figure 13: Row of LOX injection elements inside the hydrogen distribution dome

Figure 13 offers a view inside the fuel dome of the Vulcain 2 engine. A dense package of more than 550 injection elements homogenizes the hydrogen supply. Obviously precision mounting of all these elements is a time consuming and costly process. The exit of the ignition gas is visible in the centre.

Finally, a comparison of different injectors is given in table 6 which summarizes some characteristic data of large liquid propellant rocket engines, F-1, RD-170, SSME, RD-0120, LE-7A, RS-68, and Vulcain 2.

This offers interesting comparison since the first two engines

are LOX/ kerosene one gas generator and the other staged combustion cycle, the following three staged combustion engines are working with LOX/ LH2 and the final two work both the same propellants but are both gas generator cycle engines.

Engine	F-1	RD-170	SSME	RD-0120	LE-7A	RS-68	Vulcain 2
Thrust (sl) [MN]	6.9	7.6	1.8	1.52	0.86	2.9	0.94
Propellant combination	LOX / RP-1	LOX / kerosene	LOX / LH2	LOX / LH2	LOX / LH2	LOX / LH2	LOX / LH2
Injector type	impinging	Swirl coax	Shear coax	Shear coax	Shear coax	Shear coax	Shear coax
Flow rate / element [kg/s]	1.7	1.8	0.9	~1	0.85	~0.9	0.55
Thrust / element [kN]	4.6	5.5	3.8	3.4	3.1	~3.2	1.6

Table 6: Characteristic data of sample injectors [10]

2.3.3 Combustion chamber

As an integral and may be the most important component of the thrust chamber assembly, the combustion chamber must be specifically designed to satisfy the operating requirements of engine. The basic components of a combustion chamber are the coolant inlet and discharge manifolds, a cooled internal liner consisting of tubes or channels and an external structural assembly which is capable to carry all structural and flight loads such as thrust, pressure, and vibrations. The contour of the inner liner is aerodynamically designed to provide maximum performance and thrust for the engine operating conditions.

2.3.3.1 Combustion chamber cooling techniques

Combustion chambers are generally categorized by the cooling method or the configuration of the coolant passages, where the coolant pressure inside may be as high as 30 MPa. The high combustion temperatures which may exceed 3600 K and the high heat transfer rates, peak values may reach 100 MW/m² encountered in a combustion chamber present a formidable challenge to the designer. To meet this challenge, several chamber cooling techniques have been utilized successfully.

Regenerative cooling is the most widely used method of cooling a combustion chamber and is accomplished by flowing high-velocity coolant over the back side of the chamber hot



Figure 14: Cut through a combustion chamber wall with CuAgZr liner and galvanic deposited Ni outer shell

gas wall to convectively cool the hot gas liner. The coolant with the heat input from cooling the liner is then discharged into the injector and utilized as a propellant. Quite a large number of engines have a "tubular wall" combustion chamber design, i.e. H-1, J-2, F-1 and RS-27 [1]. The primary advantage of the design is its light weight and the large experience base that has accrued however this method exceed its application limits at pressures in the range of 10 MPa. The best solution to date is the "channel wall" design, so named because the hot gas wall cooling is accomplished by

flowing coolant through rectangular channels, which are machined or formed into a hot gas liner fabricated from a high-conductivity material, i.e. oxygen-free copper or copper alloys such as Narloy Z (CuAgZr), see figure 14 which shows a cut through the combustion chamber wall of the Vulcain engine.

Thrust chamber liner design is a complex process and necessitates a coupled solution of the hot gas side heat transfer, the heat transport inside the walls and the coolant side heat transfer. Due to the large thermal gradients plastic deformation occurs which has to be taken into account for an analysis of the cyclic life of the liner. Cooling channel geometry design has to account for the thermal blockage caused by the high heat fluxes and the comparatively drastic change in the fluid properties, heat capacity, density and viscosity, which take place at cryogenic temperature and high pressures.

All the design bureaus and companies apply Nusselt-type correlations to describe the heat transfer since a fully numerical solution of the coupled problems is far to complex. Major hurdles are the large differences in the length and time scales, chemical non-equilibrium or finite rate chemistry, the continuous transformation from sub- to supersonic velocities, and still missing models which describe satisfactorily dominating phenomena such as fluid atomization, near critical fluid behaviour. Additionally, effects such as dissociation due to high temperatures in the combustion chamber and recombination with appropriate heat release in the cooler wall boundary layer and, finally catalytic effects at the liner surface are far too complex and time consuming to allow for a coupled numerical solution. Usually the hot gas side heat transfer is described in form of a Bartz-type correlation [13]:

$$Nu = 0,062 Re^{0,8} Pr^{0,3} (10^7 < Re < 10^8, Pr \sim 0,5) \quad (7)$$

There are various modifications around, almost every company works with their one correlation, which try to account for local effects such as curvatures of liner and throat, area ratio, Mach number which all have an influence on the heat transfer:

$$\alpha_g = \left[\frac{0,026}{D_t^{0,2}} \left(\frac{\mu^{0,2} c_p}{Pr^{0,6}} \right)_{ns} \left(\frac{(p_c)_{ns} g}{c^*} \right) \left(\frac{D_t}{R} \right) \left(\frac{A_t}{A} \right)^{0,9} \right] \sigma \quad \text{with} \quad (8)$$

$$\sigma = \left[\frac{1}{2} \frac{T_{wg}}{(T_c)_{ns}} \left(1 + \frac{k-1}{2} Ma^2 \right) + \frac{1}{2} \right]^{-0,68} \left[1 + \frac{k-1}{2} Ma^2 \right]^{-0,12} ; Pr = \frac{4k}{9k-5} \quad \text{and} \quad \mu = (46,6 \cdot 10^{-10}) M^{0,5} T^{0,6}$$

Nusselt-type correlations are as well applied for the prediction of the coolant side heat transfer. These are usually verified nowadays by 3D CFD calculations which are still very demanding due to the operating conditions. Especially the continuous but varying asymmetric heat input which results in drastic changes of the local fluid properties (10-30% in density, heat capacity or viscosity are possible). Such variations will have an influence on the pressure loss distribution along the cooling channel and thus also on the local heat pickup. In order to minimize the pressure drop necessary for cooling the cross section of the cooling channels is adjusted to the local heat loads on the hot gas side. Obviously only a coupled iterative approach may yield the final solution of the appropriate liner and cooling channel design. A rather simple example of such a correlation may read as:

$$Nu = K Re^a Pr^b \left(\frac{T_w}{T_b} \right)^n \left(1 + \frac{2D}{L} \right)^m \quad (9)$$

or a little bit more complex

$$Nu = K Re^a Pr^b \left(\frac{\rho}{\rho_w} \right)^c \left(\frac{\mu}{\mu_w} \right)^d \left(\frac{k}{k_w} \right)^e \left(\frac{\bar{c}_p}{c_p} \right)^f \left(\frac{p}{p_{cr}} \right)^g \left(1 + \frac{2D}{L} \right)^m \quad (10)$$

Table 7 below summarizes the coefficients of the correlation (eqn. 10) for different combustion chamber pressures, temperatures, cooling channel velocities, heat fluxes and propellant type.

Fuel	P_c MPa	U_{ch} m/s	q MW/m ²	T_b K	T_w K	K	a	b	c	d	e	f	g	m	n
C ₂ H ₆	13.7	6-30		420-810		0.00538	0.80	0.4	-0.125	0.242	0.193	0.395	-0.024	1	0
	3-12.4	15-45	0.3-16.4	120-395		0.00545	0.90	0.4	-1.1	0.23	0.27	0.53	0	1	0
	7-13.8	30-60	3.1-18.2	230-300	230-810	0.0280	0.80	0.4	0	0	0	0	0	0	0
CH ₄						0.00696	0.88	0.5	0	0	0	0	0	0	-1.0
	27-34	55-238	2.6-139	146-275		0.0220	0.80	0.4	0	0	0	0	0	0	-0.45
	27-34	55-238	2.6-139	146-275		0.0230	0.80	0.4	0	0	0	0	0	0	-0.57
	7-13.8	30-60	3.1-18.2	230-300	230-810	0.0230	0.80	0.4	0	0	0	0	0	0	0
						0.0230	0.80	0.4	0	0	0	0	0	0	-0.80
RP-1	7-13.8	30-60	3.1-18.2	230-300	230-810	0.0440	0.76	0.4	0	0	0	0	0	1	0
	7-13.8	30-60	3.1-18.2	230-300	230-810	0.0068	0.94	0.4	0	0	0	0	0	0	0
						0.0056	0.90	0.4	0	0	0	0	0	0	0

Table 7: Coefficients for Nusselt –correlations coolant side heat transfer

These coefficients should describe the influence of the entry conditions of the flow, cooling channel geometry and any changes, curvature effects, catalytic surface reactions, influence of the structural heat flow, thermodynamic (real gas, cryogenic conditions, vicinity to the critical point, varying fluid properties), fluid mechanic (turbulence, stratification) or chemistry (pyrolysis). It worth mentioning that all these coefficients are the result of experiments which surely are influenced by the experimental setup, the sensors applied and the general operating conditions of the test [13, 14].

Film cooling provides protection from excessive heat by introducing a thin film of coolant or propellant through orifices around the injector periphery or in the chamber wall near the injector or chamber throat region. This method is typically used in high heat flux regions and in combination with regenerative cooling. A sample correlation for film cooling prediction is given below:

$$\frac{T_{aw} - T_{wg}}{T_{aw} - T_{co}} = \exp\left(-\frac{\alpha_g}{Fc_{pc}\eta_c}\right) \quad (11)$$

Sample engines where film cooling is applied are the SSME, F-1, J-2, RS-27, Vulcain 2, and the RD-171 and RD-180 with the latter two being the only ones where an additional cooling film is generated near the throat [3].

Transpiration cooling, which is considered a special case of film cooling provides gaseous or liquid coolant through the porous chamber liner wall at a rate sufficient to maintain the chamber hot gas wall to the desired temperature. A typical correlation to determine the chamber wall is given in equation (12) [3]:

$$\frac{T_{aw} - T_{co}}{T_{wg} - T_{co}} = \left[1 + \left\{1.18(\text{Re}_b)^{0.1} - 1\right\} - Y\right] Y^{\text{Pr}_m} \quad \text{with} \quad Y = e^{37\left(\frac{G_c}{G_g}\right)(\text{Re})^{0.1}} \quad (12)$$

This technique was applied to cool the injector faces of the J-2 and the RS-44, as well the SSME. However, the method has to date never been used to cool the chamber liner. The major reason might be that transpiration cooling in combination with a metallic porous structure doesn't offer a big advantage compared to conventional cooling since the maximum wall temperature will not change much and the continuous adjustment of the coolant mass flow rate to the local thermal loads is difficult to achieve.

With *ablative cooling*, combustion gas-side wall material is successively sacrificed by melting, vaporization and chemical changes to dissipate heat. As a result, relatively cool gases flow over the wall surface, thus lowering the boundary-layer temperature and assisting the cooling process. Ablative cooling may be applied either to the entire combustion chamber liner or to the throat section alone. Typically all solid rocket boosters have ablative cooled nozzles. Sample chambers with partially ablative cooled throat sections are the Viking or more recent the RS-68. Although successfully applied this cooling method has a major drawback since it doesn't allow for modifications of the engine burn time.

A *radiation cooled* chamber transmits the heat from its outer surface, chamber or nozzle extension. Radiation cooling is typically used for small thrust chambers with a high-temperature wall material (refractory) and in low-heat flux regions, such as a nozzle extension. An example of an entirely radiation cooled thrusters is the RS-21 Mariner/Viking Orbiter spacecraft, RL 10B or similar upper stage engines have radiation cooled ceramic nozzles [1, 3].

2.3.3.2 Combustion chamber life

Cyclic fatigue of the liner material is one of the life limiting factors for a rocket engine. During the start-up process the liner is first exposed to liquid hydrogen which causes the material to shrink and, since the inner copper alloy liner cools down faster than the outer nickel shell, the fins of the cooling channels are exposed to severe thermal stresses. At the end of the

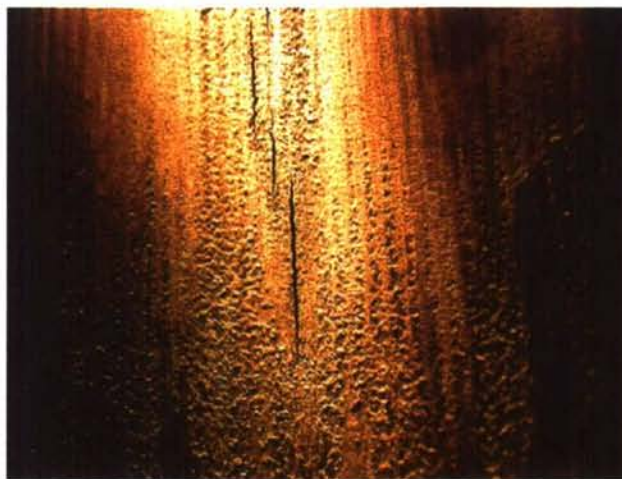


Figure 15: Chamber liner with typical longitudinal failure

cool-down the entire chamber inner shrinks about half the size of the cooling channel wall (Vulcain dimensions). After successful ignition, the temperature and pressure in the combustion chamber increase very fast and the copper wall will expand accordingly. Now, the nickel closeout is cooling by the liquid hydrogen and thus still at cryogenic temperatures. Hence, the copper has to react to the thermal expansion alone which poses additional thermal stresses to the material. With plastic deformation exceeding 3-4% a typical chamber has a life of less than 20 cycles. Figure 15 shows the liner of the Vulcain engine with its typical failures at the cooling channels.

The methods available to predict cyclic life of a combustion chamber are highly based on experience and experimental data. One reason is still missing detailed enough initial material

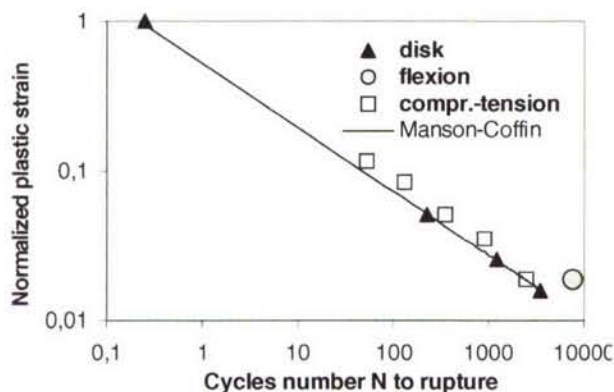


Figure 16: Cyclic material failure law

properties and their behaviour under operating conditions. Aside the above mentioned thermal stresses the liner material is exposed to additional loads which will have an impact on material properties. First, mechanical loads such as static pressure or pressure fluctuations or mechanical vibrations of various sources, second, material weakening by hydrogen embrittlement, third, high temperature fatigue or creep, and last but not least a chemical attack at the surface by OH or other radicals or a simple oxidation through exposure to

oxygen-rich gases. Anyone of these phenomena is difficult to access quantitatively in separate experiments and, even more important there is no clear understanding about the interaction of these phenomena.

A typical approach for cyclic life prediction would be to determine the hot gas side and coolant side heat transfer and then calculate the thermal field and the resulting stresses and strains in the material iteratively. Then, based on the predicted strains coming from one cyclic load case the number of cycles to failure is determined applying typical material failure relations derived from experiments, see figure 16 [15].

Quite often the thermal and mechanical analyses are performed in 2D and for a stationary thermal field, however recent investigations have shown that 3D calculations and especially transient thermal analyses are important for reliable cyclic life predictions. The numerical prediction of total number of cycles to failure is and will be for quite a while still out of reach for practical applications.

2.3.4 Nozzle

The nozzle uses the pressure generated in the combustion chamber to increase thrust by accelerating the combustion gas to a high supersonic velocity. Commonly used nozzles are bell-shaped with a parabolic contour which is either a truncated ideal or a thrust optimized one, see figure 17. While all Russian rocket engines have nozzles with an ideal contour, American, European and Japanese engines fly a thrust optimized nozzle design. The latter has a cross-sectional nozzle area which expands much faster near the throat and thus results in a shorter nozzle at the same expansion ratio compared to an ideal nozzle. This expansion however causes the formation of an internal shock and at certain stages during transient start-up

and shutdown a flow phenomenon develops which is described as restricted shock separation since the flow separates but reattaches almost immediately again. Aside severe side loads, this reattachment of a high speed hot jet poses high heat loads to the nozzles, too [16].

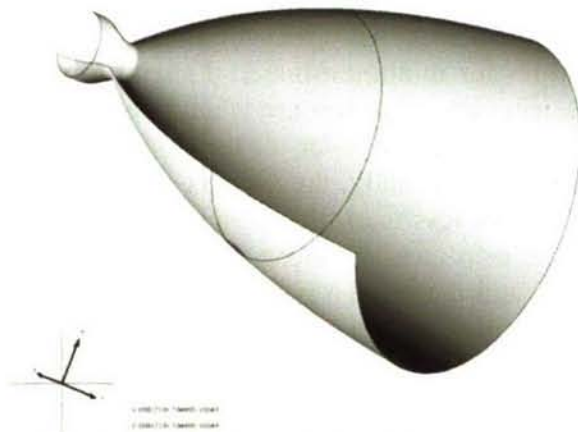


Figure 17: Typical bell-shaped nozzle

Nozzle extensions are seldom regenerative cooled more often the much simpler dump cooling is applied. The most frequent method however is ablative or radiation cooling. Materials suited for these applications are C/C or SiC structures, which infiltrated with poly-aromatic hydrocarbons and additionally incorporated additives are decomposed in an endothermic reaction route.

Radiation cooling requires appropriate high temperature materials which often have a protective coating to prevent oxidation. Only small thrusters for satellite applications have metallic nozzles build from refractory metals such as Tungsten, Rhenium or other refractory metals. A design follows based on:

$$q = \varepsilon \sigma T_{wg}^4 \quad (13)$$

with ε , the emission coefficient, σ , the Stefan-Boltzmann radiation constant and T_{wg} , the maximum hot gas side wall temperature. It is worth mentioning that in case of radiation cooling, the engine itself, its supply lines and especially sensors and cables have to be protected against high heat loads.

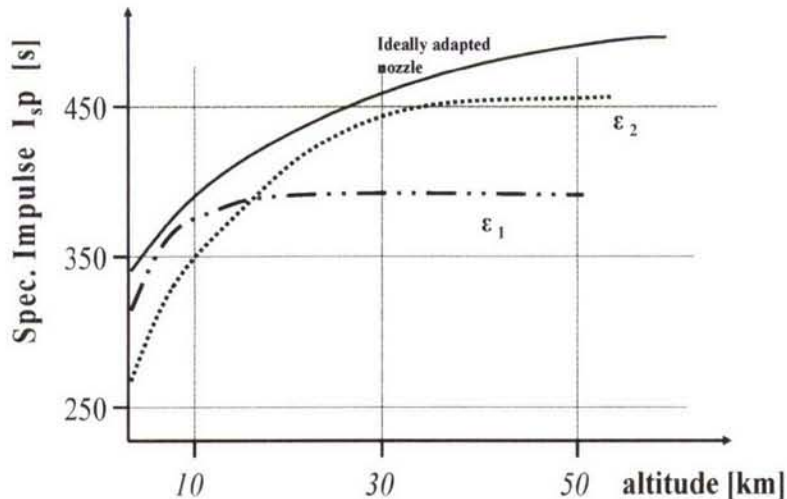


Figure 18: Potential I_{sp} penalty of main stage engines

ever, this advantage wears out soon and in the later phases of the launch the impulse penalty may exceed 15%. Engine 2 is designed for high impulse in the later flight phase and thus suffers from an impulse penalty during the first flight phase. Anyhow, however the nozzle design may be sooner or later the impulse will be less than possible.

2.3.5 Design Methodology

Current engines design techniques are based on a design methodology with load factors and safety factors determined on more than four decades of experience, and are commonly gathered under the heading of deterministic design. A deterministic structural analysis means that first, a load or condition is solely based on a set of design points and load factors which account for some variability in the specific load in order to be sure that the maximum load ever before will be accounted for, second, that values for minimum material strength or allowable fatigue are taken that ensures variations in material properties are taken into account, and, third, a safety factor is worked into the design which will cover all the remaining unknowns in analysis, loads, fabrication or even human error. Finally, the product of the design load, limiting factors, and safety factors must always be less than the strength or allowable fatigue to assure safe operation. Usually, designs have to meet different conditions such as strength, fatigue, creep, deflection, buckling or burst and therefore a typical design approach applies during the analysis maximum loads and minimum strength conditions [17].

In typical design analyses, load factors are based on previous hardware failures that were initially, analyzed by this same method - with factors that specified that none of the hardware was to fail. Taken all component and sub-systems of an engine this approach is conservative one and usually yields part which are over-designed. However, since the methodology aims at a no-failure design, there is no way to avoid a partial over-design. Numerous design reviews, audits and quality checks during the entire process of development are aimed at identifying analysis or manufacturing mistakes or integration, operation or load conditions errors. However, extensive ground testing is still necessary since any new design may yield load conditions and resulting failures that were unknown until the test [17, 18].

3. Advanced Concepts

Any new concept or design has to show the capability to improve reliability, performance or cost effectiveness of the system or component and in recent years reliability and cost became dominating. Hence, current developments deal with low cost approaches such as the RS-68 or Vulcain X design studies. In the following chapter a series of new concepts and a

The key problem of main stage engines with long burn times is illustrated demonstrated in figure 18 which shows the change in specific impulse as a function of flight altitude for an engine with two different expansion ratios ϵ_1 and ϵ_2 . In order to avoid flow separation and induced heavy side loads during the first flight phase engine 1 is designed with a short nozzle and thus has a relatively high impulse then. However,

novel design methodology approach are discussed and their potential contribution to the above mentioned drivers will be shown.

3.1 Advanced ignition devices

An ignition system is designed to meet the requirements of the mission, sea level, vacuum or multiple ignitions and accounts for further boundary conditions such as propellant phase and temperature as well as geometric and power constraints. Any improvement will have to account for these conditions and will most likely be mission specific as well.

The simplest form of system improvement is a reduction of complexity by reducing the number of parts. This may be combined with a reduction of component weight. An example could be to use the original propellants instead of additional ones. For re-ignitable engines a simple pyrotechnic system isn't sufficient and another form has to be used. Quite often gaseous pressurized propellants are applied which are sent to an ignition chamber at the appropriate mixture ratio and then injected into the combustion chamber. Multiple ignitions require a sufficient amount of propellant and thus large enough tanks. The entire system including valves ignition chamber a.s.o. may be omitted if another system with similar reliability becomes available. Although not yet used in cars yet, the automotive industry currently develops igniters for their internal combustion engines which apply semi-conductor lasers as we already use in our MP3 or CD players [19]. A change from continuous wave to pulse mode operation allows for a considerable increase in optical power. A laser-based ignition system offers the capability of distributed ignition, the energy for ignition initiation can be delivered almost everywhere. This allows for an ignition at places where unburned premixed propellants may accumulate, i.e. lifted flames, recirculation areas within injectors. Hence, this method offers a potential for risk reduction towards initiation of combustion instabilities. Nowadays, glass fibres are common for optical signal transmission. The combination of pulse mode semi-conductor lasers optical fibres allows for a safer placement of the more sensitive parts of the lasers and the above mentioned distributed ignition. This development seems worth considering since the operating conditions in a car are demanding and the required reliability is extremely high.

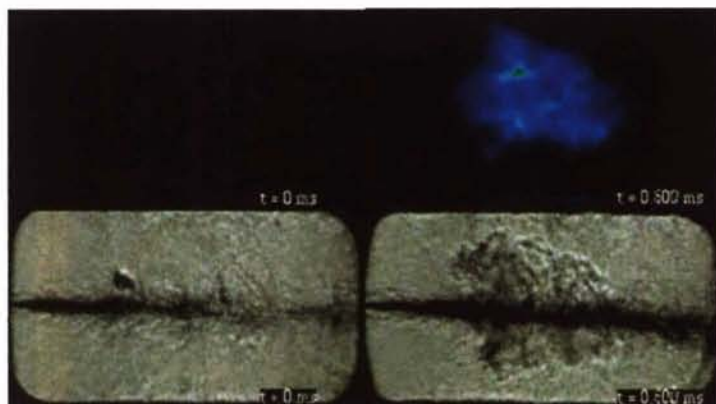


Figure 19: Laser-based ignition of a LOX/H₂ spray

There has been some effort at various places to develop this ignition technique. NASA has considered laser-based ignition as the appropriate ignition method for the individual thrust cells of the XRS-2200, the engine for the X-31 vehicle. Laser-based plasma generation and ignition of single injector cryogenic propellants was investigated for example at DLR Lampoldshausen [20]. Figure 19 shows on its left side on top the OH emission and below a Schlieren image with the dark spot just above the dark jet the result high temperature foot print of the generated plasma directly after the laser shot. On its right side, the top picture shows 800 microseconds later the OH emission of the developing flame front and below the corresponding Schlieren image. It can be seen that the flame develops within the shear layer around the oxygen jet before moving towards the injector face plate. At JAXA studies are underway which apply a laser to heat a target in the chamber sufficiently fast so that the target glows and initiates ignition of the propellant. The system might be improved if the surface of the target is activated to act as a catalyst or the target is infiltrated with a liquid which when evaporated reacts hypergolic with one of the propellants.

3.2 Advanced injection techniques

High precision fabrication, qualification inspection and testing, high precision mounting and quality assurance procedures for injector are time consuming and costly. There are two possible ways to alter the procedures mentioned above, first, a reduction of the precision requirements through a simpler injector design or, second, a reduction of the number of injection elements through an increase in the injector mass flow rate.

3.3.1 High thrust/element injectors

An increase of the thrust per injection element requires improved atomization and mixing in order to maintain similar combustion performance. In order to achieve a better atomization the area of interaction between the gas and the liquid has to be increased. An improvement of the shear coax injector with the liquid in the centre is the tri-coax injector which has a gas jet in the centre, an annular gap for the liquid and another annular gap for the remaining part of the gas. The RD-170 and RD-180 already have the hot oxygen-rich pre-burner gases in the centre and the kerosene in the annular gap around it. Examples of high thrust elements, a cross coax and tri-coax injector, which are presently under investigation at Astrium are shown in figure 20 [21]. A closer look at the thrust per element figures for different engines, see table 6, reveals that engines such as the SSME reach a thrust/element of 3.8 kN out of a mass flow rate per element of 0.9 kg/s compared to 1.6 kN out of 0.53 kg/s of the Vulcain 2 engine. Maintaining the performance and increase the flow rate per element to SSME values would cut down the number of elements by about 40%.

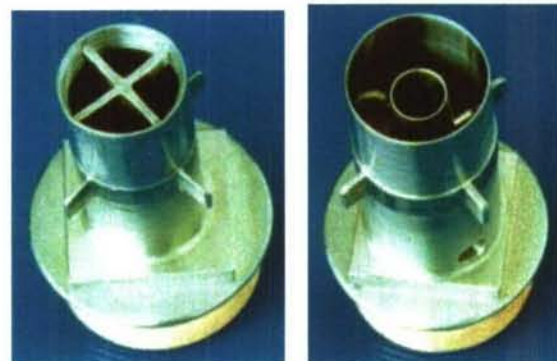


Figure 20: High thrust elements
a) cross coax b) tri-coax

3.3.2 Low precision injectors

An entirely different approach compared to the high precision requirement coax or tri-coax injectors is an approach with a porous face plate through which all the gaseous propellants are fed into the combustion chamber and large number of small LOX injectors. The advantage of this approach is that the dimensions of each element are so small that deviations from the required dimensions are tolerable since each element delivers something in the order of 0.1% of the total oxygen mass flow rate to the chamber and deviations affect only negligible parts of the combustion chamber volume.

It is worth mentioning that the atomization process with this kind of injector is different compared to the one with conventional shear coax injectors. Distribution of the gaseous fuel all over the face plate considerably lowers the hydrogen velocity which in turn reduces the available aerodynamic forces available for atomization which makes this approach less attractive. However, a closer look at the local conditions reveals that these are not that far away from typical atomization conditions in an internal combustion engine where the liquid is injected at high speeds into an almost stagnant air. Porous face plates have already been considered for the HM7B and have been tested in the J2 and SSME engines and have been flight proven with the RD-0120 although the face plate might not be consider porous since it has more than 15000 holes of less than half a millimetre in diameter. However, all these engines still have conventional shear coax injectors.

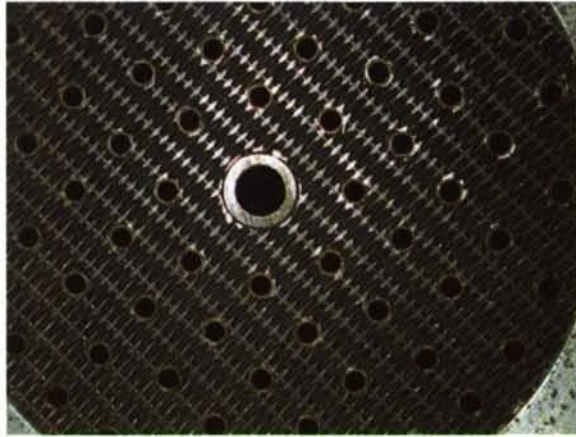


Figure 21: Sub-scale injector head with porous rigimesh face plate

indicates a more uniform heat release without any heat transfer problems to the face plate itself. Currently, investigations are underway with aim to replace both the metallic face plate and the metallic LOX post with ceramic materials and have an entire ceramic injector head.

Recently, DLR performed a series of sub-scale test campaigns with LOX/GH₂ and LOX/GCH₄ applying a porous sintered metallic (copper as well as stainless steel) and a rigimesh face plate, see figure 21, with a large number of LOX posts made of cheap pipe material. The holes for the LOX posts were simply drilled into the porous plate and the LOX posts itself were electron beam welded into the LOX dome.

The results were promising insofar as combustion efficiency determined by chamber pressure measurements turned out to be almost negligible. Furthermore, heat transfer data indicates a more uniform heat release without any heat transfer problems to the face plate itself.

3.4 Advanced thrust chamber technologies

As already stated earlier, the two approaches to improve current technologies, one driven by cost reduction constraints and the other driven by performance considerations. Improvements which increase engine reliability may be considered as cost reduction related. Any advanced thrust chamber technology will be related to heat load management, i.e. protective coatings, improved cooling, new materials or fabrication techniques with increased cyclic life behaviour, high temperature heat transfer, cooling and related component life [22-24]. It is also worth mentioning that regenerative cooling reaches its application limits when local heat fluxes exceed 80 MW/m². Typical high pressure engines apply as already mentioned a combination of regenerative and film cooling. Another method to reduce the temperature gradient across the chamber wall is deposit a thin thermal barrier coating, usually Y₂O₃-stabilized ZrO₂ on the hot gas side surface. In any case, the implementation of new materials and concepts requires the adaptation of existing design rules and tools, the determination of material properties and behaviour laws, appropriate failure detection techniques and predictive tools for failure propagation, and, first of all, reliable and reproducible material production itself.

Among the different methods which are proposed in order to meet the cooling and life requirements three approaches are worthwhile to be considered in more detail. Two more conservative approaches which maintain the concept of regenerative cooling, one which still keeps the standard combustion chamber liner material CuAgZr but protects this liner with a thermal barrier coating employing extreme thin ceramic top layers combined with appropriate metallic bond coats and another one which replaces both the conventional liner material and fabrication method by forming the liner via vacuum plasma spraying of CuCrNb powder and a more advanced approach which combines the advantages of a high temperature, low density and porous carbon-fibre reinforced carbon (C/C) based combustion chamber liner with the concept of transpiration cooling using liquid hydrogen without regenerative cooling [25-33]. While the first two techniques allow for a reduction of the thermal loads of the chamber liner and therefore aim at an increase of chamber life, which may always be traded if necessary in reduced requirements for the turbopump by a reduction of the necessary cooling pressure drop, the latter approach has almost three goals in parallel, increase of cyclic life, considerable reduction of engine weight and improved production cost.

An intermediate approach where conventional regenerative cooling is combined with non-conventional fabricated hybrid liner structure, fibre reinforced ceramic matrix composites

such as C/C or SiC/SiC, were coated applying different deposition techniques with thin metallic layers (copper, rhenium coated with tantalum) are already under investigation [25].

As has been shown earlier, main stage engines with long burn times usually suffer from an almost continuous mismatch of the nozzle expansion ratio to ambient pressure. Taking into account that none of the various plug nozzle concepts which aim at a continuous adaptation of the expansion ratio to altitude has made it from development into flight qualification [34, 35] the only remaining concept is that of a dual bell, an extendable nozzle exit cone or an expendable nozzle insert [36].

3.4.1 C/C Thrust chamber liner with effusion (transpiration) cooling

In order to fully realize the potentials of CMC materials the final development goal would be an integral thrust chamber with a CMC liner with an outer load bearing carbon-fibre reinforced polymer (CFRP) and a CMC injection head. The main challenge of transpiration cooling is the continuous adaptation of the local coolant supply to the varying heat fluxes. At each surface element of the liner static and dynamic pressure of both coolant and hot gas have to be balanced to prevent entrainment of hot gases into the porous C/C structure. A further key element will be the injector head including the injector elements which have to be different in design since the heat pickup of the propellant in the cooling channels will be missing. Especially the near injector region of the liner may need additional protection against a potential chemical attack by oxygen molecules or OH radicals.

The principle of effusion cooling bases on the following two mechanisms: Passing through the porous wall the coolant absorbs the heat conducted into the solid material of the wall. In this way, the porous wall may be considered as a counter flow heat exchanger. Heat conducted into the wall from the hot gas side is transported backwards into the hot gas. The coolant having passed through the porous wall forms a fluid film on the hot gas side wall surface and will act as a typical cooling film. Hence, a part of the convective wall heat flux is absorbed by this film. The heated coolant at the film surface is transported downstream by the momentum of the hot gas flow, partially entrained into the main flow and continuously replaced with new coolant coming out of the wall.

The porous CMC is a carbon-fibre reinforced carbon (C/C) which has a high temperature resistance of about 2500 K. The porosity can be adjusted to the application needs altering either the fabrication procedure or the raw material. Another advantage of C/C is its almost negligible thermal expansion which makes it resistive to thermal shocks or thermal cyclic fatigue. Typical high pressure rocket engines require a sufficient high Reynolds number in the cooling channels to assure the necessary cooling efficiency and to keep the wall temperatures below critical values. Pressure losses to assure sufficient cooling typically may even exceed 10 MPa while for an effusion cooled liner less than 0.5 MPa will typically be sufficient to keep the inner liner wall at tolerable temperatures. This possible pressure potential can be traded within the system for a reduced turbopump discharge pressure, lower gas generator mass flow rates, an increased engines performance or reliability or simply to enlarge the system margins.

DLR has been active for years to develop the fundamental and technological basis for this approach [37]. Material and cooling technology have been verified in different test campaigns. Key objectives were thermal cyclic fatigue tests at typical temperatures and pressure levels between 0.5 and 1 MPa, high temperature failure tests which exceeded 2500 K and sub-scale tests at P8 with typical mixture ratios and chamber pressures up to 10 MPa. One of the development goals was to overcome a potential disadvantage of this cooling concept, the loss in specific impulse. The part of the propellant which is used as coolant will enter the combustion chamber along the liner to the throat with continuously decreasing pressure and subsequently will contribute less and less to the overall thrust.

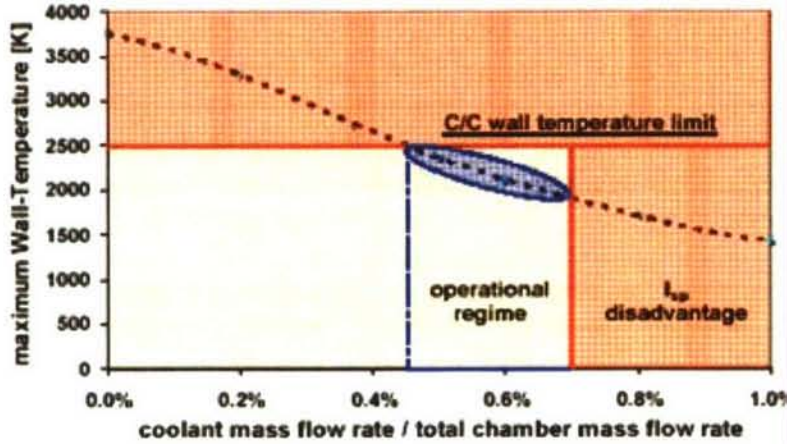


Figure 22: Operating regime of a transpiration cooled C/C liner

limit of 0.7% of the total mass flow rate. Figure 22 shows the surface temperature of the C/C as a function of the coolant mass flow rate and reveals that the material allows even for flow as low as 0.5 % and still keeping the temperature threshold of 2500 K.

3.4.2 Thermal Barrier Coating (TBC)

There exist various methods to build up protective layers for thermal protection. Among them the following techniques have been demonstrated successfully that they are suited for copper alloy substrates typical for liquid rocket engine applications: electron beam physical vapour deposition (EB-PVD), vacuum plasma spraying (VPS) and solution plasma spraying (SPS) [38-41]. A segmented sub-scale model combustor with a EB-PVD zirconia TBC was tested successfully under representative operating conditions at DLR [42].

The functional principle of a TBC, illustrated in figure 23, is to increase the hot gas side wall temperature T_w . This is achieved by applying a ceramic top layer, i.e. partially Yttrium stabilized Zirconia (PYSZ), onto the copper wall.

The PYSZ ceramic offers a thermal conductivity λ of about 1.5 W/(m K). In order to prevent a coating overheat (> 1500 K) coating thicknesses of less than 50 μm are required. These high hot gas side wall temperatures compared to the 800 K maximum temperature of the uncoated copper wall the convective wall heat flux is reduced remarkably.

There are several reasons for an application of a TBC to the liner of a combustion chamber, to provide a protective layer against chemical attack of oxygen or OH radicals and hydrogen embrittlement and to protect the copper liner from high temperatures and thermal shocks. With such a protective layer, the application range of existing regenerative cooling thrust chambers can be enlarged towards higher combustion chamber pressures or an increased thrust chamber life. In general a TBC acts as an insulator to the inner liner, reducing the wall heat flux into the copper base material.

Figure 23: Functional principle of a thermal barrier coating

3.4.3 New materials and processes for conventional regenerative cooled chamber lines

Within the last years near net-shape formation of thrust chamber liners or nozzle throat sections has been discussed intensively in the literature. Aside tungsten or rhenium which

were proposed for satellite or apogee application only recently high temperature [43, 44] high strength alloys such as CuCrNb are proposed and developed which seem to be able to replace the standard CuAgZr material. This material attracted increasing interest all over the world and in the meanwhile the technology and the material seem to be ready to be applied for thrust chamber applications [45, 46]. However, as far as the open literature shows only sub-scale level or component level testing of thermal spray formed hardware have been performed yet [47, 48]. Results about test campaigns of high thrust engines are not available in open literature. One of the reasons may be that the problems of identification, quantification and detailed control of all the process parameters which may have an impact on key material properties such as elasticity and strength, resistance to annealing or creep may not be solved yet. Furthermore, most of the engineering design tools which are used to predict the low cycle fatigue and failure of thrust chamber liners have to be adjusted to this new material.

3.4.4 High area ratio cooling channels

The basic idea behind high aspect ratio cooling channels is to enhance the heat transfer and thus influence the temperature gradients [49, 50]. A reduction in channel width will allow a larger number of channels and longer fins and both effects will increase the heat transfer area. Furthermore, narrower cooling channels allow for thinner liner walls, see figure 24. The limits for the liner walls thickness are given by the finite non-homogeneities of the liner material and by the requirements of conventional milling tools. To date thicknesses of less than 0.6 mm are hardly achievable.

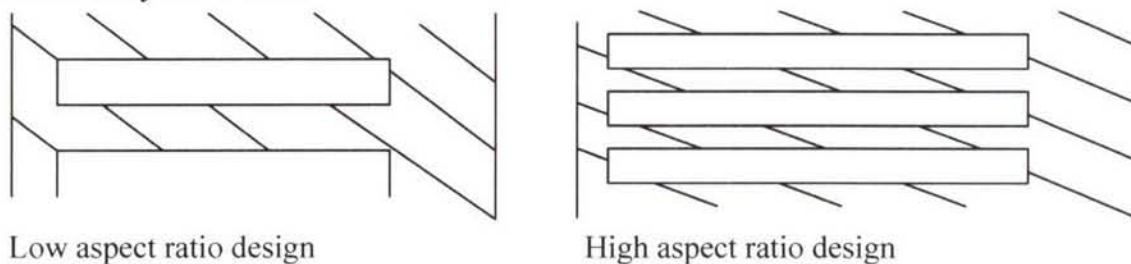


Figure 24: Sketch of a conventional and high aspect ratio cooling channel

DLR recently build and hot-fire tested a modular, sub-scale combustion chamber which had incorporated in one segment with four different aspect ratios of cooling channels to determine the effect of different aspect ratios on the heat transfer and especially on the temperature of the hot gas side liner [51].

3.4.5 Advanced nozzles concepts

As already mentioned in chapter 2.3.4, any rocket engine with a burn time considerably higher than that of a standard booster engine (~150 s) will suffer from an off design penalty of its nozzle due to the changing ambient pressure conditions during ascent. The dual bell nozzle concept, see figure 25, aims at a reduction of this performance losses. During sea level pressure conditions the flow separates at the contour inflection of the nozzle and only the first part of it, the base nozzle experience fully attached flow conditions. During ascent of the launcher, the ambient pressure decreases and at a certain altitude the flow jumps from the end of the first bell to the end of the nozzle extension, the second bell. The full flowing dual bell nozzle now works under high altitude conditions. The period of transition is sensitive to outer pressure

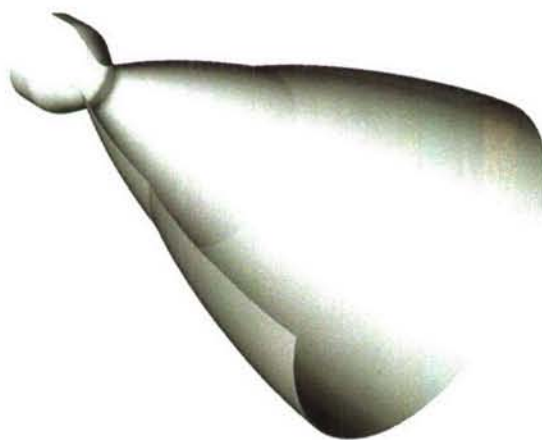


Figure 25: Dual bell nozzle

field fluctuations and therefore of special interest. Figure 26 below demonstrates the advantage of a dual bell in comparison with conventional bell nozzles with different expansion ratios. The light blue curve shows the specific impulse of a booster engine with an expansion ratio of 32, while the green, black and red curves show that of engines with expansion ratios of 45, Vulcain 2 (60), and 100, respectively. In dark blue the specific impulse of a dual bell nozzle, designed with an expansion ratio of 45 for the first bell and of 100 for the second bell are shown. Although the specific impulse drops considerably due to the jump from first to the second bell this drawback is overcome later into the flight.

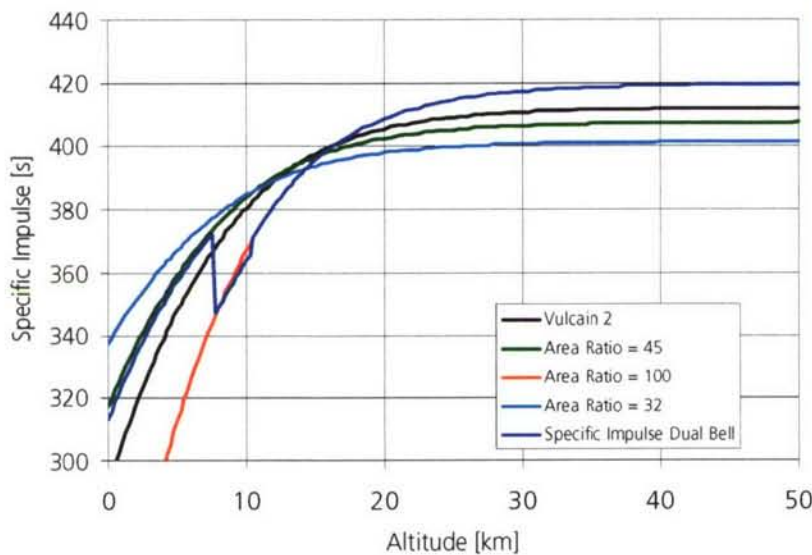


Figure 26: Specific impulse of nozzles with different expansion ratios

ratio. While the jump with increasing pressure ratio at a certain value, the back-jump at decreasing pressure ratios is delayed to a considerably lower value [52]. This stabilizing effect increases the sensitivity of the nozzle against ambient pressure fluctuations and thus enlarges the design margins of the nozzle and the nozzle operating conditions. However, the establishment of safe jump conditions during ascent require an active control of the nozzle pressure ratio by throttling of the engine.

Within the last 10 years the European FSCD consortium which features CNES, DLR, EADS, ESA, ONERA, SNECMA, Volvo Aero Corp. investigated various nozzle contours in order to identify and quantify the physical sources of flow separation and side-loads and to establish reliable criteria and models to be implemented in engineering design tools [53, 54].

3.4.6 Advanced design methodology

A clear alternative to the deterministic approach briefly described in chapter 2.3.5, is a probabilistic design approach which considers the uncertainties of material properties, operating conditions and loads in a more structured manner. In the probabilistic approach, design variables are neither seen as single values nor are they weighed to an upper or lower bounds. They are instead represented by the actual distribution or variation of the parameters. A distribution is a histogram of discrete values of the parameters or a mathematical model that represents a smooth description of the variation. When the area under the histogram or curve is normalized to a value of one, the function is called the probability density function. The parameters are termed random variables. The distribution functions, then, are used to determine the probability of occurrence of a given value of the random variable. A typical structural model for both static and dynamic analyses bases on nominal hardware geometry. Resulting displacements, loads and stresses are then compared to the material data, i.e. cyclic fatigue or ultimate strength. The material data are taken as lower bound values of the available material

The experiments performed so far with cold gas facilities revealed that the jump and back-jump from the first to the second bell and back are very fast, typically less than 10 ms. The separation from the first bell is usually not entirely symmetric however, this asymmetry is limited to angles of less than 10° which effectively limits the resulting side loads, too. Additionally, there is a hysteresis effect insofar as jump and back-jump don't occur at the same nozzle pressure

test data. The ratios between the data and the predicted values have to be within the specified safety margin. The predicted distributions show the probability for a failure and not a value or safety. The sensitivity of each variable to failure which is part of the result and this information helps the designer to get a better feeling for the impact of a variable. It is essential to become knowledgeable of inherent risk of failure and assess it, identify the mayor causes and minimize them within the design constraints.

A typical design process can be divided into conceptual design, preliminary design, detailed design and development testing. The conceptual design process is performed in the classical deterministic way and includes defining operating characteristics and configurations and the use of simplistic design guidelines for definition of configuration. Initial sizing is based on deterministic analysis for primary loads and the design features incorporate the essence of the load-carrying features of the hardware. Many details are ignored at this stage and will be handled later and whenever appropriate, simple approximations are utilized. The preliminary design typically entails a deterministic design analysis, analyses of failure modes and a list of critical items. In a probabilistic design methodology, it is at this point that the initial decisions are made as to which variables are crucial; an initial quantification of uncertainty is also determined. In addition, the design must be critically reviewed to define possible failure modes and how they relate to the uncertainty of variables. Typically the detailed design will still make use of deterministic analysis with maximum loads, minimum properties and associated deterministic models and failure techniques. Each element of a design requires a reliability estimate. Non-critical items where reliability is easily obtained, a simple reliability estimator will be utilized. Critical items however require a detailed probabilistic analysis which considers component load distributions, geometric tolerances and variations, material property unknown or uncertainties, failure model characterization such as ultimate load, buckling or fatigue, and allowances for human error, model error, fabrication and assembly. Using this detailed evaluation, loads, responses and damage assessment will be quantified as a component reliability that has considered the sensitivities of the hardware and uncertainties.

Generally, all probabilistic methods are approximate and the most common of the approximate methods is the Monte Carlo simulation or a variation of it. Repeated numerical experiments are performed that represent the total spectrum of the population of the problem. The method has an accuracy problem when small probabilities are involved. The mean value is adequately represented with a reasonable number of simulations. Sufficiently accurate solutions are with increasing numbers of simulations (less then 10,000) and the method delivers perfect answers when 20,000 to 100,000 simulations can be done in a reasonable amount of computer time. Obviously, the method has problems if each takes too time consuming which quite often happens for large finite-element analysis.

Finally, important results from probabilistic analysis are the sensitivity responses which allow for a quantitative ranking of different design variables relative to the deviation in the response of the structure. The probabilistic approach identifies areas where tolerances might be loosened with negligible effect on reliability as well as areas where additional data is required to improve reliability. Although probabilistic analysis requires more computational effort, the method provides much more information than deterministic design and it is better suited to include uncertainties such as scatter in material data, variations in thermal, mechanical, chemical static or dynamic loads tolerance in production precision. Furthermore, it is a tool which allows for risk identification.

4. Conclusions

Based on a description of the basic components and features of rocket engines areas have been identified and the physical and technological limitations given in order to pave the way for a discussion of possible improvements. The topics of gas generator or pre-burner as well

as were not included in the areas where potential advancements were proposed although some of the techniques proposed for thrust chambers, ignition systems or injector should be applicable as well for other combustion devices.

The concept of an advanced laser-based ignition system was discussed and the current status given. Additionally, an injection system design which aims at a much cheaper design with negligible impact on performance with simple LOX posts and a porous face plate was proposed and sample results were given. Various possibilities to improve thrust chamber cooling techniques involving new materials such as CuCrNb, ceramic matrix composites or effusion cooling were explained, the different aspects shown. Additionally, the advantages and the basic features of an advanced nozzle concept for a main stage engine, the dual bell nozzle was described and the current statuses of technology explained. Finally, a novel design methodology, the probabilistic design approach was briefly described.

5 References

- [1] Sutton, G.P., *History of Liquid Propellant Rocket Engines*, ISBN 1-56347-649-5, American Institute of Aeronautics and Astronautics, 2006
- [2] Isakovic, S.J., Hopkins Jr., J.P., Hopkins, J.B., *International Reference Guide to Space Launch Systems*, 3rd Ed. AIAA, 1999
- [3] Huzel, D.K., Hwang, D.H., *Modern Engineering for Design of Liquid Rocket Engines*, ISBN 1-56347-013-6, American Institute of Aeronautics and Astronautics, 1992
- [4] Sutton, J.P., *Rocket Propulsion Elements*, 3rd Edition, Wiley and Sons, New York, London, 1963
- [5] NASA Facts, *Next Generation Propulsion Technology: Integrated Powerhead Demonstrator, Technology*, FS-2005-01-05-MSFC, Pub 8-40355, 2005
- [6] Cai, C., Jin, P., Yang, L., Du, Z., Xu, K., *Experimental and Numerical Investigation of Gas-Gas Injectors for Full Flow Stage Combustion Cycle Engine*, AIAA-2005-3745, 2005.
- [7] Davis, J.A., Campell, R.L., *Advantages of a full-flow staged combustion cycle engine system*, AIAA-1997-3318, 1997
- [8] M. Wade, *Encyclopedia Astronautica*, www.astronautix.com
- [9] Farhangi, S., Hunt, K., Tuegel, L., Matthews, D., Fisher, S., *Oxidizer-Rich Pre-burner for Advanced Rocket Engine Application*, AIAA 94-3260, 1994
- [10] D. Haeseler, *private communication*
- [11] Cannon, J.L., *Turbomachinery for Liquid Rocket Engines*, "Liquid Propulsion Systems - Evolution and Advancements, American Institute of Aeronautics and Astronautics Professional Development Short Course, 2003
- [12] Albat, R., Langel, G., Haidn, O.J., "Antriebssysteme", in Ley, Wittmann, Hallmann (Eds.) "**Handbuch der Raumfahrttechnik**", Hanser Verlag, to be published 2007
- [13] Fisher, S.C., Popp, M., Quentmeyer, R.J., *Thrust Chamber Cooling and Heat Transfer*, in M. Habiballah, M. Popp, V. Yang (Eds., **LIQUID ROCKET COMBUSTION DEVICES Aspects of Modeling, Analysis and Design**, proceedings of the 2nd Int. Symposium on Liquid Rocket Propulsion, Chatillon, 1995
- [14] Liang, K., Yang, B., Zhang, Z., *Investigation of heat transfer and coking characteristics of hydrocarbons fuels*, Journal of Propulsion and Power, Vol. 14, No. 5, 1998
- [15] Riccius, J.R., Haidn, O.J., Zametaev, E.B., *Influence of Time Dependent Effects on the Estimated Life Time of Liquid Rocket Engines*, Int. Symposium on Space Propulsion, Shanghai, Sept. 25-28, 2004, China

- [16] Frey, M., Rydén, R., Alziary de Roquefort, Th., Hagemann, G., James, Ph., Kachler, Th., Reijasse, Ph., Schwane, R., Stark, R.: *European Cooperation on Flow Separation Control*, 4th International Conference on Launcher Technology, Liege, 2002.
- [17] Hammond, W., *Space Transportation: A System Approach to Analysis and Design*, ISBN 1-56347-032-2, American Institute of Aeronautics and Astronautics, 1999
- [18] Newell, J.F., Rajagopal, K.R., *Probabilistic Methodology – A Design Tool for the Future*, www.engineeringatboeing.com/articles/probabilistic.htm, 1999
- [19] Gerlinger, B., et al., *Direkteinspritzender Ottomotor und Laserzündung*, 5. Dresdner Motorenkolloquium, 2003
- [20] Gurliat O., Schmidt V., Haidn O.J., Oschwald M., *Ignition of Cryogenic H₂/LOX Sprays*, **Aerospace Science and Technology**, Vol. 7, Issue 7, pp. 517-531, 2003
- [21] Haeseler, D., Mäding, C., Rubinski, V., Khriisanfov, S., Kosmacheva, *High Flow Rate Injection Elements*, 4th Int. Conference on Launcher Technology, Liege, 2002
- [22] Popp, M., Schmidt, G., *Rocket engine combustion chamber design concepts for enhanced life*, AIAA-1996-3303, 1996.
- [23] Kindermann, R., Beyer, S., Sebald, T., Hollmann, C., Denkena, B., Friemuth, T., Kaufeld, M., Kolb, U., *Advanced Production and Process Technologies for current and future Thrust Chambers of Liquid Rocket Engines*, 4th International Conference on Launcher Technology, Liege, 2002.
- [24] Quentmeyer, R.J., *Rocket Combustion Chamber Life-Enhancing Design Concepts*, AIAA-1990-2116, 1990.
- [25] Elam, S., Effinger, M., Holmes, R., Lee, J., Jaskowiak, M., *Lightweight Chambers Thrust Cell Applications*, AIAA 2000-3131, 2000.
- [26] Shelley, J.S., LeClaire, R., Nichols, J., *Metal-Matrix Composites for Liquid Rocket Engines*, JOM, Vol. 53 No. 4, pp. 18-21, 2001.
- [27] Dembinski, L., Grosdidier, T., Coddet, C., *On the microstructure of vacuum plasma sprayed Cu-3% Ag alloys*, ITSC 2001 - Singapour - éditée par C.C. Berndt - K.A. Khor et E.F. Lugscheider - ASM-TSS - Materials park - OH-USA, p.633-637.
- [28] Leonhardt, T., Hamister, M., Carlén, J.C., Biaglow, J., Reed, B., *Near-Net Shape Powder Metallurgy Thruster*, NASA TM-2001-210373, 2001
- [29] May, L., Burkhardt, W.M., *Transpiration Cooled Throat for hydrocarbon Rocket Engines*, NASA KEE6-FR, 1991
- [30] Haeseler, D., Maeding, C., Rubinskiy, V., Gorokhov, V., Khriisanfov, S., *Experimental Investigation of Transpiration Cooled Hydrogen-Oxygen Subscale Combustion Chambers*, AIAA 98-3364, 1998
- [31] Meinert, J., Huhn, J., Serbest, E., Haidn, O.J.: *Turbulent Boundary Layers with Foreign Gas Transpiration*, Journal of Spacecraft and Rockets, 2001, volume 38, number 2, pp. 191-198.
- [32] Keener, D., Lenertz, J., Bowerson, R., Bowman, J., *Transpiration Cooling Effects on Nozzle Heat Transfer and Performance*, Journal of Spacecraft and Rockets, Vol. 32, No. 6, 1995, pp. 981 – 985.
- [33] Serbest, E., Haidn, O.J., Hald, H., Korger, G., Winkelmann, P., Fritscher, K., *Advanced Technologies and Materials for Future Liquid Rocket Engines*, 12th European Aerospace Conference, Paris, 1999
- [34] Hagemann, G., Immich, H., Nguyen TV., Dumnov, G.E., *Advanced Rocket Nozzles*, Journal of Propulsion and Power, Vol. 14, No.5, pp. 620-634, 1998

- [35] Korte, J.J., Salas, A.O., Dun, H.J., Alexandrov, N.M., Follet, W.W., Orient, G.E., Hadid, A.H., *Multidisciplinary Approach to Aerospike Nozzle Design*, NASA TM 110326, 1997.
- [36] Frey, M., Hagemann, G., *Critical Assessment of Dual-Bell Nozzles*, Journal of Propulsion and Power, Vol. 15, No. 1, pp. 137-143, 1999.
- [37] Haidn O.J., Greuel, Herbertz, A., Ortelt, M., Hald, H., *Application of Fiber Reinforced C/C Ceramic Structures in Liquid Rocket Engines*, SPACE CHALLENGE IN XXI CENTURY, Assovskiy I., Haidn OJ, (Eds), ISBN 5-94588-036-1, Moscow 2005, pp. 46-72.
- [38] Sebald, T., Beyer, S., Gawlitza, P., Mai, H., Pompe, W., *Advanced Thermal Barrier Coatings for High Heat Fluxes in Thrust Chambers of Liquid Rocket Engines*, 4th International Conference on Launcher Technology Space Launcher Propulsion, 2002, Liège.
- [39] Gell, M., Xie, L., Ma, X., Jordan, E.H., Pature, N.P., *Highly durable thermal barrier coatings made by the solution precursor plasma spray process*, Surface & Coatings Technology, 177-178 (2004) pp. 97-102.
- [40] Azzopardi, A., Mévrel, R., Saint-Ramond, B., Olson, E., Stiller, K., *Influence of aging on structure and thermal conductivity of Y-PSZ and Y-FSZ EB-PVD coatings*, Surface and Coatings Technology 177-178 (2004), pp. 131-139.
- [41] Faraoun, H., Aourag, H., Grosdidier, T., Klein, D., Coddet, C., *Development of modified embedded atom potentials for the Cu-Ag system*, Superlattices and Microstructures, Vol 30 (5), pp. 261-271, 2001.
- [42] Schulz, U., Fritscher, K., Peters, M., Greuel, D., Haidn O.J., *Fabrication of TBC- armoured rocket combustion chambers by EB-PVD methods and TLP*, Science and Technology of Advanced Materials, 6, 2005, pp. 101 – 110.
- [43] Leonhardt, T., Hamister, M., Cerlén, J.C., Biaglow, J., Reed, B., *Near-Net Shape Powder Metallurgy Rhenium Thruster*, NASA/TM-2001-210373, 2001
- [44] Flinn, E., *Tough Coating for a Smoother Rocket Cone*, Aerospace America, August 2004, pp. 24-25.
- [45] Thomas-Ogbuji, L., Humphrey, D.L., Setlock, J.A., *Oxidation-Reduction Resistance of Advanced Copper Alloys*, NASA/CR-2003-212549, 2003.
- [46] Hickmann, R., McKechnie, T., Holmes, R., Elam, S., *Material Properties of Net Shape, Vacuum Plasma Sprayed GRCop-84*, AIAA 2003-4612, 2003
- [47] Ellis, D.L., *GRCop-84: A High-Temperature Copper Alloy for High-Heat-Flux Applications*, NASA/TM-2005-213566.
- [48] Verdy, C., Coddet, C., Thomas, J.-L., Cornu, D., Choulat, M., *Highly Thickness Components for Liquid Rocket Engine Produced by Low Pressure Plasma Spraying*, International Thermal Spray Conference, Seattle, 2006.
- [49] Carlile, J.A., Quentmeyer, R.J., *An Experimental Investigation of High-Aspect-Ratio Cooling Passages*, AIAA 92-3154, 1992
- [50] Wadle, M.F., *Comparison of High Aspect Ratio Cooling Channel Designs for a Rocket Combustion Chamber with Development of an Optimum Design*, NASA/TM-1998-206313, 1998
- [51] Woschnak, A., Suslov, D., Oschwald, M., *Experimental and Numerical Investigations of Thermal Stratification Effects*, AIAA 2003-4615, 2003.
- [52] Stark, R., Haidn, O.J., Böhm, C., Zimmermann, H., *Cold Flow Testing of Dual-Bell Nozzles in Altitude Simulation Chambers*, Proc. of EUCASS European Conference for Aerospace Sciences, Moscow, 2005.

[53] Frey, M., Rydén, R., Alziary de Roquefort, Th., Hagemann, G., James, Ph., Kachler, Th., Reijasse, Ph., Schwane, R., Stark, R.: *European Cooperation on Flow Separation Control*, 4th International Conference on Launcher Technology, Liege, 2002.

[54] Winterfeldt, L. Laumert, B., Tano, R., James, P., Geneau, F., Blasi, R., Hageman, G., *Redesign of the Vulcain 2 Nozzle Extension*, AIAA-2005-4536, 2005

von Karman Institute for Fluid Dynamics

RTO-AVT-VKI Lecture Series 2007

**ADVANCES ON PROPULSION TECHNOLOGY
FOR HIGH-SPEED AIRCRAFT**

March 12-15, 2007

RAMJET AND DUAL MODE OPERATION

F. Falempin
MBDA, France

RAMJET AND DUAL MODE OPERATION

François Falempin
MBDA France

Abstract

During last twenty years, a large effort has been undertaken in Europe, and particularly in France, to improve knowledge on hypersonic air breathing propulsion, to acquire a first know-how for components design and to develop needed technologies.

On this scientific and technology basis, two families of possible application can be imagined for high-speed air breathing propulsion: reusable space launcher and military systems.

By combining the high-speed air breathing propulsion with a conventional rocket engine (combined cycle or combined propulsion system), it should be possible to improve the average installed specific impulse along the ascent trajectory and then make possible more performing launchers and, hopefully, a fully reusable one. A lot of system studies have been performed on that subject within the framework of different and consecutive programs. Nevertheless, these studies never clearly concluded if a space launcher could take advantage of using a combined propulsion system or not. Further works are under progress to design more efficient vehicle concepts taking all advantages of the air breathing operation while preserving the mechanical efficiency of the vehicle airframe.

Different possible military applications can be proposed:

- tactical missile when penetration is the key factor or when pure speed is necessary against critical time targets,
- high speed reconnaissance drone with improved mission safety and response time capability,
- global range rapid intervention system based on a large body airplane, equipped with high-speed very long range drones and missiles controlled by an on-board analysis/command team.

Considering required technology level and development risk for these both applications, it appears clearly that military application could be developed more rapidly.

Development of operational application, civilian or military, of the hypersonic air breathing propulsion depends of two key points: development of needed technologies for the fuel-cooled structure of the propulsion system, capability to predict with a reasonable accuracy and to optimize the aero-propulsive balance (or generalized thrust-minus-drag balance).

The most part of the technology development effort can be led with available ground test facilities and classical numerical simulation (thermal, mechanics ...).

On the contrary, before any operational application, it is mandatory to flight demonstrate the capability to predict the aero-propulsive balance, providing sufficient margins to start a costly development program.

R&T effort led today in France should allow better estimating advantages provided by high-speed air breathing propulsion and building a coherent development capability including methodology, facilities and adapted technologies.

On the basis of already existing and expected results of current R&T effort, some system studies have been re-started and provide very promising results for the space launcher application.

Copyright © 2007 by **MBDA France**. Published by the Von Karman Institute and RTO, with permission.

Introduction

The ramjet/scramjet concept constitutes the main air breathing propulsion system which can be used in a very large flight Mach number range up to Mach 10/12.

During last twenty years, a large effort has been undertaken in Europe, and particularly in France, to improve knowledge on hypersonic air breathing propulsion, acquire a first know-how for components design and develop needed technologies.

On this scientific and technology basis, two families of possible application can be imagined for high-speed air breathing propulsion and will be discussed hereafter.

But, prior to the development of such operational applications, it is mandatory to solve two key technology issues which are the accurate prediction of the aero-propulsive balance of an air breathing vehicle flying at high Mach number and the development of high-temperature structures for the combustion chamber, able to withstand the very severe environment generated by the heat release process while ensuring reliability and limited mass.

Ramjet/scramjet principle

In a ramjet engine, the initial compression is directly operated inside the air inlet which, by slowing the flow, raises the pressure without any compressor, so that there is also no need for a turbine. This turns to be a very simple system, avoiding all kind of turbo machinery, and associated limitations. Nevertheless, such process becomes really efficient only when the natural compression provided by the inlet is sufficiently high, i.e. approximately to Mach 1,5/2. Therefore, every ramjet-based system needs some additional propulsion for initial acceleration. As soon as the starting point is reached, the ramjet engine is able to provide performance which improves up to Mach number 3.5/4, due to the higher temperature and pressure obtained in the combustion chamber, providing better combustion conditions.

In a conventional ramjet, the airflow is slowed from supersonic speed down to subsonic speed (Mach ~0,3) through the shock system created by the forebody and the compression ramps of the air inlet, simultaneously raising the air temperature. Low speed and high temperature provide very favourable conditions for injecting, mixing, and burning the fuel.

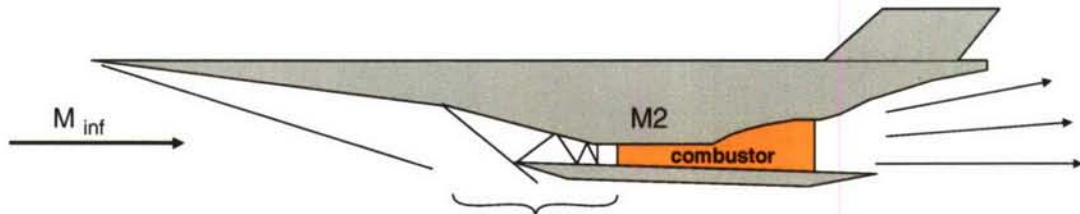
However, the shock system is also a source of entropy losses, which increase with the strength of the shocks, in direct connection with the increase of the upstream Mach number (M_{inf}). These pressure losses reduce compression efficiency. In the same time, the temperature level becomes very high at the entrance of the combustion chamber, causing two related problems:

- internal structures are exposed to high thermal loads, even before the combustor,
- heat addition to an already hot air stream becomes less efficient.

The decrease of efficiency of ramjet performance starts around Mach 5 conditions, so that its potential operation is very limited above Mach 6 or 7.

To overcome this limit, a good solution lies in decelerating the upstream flow but still maintaining supersonic conditions (Mach 2 or 3 for example), thus limiting the pressure losses, allowing an efficient heat release by combustion and lowering the thermal loads on combustor walls. Considering that the residence time at such supersonic speed is something like one

millisecond, the problem is to organise efficient injection, mixing, ignition and heat release before the fuel can escape non-burnt to the nozzle. If so, we obtain a supersonic combustion regime, and the engine is called a supersonic combustion ramjet, or scramjet.



Compression by forebody and inlet shock system
Flow slows down from M_{inf} to M_2 ($M_2 < 1$ or $M_2 > 1$)

Figure 1. Scheme of ramjet/scramjet (DMR) system

A Dual Mode Ramjet (DMR) is a ramjet engine which can be operated in both subsonic and supersonic combustion mode. DMR operation can be obtained using a fixed geometry if the overall Mach number range is not too wide (i.e. Mach 4 to 8). Extension of this Mach number range, and particularly towards lower Mach numbers, implies variable geometry for the air inlet and/or the combustion chamber. Nevertheless, different solution can be envisaged in order to obtain satisfactory operation of a DMR in the range Mach 2 to 12 within a single integrated engine.

Performances achievable by the ramjet/scramjet in term of specific impulse are illustrated by figure 2 in the case of hydrogen fuel.

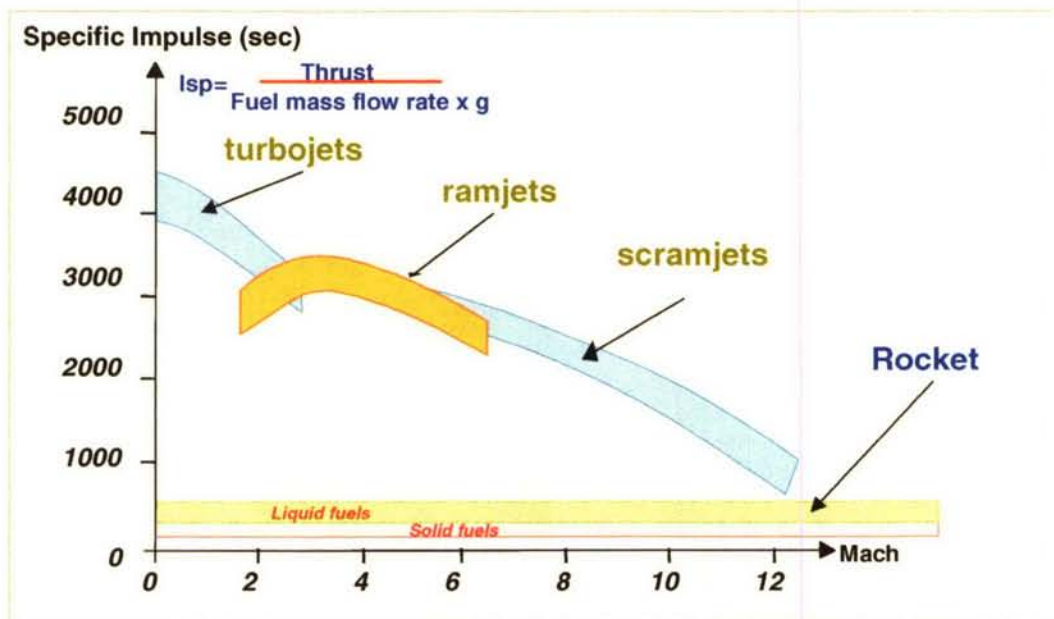


Figure 2. Achievable performance with ramjet/scramjet

Possible application

Considering the previous elements, two families of operational application can be imagined for high-speed air breathing propulsion:

- combined air breathing/rocket propulsion for space launcher,
- military systems, mainly missiles and drone.

Space launcher application

By combining the high-speed air breathing propulsion with a conventional rocket engine (combined cycle or combined propulsion system), it should be possible to improve the average installed specific impulse along the ascent trajectory and then make possible more performing launchers and, hopefully, a fully reusable one.

A lot of system studies have been performed in France on that subject within the framework of different and consecutive programs (Ref [1]). Nevertheless, these studies never clearly concluded if a space launcher could take advantage of using a combined propulsion system or not.

As a matter of fact, past studies were performed sometimes by different teams with different tools and hypothesis, sometimes for particular purpose. For example, the purpose of system studies led in the framework of the National PREPHA program (Ref [2]) was not to assess the feasibility of a fully reusable Single-Stage-To-Orbit (SSTO) space launcher but only to determine some general technical requirements for the study of a scramjet system.

By another way, these studies used systematically a very conservative approach in term of vehicle airframe configuration and it is doubtful that the best trade-off between air breathing propulsion mode needs and the mandatory low dry mass for the vehicle and its propulsion system was obtained with the considered vehicle concepts.

What could be the individual impress or opinion one can have (Ref [3]), it has to be noticed that a large worldwide effort is still under progress for developing the high-speed air breathing propulsion technology in USA, in Japan, in Australia, in Russia, in India, In China but also in France (Ref [4] to [10]).

In that context, a brief review of some of the main design issues of a future space launcher using combined propulsion leads to propose a focused approach for further new system studies which could take into account the progress made these last years in the related technologies.

SSTO

A large part of the past system studies were focused on SSTO application. As a matter of fact, it is clear that the ultimate goal must be the development of a SSTO to finally make the access to space a daily routine with corresponding low cost and, then, to develop new unexpected markets.

It is generally accepted that a fully pure rocket powered SSTO is not feasible with an achievable dry mass. By comparison, studies performed during the PREPHA program led to the conclusion that the combined propulsion could largely improve the feasibility of a SSTO if the air breathing mode can be efficiently used on a very large flight Mach number range (i.e. from Mach 1.5/2 to Mach 10/12) (Ref [11]).

Nevertheless, for such application, the payload mass is a very limited part of the total take-off mass and the remaining uncertainties related to air breathing mode performance and to achievable vehicle dry mass are of the same order of magnitude, making impossible to conclude on the real feasibility of such a SSTO launcher.

By another way, due to the extreme sensitivity of the payload mass for a SSTO launcher, the development of an operational vehicle integrating a completely new and very complex propulsion system would correspond with an unacceptable development risk level.

TSTO

On the contrary, it seems to be relatively easy to develop a Two-Stages-To-Orbit (TSTO) launcher with an air breathing first stage.

Remark : it would be also possible to place the air breathing mode on the second stage. But in this case, a large part of the problems related to the SSTO would remain (for example : heavy propulsion system placed into orbit, atmospheric re-entry of an air breathing vehicle) and would combine with the difficulty one can encounter for the flight back to the launching pad of a rocket powered first stage

First studies led in France were considering different kinds of combined propulsion systems, for the first stage, with an air breathing mode limited to Mach 6/6.5. They showed that a combined propulsion system was feasible but they also showed that this propulsion system did not improve the overall performance: the better average specific impulse being compensated by the increase in dry mass. Moreover, the pure rocket second stage remained not so easy to develop.

Other studies were performed to assess the interest of an extended air breathing mode by considering a TSTO with a first stage operating up to Mach 10/12 by using a scramjet mode. Obviously, such a solution largely eases the development of the second stage. But, it corresponds with a very complex first stage vehicle.

For all the previous studies, the staging was very close to the end of the air breathing mode. Some complementary studies showed that it would be very interesting, from the point of view of payload mass/gross weight take-off to fix the staging Mach number largely beyond the end of the air breathing mode (Ref [12]). Nevertheless, that would correspond with an even more complex first stage vehicle.

In any case, one can assume that a TSTO would be feasible with pure rocket mode on the two stages (even if it can be necessary to add a limited speed air breathing system to allow a direct and safe flight back to the launching pad for the first stage). Then, even if the combined propulsion can increase the performance in term of payload mass/total take-off mass, it would not avoid, and if fact it would reinforce, the difficulties related to the development and the operation of two complex vehicles. In these conditions, the development of a completely new propulsion system cannot make sense.

Near Earth Orbit

On the base of previous discussion, it appears that further system studies should address the concept that could be called "Near Earth Orbit" (NEO) (Ref [13]).

Indeed, the use of a very limited expendable upper stage just avoiding to really place into orbit the vehicle can largely increase the payload mass (Fig. 3). For example, the generic mission for the SSTO studied within the PREPHA program was to reach a circular orbit at 500 km. 8 metric tons of propellants were needed to circularize the vehicle orbit and, then to de-orbit. In the case of a NEO, the most part of this mass could be complementary payload improving the performance or could be considered as design margin reducing the development risk.

Even if the NEO is not a real SSTO, it would be design as a SSTO and would take into account all the requirements related to the flight outside the atmosphere (attitude control for example) and to the atmospheric re-entry. Then, considering that the number of reusable space launchers

will be limited and that these vehicles will remain some kinds of prototypes, it could be possible to integrate step by step some performance to finally reach the real SSTO mission.

Remark : It has to be noticed that the design of the vehicle could take into account the possibility to really place the vehicle without payload in orbit in order to make possible the capture of a payload in orbit before returning on ground.

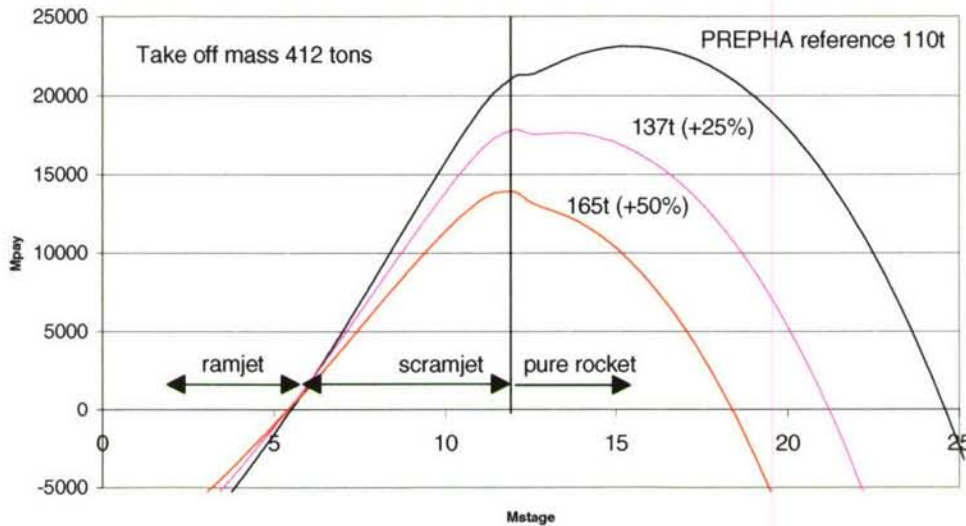


Fig. 3 –Effect of staging Mach number on payload for a TSTO using a low performance second rocket stage (Isp = 340 s and dry mass = 12% of total mass)

Such concept appears very attracting and is currently studied within MBDA France. A few specific information elements are given on that study in the last part of the present paper.

Military application

Nevertheless, considering following points, it appears clearly that military application and more specifically missile application could be developed first:

- The space application draws maximum benefit from air breathing propulsion when using it up to Mach 10-12, in order to optimize the staging of the different propulsion modes. On the contrary, the military interest of high speeds can be reached significantly below this domain. Mach 8 should not be very far from the upper limit for missile applications, and the Mach domain to be addressed through the related studies is then reduced.
- In its whole flight envelope, the space launcher has to provide a very large acceleration, which is one of the key parameters to provide sufficient payload performances into orbit. A cruising military system has naturally less needs in terms of acceleration capability at high speed.
- Test facilities, developed in the frame of PREPHA, were designed to test components of the propulsion system of a launcher at much reduced scale and in a limited Flight Mach number conditions range (up to Mach 7.5 when operational engine would have to operate up to Mach 10/12) but they nearly enable to test a missile engine at full scale. This situation contributes to reduce the uncertainties remaining after ground tests to get to flight tests. Scale effects will necessary have to be addressed for space application first by numerical simulation and then, may be, by combining step-by-step demonstration vehicles.
- Finally, it is clear that if a flight demonstration was made using a vehicle whose size would have been chosen minimal for together preserving the demonstration interest of the operation, and limiting the cost, this minimal size would probably be not very far from the size of a

missile (4 to 6m). Consequently, the success of the flight demonstration would validate the methodology used to develop the experimental vehicle, so that this methodology would also be applicable for any kind of vehicle of similar size and level of integration. With this basis, the development of an operational vehicle could be started with sufficient design margins and limited technical risk. On the contrary, even if such a demonstration would add a lot of credit for general use of dual mode ramjet, space launcher application would still require further developments before an operational vehicle program can be started.

Then, different possible military applications can be proposed (Ref [14]):

- tactical missile when penetration is the key factor or when pure speed is necessary against critical time targets,
- high speed reconnaissance drone with improved mission safety and response time capability (Ref [15], [16]),
- global range rapid intervention system based on previously mentioned missiles and drones,
- global range military aircraft or UCAV,
- short response time space launching system.

From an European point of view, it is clear that a global range military aircraft is out of possibilities (at least largely beyond the first quarter of the XXIst Century). In the same way, the development of a specific military space launcher can not be foreseen in the first half of the Century. Nevertheless, one can dream that before this time a fully reusable space launcher, mainly developed for civilian missions, will be able to provide rapid access to space for military operations (unpredictable flight over hostile zone, refurbishment or repairing of damaged satellites...).

On the contrary, it is probable that missiles and drones could appear within the two next decades.

In any case, it is clear that military application of high-speed air breathing propulsion corresponds with high value armament systems which can not be supported by only one European Nation. In the same time, related possible mission correspond with a large and direct involvement of political people. By this fact, the use of high-speed air breathing propulsion for military purposes in Europe does not just need a large, but achievable, technology step. It needs also an important, but maybe feasible, progress in European integration for Foreign Affairs and Defence issues.

Recent French background

During last fifteen years, a large effort has been undertaken in France, to improve knowledge on hypersonic air breathing propulsion, acquire a first know-how for components design and develop needed technologies.

MBDA France and ONERA brought major contributions to this effort by participating in different Research and Technology programs: PREPHA, WRR, JAPHAR, PROMETHEE...

Within the scope of the French National Research and Technology Program for Advanced Hypersonic Propulsion - PREPHA, they acquired a first know-how in scramjet and dual-mode ramjet components design (inlet, combustor, injection struts, nozzle) and hypersonic air breathing vehicle system studies (definition and performance evaluation for space launchers (Fig. 4), missiles and experimental flight vehicles) (ref [17], [2]). They also improved their test facilities and numerical means (Ref [18]) and started some activities on flight experiments.

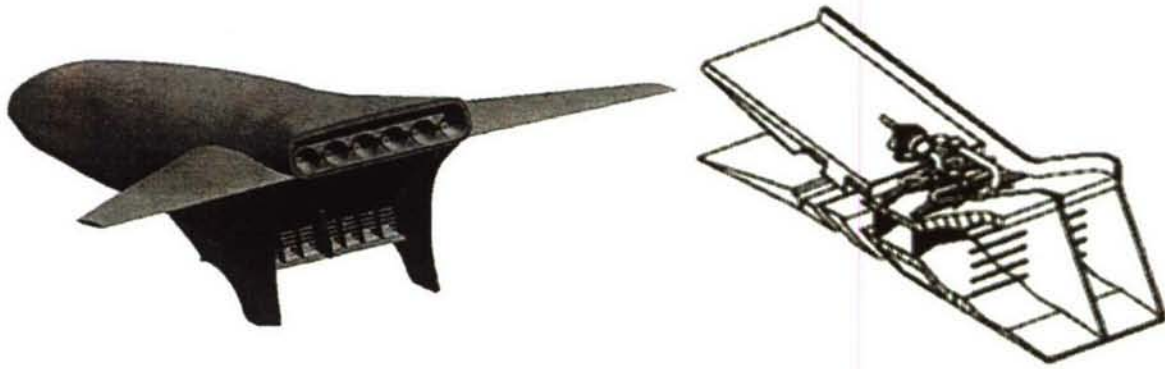


Fig. 4 – PREPHA - Generic SSTO vehicle and its air breathing propulsion system

From 1995 to 2000, and with a partial support of French Administration, MBDA France has been leading a cooperation with the Moscow Aviation Institute (MAI) to develop and test at ground a wide range ramjet dual mode ramjet (Mach 2-12), with fully variable geometry, and using kerosene and hydrogen (ref [19] to [22]). MBDA France has also been leading a cooperation with the Institute of Theoretical and Applied Mechanics (ITAM) from Novosibirsk to develop variable geometry air inlet able to operate in a very large Mach number range (2 to 8 or more) (Ref [23] to [25]- Fig.5).

MBDA France is also working with Astrium Space Transportation to develop fuel-cooled composite structures. First achievement of this cooperation was the development on a C/C hydrogen-cooled injection strut (ref [26]). Partners are now developing an innovative technology for C/SiC endothermic fuel-cooled or hydrogen-cooled structures of a complete combustion chamber (ref [27] to [30]).

In parallel, from 1997 to 2001, ONERA led an in house program in cooperation with its German counterpart DLR. This program, named JAPHAR, aimed at pursuing the basic studies engaged during PREPHA by studying a hydrogen fuelled dual mode ramjet, able to operate in the range Mach 4-8, and by developing a methodology to demonstrate the in flight aero-propulsive balance of an experimental vehicle which would use this engine (ref [31] to [37] – Fig.6).

By another way, ONERA was cooperating with SNECMA (ref [38]) to develop a composite materials technology for endothermic fuel-cooled structures in the frame of the A3CP program.



Fig.5 – Mach 2/Mach 8 variable geometry air inlet tested in ITAM wind tunnel

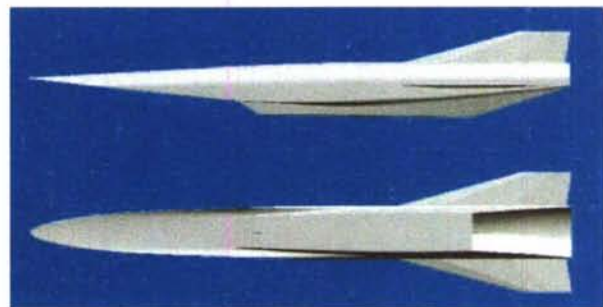


Fig.6 – JAPHAR - generic experimental vehicle

In 1999, French MoD started the PROMETHEE Program. This program, led by MBDA France and ONERA, aims at studying the main difficulties associated to hydrocarbon fuel dual mode ramjet in order to acquire a first know-how in the design and operation of a propulsion system capable of powering a hypersonic cruise missile, and taking directly some operational constraints into account (ref [39] to [41]). To federate these studies, the application to a long range air-to-ground generic missile is considered (Fig. 7).



Fig. 7 – Generic Air-to-Ground missile

Key technology issues

The feasibility of previously described application mainly depends of two key technology issues:

- capability to predict with a reasonable accuracy and to optimize the aero-propulsive balance (or generalized thrust-minus-drag),
- development of needed technologies for the propulsion system as a low weight, high robustness fuel-cooled structure for the combustor.

Aero-propulsive balance sensitivity

For an air breathing propulsion system, the net thrust (i.e. the thrust which can effectively be used for compensating the drag and accelerating the considered vehicle including the propulsion system) is the difference between the thrust provided by the exit nozzle (momentum of accelerated hot gas coming from the combustion chamber) and the drag due to air capture by the inlet. As a matter of fact, atmospheric air has initially no speed. During capturing process, some energy has first to be paid to accelerate the incoming air in the upstream direction up to 40 to 75 % of the vehicle speed. On the contrary, hot exhaust gas must be ejected through the nozzle in the rear direction at a speed exceeding flight speed (in vehicle reference).

This fact can be illustrated as follows:

- at flight Mach number 2, a net thrust of 1 is obtained by producing a thrust of 2 by the nozzle which compensates an air capture drag of 1,
- at Mach 8, a net thrust of 1 is obtained by a nozzle thrust of 7 while air capture drag is 6,
- at Mach 12, a net thrust of 1 is obtained by a nozzle thrust of 12 while air capture drag is 11.

Then, the higher the flight Mach number, the more sensitive the net thrust. At Mach 8, for example, an error of 5 % on nozzle performance leads to a reduction of 35 % in net thrust. At Mach 12, the same error will result in 60% net thrust reduction.

Then, it is more and more mandatory to optimize the integration of the propulsion system into the vehicle airframe, and vehicle and propulsion system components are operating in a much

coupled way which would require testing the overall system to determine the global performance.

But, the higher the flight Mach number, the more difficult to simulate right flight conditions with on-ground test facilities. Generally, in such test facilities, air is heated up to total temperature before being accelerated through a nozzle to enter the test section at the right Mach number. Whatever the heating process may be, that generally leads to the creation of radicals, and very often some pollution into the incoming air, which can globally change the combustion process.

This problem is largely increased when heating process is based on pre-combustion (hydrogen, gaseous or liquid hydrocarbon fuel) and oxygen completion. In this case, chemical nature and thermodynamic characteristics of the incoming air are modified, that creates change of ignition delay and modification of thermodynamics into the propulsion flow path.

By another way, for large and very large vehicles, some scaling effects are difficult (or impossible ?) to solve. Then a specific development methodology has to be defined by combining large scale partial tests (possibly corresponding with very large, then expensive test facilities) and numerical simulation in order to be able to ensure design margins for the development of an actual full scale system ; the only one validation of this methodology accessible prior to the full scale development being acquired by numerical simulation.

Propulsion system concept

As already mentioned, past studies performed in France demonstrated that combined propulsion could have an interest for space launcher only if the air breathing mode can provide a significant part of the total speed increment.

For a TSTO, a limited part of the total speed increment given by the air breathing mode will not make the launcher unfeasible but will not improve the performance (payload mass/total take-off mass) by comparison with a full rocket system : reduction in needed fuel mass being compensated by the complementary dry mass of the air breathing engine.

For a SSTO, it is clear that the complementary dry mass corresponding with the air breathing mode and its integration into the vehicle will directly reduce the possible mass of payload. Then, the benefit provided by the air breathing mode in term of specific impulse improvement must be sufficient to compensate all these negative terms:

- large Mach number range of operation,
- high installed specific impulse allowing good acceleration level in the whole air breathing mode,
- low dry mass.

Different types of air breathing combined cycles were considered for the system studies performed within the framework of the PREPHA program (Ref [1] and [11]). These studies showed that the use of turbo machinery is not pertinent by comparison with systems based on ramjet. As a matter of fact, one can only take advantage of a turbine based combined cycle in term of specific impulse on a limited Mach number range (maximum up to Mach 6) while it corresponds with a very important increase of dry mass:

- the engine by itself is heavy,
- its combination with a ramjet/scramjet system is very difficult and leads to complex and heavy air inlet consecutively ensuring the supply of a large air mass flow to two different air ducts.

At the contrary, a ramjet/scramjet (dual-mode ramjet DMR) system can be used on a large Mach number range (up to Mach 12) and corresponds with more simple system using a single air duct,

avoiding complex transition phase within the air breathing mode and more limited induced dry mass addition.

Moreover, such a ramjet/scramjet system is more capable to integrate some improvements like in-flight oxygen collection or extension to higher Mach number by adding an Oblique Detonation Wave mode or major evolution like MHD by-pass or other heat release principle which could be developed and validated during the development or the in-service life of the vehicle.

A large effort has been led, mainly in USA, on the RBCC (Rocket Based Combined Cycle) concept. Some system studies have been performed in France on that concept (particularly in the framework of the PREPHA program). It has never been confirmed that such integration of the rocket mode into the air breathing duct can improve the global performance. As a matter of fact, in order to obtain a ramjet effect at low Mach number (between 0 and 1.5/2) and then improve the specific impulse, one must reduce rapidly the thrust of the rocket mode (very rich propellants mixture). But, this action dramatically reduces the global thrust and then the vehicle specific impulse (acceleration capability). Then, it appears preferable to use the rocket mode at full power (eventually without any ramjet effect) up to the minimum Mach number for which the air breathing mode is able to provide alone a sufficient thrust to obtain an improved vehicle specific impulse. By another way, if one tries to integrate into the air breathing duct the rocket engines ensuring the final acceleration, that leads to strong integration constraints limiting the achievable performances for the air breathing mode, particularly at high Mach number (supersonic combustion), and generates new difficulties related to the thermal sizing of the air breathing combustion chamber. Finally, such RBCC system make more complex the attitude control during the flight outside the atmosphere, rocket engines thrust being not easily directed to the vehicle centre of gravity.

Need of a variable geometry concept

As a very large flight Mach number range must be considered for the dual-mode ramjet (i.e. 1.5 to 12), a variable geometry is mandatory to provide the best acceleration capability of the air breathing mode.

A fixed geometry combustion chamber associated to a variable capture area air inlet was considered (Fig.8). But, due to the fixed minimum section of the air inlet (equivalent to the fixed section of the combustion chamber entrance), the thrust was limited at low Mach number because of the blockage of incoming air. Moreover, if one tries maintain the air inlet capture area within the bow shock up to the maximum Mach number of the air breathing mode, the air inlet size is limited and consecutively the available thrust reducing the vehicle specific impulse.

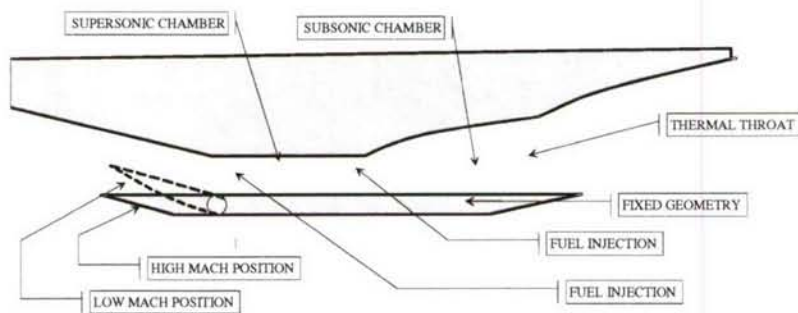


Fig.8 – fixed geometry concept of PREPHA engine

A different concept has been developed with the Moscow Aviation Institute. This concept, called WRR has a fully variable geometry –air inlet + combustion chamber (Fig.9). Then, performances can be increased by comparison with the previous concept as it is shown in Ref [42]. Nevertheless, this concept has the same limitation as the PREPHA concept (i.e. fixed minimum section of the inlet). Then, one cannot take all the benefit of the complexity related to a fully variable geometry system.

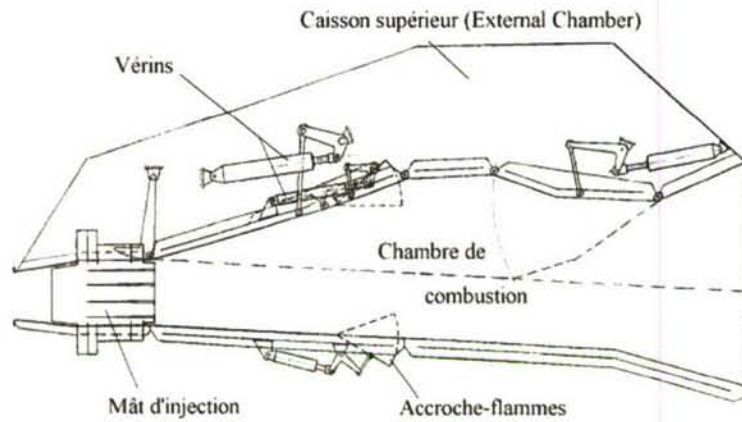


Fig.9 – variable geometry WRR engine

Other concepts have been studied, which consist in modifying in the same time the minimum section of the air inlet and the geometry of the combustion chamber by using a simple movement of the engine cowl. PROMETHEE program is focused of a rotating cowl concept (Fig.10), while PIAF studies, performed with MAI, are focused of a translating cowl (Fig.11).

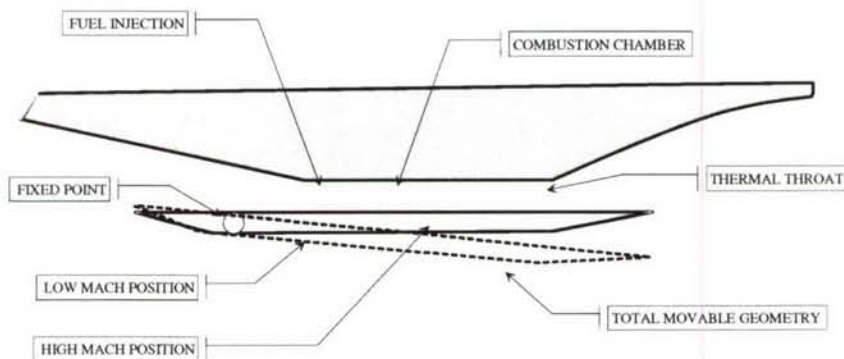


Fig.10 – variable geometry PROMETHEE engine

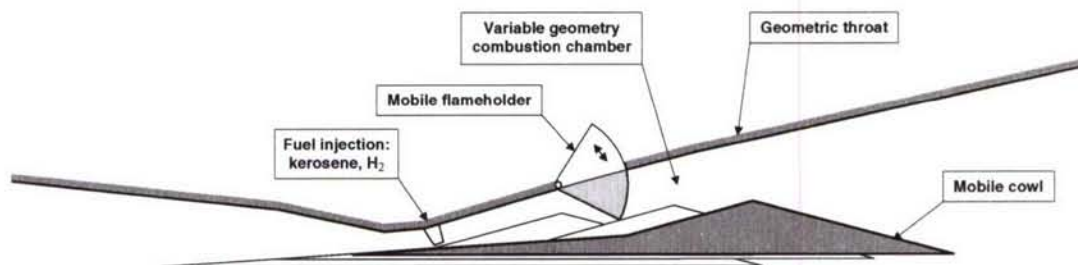


Fig.11 – variable geometry PIAF engine

For such concepts, having at disposal a variable minimum section for the air inlet avoid the need of a large variation of the air inlet capture area (i.e. increase when the Mach number increases).

Then the limitation of engine size due to the bow shock is reduced and air breathing engine can be larger at low Mach number providing high thrust level and then better vehicle specific impulse. In these conditions, it is possible to switch to air breathing mode earlier increasing subsequently the overall performance.

Air breathing engine integration

Dual-mode ramjet has obviously the drawbacks of its advantages: a low specific thrust associated with a high specific impulse. The size of the required engine is then quite big, and its weight is about 1000 kg per square meter of air inlet capture area (a benefit of 30 % can be expected by using ceramic composite materials (Ref [43])).

Most of the current launchers projects have quite conventional shapes and the need to integrate a large air breathing propulsion system leads to very low structural efficiency for the flat airframe which is mainly a pressurized fuel tank.

However, other concepts could be studied to try to ensure better trade-off between air breathing propulsion system needs and airframe structural efficiency (Ref [13]).

The first example of these possible vehicles consists in twin axi-symmetric fuel tanks, which are linked by a large 2 D air breathing propulsion system while the rocket engines are placed on the base of cylindrical fuel tanks (Figure 12).

This configuration lends itself a very large, fully variable geometry air breathing system, which has no limitation at low Mach number and then can provide a very high level of thrust. The upstream position of the air breathing mode make possible an inversed SERN nozzle that contributes to the lift at low Mach number rather than increasing the apparent weight. This said, the problem of large base drag created by the two rocket engines still remains and the re-entry phase (air inlet closed of-course) is questionable.

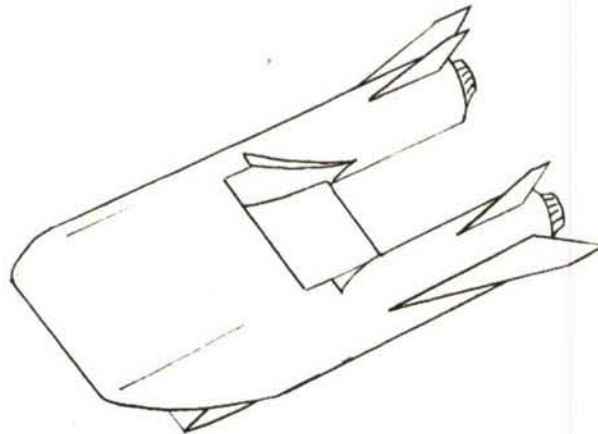


Figure 12 : Twin fuel tank concept

Another concept can be proposed as shown on Figure 13. It is based on a double cone fuselage, which corresponds with a very good structural efficiency. The air breathing engine is semi-annular and takes advantage of a very large air capture section provided by the cone. It can be considered as a series of relatively small modules, which could be more easily tested on ground. The rocket mode can be integrated in the external part of the SERN nozzle. The wing is designed to provide protection of the propulsion system during the re-entry phase (180° vehicle turn

before re-entry). Telescopic aerodynamics could provide performing pre-compression while allowing a large nose radius during the re-entry phase.

A completely axi-symmetric concept can be also proposed as shown on Figure 14. This concept will be a little bit further discussed hereafter.

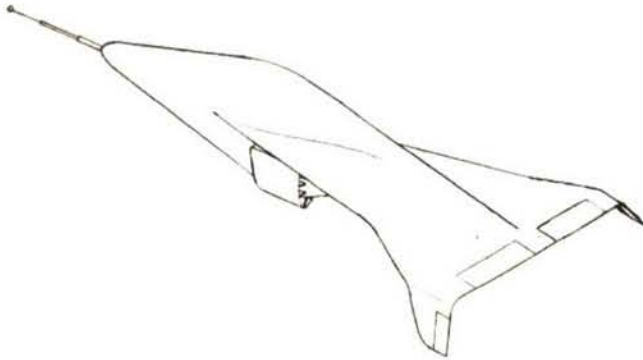


Fig. 13 – double cone airframe concept

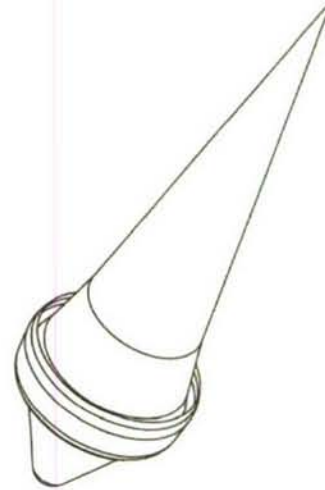


Fig.14 – Fully axi-symmetric concept

Rocket engines are placed in the downstream cone, which constitutes the external part of the SERN nozzle. It is then very easy to control the vehicle including during the flight outside the atmosphere while taking advantage of maximum expansion. The movable cowl of the air breathing engine can be moved upstream to the maximum diameter of the fuselage in order to create a circular wing on the back of the vehicle, allowing to land horizontally after re-entry and deceleration phases (already designed for very large thermal loading). Such a concept leads to a very large engine (2 to 2.5 times larger than that of PREPHA for the same vehicle size). Then the air breathing phase is very efficient and can be performed with a high slope angle, which dramatically reduces the duration of the atmospheric flight (Mach 0 to 12 in 250 seconds instead 1100 seconds for the PREPHA generic vehicle) and then improves the overall efficiency and maybe relaxes the constraints for the sizing of the thermal protection system.

Development methodology

The here above described extreme sensitivity of the aero-propulsive balance on one hand, and the corresponding limited capability of ground test facilities to represent right flight conditions on the other hand make mandatory the definition of a specific on-ground development methodology coupling very closely experimental and numerical approaches.

In such a methodology, the in-flight performance can be predicted only by a nose-to-tail numerical simulation. Then on-ground test facilities will be used to performed partial test of vehicle and propulsion system components separated or coupled one to the other.

These tests have different goals:

- to allow components design tuning and verify a minimum performance,
- to verify, step by step, the ability of numerical simulation to predict accurately performance in conditions as close as possible to the actual flight,
- to acquire a minimum knowledge related to coupled operation of components.

Obviously, such methodology is very challenging. So, before starting any operational development, it must be demonstrated that applying this approach will give an accurate value of

the performance, allowing to guarantee design margins and to identify properly right directions for optimizing system design. That is why; a flight experimental program is a mandatory step towards future operational developments.

First approaches for a flight test program

In 1993/1995, a first flight test program was performed with system Kholod developed by the Central Institute of Aviation Motors from Moscow (CIAM). But, this program was based on a hydrogen fuelled axi-symmetrical engine placed on top of a Russian SA6 missile during the whole flight (Fig.15 - Ref[43]).



Fig.15 – Kholod system developed by CIAM

A successful test was performed at Mach 5.7. A new test aiming at flying at Mach 6.3 had a failure. Nevertheless, engine configuration was considered having low interest for future application. Moreover, due to the engine/booster integration it was not possible to establish a clear thrust-minus-drag. Then it was decided to stop this cooperation which has been pursued by CIAM with NASA for a complementary flight.

Beyond this first experiment and in the framework of the PREPHA program, an analysis of flight test needs allowed evaluating the capacity of a large set of typical experimental vehicles to comply with these requirements (Ref [44]). This study resulted in the demonstration of the mandatory need of testing an autonomous vehicle to assess the aero-propulsive balance. It also demonstrated that a small and simplified vehicle would be sufficient for this essential demonstration even if it would not give right answer to some others flight experimental needs.

Assuming obtained results, ONERA and MBDA France sketched a few self-powered experimental vehicles (Ref [45]).

In 1997, ONERA and DLR started the already mentioned JAPHAR program. This program aimed at defining a development methodology and at designing a flight experimental vehicle allowing validating this methodology by flying between Mach 4 and Mach 8. The propulsion system size – height of engine entrance section equal 100 mm – led to a relatively large vehicle (~11 meters long) which corresponds with a cost largely exceeding possibly available budget in France (and Europe up to now).

Finally, MBDA France had a limited participation in the HyShot experiment led by the University of Queensland – Australia and QinetiQ (Ref [46]).

The LEA flight test program

Beyond all current technology development works mentioned here above, and on the base of previous acquired results, MBDA France and ONERA started a flight test program, called LEA, in January 2003 with the support of French Administration (Ref [47] and [48]). In order to limit the cost, this flight test program would be performed with a 4 meters long experimental vehicle having no technology demonstration purpose (use of existing technologies as often as possible) (Fig. 16). In the same view this vehicle would be non-recoverable, then non-reusable. Specifically addressing the aero-propulsive balance, this flight test program is supposed to be performed in cooperation with Russian organizations.

Today, different possible configurations are still considered for the launching and accelerating system and corresponding Russian partners. Nevertheless, an air-launched experimental system would be preferred because it gives some flexibility and reduces range clearance problems.

The test principle consists in accelerating the flight experimental vehicle specimen thanks to an air-launched booster up to the given test Mach number, chosen in the range 4 to 8. Then, after booster separation and stabilization, the experimental vehicle will fly autonomously during 20 to 30 seconds. During this flight, the air breathing propulsion system will be ignited during about 5 seconds with a fuel-to-air equivalence ratio variation (Fig. 17).

The vehicle would be specifically instrumented to give a precise evaluation of the aero-propulsive balance with and without combustion and to determine the contribution of each propulsion system component to this balance. All measured parameters will be transmitted to ground by telemetry and recorded with an on-board data recorder which will be recovered after the crash of the vehicle.

The program should result in 6 flight tests, planned between 2010 and 2012 for exploring Mach 4 to Mach 8 Mach number range. As explained previously, and beyond a detailed understanding of the aero-propulsive balance, such a flight test program will give the opportunity to define, implement and validate a development methodology applicable to any future operational development.

For this experimental vehicle, the airbreathing propulsion system concept has been chosen by taking into account all results acquired during engines developments performed these last years. The finally selected concept is a variable geometry one using a simple translation movement of the engine cowl, like PIAF engine (Fig. 11) but with a thermal throttling. Nevertheless, as each flight test will be performed at a quite constant Mach number, a fixed geometry engine will be used on board of each LEA test vehicle, this engine configuration being representative of the selected variable geometry concept at the tested flight Mach number.



Fig. 16 – CAD view of LEA vehicle

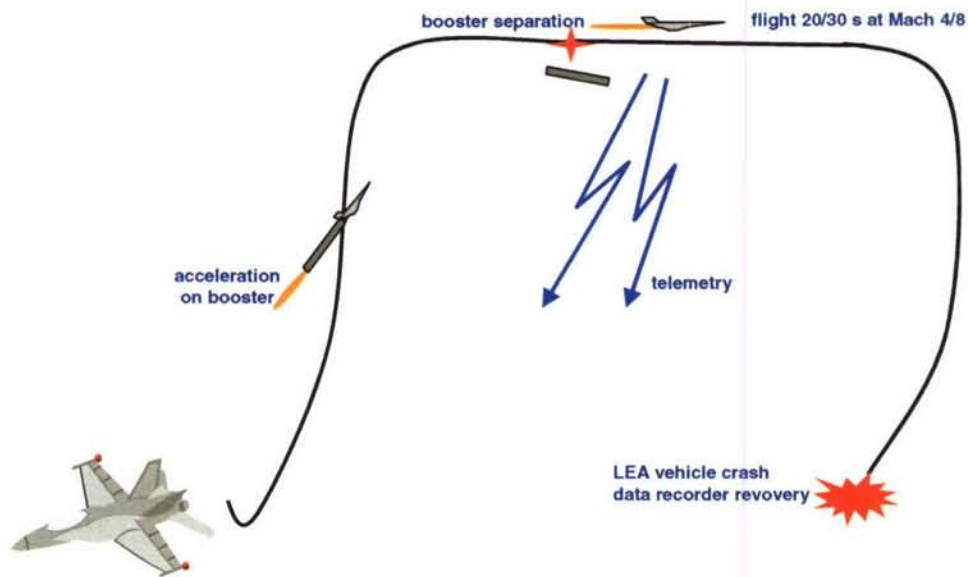


Fig.17 – LEA flight testing sequence

A parametric study has been performed on the possible technology for the combustion chamber. The finally selected solution is based on metallic heat sink solution with a high temperature low thermal conductivity coating.

The fuel has also been chosen. The most part of French experience in supersonic combustion is related to Hydrogen. But, considering the very low density of Hydrogen, it is preferable to avoid this fuel in order to limit the size of the tank, then the size of the vehicle and consecutive difficulties to find a possible acceleration system complying with the needs (integration constraints, needed total energy release...).

On the other hand, liquid hydrocarbon fuel could be considered. But, our experience is very limited with such a fuel and it would be difficult to ensure a robust ignition and a good combustion efficiency without previous reforming in a regenerative cooling system (simplest technology used on board of the experimental vehicle).

Finally, a mixture of gaseous Methane and gaseous Hydrogen has been selected. By using this mixture, it is possible to increase the fuel density then limit the fuel tank size. It will be also possible to vary the H₂/CH₄ ratio during the flight to ensure a robust ignition and control the heat release along the combustor.

Some specific works have been performed to adapt used computation codes to this particular fuel. These codes have been validated thanks to basic experiments led in updated ONERA LAERTE test facility. Moreover, ONERA ATD 5 test facility has been updated to allow future CH₄/H₂ tests for the LEA engine. By waiting, a first test series has been performed with already existing JAPHAR combustion chamber to acquire a first experience with such a fuel.

The forebody has been specifically studied. Some parametric studies have been carried out in order to determine a set of design parameters allowing a satisfactory pre-compression while complying with technology constraints.

On the base of an air inlet design and corresponding performances, a first design of the combustion chamber has been realized thanks to 1D, then 2 and 3D computation. On this basis, a full scale mock-up is under manufacturing for future test in ATD 5 ONERA test facility.

Due to the particular configuration of the afterbody/nozzle, a specific effort is still under progress to well understand the interaction between the propulsive jet and the external flow to accurately determine the effect of propulsion on external aerodynamic (Fig.18).

Aerodynamic behaviours of the LEA vehicle and of the Flight Experimental Composite constituted by LEA and its booster have been evaluated by computation for preparing future aerodynamic tests.

Finally, a large effort has been dedicated to the development of Nose-to-Tail computation tools. Thanks to this, two approaches – NtT computation by blocks or integral NtT computation – are available and daily used to evaluate and optimize the aero-propulsive balance of the vehicle (Fig.18).

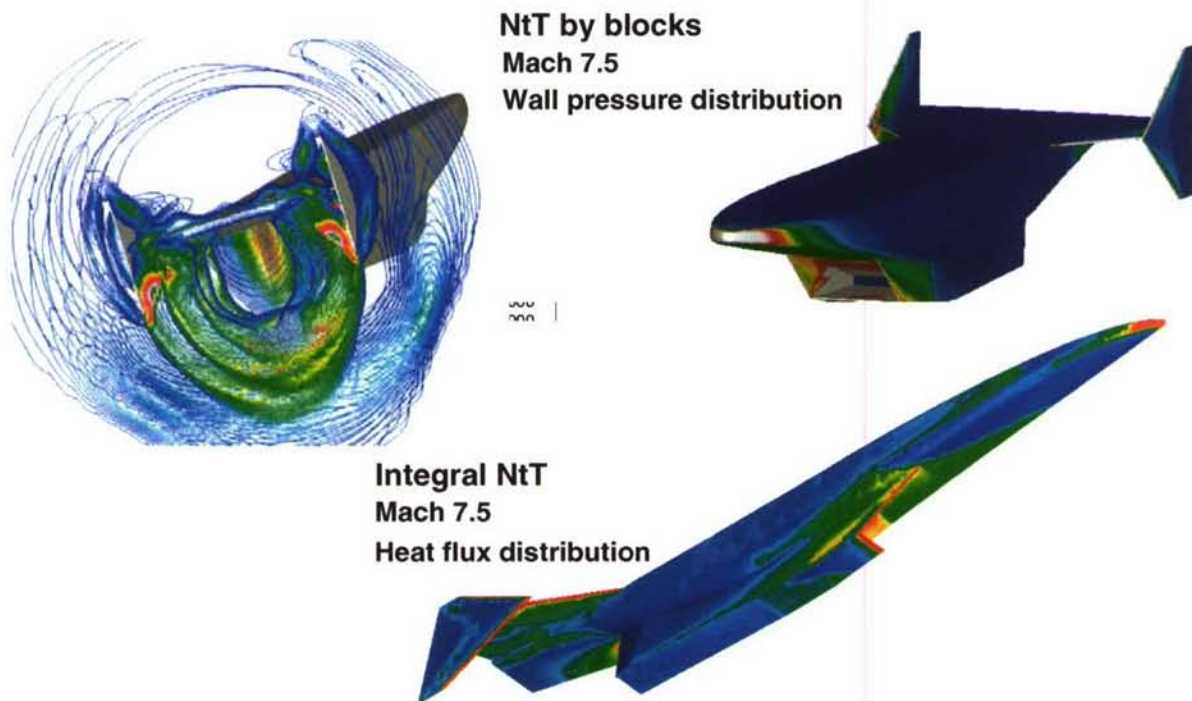


Fig.18 – Some example of Nose-to-Tail computation results

All the previous elements have been used in a detailed flight simulation in order to obtain a first evaluation of reachable maximum LEA/booster separation conditions. This flight simulation allows simulating a complete flight test sequence including LEA/booster dropping from air carrier, acceleration on booster, separation, descent trajectory of booster, LEA autonomous flight up to final crash.

Other activities have also been carried out to chose the basic technologies used for the LEA vehicle and its propulsion system and a preliminary design has been performed and validated by a Preliminary Design Review (Fig.19).

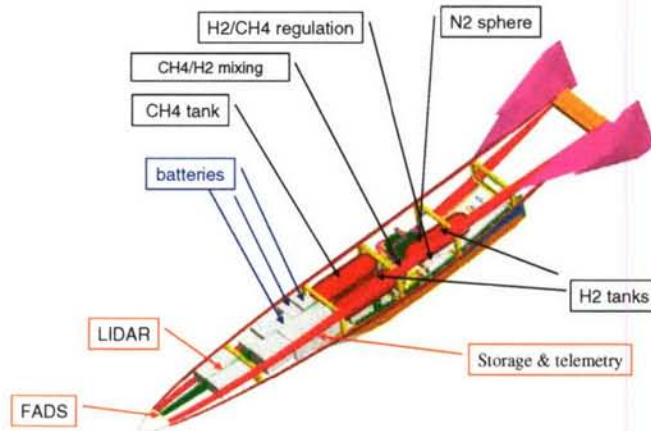


Fig.19 – LEA vehicle Internal layout

By another way, a general approach for on-ground testing has been defined but it still remain to be refined and confirmed. Indeed, as Fig.20 shows and on the base of previous studies [49], a large part of the on-ground testing program should be realized in the S4Ma wind tunnel located in ONERA Modane test Center in the French Alps.

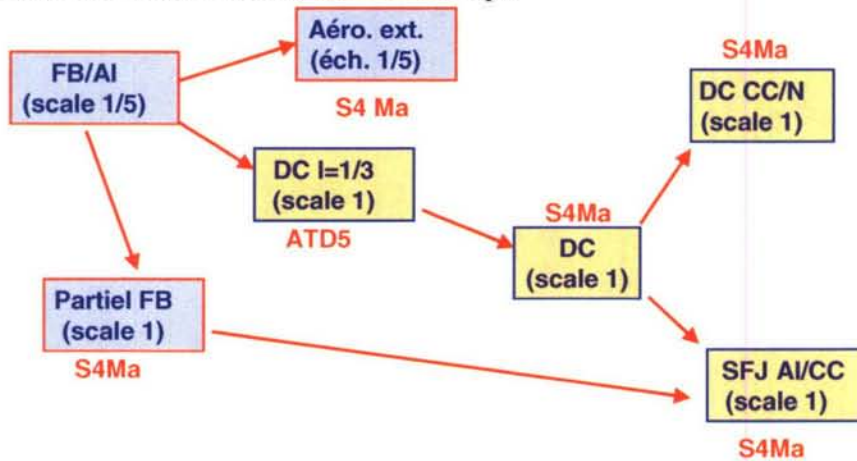


Fig. 20 – general approach for on-ground testing

It is intended to upgrade this test facility in order to take advantage of the existing alumina pebble bed heater which allows to perform test with air non vitiated by water vapour up to Mach 6.5 conditions (1800 K). Thanks to a complementary pre-burner or to an updating of the pebble bed heater, tests corresponding to Mach 7.5/8 flight conditions should be also easily feasible. Detailed design studies, as for example free jet test configuration (Fig.21), have been performed to verify the feasibility of such an upgrading and evaluate precisely the corresponding cost.

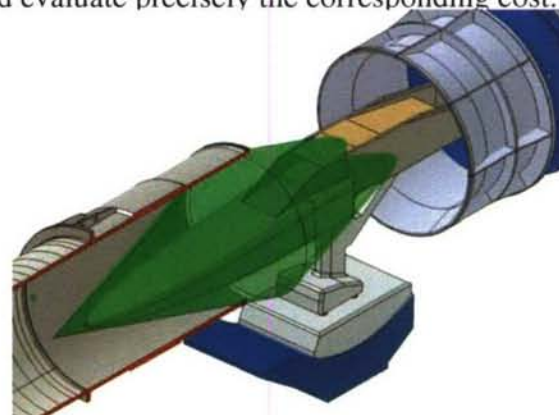


Fig. 21 – Study of LEA free-jet test installation in S4Ma ONERA test facility

Combustion chamber technology

The combustion chamber technology covers different aspects which contribute to ensure the thermal and mechanical strength:

- variable geometry needed to optimize the performance on the overall flight Mach number range,
- fuel used as coolant for combustion chamber structure,
- fuel-cooled structure itself.

Variable geometry

Some developments have already been performed in the scope of the WRR program led by MBDA France in cooperation with MAI. Corresponding technologies (cooled hinges, high temperature sealing system between movable and fixed walls...Fig.22) have been tested separately, then reused in the PIAF combustion chamber which have been successfully tested at MAI in the Mach number range from 2 to 7.5.

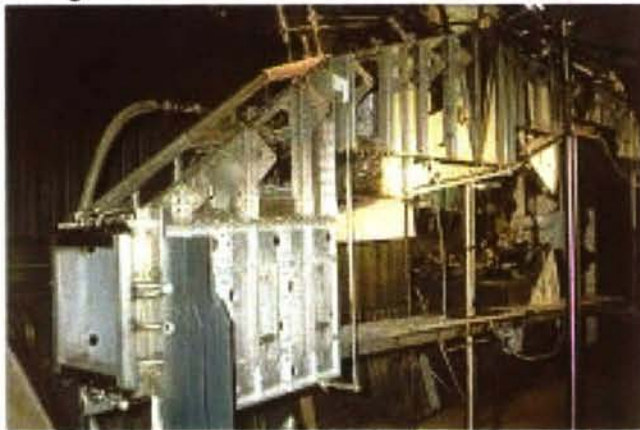
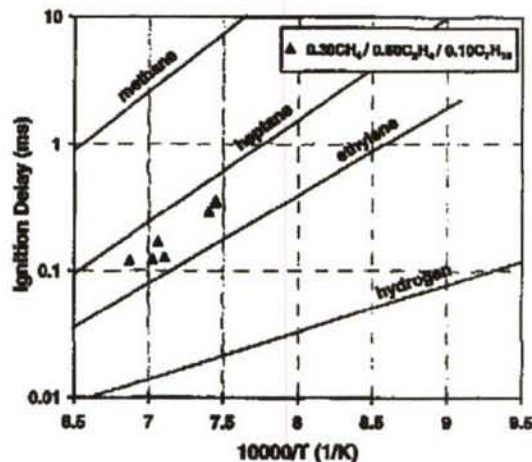


Fig.22 – WRR Prototype with removed lateral wall

Endothermic fuel

The cooling capacity of the hydrocarbon fuels is less than hydrogen one, and cannot easily ensure the cooling of the combustion chamber of the dual-mode ramjet, which is absolutely mandatory at high Mach numbers first to ensure thermal resistance of the combustion chamber and second also to improve mixing and combustion process (gaseous fuel with radicals promoting ignition – see Fig.23) and maximize the net thrust (by re-injecting heat lost along combustor walls into the propulsive thermodynamic cycle).

Fig.23 – example of ignition delay for a hydrocarbon mixture representing fuel reforming products



In order to obtain sufficient cooling capability, one way is to use the endothermic effect which is produced by thermal reforming of the liquid fuel into lighter components. Figure 24 shows how the decomposition of the fuel can significantly increase the thermal absorption capacity.

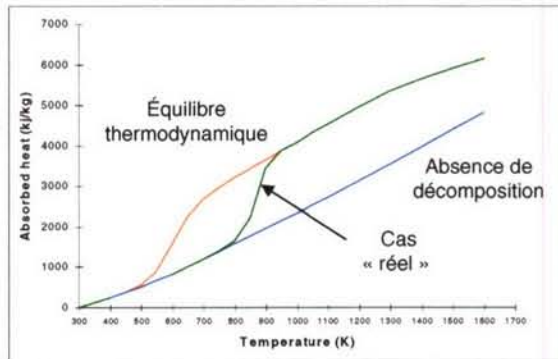


Fig.24 - Endothermic effect

In order to analyze and get to a better understanding of the different thermo chemical mechanisms associated to fuel reforming process inside the cooling system, a pilot system has been developed (Fig.25). The pilot system is organized around a tube which is placed inside a thick copper bloc. The block is heated by electrical resistances progressively, and it then operates as a heat capacity when the fuel flow is started into the tube. This system aims at studying, for different mass flow rates and heating conditions, the evolution of the composition of the products at the exhaust of the tube.

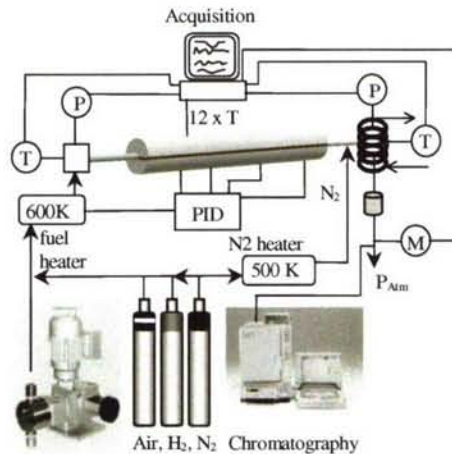


Fig. 25 - Pilot system in operation at ONERA

Complex reactions are located in the cooling circuit elements. The design of a combustion chamber cooled by this method requires perfect mastering of the following points:

- thermal loads evaluation, along the whole flight trajectory
- structural design of an integrated cooled chamber
- fuel thermal reforming process
- fuel injection system capable of managing the different situations encountered during the flight (variable mass flow rate, thermodynamic state of the products, different location of the injection points...)

Some works are led in cooperation with CNRS to be able to simulate the complete operation of the cooling circuit (Ref [50] and [51] - Fig.26) taking into account in the same computation the reforming process (Fig.27)

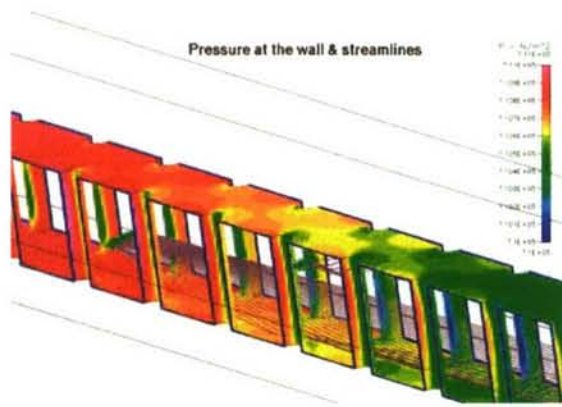


Fig.26 – Example of computation in Ptah-Socar cooling circuit

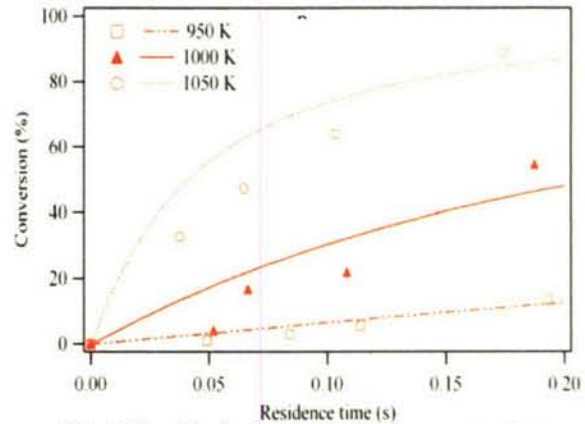


Fig.27 – Endothermic fuel conversion as function of residence time

At the beginning of the flight, the wall of the combustion chamber is not necessarily hot enough to reach the conditions where decomposition of the fuel is obtained. The tuning of the engine has to be made, especially for a certain part of the flight trajectory, using at least partially liquid fuel. On the contrary, when the missile is flying at very high speed, the fuel can reach a very high level of decomposition. Its chemical composition becomes complex, and the combustion parameters of this hot multi-component fuel is no more like the combustion of the original cold liquid fuel.

However, it is not easy to tune the engine using a technological chamber (integrating cooling system), and it also very difficult to produce appropriate mass flow of appropriate composition with external devices. Then the problem becomes to ensure sufficient similitude for the combustion using more convenient and available fuels.

Combustion chamber fuel-cooled structure

From the point of view of materials, the major technological difficulty for the development of hypersonic air breathing vehicles, powered by dual-mode ramjet or scramjet, is to design and realize the structure of the combustion chamber. As a matter of fact, the combustion chamber and the fuel injection and/or flame stabilization systems, possibly placed in the flow, must be able to sustain a rarely so severe thermo-mechanical environment.

Moreover, in the case of variable geometry combustion chamber, it is necessary to ensure a sufficiently controlled geometry to ensure tightness between movable and fixed surfaces of the chamber.

These elements lead to consider combustion chamber technologies based on the use of thermo-structural composite materials cooled by the fuel. By comparison with metallic solutions, such a technology should give large design margin and should correspond with relatively low cost systems while ensuring good reliability and safety characteristics.

In this field, very limited works have been performed by EADS Space Transportation (now Astrium ST) and SNECMA during the PREPHA program and led to basic test, performed at ONERA (Ref [2]). In parallel, MBDA France and Astrium ST led in house development of hydrogen or hydrocarbon fuel-cooled injection strut (St ELME) (Ref [52] – Fig.28).

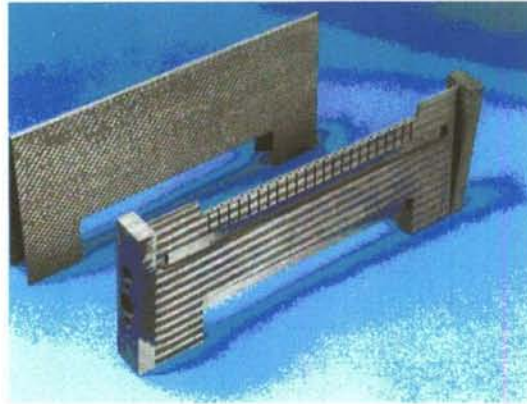


Fig.28 – H2 cooled C/C injection strut

By another way, the cooperation led by MBDA France and MAI for developing a fully variable geometry dual-mode ramjet was also an opportunity to acquire a large know-how in the field of fuel-cooled structures. More than 30 concepts of cooled panels have been developed for protecting the fixed and movable combustion chamber walls.

Most of these studied cooled panels were based on metallic structures. Then, in order to maintain the temperature of the hot wall under the relatively limited capacity of the steel alloys it is necessary to use:

- 3D configurations, in particular multi-layer architectures,
- heat exchange enhancement systems in the cooling channels.

Each of cooled panel has been tested in MAI test facility, in which hydrogen fueled scramjet combustion chamber is used as high temperature gas generator. The tested cooled-panel (100x200 mm²) is placed at the scramjet chamber exit (Fig.29). A wedge is facing the tested panel in order to create a shock wave whose interaction with the tested panel increases the heat flux, which can reach 3 MW/m².

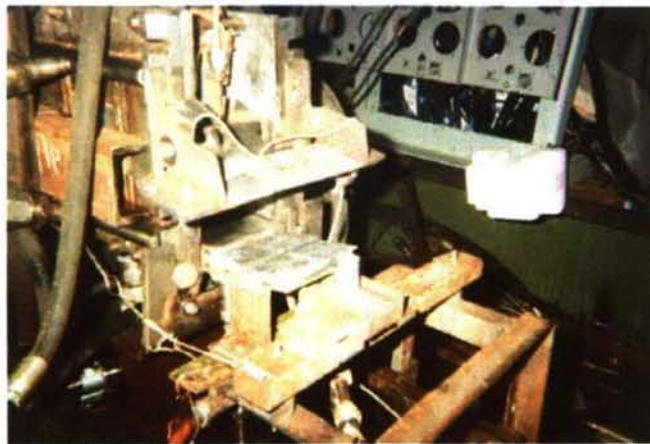


Fig. 29 – Cooled panel test facility at MAI

Today, MBDA France and Astrium ST are focusing their in house effort on the development of a low cost, highly reliable and effectiveness technology for the fuel-cooled composite material structure, particularly usable for the walls of ramjet/scramjet combustion chamber. This technology, called PTAH-SOCAR, takes advantage of the Astrium ST know-how in the field of

pre-form manufacturing and particularly of its mastery for weaving the fibrous structure (Ref [53] to [56]).

By comparison with more classical solution, this know-how enables us to create a C/SiC structure, which has the following advantages:

- It avoids any bonding system (brazing, gluing...), which constitutes a weakness for classical systems for sustaining the high pressure of the internal cooling flow and implies limitation of maximum temperature in the bonding region.
- It enables us to obtain a complete combustion chamber structure in one part. That led to :
 - limit the connecting problems to one inlet and one outlet connection,
 - avoid any problem generally encountered with classical plane cooled panels for realization of the corners of a 2D combustor,
 - increase the reliability by limiting the possible leakage problems.
- It considerably reduces the part of the cooled-structure wall, exposed to the hot heat flux, which is not directly in contact with the coolant fuel.
- It avoids to machine internal channels and, by this way, makes easier the integration of specific systems like injectors, injection struts or flame-holders.

Moreover, this technology can be easily adapted to other applications as injection struts or cooled nozzle expansion ramp.

A first test series has been performed with PTAH-SOCAR cooled-panels densified by CVI process (Fig.30). Tests were performed with nitrogen and kerosene as coolant. By reducing step by step the coolant mass flow it has been possible to obtain the maximum temperature on the hot wall which would be reached in an operational application (Fig.31).

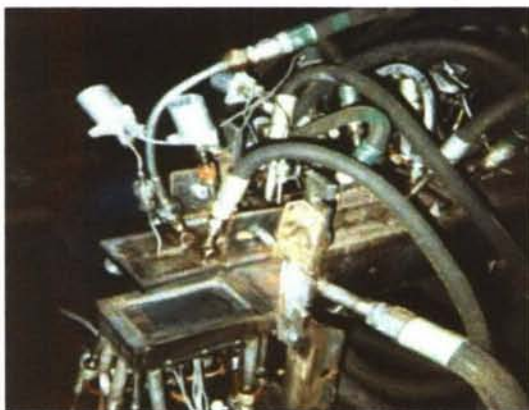


Fig.30 – PTAH-SOCAR panel in test at MAI

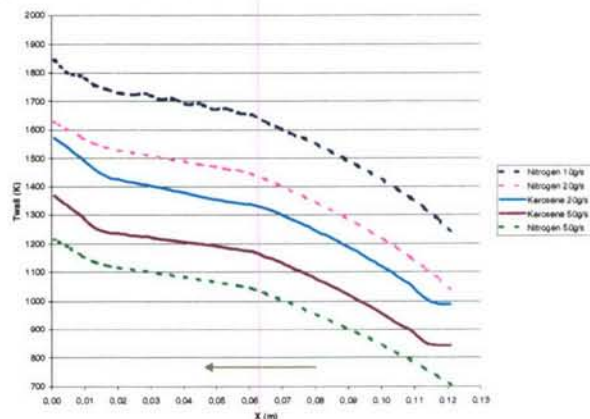


Fig. 31 – Hot wall temperature evolution

A key point for using composite materials for fuel-cooled panels is their natural porosity which could generate safety hazard and reduce the performance (with natural porosity, the total injected fuel would completely leak through combustion chamber walls and no fuel would reach the injection system). It is then very important to master the permeability of the material. However, a preliminary study indicates that a small leakage to the combustion chamber side could be interesting from the point of view of performance. As a matter of fact (Fig. 32):

- If the porosity is too large, an important part of the fuel mass-flow will leak out through the combustion chamber wall. Then, specific impulse will decrease (no combustion of the corresponding mass of fuel) or it will create thermal overloading on the wall (in case of partial or total combustion of the fuel damaging the wall).

- If the porosity is limited, the fuel leaking out through the wall will reduce skin friction losses while the main part of fuel will burn normally resulting in an improved specific impulse by comparison with a perfectly fuel-tight material.

In order to solve this problem, but also to reduce the production cost, the PTAH-SOCAR has been adapted to liquid infiltration by using the LSI process developed by Astrium ST Germany). This new version has already been tested at component level (mechanic and thermal characterisation and cooled panel). After several iterations, this technology present today the permeability needed to ensure an optimum fuel leakage in the case of a propulsion system for a missile.

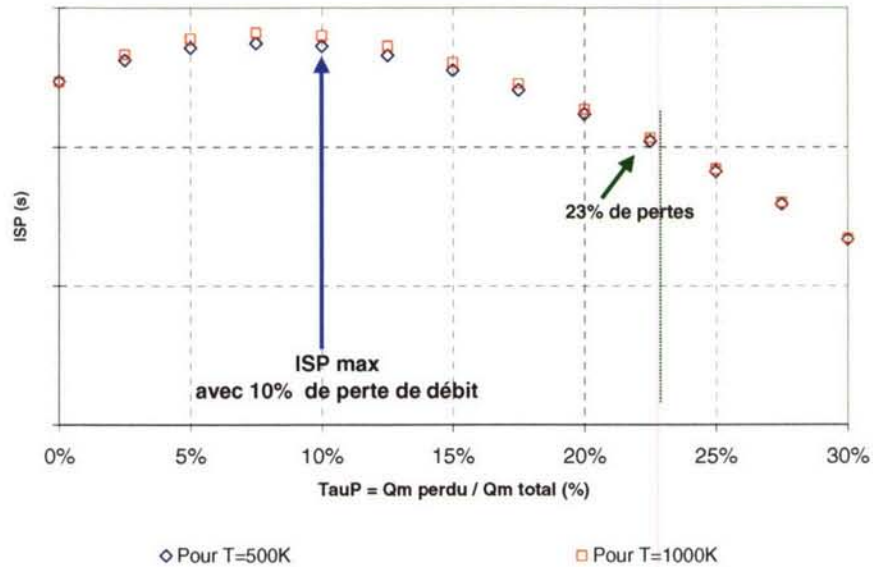


Fig.32 – Fuel leakage effect on specific impulse

On the basis of these technology development works, a demonstration part constituting a portion of cooled combustion chamber, called PSD, has been designed, manufactured and successfully tested in 2006 at ONERA test bench ATD 5 (Fig. 33 - Ref [57]).

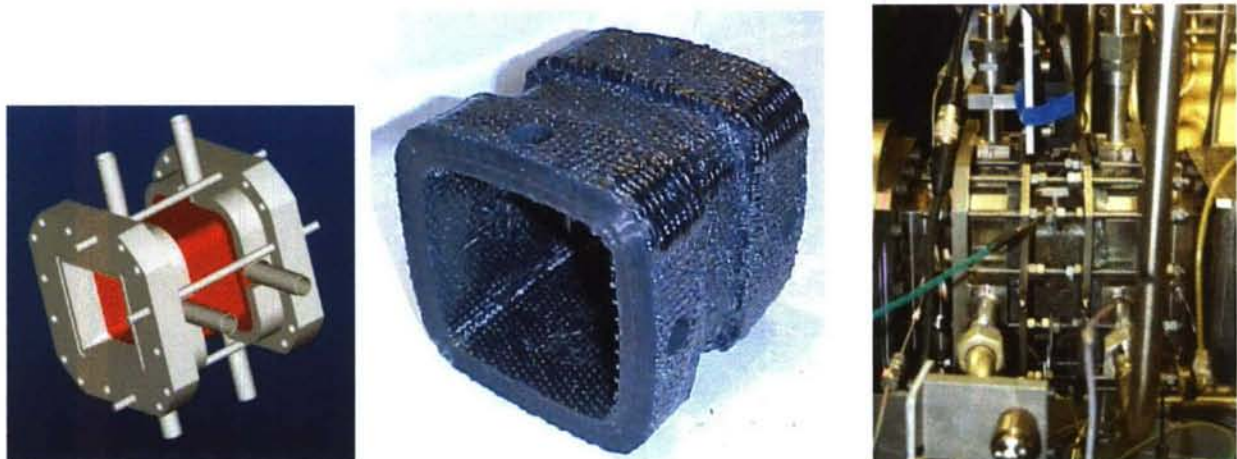


Fig.33 – PTAH-SOCAR PSD demo tested at ONERA ATD 5 test bench

Further works

Beyond the works already in progress, the test facility, developed by MBDA France and ROXEL in their Bourges Subdray test centre in the framework of PREPHA program (Ref [49] – Fig.34), is under upgrading. The new test facility, called METHYLE, will allow to perform long endurance test in representative conditions to pursue and reinforce technology development by using a modular water-cooled dual mode ramjet combustion chamber able to integrate different kind of testing parts as for : element of variable geometry, sealing system, fuel-cooled structure, measurement techniques, engine control system...) (Fig.35).

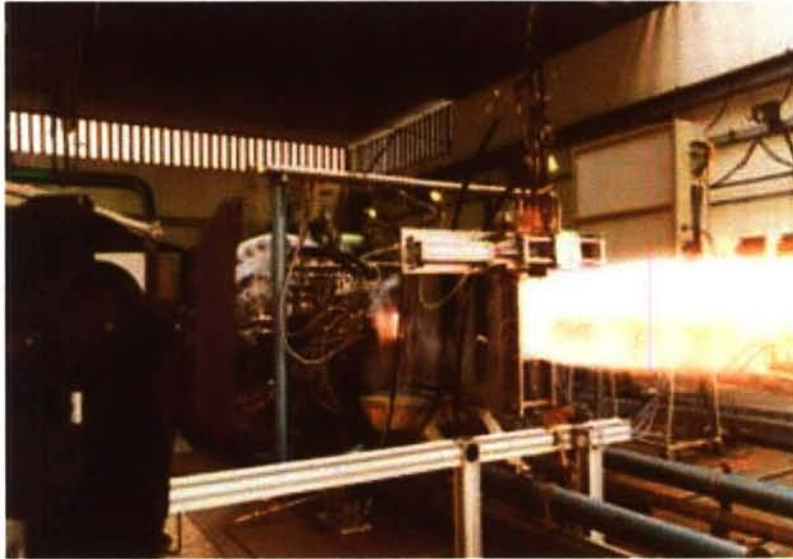


Fig.34 – Hypersonic test bench in Bourges Subdray test centre

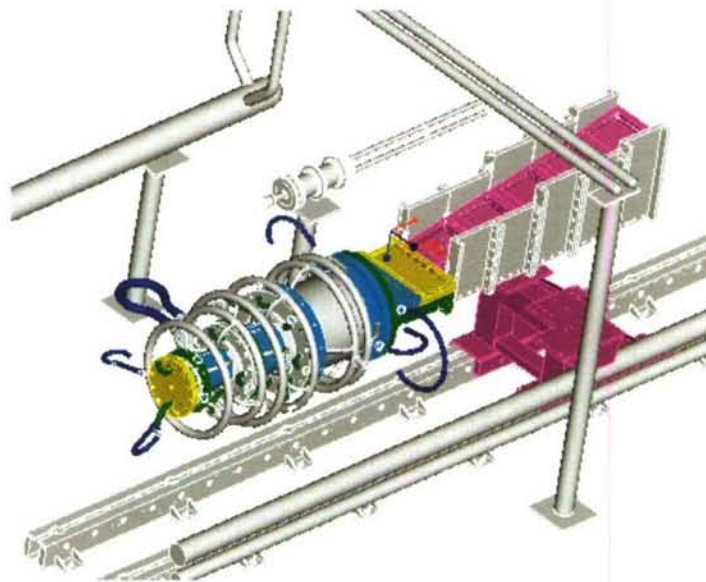


Fig.35 – METHYLE test facility (under development)

Further possible development

The LEA flight test program constitutes a very important first step in the definition and the validation of a development methodology for hypersonic air breathing vehicles. Nevertheless, if we consider the possible application of high-speed air breathing propulsion to future reusable space launcher, it is clear that the air breathing phase will have to be extended up to Mach 10/12.

In that view, a minimum R&T program has been proposed (Ref [58]). It includes an extension of the flight domain of the LEA vehicle (LEA+) thanks to the upgrading of the present acceleration system or by selecting another one with higher capabilities. At least, taking into account the corresponding background and associated working partnership, it should be possible to define the most efficient flight test program (in term of scientific and technological return to financial investment).

It has to be noticed that such extended flight experimental program could take advantage of other already existing experimental systems and programs as, for example, the HyShot program which could be used to perform partial technology flight validation for LEA vehicle and propulsion system or for instrumentation.

But, the budget which could be potentially available in Europe within the next years for such a flight test program will be limited. By another way, the on-going LEA flight test program between Mach 4 and Mach 8 has to be first performed. That is why, considering these two points, a proposal has been submitted to ESA regarding a preliminary and less ambitious flight test program, called EAST for European Advanced Scramjet Test, which could be performed by 2010.

The EAST program would consider a subscale ($\sim 1/4$) twin engines configuration derived from LEA vehicle (Fig.36). EAST would not be a simple supersonic combustion experiment within an academic combustor but would consist in testing the system forebody / air inlet / combustion chamber / partial nozzle during a captive flight on top of a booster derived from a sounding rocket system (Fig.37). The EAST experiment would be fixed on the booster thanks to a strut equipped with a thrust measuring system.

Such a program, dealing with an integrated propulsion system, would allow extending the already defined development methodology by taking into account new ground test possibilities as, for example, high enthalpy short time wind tunnels F4 at ONERA Fauga or HEG at DLR Göttingen and to acquire a first flight validation. By another way it would be possible to take advantage of the quite complete propulsion system configuration to flight test the needed improvements of LEA technology to sustain higher flight Mach number conditions.



Fig. 36 – EAST configuration

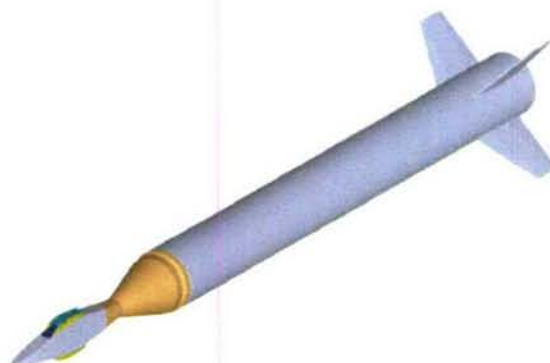


Fig. 37 – EAST on top of the sounding rocket

Beyond these technology development efforts, the need was also clearly identified to restart system studies taking advantage of recent progress made regarding knowledge, tools and technology and focusing on more innovative airframe/propulsion system concepts enabling better trade-off between structural efficiency and propulsion system performance.

In that field, a fully axi-symmetric configuration has been considered for a reusable micro-space launcher (10 kg payload). The vehicle, based on a double cone fuselage providing good structural efficiency, is constituted by a main stage powered by air breathing propulsion, combined or not with liquid rocket mode. A “kick stage”, powered by a low performance solid rocket engine provides the final acceleration (NEO concept) (Fig.38).

The air breathing engine is annular and can also be constituted by a series of modules, each easily testable on ground (in any case corresponding to a limited scaling effect by comparison with possible ground testing). This engine has fully variable geometry one using a concept derived from the LEA engine. Taking advantage of the translating movement of the cowl, the rear part of the engine can be closed to ensure a safe re-entry on the back using the aerospike nozzle as blunt nose providing the needed thermal protection.

**New configuration studies for NEO concept to improve the trade-off
 Propulsion performance ↔ Vehicle dry mass**

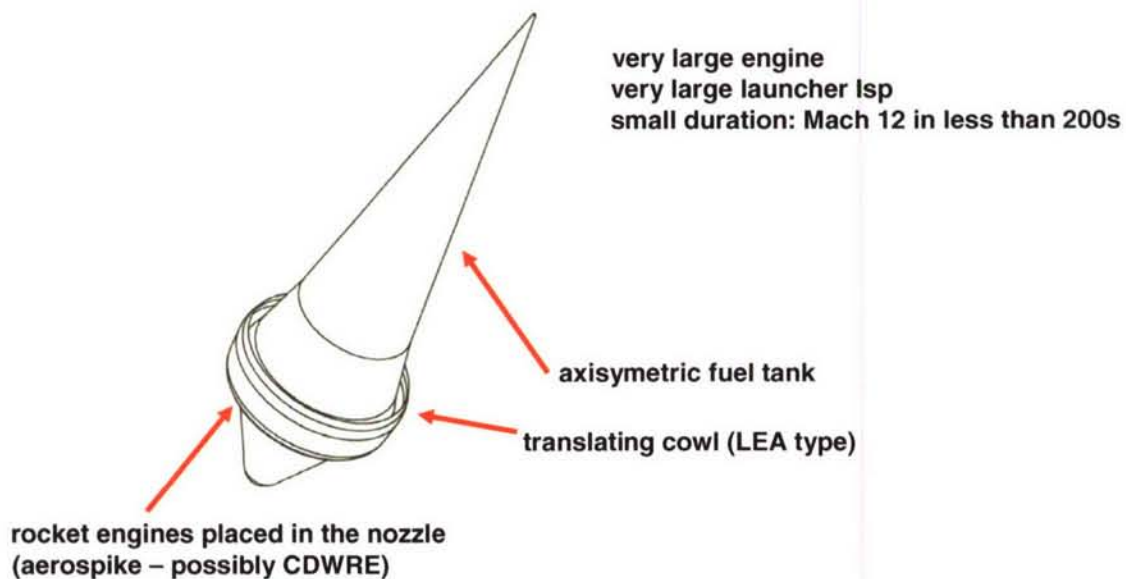


Fig.38 – Axi-symmetric NEO concept

A preliminary design has been performed for different variants : one using a separated booster and a purely air breathing main stage, a second one using a booster and a main stage combining air breathing and rocket mode, a third one without separated booster, the main stage ensuring the initial acceleration in liquid rocket mode and a complementary acceleration phase in rocket mode beyond the air breathing propulsion system operation (Fig.39).

On this basis, performance assessment has been carried-out thanks to trajectory simulation. The main conclusions are the following :

- The very large air breathing engine delivers a very large thrust level.
- This thrust level provides a very high acceleration capability and then a very good launcher specific impulse.

- It also allows starting the air breathing mode very early (at about Mach 1.5) reducing the needed on-board oxidizer mass then the corresponding tank mass.
- The acceleration capability allows to reach Mach 12 in less than 200s (to be compared with 1000 to 1200 s needed with an airplane-like vehicle (PREPHA vehicle for example).
- Then the air breathing mode, and consecutive trajectory in the atmosphere, doesn't lead to thermal protection oversizing.
- The large air breathing engine corresponds with a limited dry mass increase as it is mainly constituted by a short annular cowl.
- All the previous elements lead to the feasibility of a reusable main stage with a staging at Mach 14.5 corresponding to a 8.5 m long, 3.0 m diameter vehicle with a gross take-off weight of about 4.5 metric tons, able to place in a 250km circular orbit a payload of 10 kg + 30 kg of avionics.
- Finally, there will be a clear advantage in replacing the liquid rocket engine of this third variant by a continuous detonation wave rocket engine for which integration will largely easier and more efficient (including a very simple way to control the thrust vector and to close the engine for the re-entry phase).

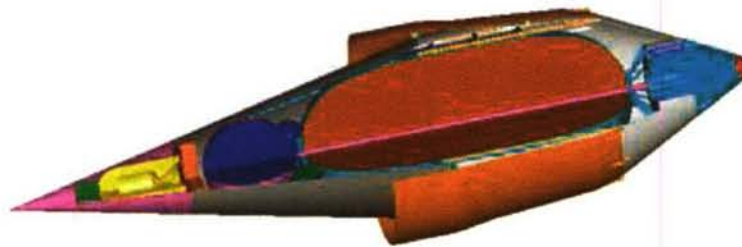


Fig. 39 – Axi-symmetric NEO micro-space launcher – internal layout

Conclusion

The ramjet/scramjet concept constitutes the main air breathing propulsion system which can be used in a very large flight Mach number range up to Mach 10/12 and then could allow developing future fully reusable space launcher and military systems.

Beside international activities, mainly in USA and Japan, a permanent Research and Technology effort has been pursued in Europe since twenty years. Today, the effort led in France aims at addressing the two key technology issues which are the accurate prediction of the aero-propulsive balance of an air breathing vehicle flying at high Mach number and the development of high-temperature structures for the combustion chamber able to withstand the very severe environment generated by the heat release process while ensuring reliability and limited mass and should allow to conclude on the feasibility and interest of the two possible application within the next five to six years (2012/2013).

References

- [1] **F. FALEMPIN, Ph. NOVELLI, P. HENDRICK, A. SOUCHIER**
Air breathing/rocket combined cycle propulsion efforts in Europe
AAAF – 2002 – 268 – Versailles
- [2] **FALEMPIN, D. SCHERRER, G. LARUELLE, Ph. ROSTAND, G. FRATACCI**
French Hypersonic Propulsion programme PREPHA - Results, Lessons and Perspectives
AIAA - 98 – 1565 - Norfolk
- [3] **A. LENTSCH, R. BEC, F. DENEU, Ph. NOVELLI, M. RIGAULT, J.-M. CONRARDY**
Air-Breathing Launch Vehicle Activities in France - The Last and the Next 20 Years
AIAA 2003-6949, Norfolk, December 2003.
- [4] **J. HUTT**
Space Launch Roadmap
AIAA-2003-6941
- [5] **A. BOUDREAU**
Status of the Air Force HyTech Program
AIAA-2003-6947
- [6] **K. FUJII, T. NAKAMURA, H. KAWATO and S. WATANABE**
Concepts and Studies of Flight Experiment Vehicles for Reusable Space Transportation System
AIAA-2003-6984
- [7] **R. BOYCE, S. GERARD, A. PAULL**
The HyShot Scramjet Flight Experiment - Flight Data and CFD Calculations Compared
AIAA-2003-7029
- [8] **M. NAIR, N. KUMAR and S. SAXENA**
Reynolds Averaged Navier-Stokes Based Aerodynamic Analysis of Inlet for a Hypersonic Research Vehicle
AIAA-2003-7067
- [9] **J. LE, W. LIU, Y. TAN and W. HE**
Performance Study of Model Scramjet with Fuel of Kerosene in Pulse Facility
AIAA-2003-6936
- [10] **F. FALEMPIN**
High-speed air breathing propulsion French activities
AIAA - 2002 – 5232
- [11] **F. FALEMPIN**
French hypersonic program PREPHA - System studies synthesis
XIII ISABE - Chattanooga - 1997
- [12] **L. SERRE**
Towards a low risk air breathing SSTO program : a continuous robust PREPHA based TSTO
AIAA - 99 - 4946 - Norfolk
- [13] **F. FALEMPIN**
The fully reusable launcher : a new concept asking new visions
AIAA - 2003 – 7031
- [14] **F. FALEMPIN**
Possible military application of high-speed air breathing propulsion in the XXIst Century
an European vision
AIAA - 2003 – 2733
- [15] **L. SERRE**
Hypersonic UAV for reconnaissance in the depth
AGARD 594 - Athens – 1997
- [16] **L. SERRE, F. FALEMPIN**
High altitude high-speed UAV for reconnaissance operations - Projection of forces international symposium
AAAF – Paris – Dec. 99
- [17] **M. SANCHO, Y. COLIN, C. JOHNSON**
The French hypersonic research program PREPHA
AIAA-96-Norfolk
- [18] **F. FALEMPIN**
Ramjet/Scramjet technology – French capabilities
AIAA - 99 – 2377 – Los Angeles
- [19] **F. FALEMPIN, V. LEVINE, V. AVRASHKOV, D. DAVIDENKO, M. BOUCHEZ**
MAI/AEROSPATIALE Cooperation on a hypersonic WRR: evaluation of thermal protection systems
XIV ISABE - Florence - IS 7140 – 1999
- [20] **M. BOUCHEZ, V. LEVINE, V. AVRASHKOV, D. DAVIDENKO, F. FALEMPIN**
France-Russia partnership on hypersonic Wide Range Ramjet : status in 1999
AIAA – 99 – 4845 - Norfolk
- [21] **M. BOUCHEZ, F. FALEMPIN, V. LEVINE, V. AVRASHKOV, D. DAVIDENKO**
French-Russian partnership on hypersonic Wide Range Ramjet : status in 2001
AIAA-2001-1872 – Kyoto
- [22] **M. BOUCHEZ, J.-P. MINARD, V. LEVINE, V. AVRASHKOV, D. DAVIDENKO**
French-Russian partnership on hypersonic Wide Range Ramjet : status in 2002
AIAA-2002 - 5254 – Orléans
- [23] **F. FALEMPIN, M. GOLDFELD**
Design and experimental evaluation of a M 2– M 8 Inlet
AIAA-2001-1890 – Kyoto

- [24] **F. FALEMPIN, M. GOLDFELD, R. NESTOULIA, A. STAROV**
Evaluation of a variable geometry inlet for dual mode ramjet
AIAA-2002 - 5232 - Orléans
- [25] **F. FALEMPIN, M. GOLDFELD, R. NESTOULIA, A. STAROV**
Experimental investigation of variable geometry inlet at mach number 2 to 8
ISABE 2003-1162
- [26] **M. BOUCHEZ, E. SAUNIER, P. PERES, J. LANSALOT**
Advanced carbon/carbon injection strut for actual scramjet
AIAA - 96 - 4567
- [27] **F. FALEMPIN, T. SALMON, V. AVRASHKOV**
Fuel-cooled composite materials structures - status at AEROSPATIALE MATRA
AIAA - 2000 - 3343 - Huntsville
- [28] **F. FALEMPIN, M. BOUCHEZ, T. SALMON, P. LESPADE, V. AVRASHKOV**
An innovative technology for fuel-cooled composite materials structures
AIAA -2001- 1880 - Kyoto
- [29] **M. BOUCHEZ, F. FALEMPIN**
PTAH-SOCAR Fuel-cooled composite materials structure
AIAA - 2002 - 5135 - Orléans
- [30] **E. DUFOUR, M. BOUCHEZ**
Semi-empirical and CFD analysis of actively cooled dual mode ramjets
AIAA - 2002 - 5126 - Orléans
- [31] **F. FALEMPIN, W. KOSCHEL**
Combined rocket and air-breathing Propulsion - European perspectives
3d International Symposium on Space Propulsion - Beijing - 1997
- [32] **Ph. NOVELLI, W. KOSCHEL**
JAPHAR : a joint ONERA-DLR research project for high-speed air breathing propulsion
XIV ISABE - Florence - IS 7091 - 1999
- [33] **Ph. NOVELLI**
Progress of the JAPHAR cooperation between ONERA and DLR on hypersonic air breathing propulsion
AIAA-2001- - Kyoto
- [34] **Th. EGGERS, Ph. NOVELLI**
Design studies for a M 8 dual mode ramjet flight test vehicle
AIAA - 99 - 4877 - Norfolk
- [35] **Ph. DUVEAU, R. HALLARD, Ph. NOVELLI, Th. EGGERS**
Aerodynamic performance analysis of the hypersonic air breathing vehicle JAPHAR
XIV ISABE - Florence - IS 7286 - 1999
- [36] **O. DESSORNES**
Tests of the JAPHAR dual-mode ramjet engine
AIAA-2001- - Kyoto
- [37] **O. DESSORNES**
Weighing of the JAPHAR dual mode ramjet engine
AIAA - 2002 - 5187 - Orléans
- [38] **D.G. MEDWICK, J.H. CASTRO, D.R. SOBEL, G. BOYET, J.P. VIDAL**
Direct fuel cooled composite structure
XIV ISABE - Florence - IS 7284 - 1999
- [39] **F. FALEMPIN, L. SERRE**
The French PROMETHEE Program - status in 2000
AIAA - 2000 - 3341 - Huntsville
- [40] **L. SERRE, F. FALEMPIN**
The French PROMETHEE Program on hydrocarbon fueled dual-mode ramjet - status in 2001
AIAA-2001-1871 - Kyoto
- [41] **L. SERRE, F. FALEMPIN**
PROMETHEE : The French military hypersonic propulsion Program
AIAA - 2002 - 5141 - Orléans
- [42] **M. BOUCHEZ, V. LEVINE, V. AVRASHKOV, D. DAVIDENKO, P. GENEVIEVE**
Air breathing space launcher interest of a fully variable propulsion system
AIAA - 2000 - 3340 - Huntsville
- [43] **A. ROUDAKOV, Y. SCHICKMANN, V. SEMENOV, Ph. NOVELLI, O. FOURT**
Flight testing an axisymmetric scramjet - Russian recent advances
IAF - 93 - S.4.485 - Graz
- [44] **F. FALEMPIN, B. FORRAT, J. BALDECK, E. HERMANT**
Hypersonic air breathing propulsion - flight test needs
AIAA-95-6013 - Chattanooga
- [45] **F. FALEMPIN, B. FORRAT, J. BALDECK, E. HERMANT**
Flight test vehicles : a mandatory step in scramjet development
AIAA - 92 - 5052 - Orlando
- [46] **A. PAULL**
The HyShot flight program and how it was developed
AIAA-2002-5248-Orléans
- [47] **F. FALEMPIN, L. SERRE**
LEA Flight Test Program - A First Step towards an Operational Application of High-Speed Air breathing Propulsion
AIAA - 2002 - 5249 - Orléans

- [48] **F. FALEMPIN, L. SERRE**
LEA Flight Test Program - A First Step to an Operational Application of High-Speed Air breathing Propulsion
AIAA – 2003 - 7031 – Norfolk
- [49] **J-P. MINARD**
French potential for semi-free jet test of an experimental dual mode ramjet in Mach 4-8 conditions
AIAA – 2002 - 5241 – Orléans
- [50] **E. DUFOUR, M. BOUCHEZ**
Semi-empirical and CFD analysis of actively cooled dual mode ramjets
AIAA – 2002 – 5126 – Orléans
- [51] **E. DANIAU, M. BOUCHEZ, R. BOUNACEUR, F. BATTIN-LECLERC, P.-M. MARQUAIRE, R. FOURNET**
Contribution to Scramjet active cooling analysis using n-dodecane decomposition model as a generic endothermic fuel
AIAA-2003-6920 - Norfolk
- [52] **M. BOUCHEZ, E. SAUNIER, P. PERES, J. LANSALOT**
Advanced carbon/carbon injection strut for actual scramjet
AIAA – 96 – 4567
- [53] **F. FALEMPIN, V. LEVINE, V. AVRASHKOV, D. DAVIDENKO, M. BOUCHEZ**
MA/aerospatiale Cooperation on a hypersonic Wide Range Ramjet : evaluation of thermal protection systems
XIV ISABE - Florence - IS 7140 - 1999
- [54] **F. FALEMPIN, T. SALMON, V. AVRASHKOV**
Fuel-cooled composite materials structures - status at AEROSPATIALE MATRA
AIAA - 2000 - 3343 - Huntsville
- [55] **F. FALEMPIN, M. BOUCHEZ, T. SALMON, P. LESPADE, V. AVRASHKOV**
An innovative technology for fuel-cooled composite materials structures
AIAA -2001- 1880 - Kyoto
- [56] **M. BOUCHEZ, F. FALEMPIN**
PTAH-SOCAR Fuel-cooled composite materials structure
AIAA – 2002 – 5135 – Orléans
- [57] **M. BOUCHEZ, V. LEVINE, V. AVRASHKOV**
French-Russian Cooperation on Dual-Mode Ramjet : significant step passed for technology and combustion processes mastering
AIAA-2003-7004 – Norfolk
- [57] **M. BOUCHEZ, S. BEYER**
PTAH-SOCAR Fuel-cooled Composite Materials Structure for Dual-Mode Ramjet and Liquid Rocket Engines - 2006 status
AIAA-2006-Canberra
- [58] **F. FALEMPIN, M. BOUCHEZ, L. SERRE, C. BRUNO, P. HENDRICK**
Airbreathing Propulsion for Future Space Launchers – Proposal for a Minimum R&T Program for Europe
AIAA – 2005 – 3362 – Capua